# WASHINGTON UNIVERSITY IN ST. LOUIS

## 2023 NASA USLI Team

Lopata 303
1 Brookings Drive
St. Louis, MO 63105

**Project Behnken 1**

---

CRITICAL DESIGN REVIEW

---

JANUARY 9, 2023

# Contents

# List of Figures

# List of Tables

# 1 Summary of Critical Design Review Report

## 1.1 Team Summary

### 1.1.1 Team Name and Location

The team name of Washington University in St. Louis's NASA Student Launch team is WURocketry. The mailing address of WURocketry is: Lopata 303, 1 Brookings Drive St. Louis, MO 63105.

### 1.1.2 Mentor Information

Table 1: Mentor Information

| | |
|---|---|
| **Name** | Michael Walsh |
| **Professional Title** | Engineering Analyst - Casting for Toyota Motor Manufacturing |
| **Contact Information** | Michael.Walsh@toyota.com, (636) 358-2490 |
| **NAR/TRA Number, Certification Level** | TRA: 09969, NAR: 85317, Certification Level 3 |

### 1.1.3 Final Launch Location and Date

The team will participate in the launch week held in Huntsville, AL between April 13th and 16th, 2022. WURocketry will complete the final launch during launch day.

### 1.1.4 Time Spent on Flight Readiness Review

Table 2: Time Spent on Critical Design Review Broken Down by Group

| **Group** | Avionics | Payload | Structures | Recovery & Propulsion | Business/ Funding | STEM Engagement | Executive Team | **Total** |
|---|---|---|---|---|---|---|---|---|
| **Time (Hours)** | 50 | 55 | 160 | 44 | 10 | 20 | 120 | 459 |

## 1.2 Launch Vehicle Summary

Table 3: Launch Vehicle Summary

| | |
|---|---|
| **Target Altitude** – 4650 ft | **Final Motor Choice** – Aerotech L1390G-P |
| **Individual Sections:**<br>Forward – 64.725 in, 18.012 lb<br>Mid – 14.75 in, 5.59 lb<br>Aft – 31.525 in, 19.24 lb wet (14.88 lb dry) | **Recovery System** – 18 in Elliptical drogue parachute released at apogee, 120 in Iris Ultra Standard parachute released at 600 ft |
| **Wet Mass** – 42.842 lb | **Burnout Mass -** 38.482 lb |
| **Landing Mass** – 38.482 lb | **Dry Mass without Ballast** – 38.482 lb |
| **Rail size** – 1515 Rail, 144 in | **Dry Mass with Ballast -** N/A |

## 1.3 Payload Summary

The WURocketry 2022-2023 VISiON (Virtual Interactive Snapshot in Operational eNvironment) payload experiment is an imaging system capable of receiving RAFCO (radio frequency commands) over an automatic packet reporting system that provides a variety of instructions for the system to take images of the surrounding landing site of the vehicle. The mechanism is located within the payload bay in the forward section of the rocket, situated behind the nosecone. The entire mechanism has an estimated weight of 5 lb and occupies a length of 15.5 in. The mechanical design responsibilities include mechanism retention, self-righting, and finally deployment involving separation of the vehicle and extending the camera system. Electrical design responsibilities include power distribution, electromotive control, and developing logic for performing the required imaging system capabilities.

# 2 Changes Made Since PDR

## 2.1 Changes Made to Vehicle Criteria

### Changes Made to Launch Vehicle Layout

With the beginning of construction, some masses shifted slightly from the predictions from the PDR as the team machined and built components. The overall launch vehicle wet weight is currently 42.842 lb, while at the PDR milestone it was estimated to be 41.50 lb. The launch vehicle length is now 111 in instead of 110 in because the retaining ring was added to the OpenRocket figure in Section 3.1.3. The same avionics bay board will no longer be used for both the sub-scale and full-scale rocket. The team determined that the added sensors for the full-scale rocket would not fit on a sub-scale-sized board.

### Changes Made to Recovery Subsystem

Black powder testing indicated weakness in the nylon shock cords as the exterior surface of the nylon was singed during black powder ejection. Due to this, the Recovery and Propulsion team chose to use Nomex sleeves to protect the shock cords. 6 in shock cord protectors will be attached to all shock cords secured to the avionics bulkheads. This will be further discussed in Section 3.2. Sub-scale flight results indicated a large risk of shock cord tangling, as well as improper inflation of the main parachute, due to the layout of the shock cord harness. As a result of these risks, changes have been made to the lengths and layout of the shock cord harness, as discussed in Section 3.3.

### Changes Made to Avionics Subsystem

After receiving and attempting to demonstrate the Sparkfun NEO-M9N Breakout, it became evident that the Breakout would not be able to function properly for the needs of the Avionics Vehicle Tracking system. The NEO-M9N is not meant to interface with a telemetry downlink but rather to be used for providing data to a microcontroller. Because of this oversight in design selection for the GPS, the team has decided to instead use the Altus Metrum TeleGPS paired with the Altus Metrum TeleBT for our vehicle tracking telemetry downlink system. The new system will communicate on the 70cm frequency band. Additional information on the updated vehicle tracking system can be found in Section 3.3.10 Recovery System Avionics under Vehicle Tracking.

## 2.2 Changes Made to Payload Criteria

### Solenoid Retention Mechanisms

Since the PDR, the team has decided to use a linear solenoid rather than a linear actuator for the nosecone and rotating track retention systems. The two main reasons for this change involve the weight and size of the actuator when compared to the solenoid. The linear actuator weighs more and takes up large amounts of space. Furthermore, there are varying sizes of solenoids while it was difficult to find any actuators that were small enough to fit into the payload. Considering there are at least 3 solenoids in the design, changing from an actuator to a solenoid will help save room for other components, as well as reduce the total weight of the payload section.

### Improved Payload Separation Distance

Originally, the design in the PDR placed the main payload setup of the board, centering rings, and rack and pinion near the motor and bulkhead between the payload and main body sections. There was a distance about 4 inches behind the setup, however now the design has increased the separation distance to a minimum of 6 in. This is done by having the centering rings and other components closer to the nosecone, as well as increasing the length of the racks to 18 in to give the separation mechanism additional clearance to separate.

**Scissor Lift Camera Deployment**

In the PDR design, the camera and servo motor were initially mounted on top of a linear actuator that would extend the camera out of the separated vehicle for imaging. Due to increasing physical volume constraints, the linear actuator deemed too lengthy to fit within the payload electronics board while remaining effectively self-righting. Therefore, we moved the linear actuator deployment into a scissor lift design.

**Improved Camera Servo Feedback**

After extensive tests in operating with the former SG90 continuous rotation servos to control the imaging system rotation, it was determined that there was not enough consistency and control in obtaining a 60 degree rotation of the camera. The original design that proposed running multiple tests to calculate the necessary amount of time and speed to run the servo such that 60 degrees was achieved (left and right) was unreliable, thus the team switched to using a 360 degree rotation with angle feedback.

**Model G Raspberry Pi Camera**

After receiving orders of the original Smraza 160 degree camera, the unit was deemed defective after several electrical tests (continuity, VIN voltage, etc.). As a result, the team has decided on ordering another model of the Raspberry Pi camera, specifically Model G, which provides the same 160 degree FoV capability via its lenses. The component successfully captured still images when issued commands from the Raspberry Pi and will thus replace the original Smraza camera.

## 2.3 Changes Made to Project Plan

Minor changes were made to the project plan since the PDR. Most of the changes made involve the addition of STEM Engagement activities to the spring schedule by reaching out to school districts in less-privileged communities. In order to get a better picture of the status of the project, the Gantt chart schedule was remade using Microsoft Project, where the team was able to assign tasks to certain subteams, therefore making the schedule and allocations more clear. Pivot charts were also used to create a snapshot of the current progress of the project. The business and funding side of the project plan has remained relatively similar with the exception of a greater focus on forming relationships with businesses to begin developing sponsorship opportunities.

# 3 Vehicle Criteria

## 3.1 Design and Verification of Launch Vehicle

### 3.1.1 Mission Statement

WURocketry aims to design, manufacture, test, assemble, document, present, and launch a recoverable and reusable rocket attaining an apogee of 4650 ft while carrying a functioning payload for the 2022-2023 NASA Student Launch.

### 3.1.2 Mission Success Criteria

The mission will be considered successful if it meets all requirements and specifications (vehicle, recovery, safety, and payload) outlined in the 2022-2023 Student Launch Handbook as well as all team derived requirements listed in Section 6.2.

### 3.1.3 Launch Vehicle Overview

The launch vehicle is designed to be 111 in long with an outer diameter of 6.17 in. The wet weight of the vehicle is 42.842 lb and the dry weight is 38.482 lb. The primary motor will be the Aerotech L1390G-P motor with a wet weight of 8.55 lb.

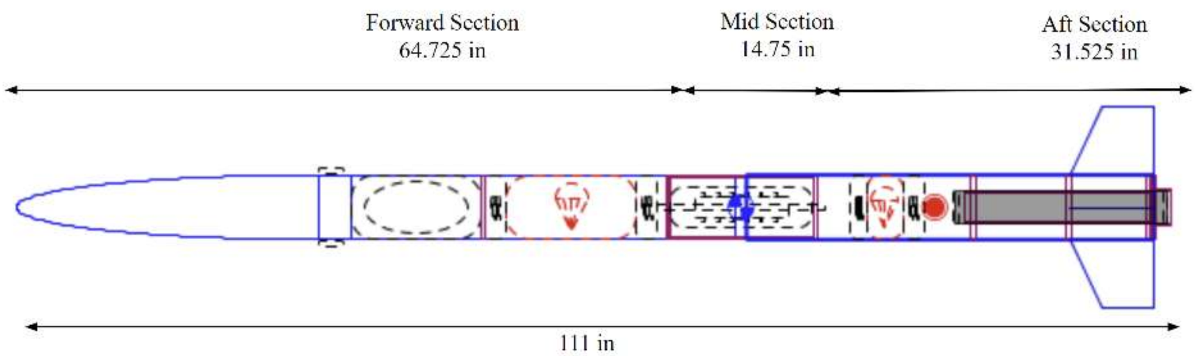


Figure 1: Current Vehicle Design Layout

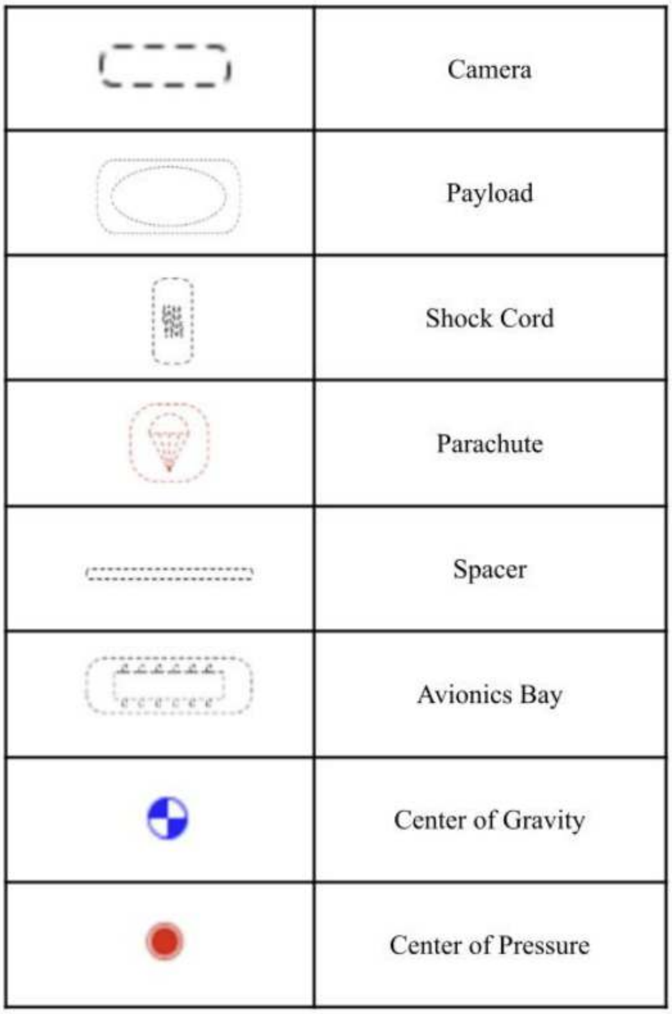


Figure 2: Launch Vehicle Component Layout.

The forward section of the rocket is made up of a 5:1 elliptical nose cone, cameras, payload, main parachute, shock cords, and a bulkhead. There is an in-flight separation point located in between the forward and mid sections. The main parachute is to be released from this separation point. This combines to a length of 64.725 in. and a weight of 18.012 lb with payload and 13.012 lb without payload.

The mid-section is made up of the avionics bay, a coupler connecting the forward and aft section, two bulkheads, and a spacer. The avionics bay will be located entirely in the coupler between two bulkheads secured via threaded rod spacers. The bulkhead forward of the avionics capsule (mid bulkhead) is attached to the aft bulkhead on the opposite side of the coupler via threaded rods and nuts. Four 4-40 nylon shear pins secure the forward body tube to the coupler tube. The aft side of the coupler tube is attached to the aft body tube with two 4-40 nylon shear pins. The mid body tube "ring" is epoxied to the coupler. The mid section with the bulkheads and coupler combines to a length of 14.75 in. and a weight of 5.59 lb.

The aft section consists of aft body tube, drogue parachute and shock cords, motor tube and closures, motor retention, centering rings, fins and fin shells. The fins are fitted through slots machined into the aft tube and held in place by cutouts in the centering rings and epoxy set on either side of the interface between the fin and airframe. This combines to a length of 31.525 in., with a wet weight of 19.24 lb and a dry weight of 14.88 lb.

Below, in Tables 4-6, the final components of the launch vehicle are shown. Additionally, the mass of each component is included in the table. Masses in green have been physically measured while masses in black are estimated masses.

Table 4: Table of Forward Vehicle Components

| Component | Design Choice | Material | Dimensions | Weight (lb) | Image |
|---|---|---|---|---|---|
| *Forward Section* | | | | *18.012* | |
| Nose Cone | 5:1 Elliptical | G10 Fiberglass with aluminum tip | 29 in long by 6.17 in wide at base | 4.3 |  |
| Cameras | Universal AstroCam HD Rocket Cameras | PETG camera holders | 2.32 in long by 0.67 in wide | 0.062 |  |
| Forward Body Tube | 6.17 in outer diameter, 6 in inner diameter | G12 Fiberglass | 40 in long | 4.53 |  |
| Payload | Board between two rotating tracks, electronics/camera deployment on top of board with battery on bottom | Plywood, PLA/PETG, alumininum | 17 in long, 6 in diameter | 5 |  |
| Forward Bulkhead | Disk with central hole eyebolt. Tapped holes on sides to be screwed into body tube | 6061-T6 Aluminum | 5.98 in diameter | 1.03 |  |
| Main Forward Shock Cord | Tubular | Nylon | 15ft 5/8" | 0.38 |  |
| Main Aft Shock Cord | Tubular | Nylon | 25ft 5/8" | 0.46 | |
| Main Parachute | Iris Ultra Standard Toroidal | Ripstop nylon | 120" Diameter | 2.25 |  |

Table 5: Table of Mid Vehicle Components

| Component | Design Choice | Material | Dimensions | Weight (lb) | Image |
|---|---|---|---|---|---|
| *Mid Section* | | | | *5.59* | |
| Mid Body Tube | 6.17 in outer diameter, 6 in inner diameter | G12 Fiberglass | 1 in long | 0.31 |  |
| Tube Coupler | 6 in outer diameter, 5.83 in inner diameter | G12 Fiberglass | 14 in long | 1.48 | |
| Mid Bulkhead | Disk with slots and holes for avionics and recovery/separation systems | 6061-T6 Aluminum | 5.98 in diameter | 0.99 |  |
| Avionics Bay and Spacers | Basswood board between mid and aft bulkheads, 15 in threaded spacers on each side of bay board | Basswood board, steel threaded rods | 14 in long, 5.75 in wide | 1.82 | 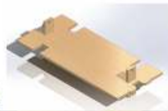 |
| Aft Bulkhead | Disk with slots and holes for avionics and recovery/separation systems | 6061-T6 Aluminum | 5.98 in diameter | 0.99 |  |

Table 6: Table of Aft Vehicle Components

| Component | Design Choice | Material | Dimensions | Weight (lb) | Image |
|---|---|---|---|---|---|
| *Aft Section* | | | | *19.24* | |
| Aft Body Tube | 6.17 in outer diameter, 6 in inner diameter | G12 Fiberglass | 39 in long | 4.81 |  |
| Drogue Parachute | Elliptical | Ripstop nylon | 18" Diameter | 0.11 | 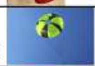 |
| Drogue Shock Cords | Tubular | Nylon | 15ft + 30ft 5/8" | 0.46 |  |
| Motor Tube | 3.08 in outer diameter, 2.88 in inner diameter | Cardboard | 18.9 in long | 0.58 |  |
| Motor Closures and Casing | 75mm diameter, Green Propellant | Aluminium | Width: 3" (7.62 cm) | 0.9 |  |
| Forward Centering Ring | 6 in outer diameter, 3.08 in inner diameter | PLA Plastic | 0.5 in long | 0.15 |  |
| Aft Centering Rings | Slots for fin cores, 6 in outer diameter, 3.08 in inner diameter | PLA Plastic | 0.5 in long | 0.31 |  |
| Fin Cores | Clipped delta shape, epoxied to airframe | G10 Fiberglass | 8 in long, 6.5 in wide, 0.25 in thick | 1.85 |  |
| Fin Shells | NACA 0012 Airfoil Shell, glued to top of fin cores | PLA Plastic | 5.7 in root cord, 2.5 in tip chord, 6.5 in width, 0.6 in thick | 0.44 |  |
| Thrust Plate | 6 in outer diameter, 2.95 in inner diameter | 6061-T6 Aluminum | 0.375 in thick | 0.77 |  |
| Retaining Ring | 3.65 in outer diameter, 3.26 in inner diameter | Aluminum | 1.4 in long | 0.31 |  |
| Wet Motor | AeroTech L1390G, 3946 Ns Impulse | Solid propellant | 20.4 in long, 2.95 in diameter | 8.55 | N/A |
| *Combined Total* | | | | *42.842* | |

WURocketry created various designs for the energetics and separation of the rocket. The chosen design, as shown in Fig. 3, has separation points at the avionics bay. The team can use two longer body tubes that sit on either side of a 1 inch body tube "ring" epoxied to the exterior middle of the coupler.

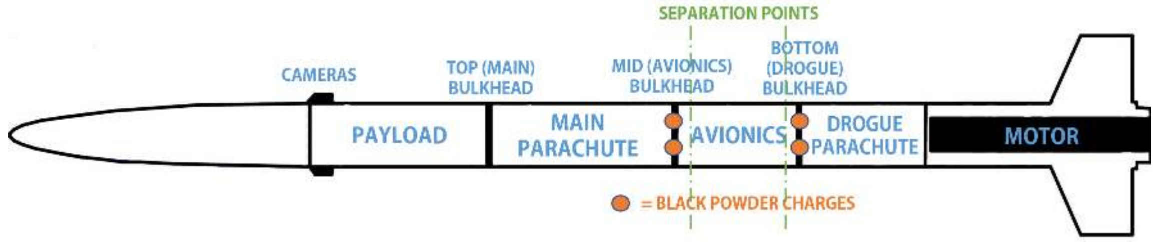


Figure 3: Vehicle In Flight Separation Point and Energetics

When determining which design will be the simplest, lightest, and easiest to assemble, the Structures subteam chose the design in Fig. 3. Other design ideas located the separation events further away from the avionics coupler, which would protect the on-board electronics, but would require more time to assemble with extra body tubes and couplers. Fig. 3 relies on the positioning of two body tubes relative to a singular object (the avionics coupler), thus decreasing assembly time. It diminishes the need for an extra coupler and centering ring for the motor, which reduces overall rocket weight.

### 3.1.4 Launch Vehicle Material Summary

The launch vehicle is constructed mainly out of fiberglass, aluminum, basswood, plywood, and PLA. The airframe, nosecone, and couplers are made of G12 fiberglass. The fin cores are machined out of a G10 fiberglass sheet, and the fin shells are printed with PLA plastic. The bulkheads are milled out of 6061-T6 aluminum. The centering rings are printed from PLA plastic. The structure that supports the avionics component is laser cut from 1/4 in basswood. The payload bay board is laser cut from 1/4 in plywood. Phenolic tube is used for the motor mount as all thrust forces are directly transferred into the airframe from the motor retention system.

### 3.1.5 Launch Vehicle Full SolidWorks Assembly

Figure 4 shows an exploded view of the Full Rocket Assembly with the different independent components labelled.

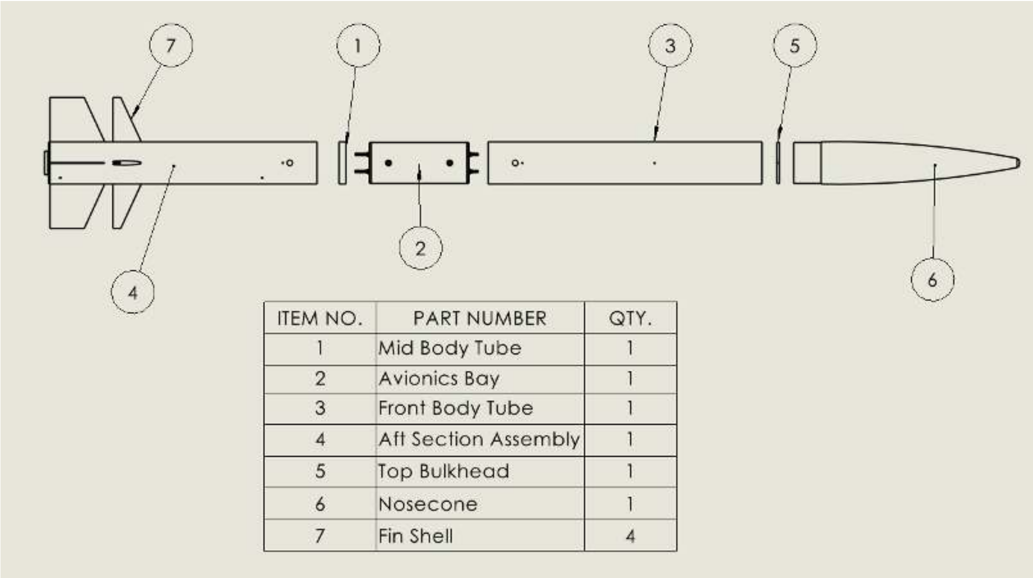


Figure 4: Full Assembly Exploded View

#### 3.1.6 Airframe

Of all the possible options for the airframe, the team decided to choose G12 fiberglass for the airframe and couplers of the rocket based on its availability, cost, RF transparency, and compressive strength. Based on the launch vehicle diameter of 6.17 in and length of 111 in, G12 fiberglass was the best option for the airframe. It is low cost and readily available, while still meeting the team's desired design requirements of RF transparency and large compressive strength. Fiberglass is an insulator, so a fiberglass airframe will be transparent to radio waves. G12 fiberglass has a compressive strength of around 22 ksi, making it suitable for use as the body tube of the rocket, as demonstrated by the calculation using a maximum thrust force of 300 lb.

$$\sigma = \frac{F}{A}$$

$$\sigma = \frac{300lb}{\frac{\pi}{4} \times (6.17in - 6.0in)^2}$$

$$\sigma = 13.22ksi < 22ksi$$

A 6.17 in diameter body tube allows ample room for the avionics, payload, and recovery systems, while providing easy access to the interior of the rocket. The figures listed below detail cross-sectional assembly drawings of each individual section of the rocket, excluding the nose cone, cameras, and fasteners. Fig. 5 displays the forward body tube with the payload bay model, forward bulkhead, and main parachute simplified model.

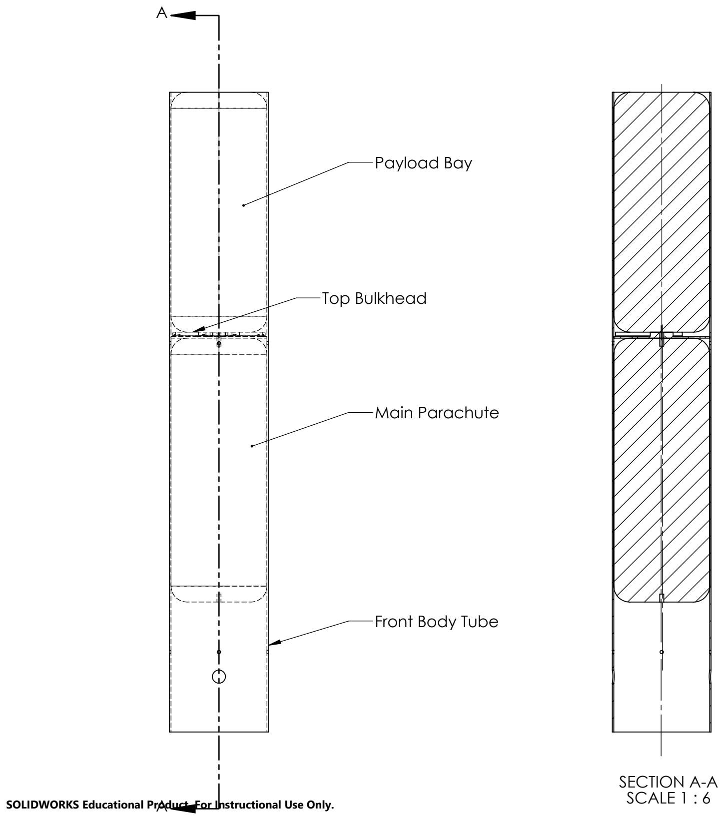


Figure 5: Forward Body Tube Sectional View

Fig. 6 displays the mid bulkhead, mid body tube, avionics coupler, avionics bay board, lead screws, flange nuts, and aft bulkhead.

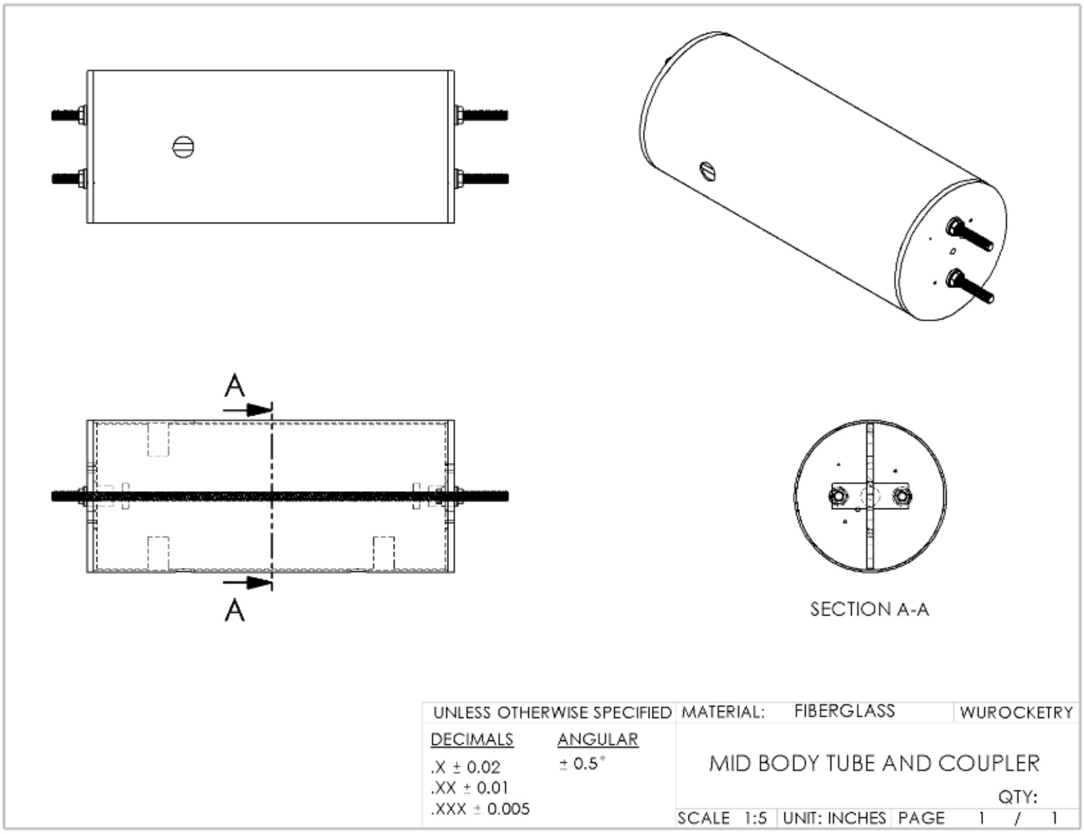


Figure 6: Mid Body Tube and Coupler Sectional View

Fig. 7 displays the drogue parachute model, aft body tube, motor tube, motor retention, centering rings, fin cores, and fin shells.

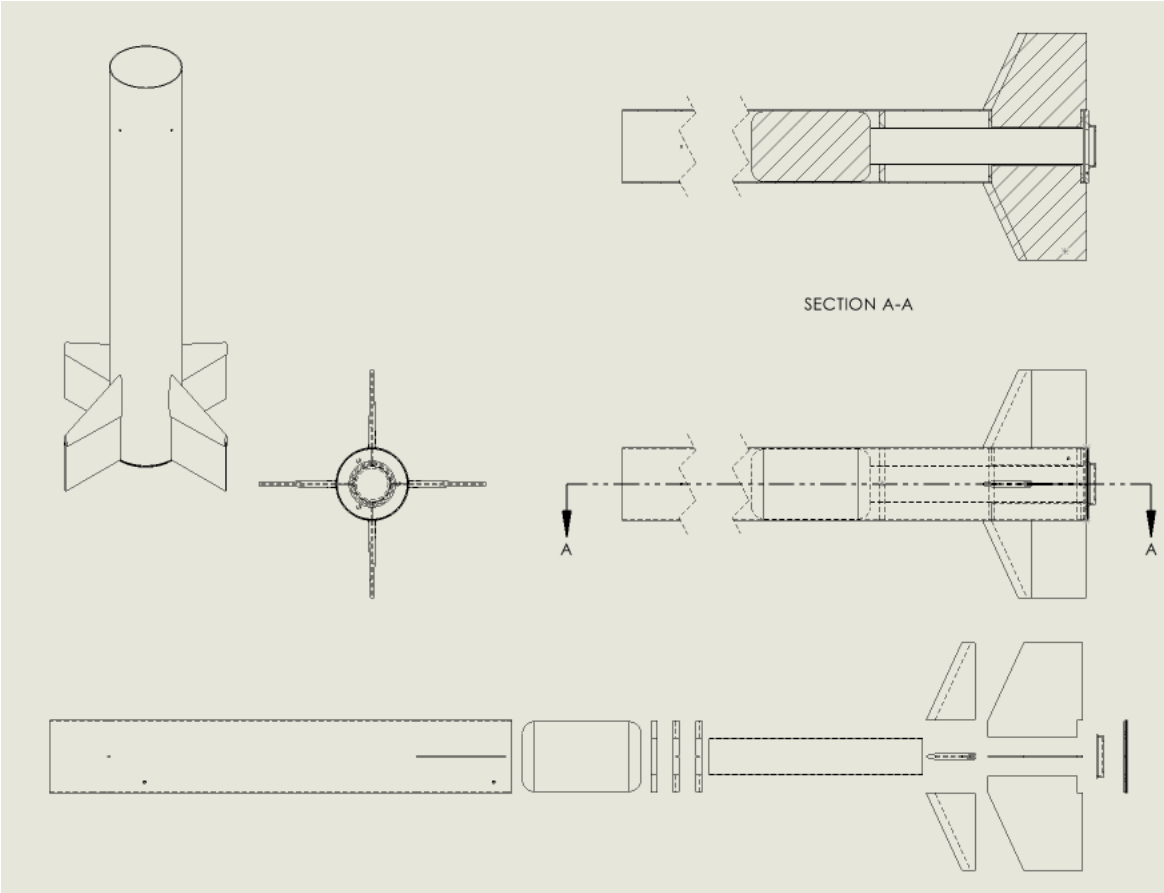


Figure 7: Aft Assembly Drawing and Sectional View

### 3.1.7 Bulkheads

The rocket will have three bulkheads. The mid and aft bulkhead form the forward and aft sides of the avionics bay. The forward bulkhead sits aft of the payload bay towards the nose cone of the rocket. Bulkheads support the loads that the rocket undergoes during flight and transfer the loads to the airframe. Each bulkhead needs a central 1/4 in hole to support an eye bolt, which connects the rocket section to the parachute. Additionally, the forward bulkhead requires four equally spaced 6-32 screw holes around the edge of the bulkhead to be fastened to the body tube. The mid and aft bulkheads have a 1/8 in lip that allows for them to rest on each end of the coupler tube and transfer perpendicular forces to the body tube. Additionally, the mid and aft bulkheads need two 3/8 in through holes for the avionics bay spacers that serve to hold the avionics coupler together. The mid and aft bulkheads will also have two #6-32 screw holes for the black powder charges as well as a 3/16 in hole for the wiring for the black powder igniters. There will be an additional 1/8 in hole in both the mid and aft bulkhead to facilitate measuring the air pressure in the parachute compartments with a pressure transducer.

The team estimates that the snatch force from the opening of the main parachute to have an approximate magnitude of 11488 N. Taking into account a 1.5x factor of safety, the forward bulkhead and mid bulkhead, which are directly attached to the main parachute, must withstand a force of 17232 N acting though the centered eye bolt. Because this force is transferred across the avionics bay through the two lead screws, this 17232 N force also acts on the bottom bulkhead's two 3/8 in holes. The bulkhead design was evaluated with SolidWorks Finite Element Analyses (FEAs), allowing for the comparison of the performance of multiple materials. The snatch force is applied over a circular area surrounding the eye bolt and lead screw holes because the snatch force is distributed over the area in contact with the nut's integrated washer. Specifically, for the middle bulkhead, the snatch force is applied around the eye bolt hole because the main parachute connects to that eye bolt. For the aft bulkhead, the snatch force is applied around the two lead screw holes because the bulkhead is constrained by them. The normal and frictional forces applied to the bulkheads by their respective body tubes were also taken into account in this study. Comparing Delrin, 6061 Aluminum, and 7075 Aluminum with this method shows that 6061 Aluminum is the best choice. Because the bulkhead needs to be used multiple times, they could not have permanent plastic deformation. Because of this, each material's yield strength was used to evaluate its suitability for the application. Generally, Delrin was not chosen because a large fraction of the bulkhead's volume had a stress that was greater than Delrin's yield strength, indicating that a bulkhead made of Delrin would plastically deform. Figure 8 is the result of the SolidWorks FEA that only shows the portion of the volume where the stress is greater than the yield stress.

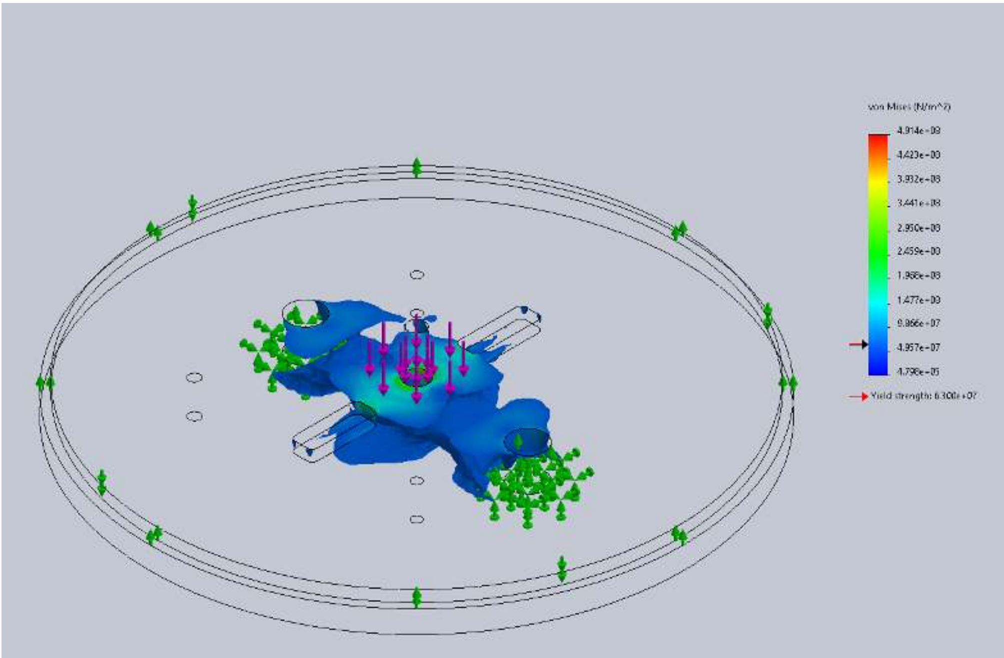


Figure 8: Delrin Mid Bulkhead FEA Result Iso Clip

In comparison, Aluminum 7075 has no significant volume where the stress is greater than the yield stress. Figure 9 shows the result of the SolidWorks FEA that only shows the portion of the volume where the stress is greater than the yield stress.

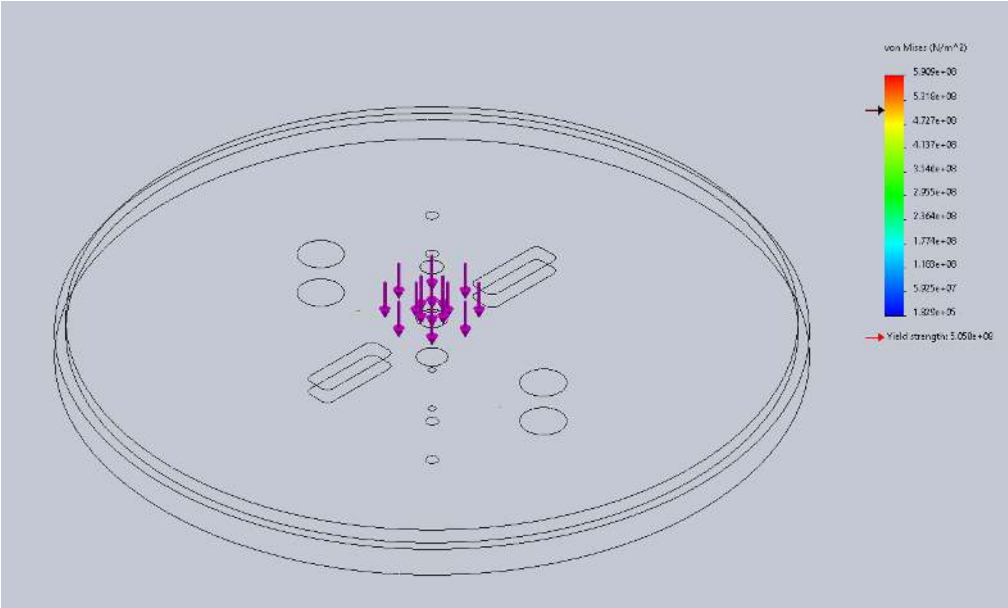


Figure 9: Aluminum 7075 Mid Bulkhead FEA Result Iso Clip

Finally, Aluminum 6061 has a small area where the stress is greater than the yield stress, but this is likely caused by the discontinuous boundary conditions imposed in the simulation rather than being a physical phenomenon. As an approximation for the nut, the geometry around the lead screw holes is fixed in space, causing its curvature to be fixed flat. As the bulkhead deflects under the applied load, the curvature right next to this boundary condition will be very high in order to match this deflection. This very high curvature turns into an apparent stress concentration. In actual usage, the geometry in contact with the nut is not truly fixed, so this stress concentration will not happen to such a high degree. This will be verified with testing as described in the testing section. Figure 10 shows the result of the Soldiworks FEA that only shows the portion of the volume where the stress is greater than the yield stress.

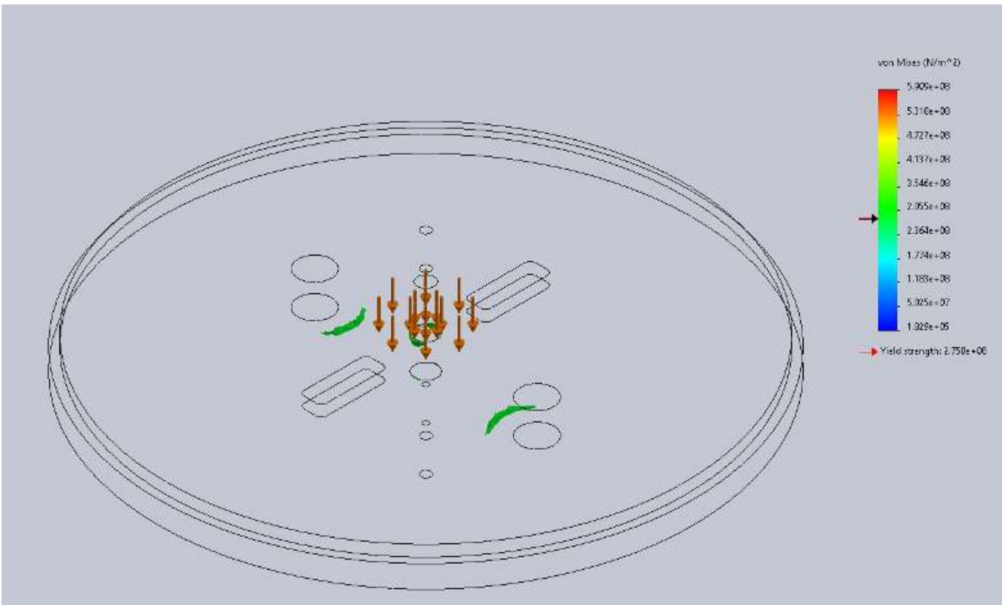


Figure 10: Aluminum 6061 Mid Bulkhead FEA Result Iso Clip

The Structures subteam conducted similar analysis for the forward and aft bulkheads and obtained similar results. Therefore, both 7075 and 6061 Aluminum are feasible options for the bulkheads. The team chose 6061 Aluminum for all three bulkheads because it is cheaper and lighter than 7075 Aluminum.

Figures 11 through 13 show the technical drawings of the bulkheads.

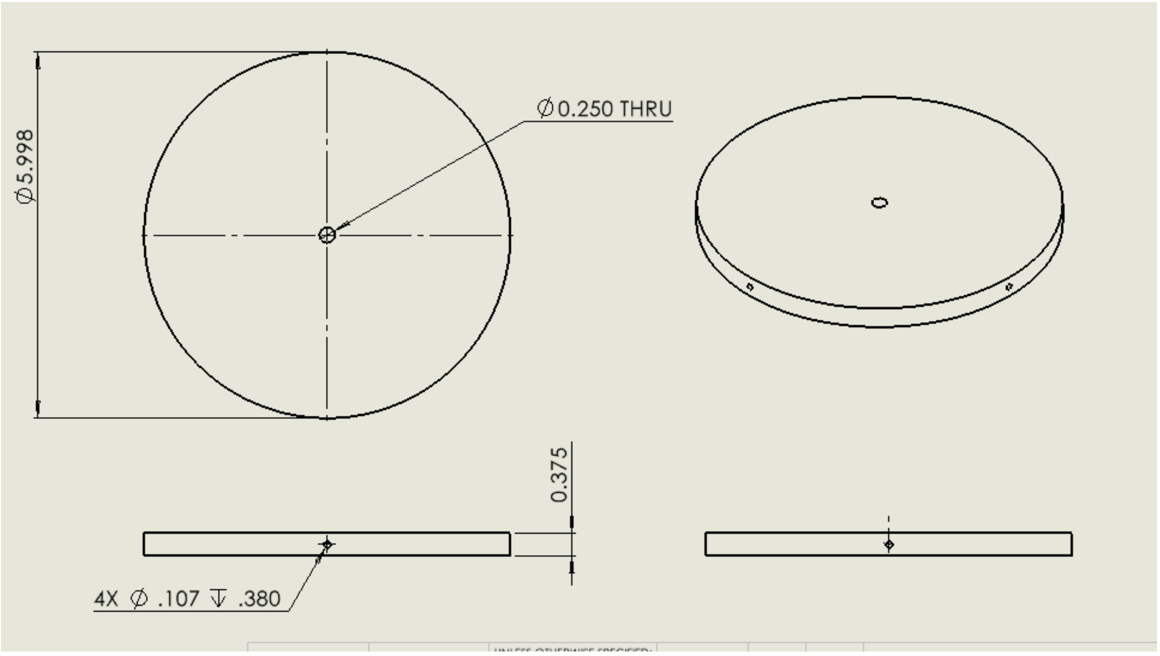


Figure 11: Forward Bulkhead Drawing

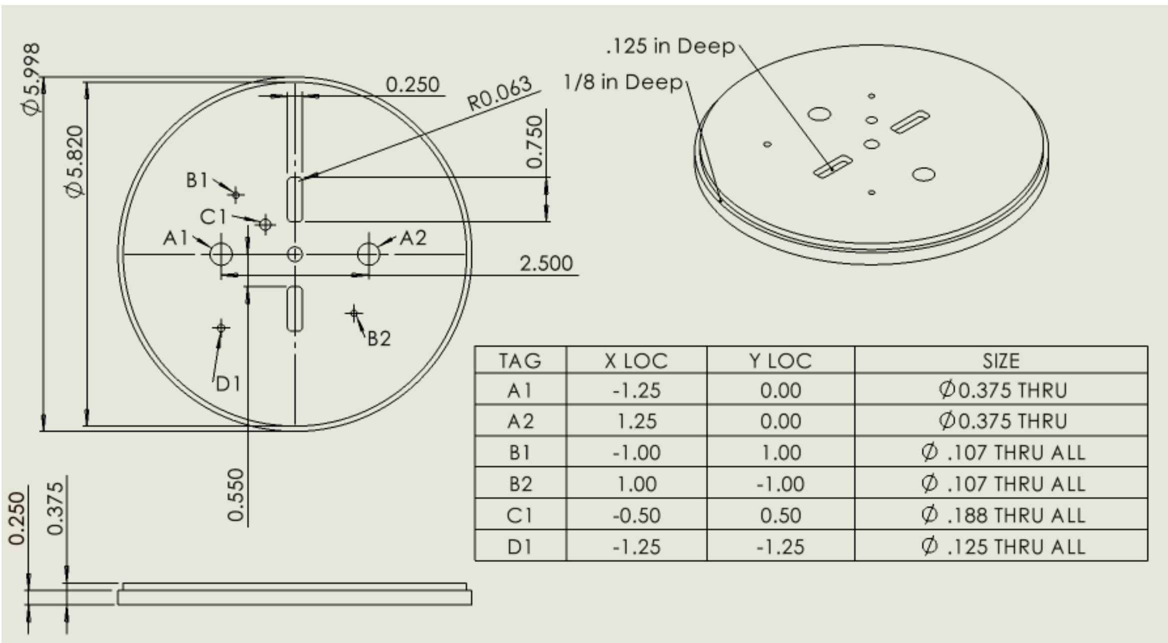


Figure 12: Mid Bulkhead Drawing

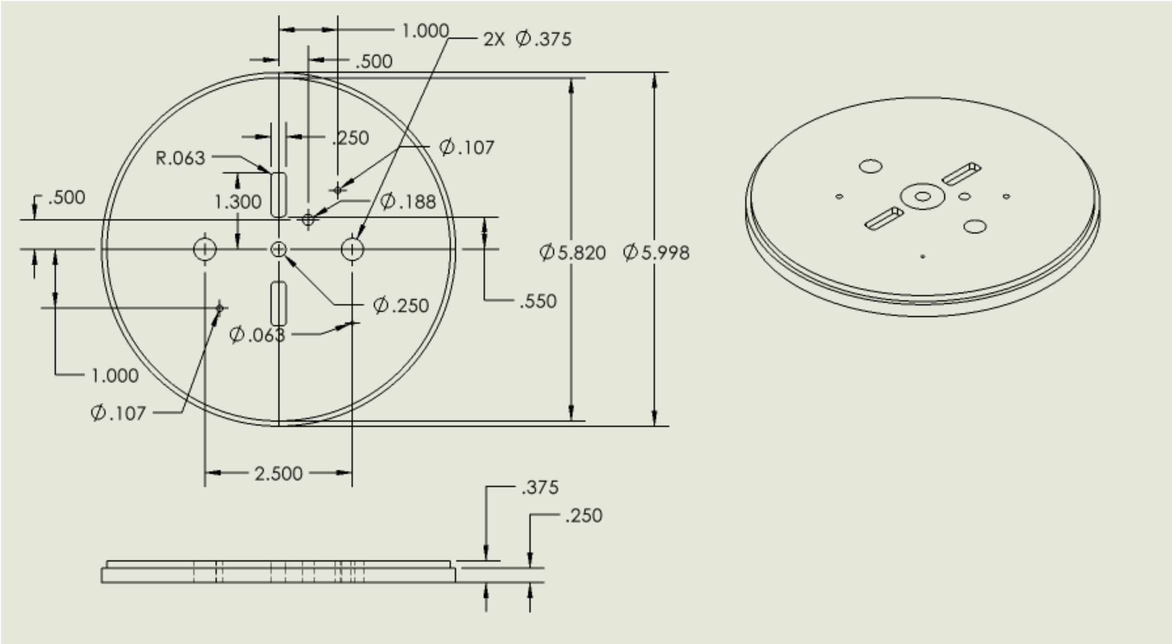


Figure 13: Aft Bulkhead Drawing

### 3.1.8 Nose Cone

The nose cone keeps the balance of the rocket in check, and with the right shape, it could greatly decrease the drag force effect on the rocket. The Structures subteam considered using a tangent ogive, elliptical, parabolic, and Von-Karman shaped nose cone. The 5:1 elliptical nose cone was chosen for its aerodynamics and lower drag force.

For materials, the Structures team was between fiberglass, plastic, and carbon fiber. The three materials were ranked based off of strength to weight ratio, availability, and RF transparency. Plastic nosecones are light but lack strength and are not widely available. On the other hand, carbon fiber has an advantageous strength-to-weight ratio, but it is expensive, difficult to find, and not RF transparent. G12 fiberglass was picked for its RF transparency, high strength-to-weight ratio, and ease of access. Fig. 14 displays a dimensional drawing of the 5:1 elliptical nose cone chosen for this year's launch vehicle with a 3.1 in shoulder attached.

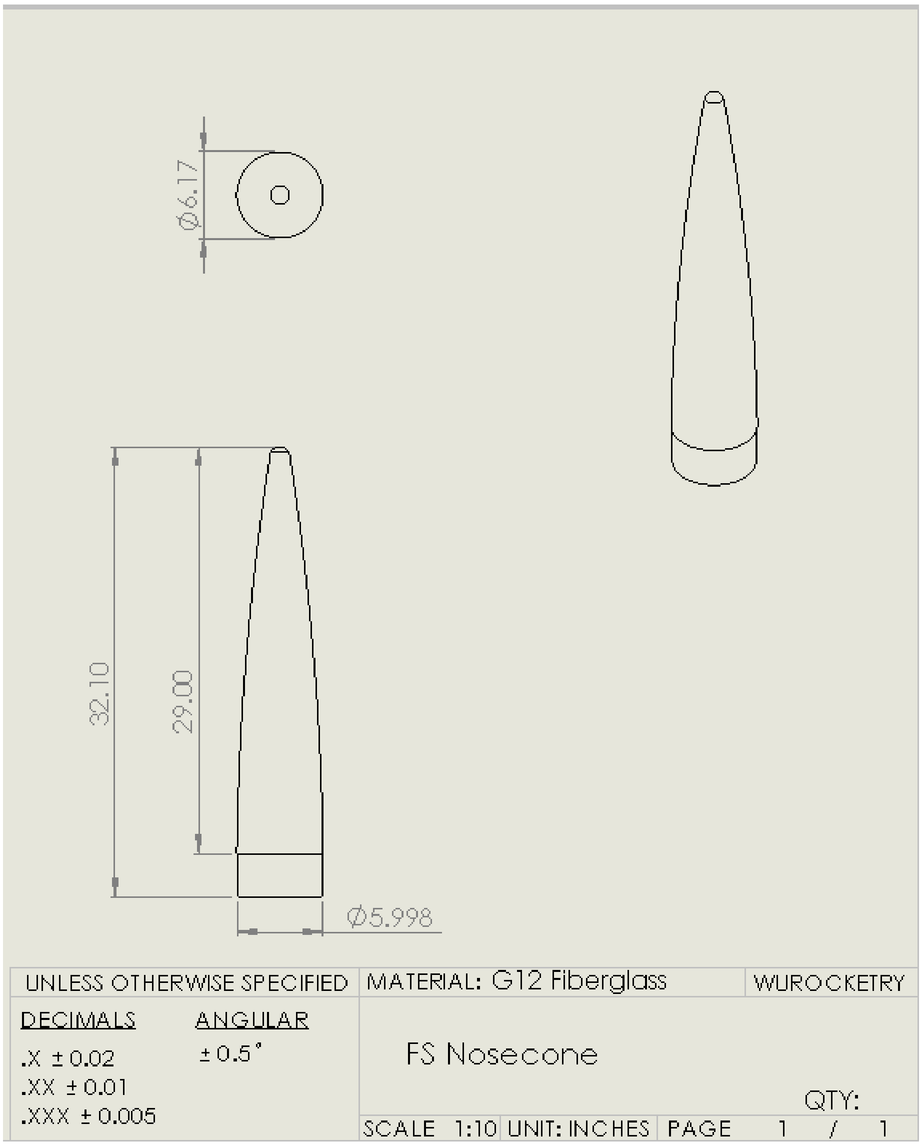


Figure 14: Nose Cone Dimensional Drawing

#### 3.1.9 Fins

Fins are used to increase the rocket's stability by bringing the rocket's center of pressure lower to the base of the rocket. Although the introduction of fins adds drag to the launch vehicle, the team designed NACA 0012 airfoil fin shells to decrease some of the drag effects and improve the rocket's aerodynamics. The Structures subteam selected materials and designs that would minimize these drag effects.

The number of fins greatly determines the stability of the rocket, but a higher number of fins could unnecessarily increase the weight and drag of the rocket. For the highest stability-to-weight ratio, the team decided to use 4 fins placed 90 degrees apart. This spacing made the fin slots easy to manufacture on a vertical mill.

The team analyzed the use of removable and non-removable fins. Removable fins allow the team to experiment with different shapes and materials. Since the Structures subteam prioritizes structural integrity, they decided a non-removable fin would be stronger, epoxying a solid G10 fiberglass clipped delta fin core to two centering rings inside the aft body tube. The team found that the square cross-section was decreasing the rocket's aerodynamics due to the increase of drag. With this flaw in mind, the Structures subteam developed airfoil shaped fin shells that would be superglued to the leading edge of the fin.

For the fin shells, the team used PLA, a material that is exceptionally stiff with a flexural strength of 103 MPa. Additionally, plastic is accessible and affordable to 3D print. In the event that fin shell fracture does occur, the 3D-printed components can be easily replaced. The fin core, on the other hand, must be strong and light as it cannot be replaced easily. The team chose to use G10 fiberglass for its high strength-to-weight ratio.

Figure 15 below displays a dimensional drawing of the G10 fiberglass fin cores.

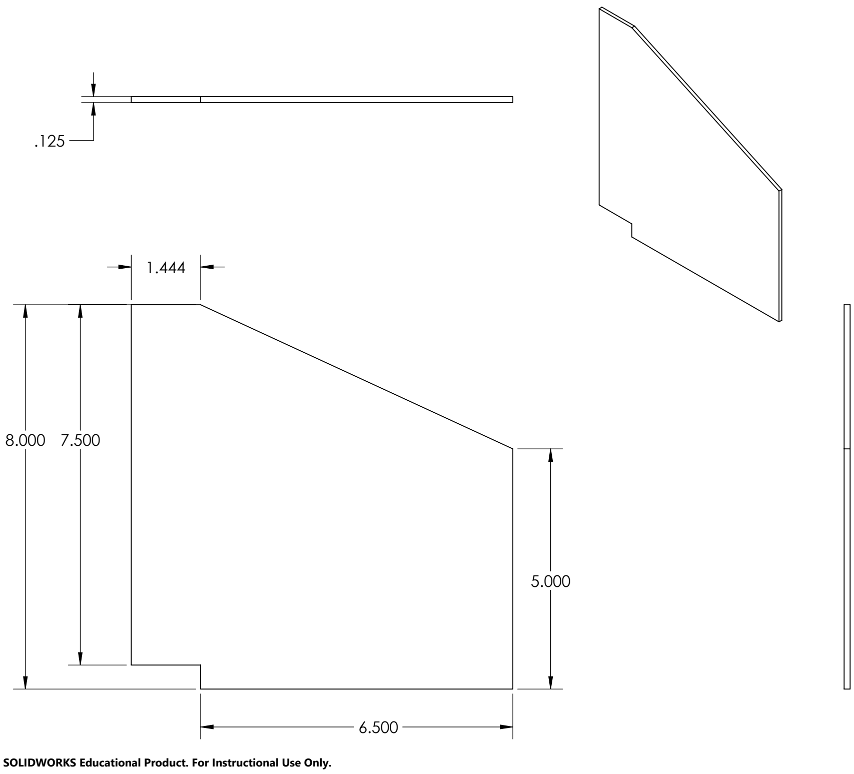


Figure 15: Fin Core Dimensional Drawing

Table 7 summarizes the clipped delta fin dimensions.

Table 7: Fin Core Dimension Summary

| | |
|---|---|
| Number of Fins | 4 |
| Root Chord | 8 in |
| Tip Chord | 5 in |
| Height | 6.5 in |
| Thickness | 0.125 in |
| Sweep Length | 3 in |
| Sweep Angle | 24.78 degrees |

Figure 16 below displays a dimensional drawing of the PLA airfoil fin shells.

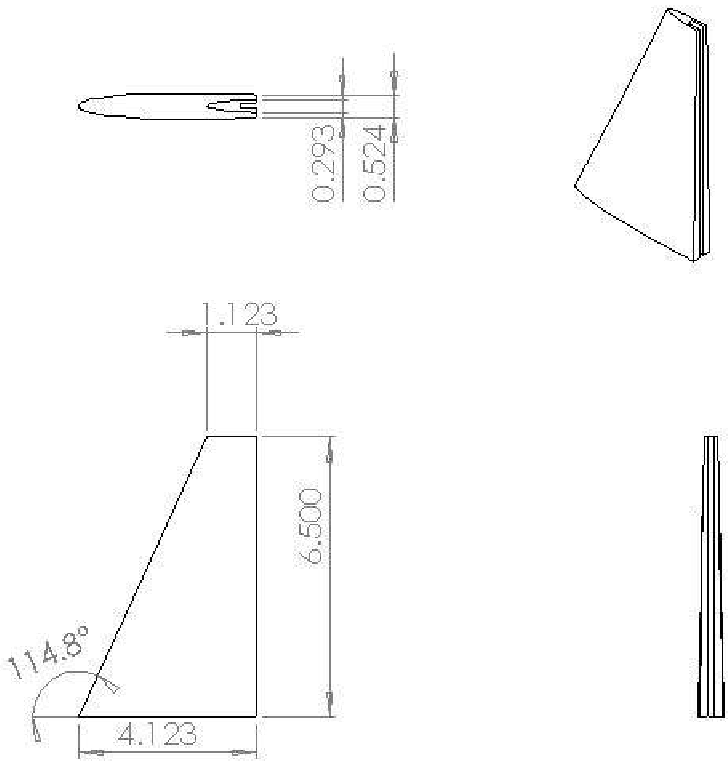


Figure 16: Fin Shell Dimensional Drawing

**Fin Flutter Calculation**
As the speed at which the rocket is going increases, so does the chance for fin flutter. To ensure the safety of the fins and rocket, the structures team calculated the minimum velocity at which the fins begin to flutter. They then applied a factor of safety of 1.5 to guarantee the likelihood of the fins fluttering being 0. Fin flutter can be calculated using the below equation.

$$V_f = 1.223\, C_s \sqrt{\frac{G}{P}} \sqrt{\left(\frac{T}{B}\right)^3 \left(\frac{2+B}{1+\lambda}\right)}$$

Figure 17: Fin Flutter Equation

Each variable represents a fin, an atmospheric, or a derived parameter. In the figure below, all these variables are defined in order to simplify calculations.

fin parameters

$$c_r = \text{root chord}, L$$
$$c_t = \text{tip chord}, L$$
$$b = \text{fin height}, L$$
$$t = \text{fin thickness}, L$$
$$G = \text{fin material shear modulus}, R$$

atmospheric parameters

$$P(h) = \text{pressure (function of altitude)}, R$$
$$C_s(h) = \text{sound speed (function of altitude)}, V$$

derived parameters

$$S = \frac{h}{2}(c_r + c_t) \text{ fin area}, L^2$$
$$\lambda = \frac{c_t}{c_r} \quad \text{fin taper ratio}$$
$$B = \frac{b^2}{S} \quad \text{aspect ratio}$$
$$T = \frac{t}{c_r} \quad \text{normalized thickness}$$

$$C_s(h) = C_{s0}\left(1 - 0.20\frac{h}{H}\right)^{1/2}$$
$$P(h) = P_0\left(1 - 0.190\frac{h}{H}\right)^{5.256}$$

Figure 18: Fin Flutter Variable Definition

Starting with the derived parameters, the surface area of the fins can be found using the root cord, tip chord, and the height of the fins.

$$S = \frac{C_r + C_t}{2}h = \frac{8+5}{2}6.5 = 42.25\ in$$

Then the fin taper ratio is calculated.

$$\lambda = \frac{C_t}{C_r} = \frac{5}{8} = 0.625$$

Using the surface area the aspect ratio is calculated.

$$B = \frac{b^2}{S} = \frac{(6.5)^2}{42.25} = 1$$

Then the normalized thickness is found using the fin core thickness

$$T = \frac{t}{C_r} = \frac{0.125}{8} = 0.01562$$

The pressure and speed of sound is solved for the respective altitude of 1141.5 ft (the height at which maximum velocity is achieved). The pressure and speed of sound at sea level is 2116.2 pft and 1100 ft/s respectively.

$$C_s(h) = C_{s0}\left(1 - 0.2\left(\frac{1141.5}{26500}\right)\right)^{\frac{1}{2}} = \qquad P(h) = P_0\left(1 - 0.19\left(\frac{1141.5}{26500}\right)\right)^{5.256} =$$

$$(1100)\left(1 - 0.2\left(\frac{1141.5}{26500}\right)\right)^{\frac{1}{2}} = 1095.25 \quad (2116.2)\left(1 - 0.19\left(\frac{1141.5}{26500}\right)\right)^{5.256} = 2026.73$$

Using the values for Young's modulus (E) and Poisson's ratio (v) of G10 fiberglass (the material used for the fin core), the Shear Modulus is found (G). E is 2,000,000 psi and v is 0.12.

$$G = \frac{E}{2(1+v)} = \frac{2000000}{2(1+0.12)} = 892857.14\, psi$$

Plugging in all the values into the fin flutter equation in Fig. 17

$$v_f = 1.223(1095.25)\sqrt{\frac{892857.14 \cdot 144}{2026.73}}$$
$$\left(\sqrt{\left(\frac{0.01562}{1}\right)^3\left(\frac{2+1}{1+0.625}\right)}\right) = 894.89\,\frac{ft}{s}$$

The structures subteam determined a factor of safety above 1.5 is sufficient in order to guarantee the low likelihood of fin flutter. Using the ratio of the fin flutter velocity (894.89 ft/s) and the current max velocity (580 ft/s), the number comes out to be 1.54, which is above the factor of safety.

#### 3.1.10 Stability

Using OpenRocket as the main software, the structures subteam was able to calculate the rocket's stability, which is determined the center of pressure (CP), the center of gravity (CG), and the rocket diameter. Stability is a high priority as it keeps the rocket following a correct flight path, ensuring the safety of the rocket components and the accuracy of apogee calculations. Due to the importance of stability, this section will focus on double-checking the OpenRocket calculations by hand, seeing if the software gives a reasonable number for stability.

Figure 19 below shows a stability vs time simulation created by OpenRocket. This helps the team visualize the stability during the launch.

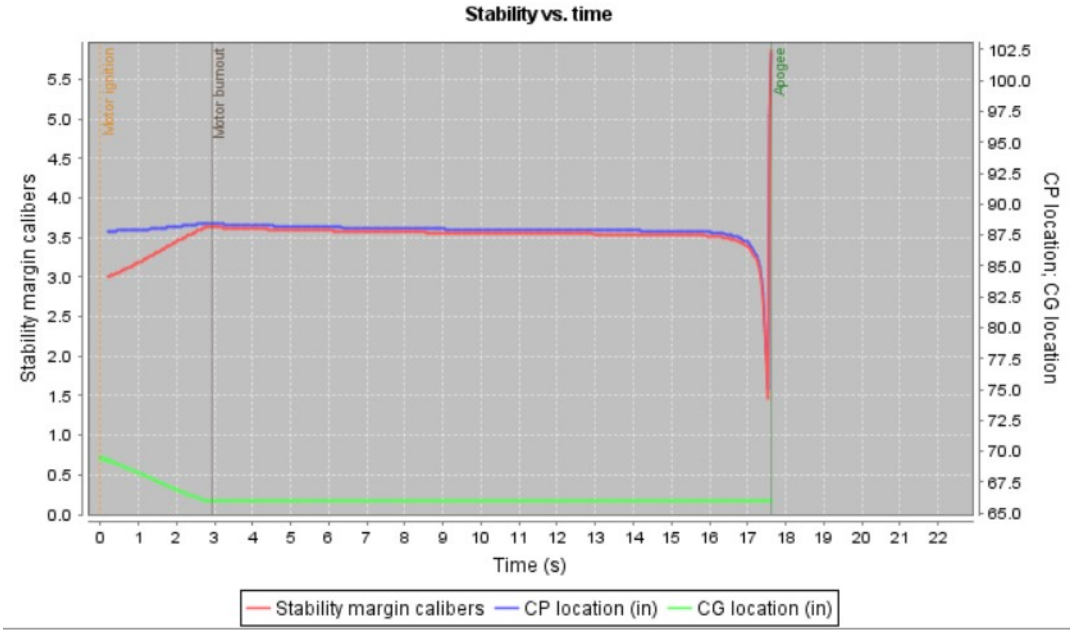


Figure 19: Open Rocket Vehicle Stability with Vertical Take off and 0 mph Wind

Figures 20-21 display the OpenRocket stability of the vehicle with and without a motor. Table 22 summarizes the OpenRocket CP, CG, and stability.

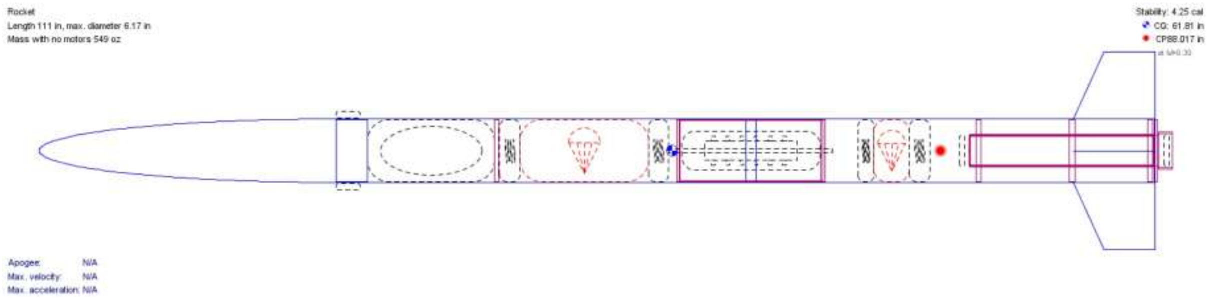


Figure 20: Open Rocket Vehicle without Motor

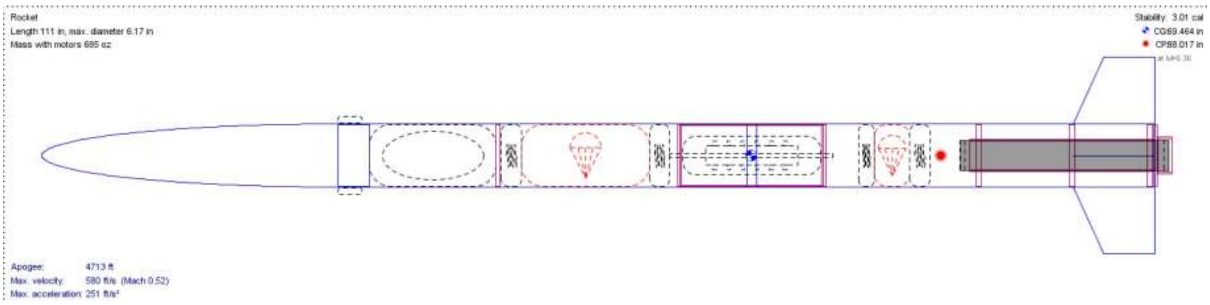


Figure 21: Open Rocket Vehicle with Motor

| | Center of Pressure from the tip of the rocket (in) | Center of Gravity from the tip of the rocket (in) | Stability (cal) |
|---|---|---|---|
| With Motor | 88.017 | 69.464 | 3.01 |
| Without Motor | 88.017 | 61.81 | 4.25 |

Figure 22: Open Rocket Vehicle with Motor

The structures subteam calculated the center of pressure using the Barrowman equations. An equation to find the center of gravity is provided but the final calculations for the center of gravity are calculated by OpenRocket due to the exact accuracy of the center of gravity and weights of all components. Figures 23-24 display the equations used along with variable definitions.

$$(C_N)_F = \left[1+\frac{R}{S+R}\right]\left[\frac{4N\left(\frac{S}{d}\right)^2}{1+\sqrt{1+\left(\frac{2L_F}{C_R+C_T}\right)^2}}\right] \longrightarrow X_F = X_B + \frac{X_R}{3}\frac{(C_R+2C_T)}{(C_R+C_T)} + \frac{1}{6}\left[(C_R+C_T) - \frac{(C_R C_T)}{(C_R+C_T)}\right]$$

$$CP\ Distance = \frac{\left(\left(C_N\right)_N\right)\left(X_N\right) + \left(\left(C_N\right)_F\right)\left(X_F\right)}{\left(\left(C_N\right)_N\right) + \left(\left(C_N\right)_F\right)}$$

$$CG\ Distance = \frac{D_F W_F + D_M W_M + D_A W_A}{W}$$

Figure 23: Stability Equations

$L_N$ = length of nose

$d$ = diameter at base of nose

$C_R$ = fin root chord

$C_T$ = fin tip chord

$S$ = fin semispan

$L_F$ = length of fin mid-chord line

$R$ = radius of body at aft end

$X_R$ = distance between fin root leading edge and fin tip leading edge parallel to body

$X_B$ = distance from nose tip to fin root chord leading edge

$N$ = number of fins

$X_N$ = $0.446(L_N)$

$(C_N)_N$ = 2

$D_M$ = distance to mid section centroid from the tip of the nose cone

$D_A$ = distance to aft section centroid from the tip of the nose cone

$D_F$ = distance to forward section centroid from the tip of the nose cone

$W_A$ = weight of aft section

$W_F$ = weight of forward section

$W_M$ = weight of mid section

$W$ = total weight

Figure 24: Stability Variable Definitions

First, the fin coefficients are calculated in the below figure 25:

$$(C_N)_F = \left(1 + \frac{3}{3+6.5}\right)\left(\frac{4(4)\left(\frac{6.5}{6}\right)^2}{1+\sqrt{1+\left(\frac{2\cdot 6.67}{5+8}\right)^2}}\right) = 10.156$$

$$X_F = (101) + \left(\frac{3}{3}\right)\left(\frac{8+(5\cdot 2)}{8+5}\right) + \frac{1}{6}\left((8+5) - \left(\frac{8\cdot 5}{8+5}\right)\right) = 104.038$$

Figure 25: Fin Coefficients Calculation

Second, the center of pressure is calculated in the below figure 26:

$$CP\ Distance = \frac{(2)(0.466\cdot 29) + (10.156)(104.038)}{(2) + (10.156)} = 89.144$$

Figure 26: Center of Pressure Calculation

Using the calculated CP and the OpenRocket CG, the team verified OpenRocket's stability in the below figure 27:

$$Stability = \frac{CP - CG}{d} = \frac{89.144 - 69.464}{6} = 3.28$$

Figure 27: Center of Pressure Calculation

The hand calculations resulted in a stability of 3.28 which is slightly above the 3.01 OpenRocket stability calculation. This is due to the higher value of the center of pressure the hand calculations computed, so the OpenRocket calculation is still reasonable. The structures subteam determined the minimum stability that would be accepted would be 2.00 based on competition requirements and both values are well above this value.

#### 3.1.11 Avionics Bay

WURocketry originally decided on using the same avionics bay for both the full-scale and sub-scale rocket. This would allow the bay to be easily transferred between the full-scale and sub-scale rocket, reducing assembly time. WURocketry decided to use a basswood board because of its light, sturdy, and avaliabliity in the size we need. Additionally, since the electronics on the bay are too expensive to duplicate, using the same bay would save expenses for the team. However, WURocketry has now decided to use two separate avionics bay boards: one for the sub-scale rocket and one for the full-scale rocket. The Avionics subteam plans to include more sensors on the full-scale rocket, which requires more room on the board than the sub-scale board would have offered. Below is the dimensional drawing of the avionics bay and the mass of each material used for the bay, along with the total avionics bay mass, excluding the electronics.

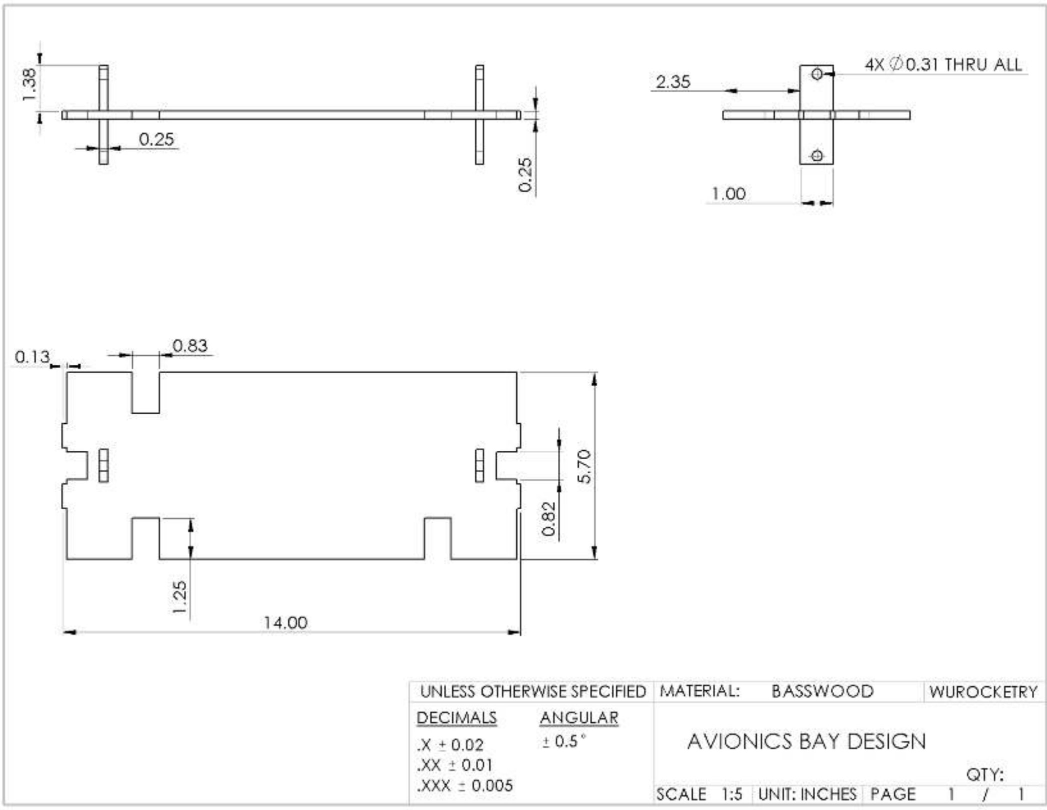


Figure 28: Dimensional Drawing of Avionics Bay

Table 8: Total Mass of Avionics Bay Without Electronics

| **Component** | **Mass (lb)** |
|---|---|
| Basswood Bay Board | 0.37 |
| Flange Nuts (x6) | 0.0174 |
| Lead Screws (x2) | 0.12 |
| Full-scale Mid Bulkhead | 0.52 |
| Full-scale Bottom Bulkhead | 0.99 |
| *Combined Full-scale Total* | 1.8874 |

When determining a design for the avionics bay, WURocketry took ease of manufacturing, cost, assembly time, reusability, and size of bay components into consideration. The team considered three designs for the avionics bay based on how the lead screws would be embedded in the bay and attached to the bulkheads. Ultimately, the team decided on a design incorporating ideas from earlier iterations. Figure 29 displays the final design, which allows the team to use both sides of the bay, is easy to manufacture, and does not interfere with any holes or slots on the bulkhead. Elevating the lead screws off the board and having them secured in holders meant they would not interfere with the bay components. Additionally, the elevated lead screws allow for the bay to be easily transferred between the full-scale and sub-scale rocket, which is what the team's primary focus was on when originally designing the avionics bay. The elevated height for the lead screws was determined using the tallest height of the bay components.

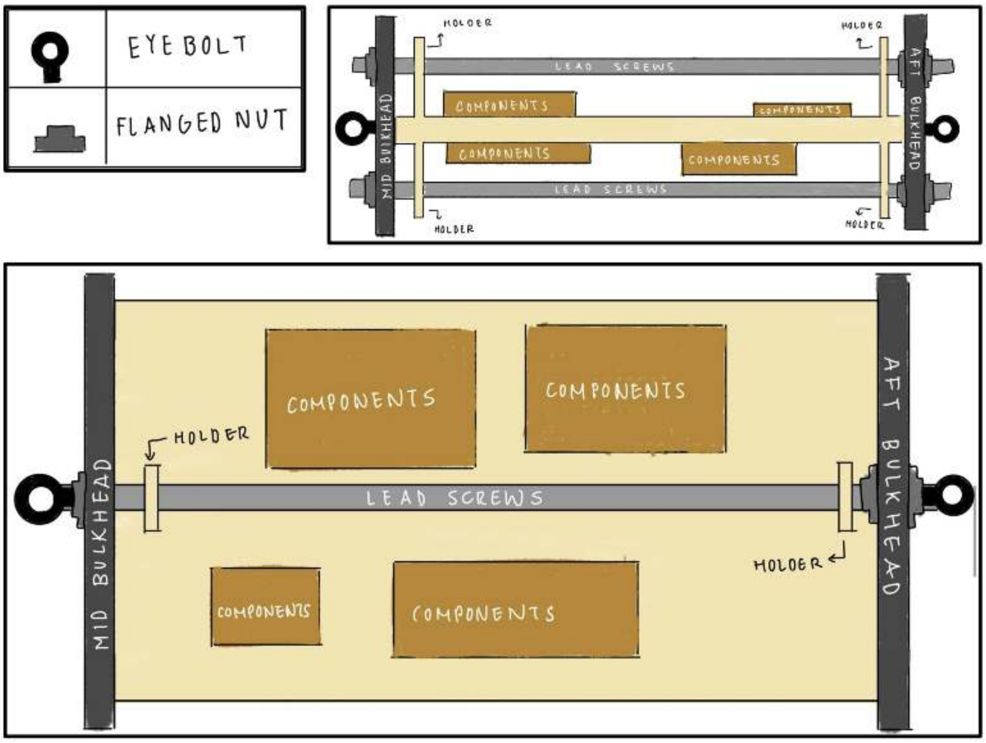


Figure 29: Using Both Sides of the Board with Elevated Lead Screws

A 14 in. coupler was chosen for the avionics bay to satisfy the NASA requirement of coupler lengths being at least two times greater than that of the diameter of the body tube. Additionally, 14 in. couplers are readily available from manufacturers. Figure 30 displays the dimensional drawing of the avionics bay assembly with the mid and aft bulkheads, lead screws, and flange nuts.

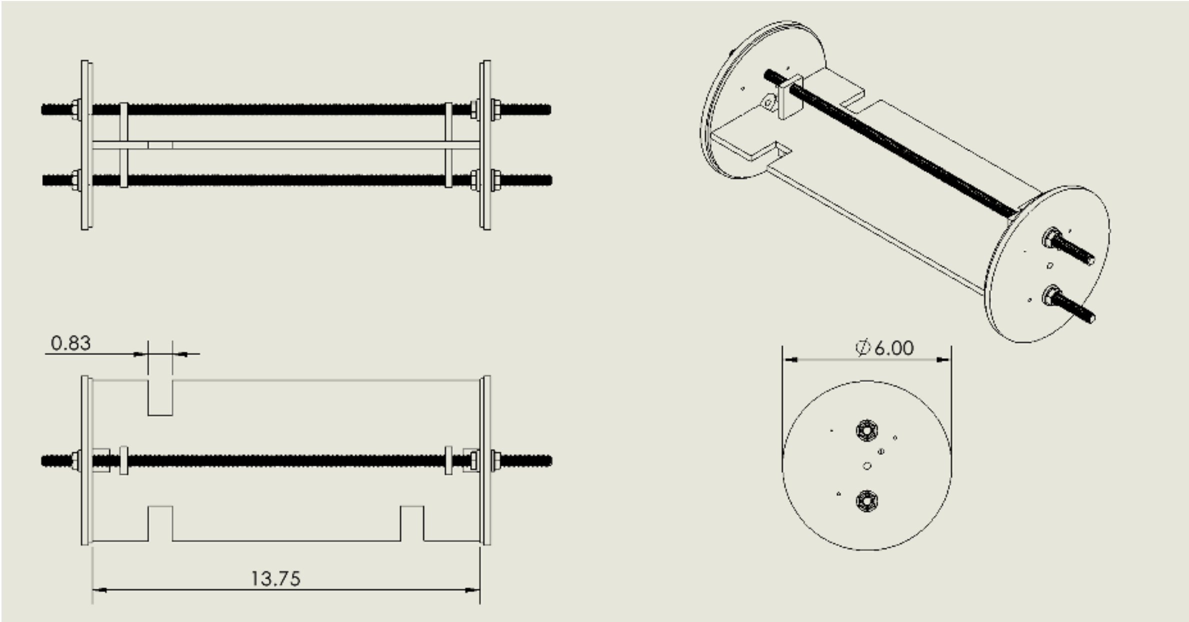


Figure 30: Full-Scale Avionics Bay Assembly

#### 3.1.12 Centering Rings

WURocketry designed three centering rings to secure the motor in place in the aft tube of the launch vehicle. They will be spaced apart to ensure that the motor's axis is collinear with that of the rocket's aft tube. The aft-most, middle, and forward centering rings will be located 0.250 in, 7.75 in, and 17.000 in from the aft face the aft body tube respectively. 3D printers will be used to manufacture the centering rings because 3D printers are easily accessible by WURocketry and the material cost for both PETG and PLA plastic are low. Additionally, PLA is lighter than PETG while both have relatively similar yield strengths.

A circular design for the PLA centering rings was selected because it would maximize contact with the motor tube's exterior as well as the interior of the rocket's aft tube. The weight of each of the centering rings is 0.15 lb. All three centering rings will be secured to the launch vehicle's aft tube with epoxy. The forward centering ring (nearer to the nose cone) is shown in Fig. 31. The aft two centering rings are differentiated from the forward centering ring by the presence of slots in which the G10 fin cores will be epoxied to the launch vehicle. These aft centering rings can be seen in Fig. 32. The aft-most centering ring will be secured to the motor's thrust plate with wood screws.

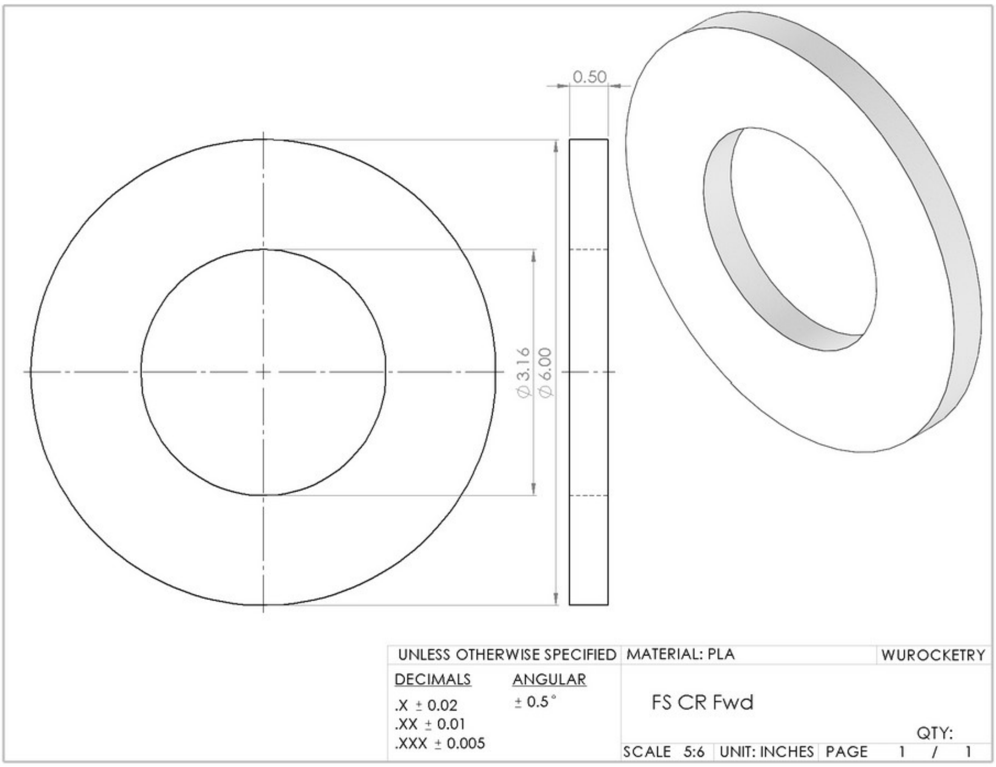


Figure 31: Forward Centering Ring

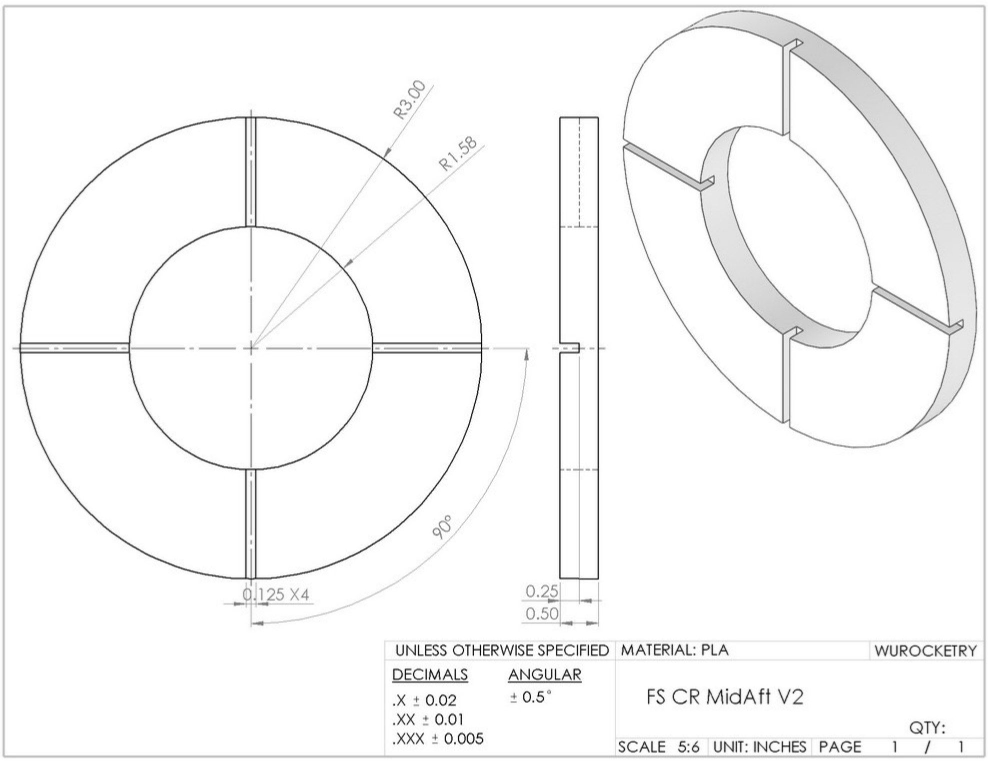


Figure 32: Aft Centering Rings

### 3.1.13 Thrust Plate

The team purchased the thrust plate for the L1390G-P motor from Apogee Components. The Structures subteam created a 3D model of the component in SolidWorks. A dimensional drawing of the thrust plate is shown in Fig. 33. WURocketry ran a Finite Element Analysis to confirm that the thrust plate would not yield under the thrust force from the motor. Fig. 34 displays the von Mises stress at various locations on the component with a deformation scale of 552.4. The team concluded that the chosen thrust plate will not yield in the presence of thrust forces from the motor.

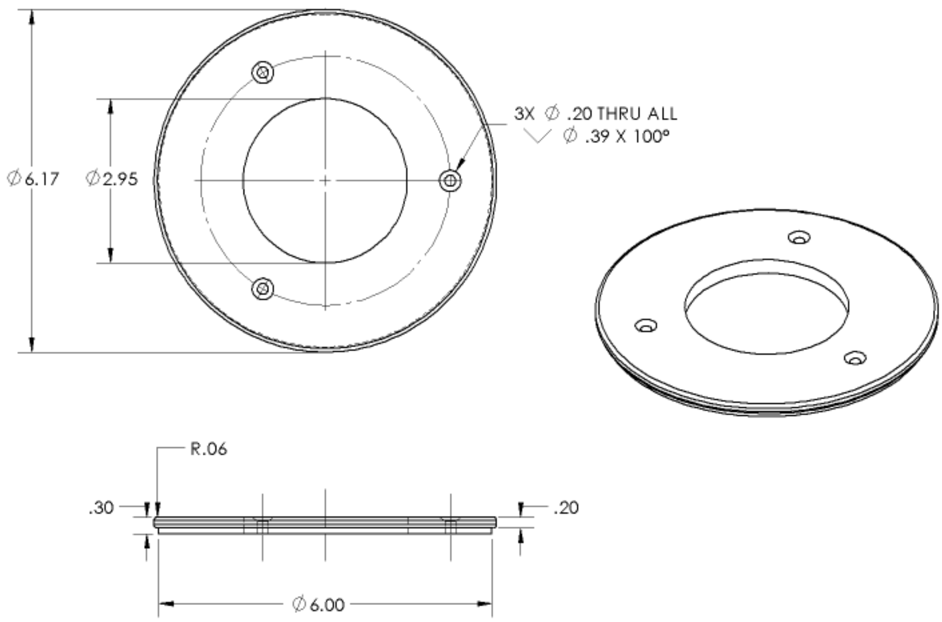


Figure 33: Dimensional Drawing of Aluminum Thrust Plate

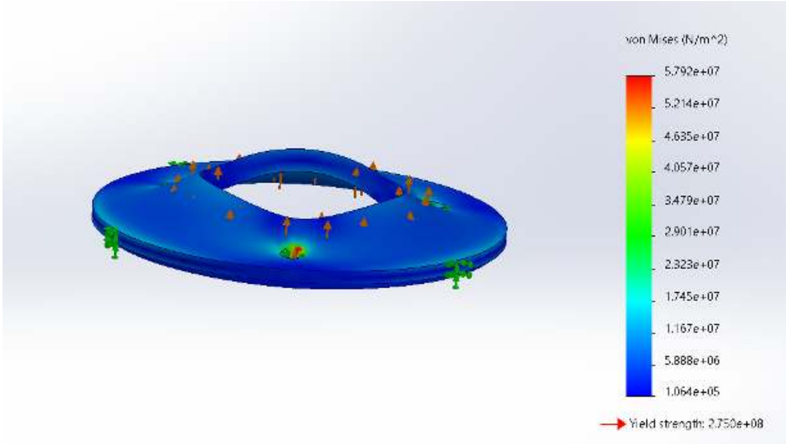


Figure 34: FEA of Aluminum Thrust Plate

#### 3.1.14 Fasteners

Two types of screws will be used for the rocket: stainless steel Phillips head screws and nylon round head slotted shear screws. Four 6-32 3/8 in Phillips head screws will be used to secure the forward bulkhead in the airframe of the rocket. The 4-40 3/16 in slotted shear screws will be used at each of the two separation points of the rocket. They will secure the forward body tube to the avionics coupler and the avionics coupler to the aft body tube until black powder charges isolate each section of the rocket.

Titanium was also considered for the bulkhead screws because it is stronger and has a higher melting point than stainless steel, but titanium costs almost $6 per 6-32 3/8 in screw, which falls outside the team's budget. Nylon was also considered for the bulkhead and ballast screws for their lightweight nature (in comparison to that of comparable metal screws) and their cost, but their tensile strength of 10000 psi (one-tenth that of the stainless steel alternative) is too low for the team's application. Nylon was chosen for the shear screws because it is lightweight and has high tensile strength for a plastic, but black powder charges will still shear them. WURocketry chose a Phillips head over a hex head screw because hex heads are more likely to strip under the stress of continual use. Additionally, the team chose button head over countersink head screws because button head screws are less likely to rip through the airframe. Furthermore, the button head screws only require drilling a simple hole while countersink head screws necessitate the drilling of a tapered hole in order to take full advantage of their more aerodynamic form. Finally, nuts and washers are placed in the avionics coupler to hold each lead screw spacer in place. WURocketry will purchase the screws, nuts, and washers from McMaster-Carr. The combined mass of every fastener on the launch vehicle is less than 0.1 lb.

Eye bolts in the rocket are used to attach recovery parachutes to the bulkheads. The 1/4"-28 stainless steel eye bolts help to absorb the stress of deploying the recovery system. WURocketry chose eye bolts over U-bolts because manufacturing a bulkhead for an eye bolt is more efficient than for a U-bolt, which requires two holes to be drilled. A singular eye bolt also occupies less space on the bulkhead and within the rocket airframe, allowing for avionics, payload, and recovery systems to fit more comfortably.

3/8"-16 stainless steel flange nuts were chosen for the rocket. The protruding rims of flange nuts make them an ideal fastener. Their washer-like bases cover more surface area, distributing the load pressure of the nut uniformly. This reduces possible damage to the attached part and decreases the likelihood of the nut loosening due to an uneven surface. In addition, the hexagonal shape of the flange nut also allows the nut to be easily tightened or loosened with a wrench.

The drawings of the Phillips head screw, nylon shear screw, eye bolt, and flange nut provided by McMaster-Carr are shown below in Figs. 35, 36, 37, and 38, respectively.

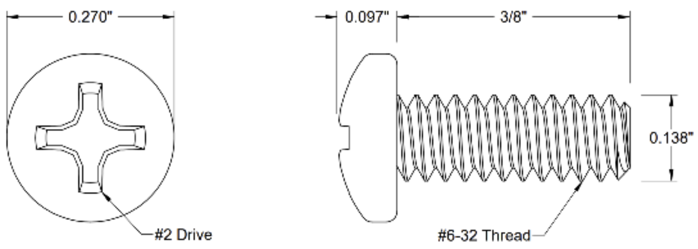


Figure 35: Phillips Head Screw

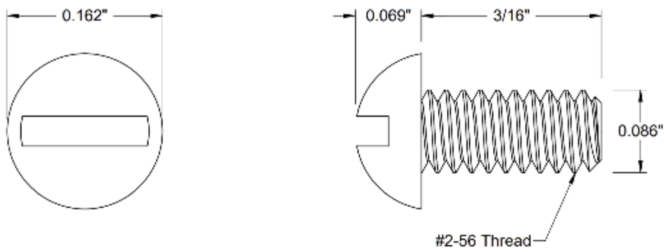


Figure 36: Nylon Shear Screw

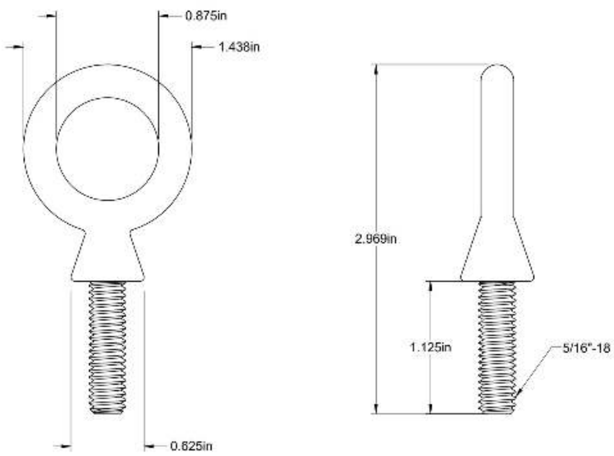


Figure 37: Eye Bolt

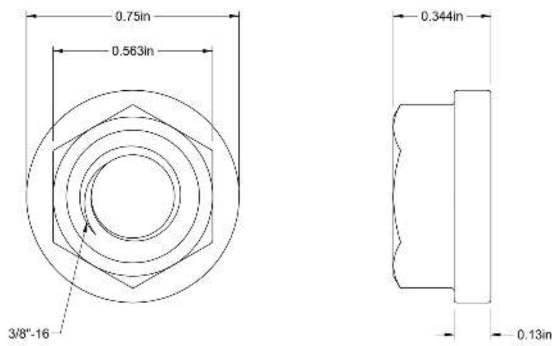


Figure 38: Flange Nut

#### 3.1.15 Cameras

WURocketry has decided to implement the addition of two Universal AstroCam HD Rocket Cameras on either side of the rocket immediately aft of the nosecone. These allow the team to clearly view the rocket and its flight for the duration of the ascent to apogee and also provide visual data for the deployment of the drogue and main parachutes. This data is vital in determining potential root causes of failures during testing and visual feedback of the impact of launch condition changes. Fig. 39 shows a dimensional drawing of the camera and its holder.

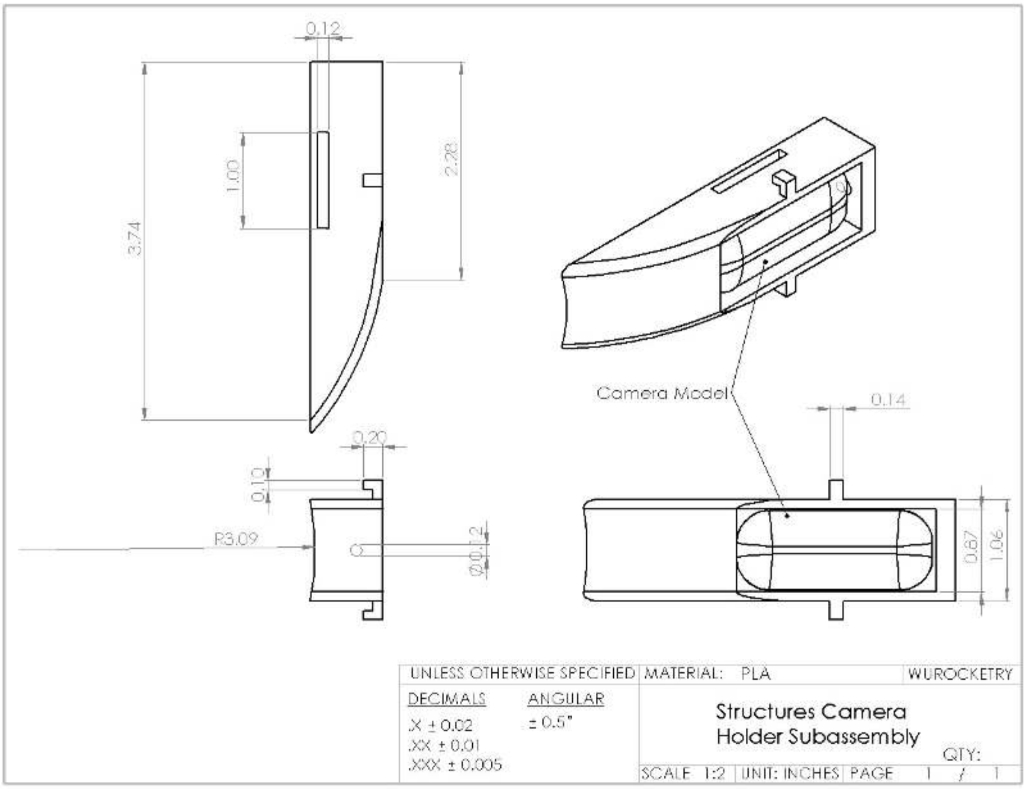


Figure 39: Dimensional Drawing of Camera Holder

### 3.1.16 Motor Selection

The motor chosen is the AeroTech L1390G-P. The L1390G motor provides an average thrust of 1,390.0 N and simulated maximum thrust of 1,649.8 N, resulting in a thrust to weight ratio of approximately 8:1. Using OpenRocket simulations, the thrust was confirmed to be sufficient to achieve an apogee of 4,650 ft with an anticipated rocket wet mass of 42.8 lbs. The rocket's stability, exit rail velocity, and maximum mach speed were also determined in OpenRocket to be 3.01 cal, 71.8 fps, and 0.52, respectively. This meets the respective minimum 2.0 cal stability, 52 fps exit velocity, and maximum 1.0 mach speed requirements. Additionally, the team chose this motor due to the 530mm length and 75mm diameter dimensions to provide sufficient packing space for the drogue parachute and shock cords. Lastly, the L1390G meets requirements of APCP propulsion, NAR/CAR/TRA certifications, and reusability.

Table 9: L1390G Motor Specifications

| | |
|---|---|
| Diameter | 75 mm |
| Length | 530 mm |
| Wet Mass | 3879 g |
| Average Thrust | 1390 N |
| Total Impulse | 3949 Ns |
| Burn Time | 2.6 s |

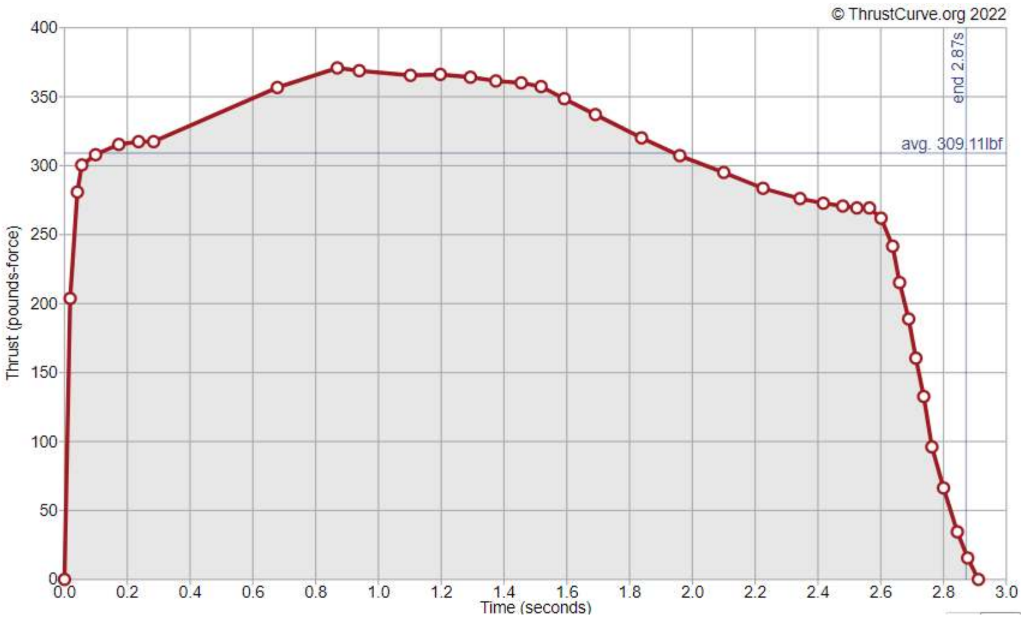


Figure 40: L1390G Thrust Curve

### 3.1.17 Motor Mounting and Retention

The L1390G-P motor has a 75 mm diameter and 530 mm length. Due to these dimensions, the motor is secured within the Aerotech RMS 75/3840 Rocket Motor Casing, with Aerotech 75 mm Forward Closure, Aft Closure, and Seal Disk. A 75 mm, 18 in long Kraft phenolic tube is used to house the motor casing and assembly within the rocket. A 6 in - 75 mm thrust plate from SC Precision centers the motor assembly within the

6 in inner diameter aft tube. Aeropack's 75 mm Flanged Retainer Ring Set secures the motor casing inside the rocket.

## 3.2 Sub-Scale Flight Results

### 3.2.1 Scaling Factors

The sub-scale launch is important in verifying the viability of the full-scale design by accurately scaling down aspects of the full-scale to match launch characteristics. The Structures subteam chose a scale factor using the body tube dimensions since the body tubes will not be manufactured by the team. The scaling factor was chosen to be around $\frac{2}{3}$ and was applied to most calculations including the length, diameter, the CG, and the CP of the sub-scale rocket. The stability of the sub-scale does not scale by $\frac{2}{3}$ with the full-scale stability because the team wanted to ensure that the sub-scale would have a higher tendency to launch straight into the air. Percent difference is also present as the subteam tried to get the values as close as possible to the predicted value, but for some cases it simply was not possible.

Table 10: Sub-Scale Scaling Factors

| **Parameter** | Full-Scale Dimensions | Sub-Scale Dimensions | Factor of $\frac{2}{3}$ | Percent Difference |
|---|---|---|---|---|
| **Length** | 111 in | 73.3 in | 74.0 in | 0.95 % |
| **Mass** | 42.8 lb | 18.3 lb | 28.5 lb | 35.78 % |
| **Diameter** | 6.17 in | 4.02 in | 4.12 in | 2.43 % |
| **CG (from tip of NC)** | 69.465 in | 46.015 in | 46.31 in | 0.64 % |
| **CP (from tip of NC)** | 88.017 in | 57.319 in | 58.70 in | 2.35 % |
| **Stability** | 3.01 cal | 2.82 cal | 2.01 cal | 40.3 % |

### 3.2.2 Flight Results - October 29th, 2022

**Launch Day Conditions and Simulation** On launch day in Ohio, IL, the average wind speed was 5 mph SW at 902 ft elevation. The latitude and longitude of Ohio is 41.5° N, 89.5° W. The temperature was 61 °F and the barometric pressure was 29.8 inHg. The sub-scale rocket was launched on a 144 in rail at a 0° angle. Figure 41 is an Open Rocket simulation of the sub-scale launch with the same input conditions.

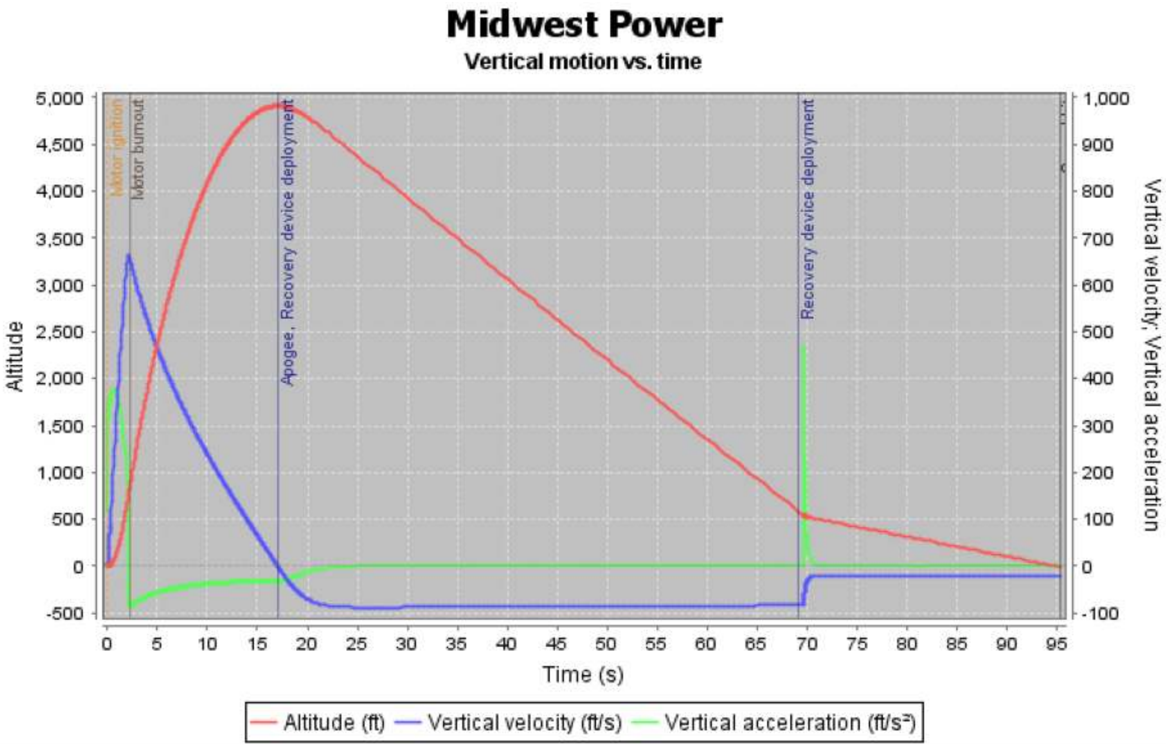


Figure 41: Sub-Scale Rocket Simulation

Additionally, the camera facing aft of the launch vehicle yielded video data of the sub-scale launch. The figures that follow (Fig. 42-43) display screenshots from the camera video during the various events of the launch and recovery.

Figure 42: 5 Seconds After Liftoff - Camera Screenshot

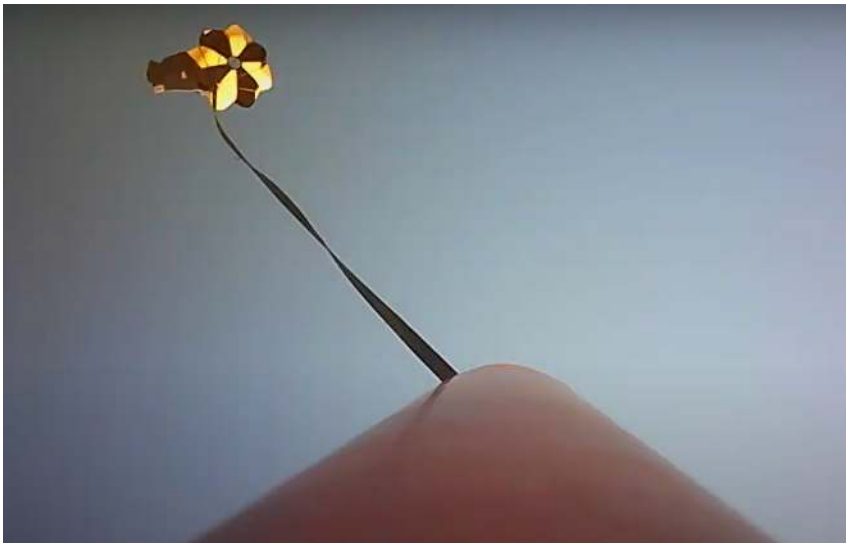

Figure 43: Drogue Parachute Deployment - Camera Screenshot

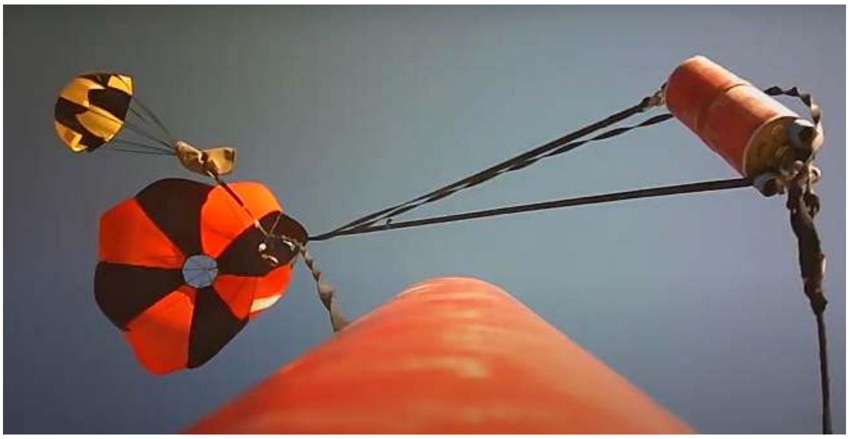

Figure 44: Main Parachute Deployment - Camera Screenshot

**Flight Data** Figure 45 displays sub-scale flight data recorded by the primary flight computer. The main apogee recorded was 4764 ft.

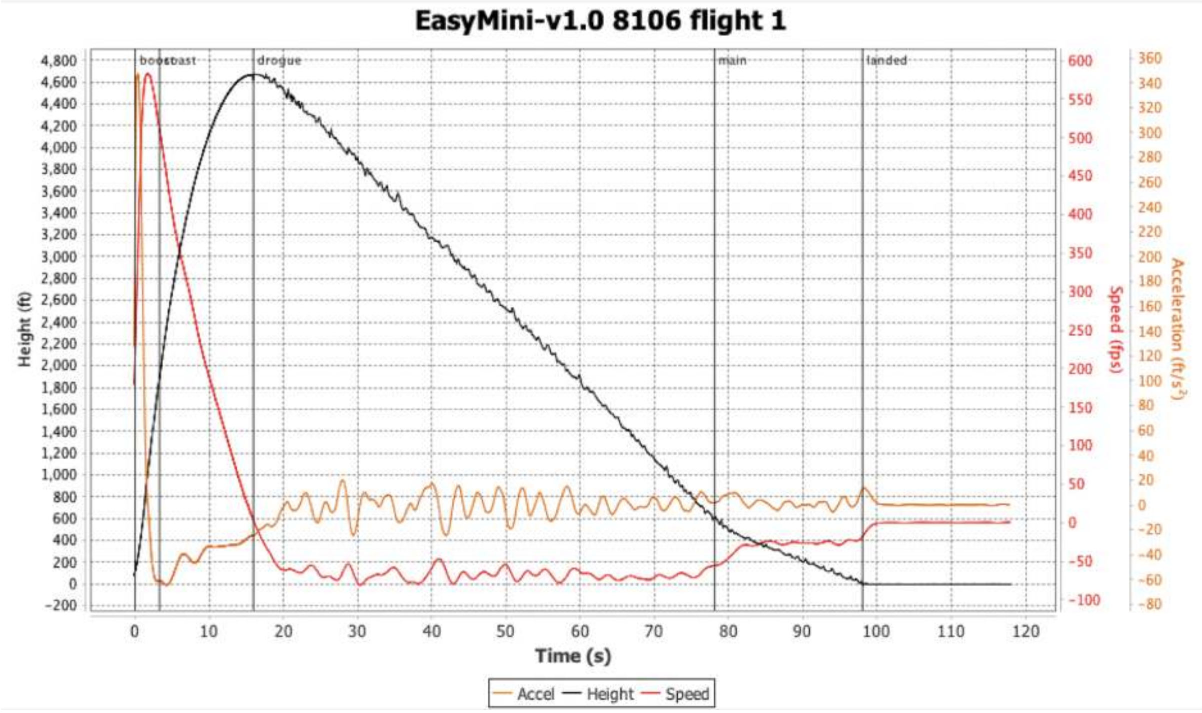


Figure 45: 10/29/2022 Sub-scale Primary Altimeter Data

Table 11: Sub-Scale Primary Altimeter Data Summary

| Vehicle Property | Simulated Value | Recorded Value | Percent Error |
|---|---|---|---|
| Maximum Velocity | 663 ft/s | 583 ft/s | 12.1% |
| Time of Maximum Velocity | 2.07 s | 2.20 s | 6.28% |
| Apogee | 4907 ft | 4764 ft | 2.91% |
| Ascent Time | 17.1 s | 15.9 s | 7.01% |
| Descent Time | 78.2 s | 82.1 s | 4.99% |

Figure 46 displays sub-scale flight data recorded by the redundant flight computer. The redundant apogee recorded was 4706 ft.

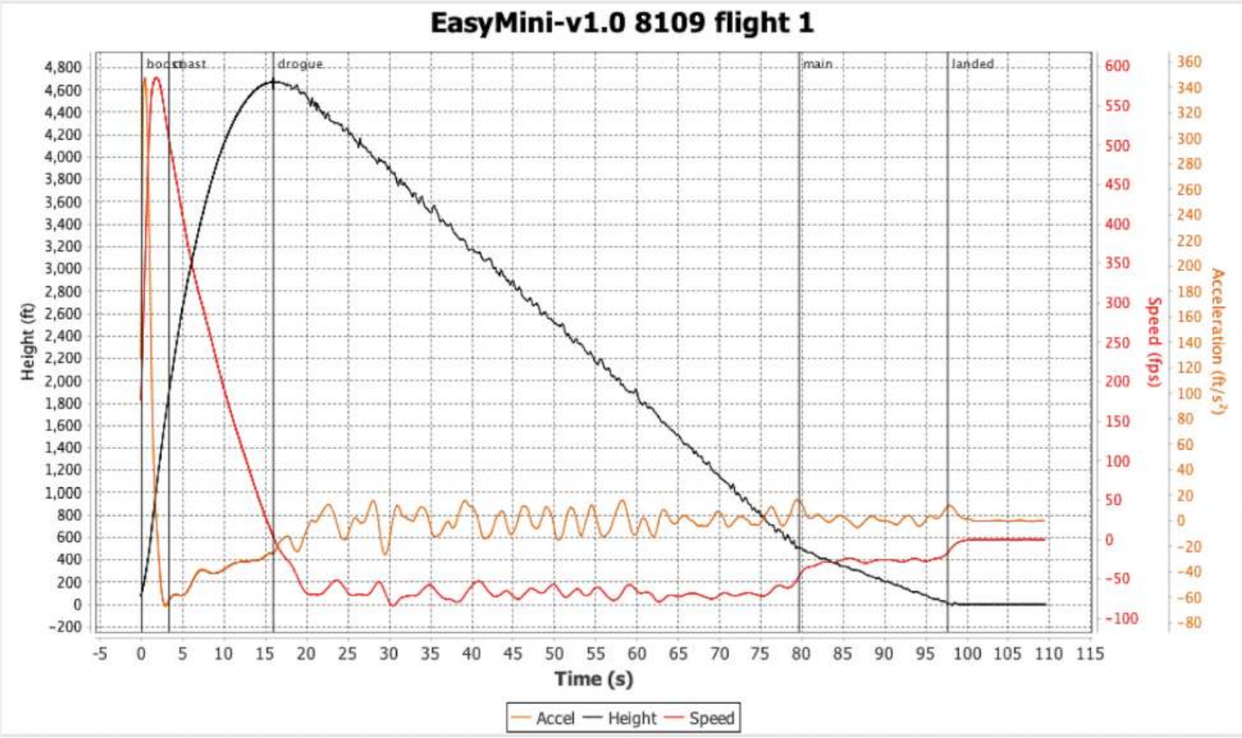


Figure 46: 10/29/2022 Sub-scale Redundant Charge Altimeter Data

Table 12: Sub-Scale Redundant Altimeter Data Summary

| Vehicle Property | Simulated Value | Recorded Value | Percent Error |
|---|---|---|---|
| Maximum Velocity | 663 ft/s | 585 ft/s | 11.8% |
| Time of Maximum Velocity | 2.07 s | 2.20 s | 6.28% |
| Apogee | 4907 ft | 4706 ft | 4.10% |
| Ascent Time | 17.1 s | 15.9 s | 7.01% |
| Descent Time | 78.2 s | 81.7 s | 4.48 % |

**Sub-Scale Flight Analysis** The sub-scale launch and flight on October 29th, 2022, was successful in verifying the team's overall structure, weight distribution, and method for calculating black powder charges. The sub-scale flight showed that the motor chosen, the Aerotech K805G, was capable of launching the rocket successfully. As the full-scale motor is using the same type of propellant, Mojave Green, this is a good indicator that the full-scale motor will function 45 properly as well. The predicted apogee of the sub-scale rocket was 4907 ft and the actual apogee recorded by the main altimeter and reported by the avionics subteam was 4,764 ft for the sub-scale launch. This is a 2.91% undershoot, and verifies the team's calculations and approach to predict apogee based on the motor specifications. One source for the undershoot is additional drag produced by the camera assembly. The camera mount was not 3D printed in time for the launch, leading to the cameras being taped onto the rocket via electrical tape. This electrical tape was not flush with the rocket body near the cameras which added unaccounted for drag, thereby decreasing the rocket's apogee. Photos of the landed sub-scale vehicle are displayed in Figs. 47 - 51.

The camera video recording allowed the team to view the separation events closely. As shown in Figure 44, the team observed the forward shock cord wrap around the avionics coupler and become twisted with the forward eyebolt after the main parachute deployment. Additionally, the drogue parachute shock cord was found to be too long or close to the main shock cord as they tangled and risked improper main parachute inflation. Despite the tangling of the shock cords with the coupler and main parachute cord, the rocket was not damaged and experienced a controlled descent.

Figure 47: All landed sections of Sub-Scale vehicle

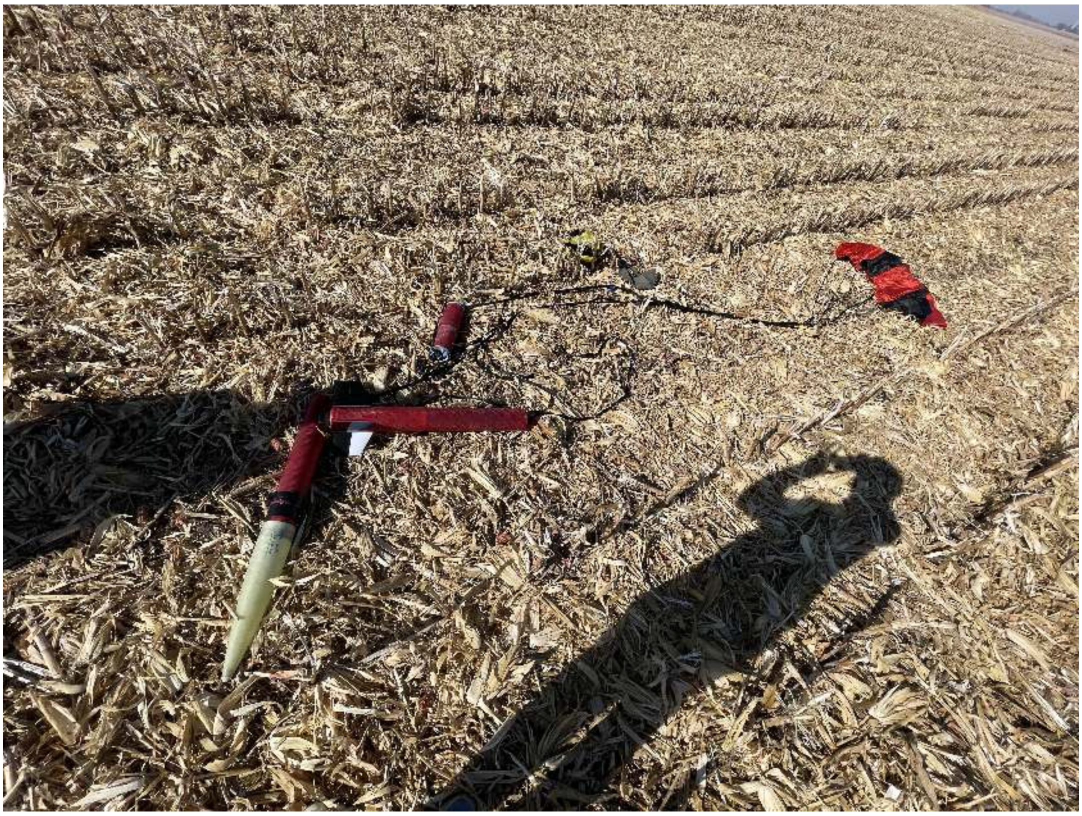

Figure 48: All landed sections with parachutes of Sub-Scale vehicle

Figure 49: Aft section of landed Sub-Scale vehicle

Figure 50: All sections of landed Sub-Scale vehicle

Figure 51: Landed parachutes of Sub-Scale vehicle

**Design Changes Due To Sub-Scale Flight** To reduce the risk of tangling and ensure proper inflation of the main parachute, the shock cord attachment method and layout was reconfigured. As the avionics bay bulkhead eyebolts were perpendicular in alignment with the ejection canisters, there were tight gaps at which shock cords may get stuck. To prevent this going forward, the eyebolts will be fastened parallel to the canisters. Additionally, the forward section shock cords have been reconfigured to provide a greater distance between the drogue and main parachutes while expectantly reducing rotational energy experienced in descent. In the initial configuration, a 15 ft shock cord connected the main parachute to the avionics bay; the same eyebolt at which a 30 ft shock cord connected the forward body to the avionics bay. A 15 ft drogue shock cord was attached at the opposite bulkhead of the avionics bay, with only a 14.75 in distance of separation (length of avionics bay). In the updated configuration, the 30 ft shock cord connects the main parachute to the mid section avionics bulkhead, allowing 15 ft of additional space such that the drogue cannot reach the main parachute's canopy. Additionally, the 15 ft shock cord attached to the forward body is now attached to the main parachute rather than the avionics bay. The attachment of the forward section directly to the main parachute should reduce the rotations experienced after main deployment once the main parachute is fully inflated. Additionally, all shock cord lengths were chosen to prevent collision of sections in descent.

### 3.2.3 Drag Coefficient Estimation

Using Newton's second law, seen in Eq. 1, the drag force on the rocket was calculated based on the acceleration and velocity data from the subscale flight. This drag was used to find a drag coefficient value and compare this value to the predicted drag coefficient from OpenRocket. In the equations, $a_r$ is the average acceleration of the rocket during ascent, $F_T$ is the average thrust of the subscale motor, and $m_r$ is the average of the dry mass and wet mass of the rocket. This average mass is used because during ascent, the total mass is changing and it would be a poor approximation to use either the dry or wet mass. The flight data from the subscale test launch in tabulated.

$$m_r * a_r = F_T - F_D - m_r * g \tag{1}$$

Solving for $F_D$ yields,

$$F_D = F_T - m_r * (a_r + g) \tag{2}$$

Eq. 3 shows the drag coefficient calculation with $\rho$ being the air density, $A$ being the effective frontal area of the rocket, which is just the area of a circle, and $v$ being the velocity of the rocket.

$$C_d = \frac{F_D}{0.5(\rho)(A)(v^2)} \tag{3}$$

Using the values in the table and the equations outlined above, the calculation yields a drag coefficient of $C_d = 1.52$. This value is larger than the OpenRocket subscale drag coefficient of $C_d = 0.6$ during flight at maximum velocity. This method of obtaining a drag coefficient with flight test data does not account for the fin drag and the camera protrusions drag, including electrical tape used to attach the cameras. All of these components add drag to the rocket, so it makes sense that using flight data from the rocket that was flown with these added components will yield a higher drag coefficient than the simulated values.

Table 13: Data for Drag Coefficient Calculation

| Variable | Value |
|---|---|
| $m_r$ | 0.569 slugs |
| $a_r$ | 190.0 ft/s$^2$ |
| $F_T$ | 181.0 lbf |
| $F_D$ | 54.57 lbf |
| g | 32.2 ft/s$^2$ |
| $\rho$ | 0.002377 slugs/ft$^3$ |
| d | 0.33 ft |
| A | 0.087 ft$^2$ |
| $v_{max}$ | 583 ft/s |

## 3.3 Recovery Subsystem

### 3.3.1 Materials Overview

Table 14 lists the parts used for in the Recovery & Propulsion subsystem for the 2022-2023 competition year.

Table 14: Recovery & Propulsion Materials

| Item | Model | Manufacturer | Material/Dimensions |
|---|---|---|---|
| Main Parachute | Iris Ultra Standard | Fruity Chutes Inc. | 120 in diameter Nylon |
| Drogue Parachute | Elliptical | Fruity Chutes Inc. | 18 in diamter Nylon |
| Shock Cords | | The Rocketman | 15, 15, 25, 30 ft Nylon |
| Deployment Bag | CDB-55-10 | Fruity Chutes Inc. | 247 in$^3$ packing volume |
| Nomex Blanket | NB-13 | Fruity Chutes Inc. | 13 in diameter |

### 3.3.2 Flight Sequence

There are two stages to recovery system operations, the first of which happens as the rocket reaches apogee. A black powder charge ignites, pressurizing the chamber, which separates the middle and aft body and deploys the drogue parachute. Next, one second after apogee is reached, a redundant black powder charge is ignited to ensure separation and release of the drogue parachute. The second stage takes place when the rocket reaches 600ft AGL. Another black powder charge is ignited between the forward and middle sections, separating them and deploying the main parachute. Once the rocket reaches 500ft AGL, a redundant black powder charge will fire to ensure proper separation and deployment of the main parachute. A description of recovery subsystem operations can be found in Table 15, and a flowchart detailing these operations can be found in Section 3.3.4.

Table 15: Vehicle Section Details

| Event | Description | Location | Redundancy |
|---|---|---|---|
| 1 | Middle and aft sections separate | Apogee | Apogee + 1 sec |
| 2 | Drogue parachute deployment | Apogee | Apogee + 1 sec |
| 3 | Forward and middle sections separate | 600 ft | 500 ft |
| 4 | Main parachute deployment | 600 ft | 500 ft |

### 3.3.3 System Layout

The recovery system is separated into two different sections within the rocket: the drogue parachute recovery section, and the main parachute recovery section. Both sections are on opposing sides of the avionics bay. The avionics bay is contained by a forward bulkhead and an aft bulkhead. In the drogue section configuration, an eyebolt is attached to the aft bulkhead, along with a quick link. The drogue parachute is connected by a 15 ft shock cord to the aft bulkhead quicklink using an eye-to-eye swivel. Additionally, the aft section of the rocket is connected by a second 25 ft shock cord to the same aft bulkhead quick link. A Nomex blanket is wrapped around the drogue parachute acting as a shield between the parachute and the black powder ejection cap canisters during black powder ignition. Two black powder canisters are secured to the aft-side bulkhead. Figure 52 summarizes the order at which hardware is connected between components, and Figure 53 provides a visual of the drogue parachute packing system.

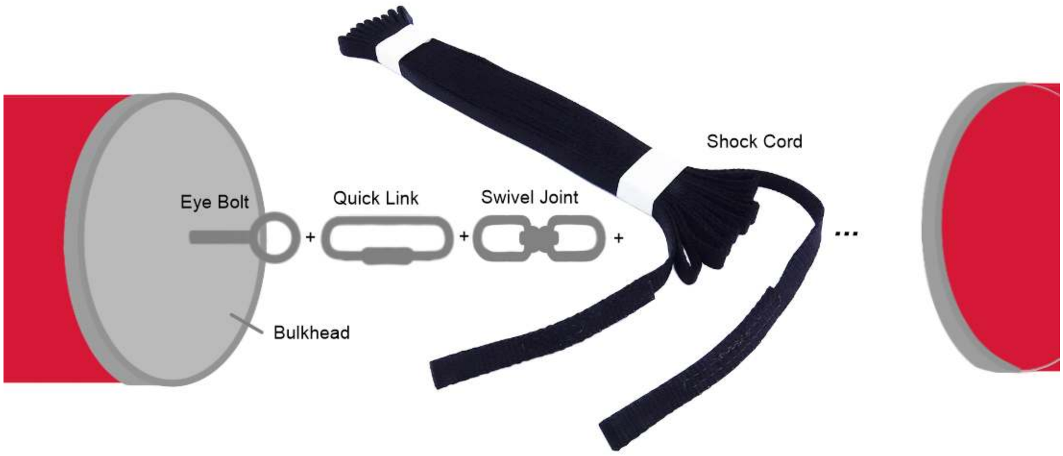


Figure 52: Hardware Diagram of Linkage Order

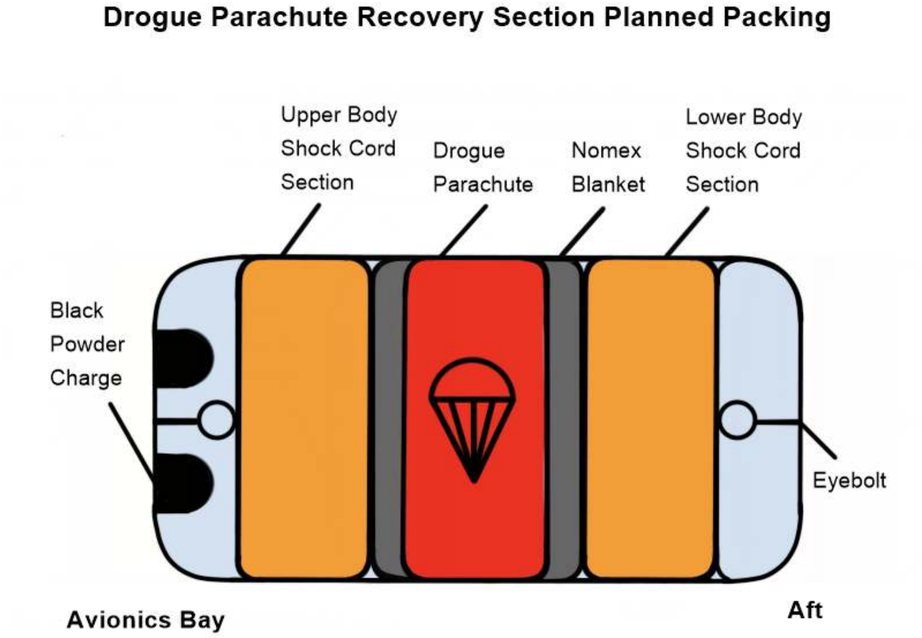


Figure 53: Drogue Parachute Packing Diagram

The main parachute recovery section will be packed in a similar manner to the drogue parachute recovery section. In the main section configuration, an eyebolt is attached to the forward bulkhead, along with a quick link. The main parachute is connected by a 30 ft shock cord to the forward bulkhead quick link using an eye-to-eye swivel. The forward section is connected by a 15 ft shock cord to the main parachute. The main parachute is located in the middle of the section, packed within a Nomex deployment bag. Identical to the drogue configuration; two black powder canisters are secured to the forward-side bulkhead. A visual of the packing system can be referenced below.

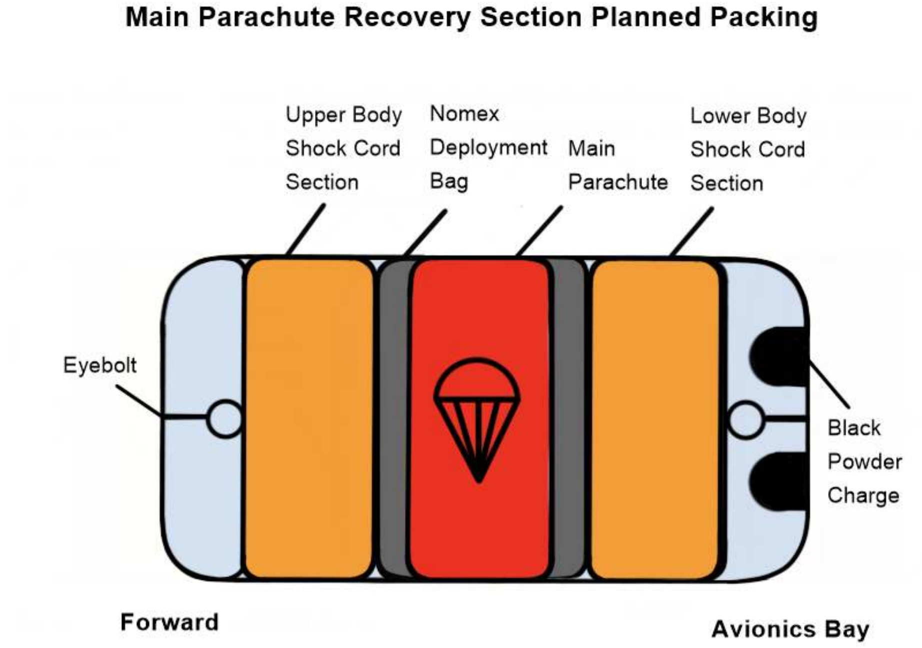


Figure 54: Main Parachute Packing Diagram

Figures 55 and 56 display the drogue and main parachute shock cord layouts and dimensions. The lengths of the shock cords were selected after considering risk of collision, bounce from the nylon shock cord's elasticity, and risk of tangling after main deployment.

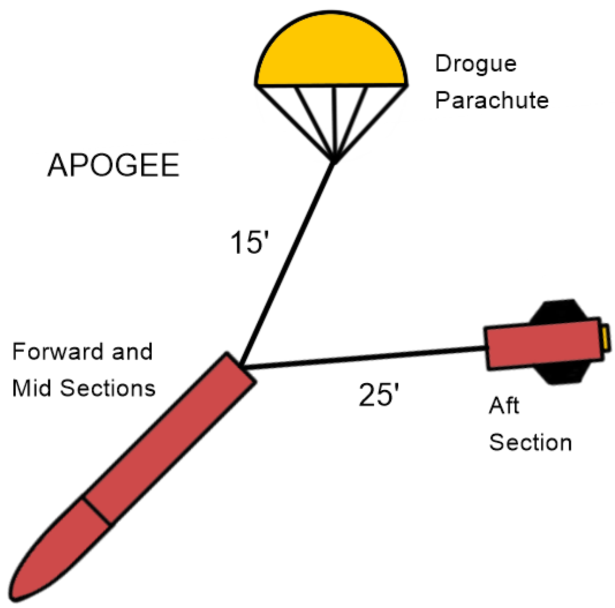


Figure 55: Drogue Deployment Schematic

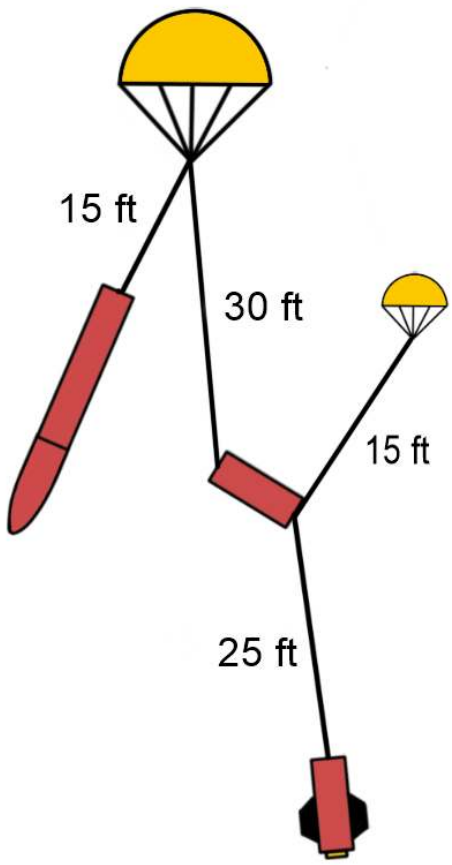


Figure 56: Main Deployment Schematic

### 3.3.4 Concept of Operations (CONOPS)

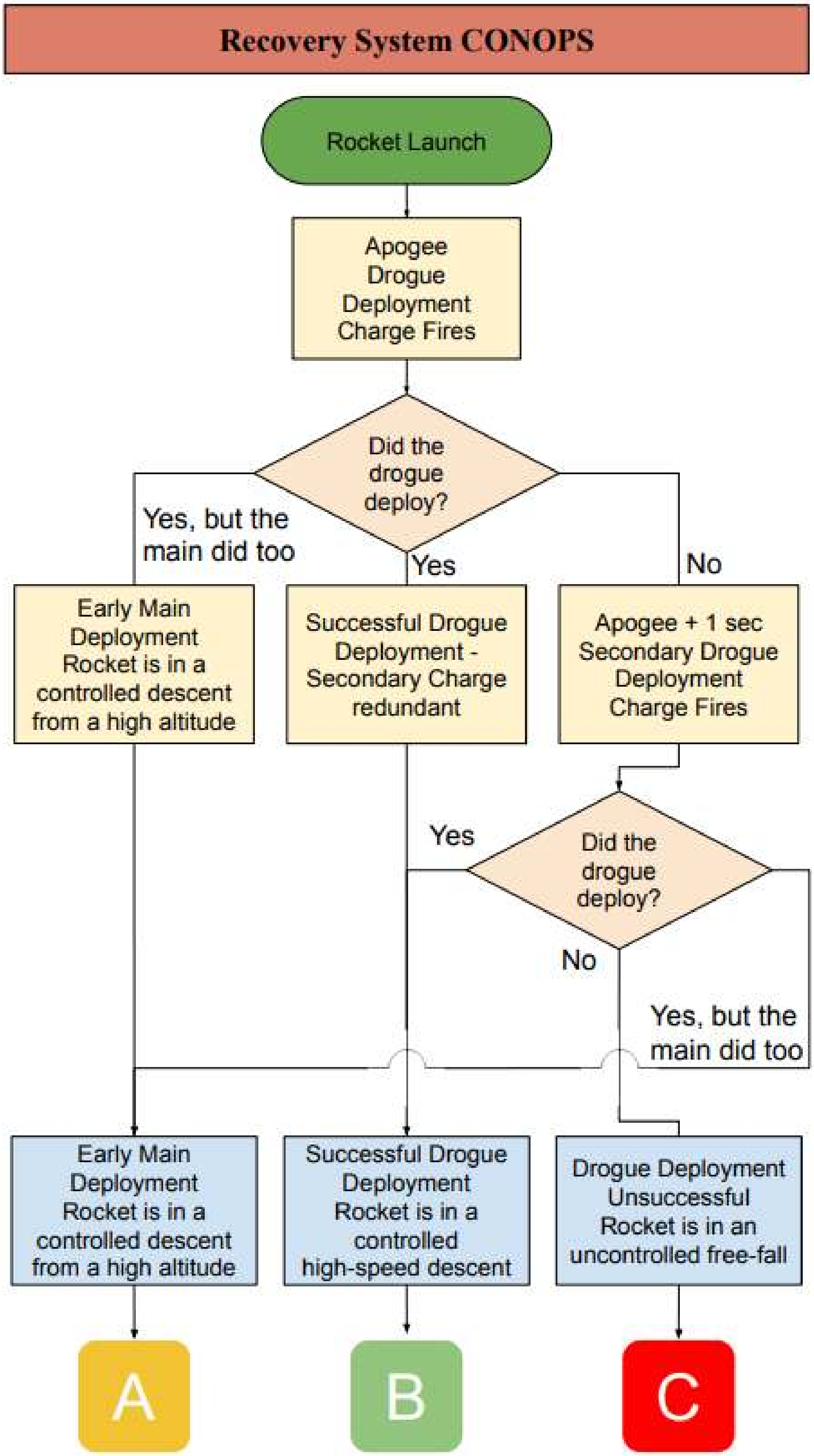


Figure 57: Concept of Operations Flowchart: Section 1

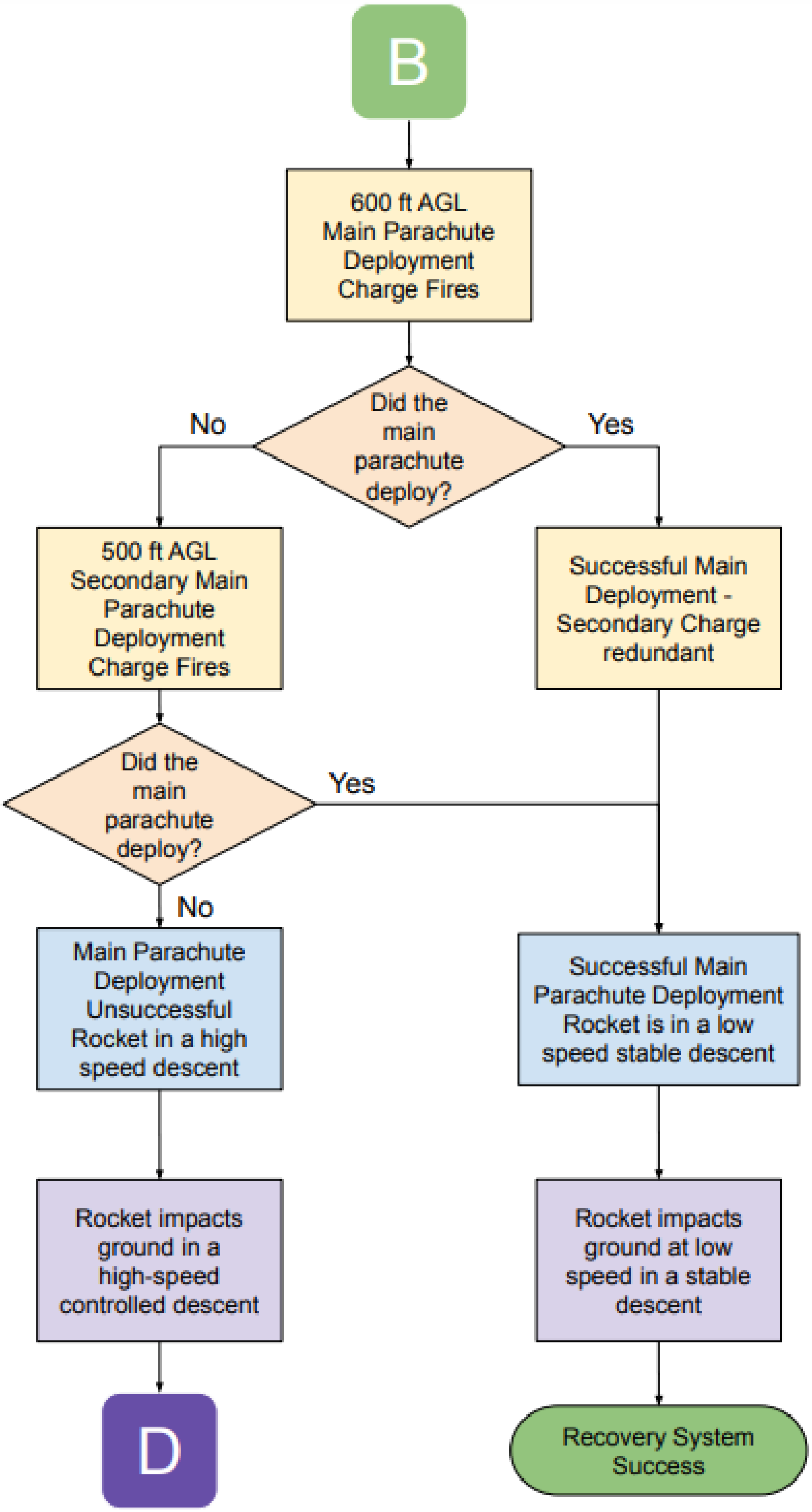


Figure 58: Concept of Operations Flowchart: Section 2

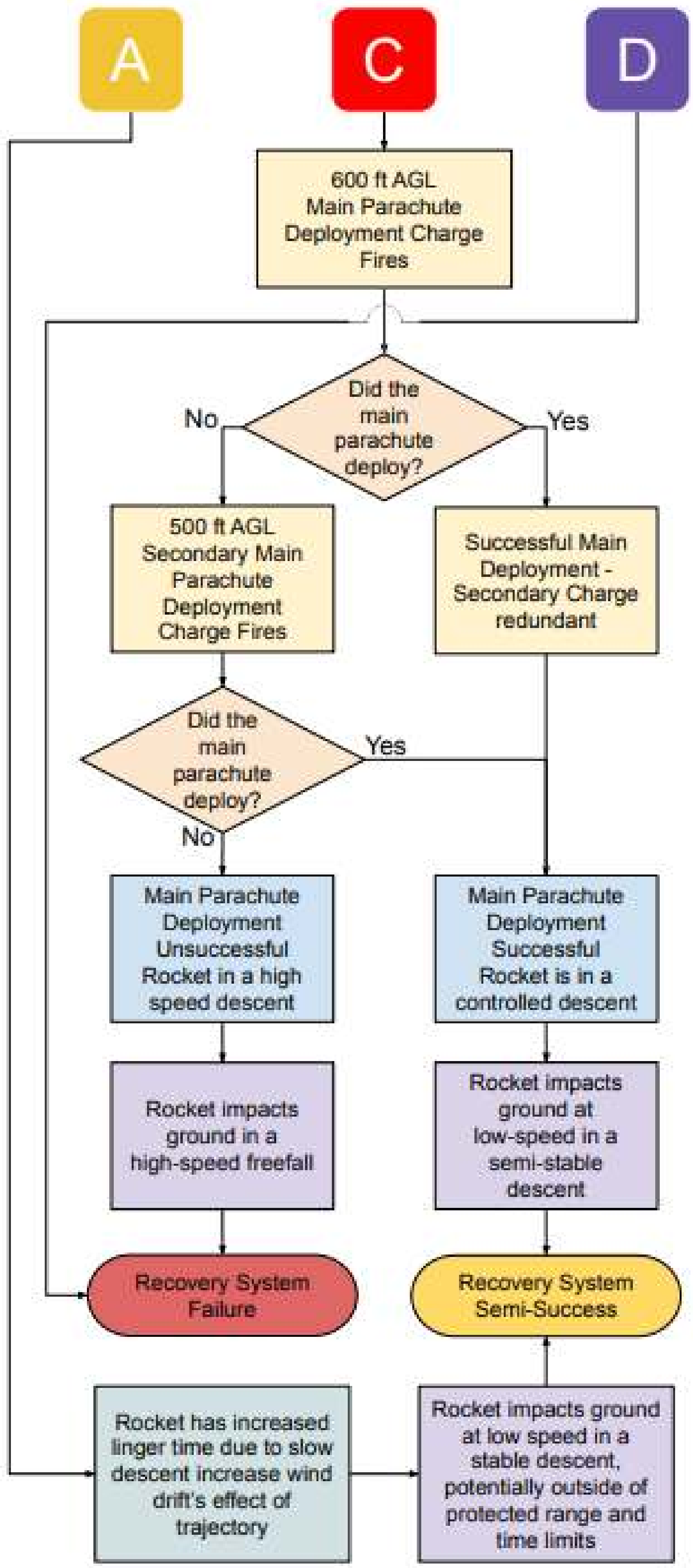


Figure 59: Concept of Operations Flowchart: Section 3

### 3.3.5 Design Selection Matrix

Table 16 below displays the final component/design decisions for the recovery system. The table explains the purpose of each component or design and why it was chosen over alternative designs.

Table 16: Recovery & Propulsion Components

| **Component** | **Purpose** | **Reason Chosen** | **Picture** |
|---|---|---|---|
| Parachute Deployment Sections | To stable ascent and descent of the rocket | The main parachute is located in the forward section to bring the CG forward, increasing stability | 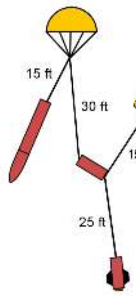 |
| Parachute Shape | To slow the descent of the rocket | The toroidal shaped main parachute has a high drag coefficient of 2.2, allowing for an impact kinetic energy within competition constraints |  |
| Parachute Material | To withstand rough environmental conditions upon landing | The Iris Ultra Standard parachute model has a thicker and more durable material than alternatives; preventing harsh tears upon landing and dragging along the ground |  |
| Shock Cord Material | To withstand the high temperatures from the ejection charges and supply enough elasticity and tensile strength to absorb the snatch force experienced | Nylon shock cords provide the necessary elasticity and tensile strength, and is capable of withstanding the flames from the black powder detonation |  |
| Ejection Method | To reliably and repeatably deploy main and drogue parachutes | Black powder is easy and inexpensive to test repeatedly and is a reliable ejection method at lower altitudes |  |

### 3.3.6 Packing Method

The Recovery and Propulsion subteam follows a *Parachute Packing Procedure* developed with reference to Fruity Chutes Inc.'s *How to Fold a Parachute* instructions. The main parachute is packed into a 5.5 in diameter by 13 in length deployment bag, and the drogue is wrapped inside of a 13 in Nomex blanket, based on respective packing volumes.

### 3.3.7 Black Powder Calculation

The force required to shear the #4-40 shear screws was calculated to determine pressures required to separate the forward and aft ejection chambers. Both chambers have different quantities of shear screws do withstand different forces. The aft chamber is secured with two shear screws, and the forward chamber is secured with four to ensure the main parachute does not deploy during drogue parachute ejection. Using the pressures and volumes of the chambers, the quantities of black powder charges can be calculated using stoichiometry. A 25% FoS is applied to the primary black powder charges, and a 50% FoS is applied to the redundant charges.

Table 17 displays the given variables used to calculate the black powder quantities within the full-scale rocket.

Table 17: Given Variables for Black Powder Calculations

| Symbol | Definition | Value | Units |
|---|---|---|---|
| Sy | Shear Strength of Shear Screw | 10000 | $psi$ |
| d | #4 Shear Screw Diameter | 0.112 | $in$ |
| $n_1$ | Shear Screw Quantity | * | unitless |
| R | Boltzmann Gas Constant | 0.0832 | $L * atm/mol * K$ |
| T | Black Powder Ignition Temperature | 1837 | $K$ |
| ID | Full-scale Body Inner Diameter | 6 | $in$ |
| $L_1$ | Forward Ejection Chamber Length | 17 | $in$ |
| $L_2$ | Aft Ejection Chamber Length | 15 | $in$ |

* Two #4-40 shear screws are used in the aft section for drogue deployment, and four #4-40 shear screws are used in the forward section for main deployment.

The following equations were used to determine the final black powder quantities listed in Table 18.

Volume of Chamber:

$$V = L * \pi * (\frac{ID}{2})^2 \qquad [in^3] \tag{4}$$

Volume Converted from $[in^3]$ to [L]

Max Force on Shear Pins:

$$F = \frac{\pi * Sy * n_1 * d^2}{4} \qquad [lbf] \tag{5}$$

Max Pressure on Shear Pins:

$$P = \frac{4 * F}{\pi * ID^2} \qquad [\frac{lbf}{in^2}] \tag{6}$$

Pressure converted from $[\frac{lbf}{in^2}]$ to [ATM]

Moles of Gas Required for Max Pressure:

$$n_2 = \frac{P * V}{R * T} \qquad [mol] \tag{7}$$

Black Powder Chemical Formula:

$$2KNO_3 + S + 3C \rightarrow K_2S + N_2 + 3CO_2 \tag{8}$$

Required Mass of Potassium Nitrate:

$$m_{KNO_3} = (\frac{n_2}{1}) * (\frac{2}{4}) * (\frac{101.1}{1}) \qquad [g] \tag{9}$$

Required Mass of Sulfur:

$$m_S = (\frac{n_2}{1}) * (\frac{1}{4}) * (\frac{32.1}{1}) \qquad [g] \tag{10}$$

Required Mass of Carbon:

$$m_C = (\frac{n_2}{1}) * (\frac{3}{4}) * (\frac{12}{1}) \qquad [g] \tag{11}$$

Required Mass of Black Powder:

$$m_{BP} = m_{KNO_3} + m_S + m_c \qquad [g] \tag{12}$$

Mass of Primary Charge:

$$m_1 = 1.25 * m_{BP} \qquad [g] \tag{13}$$

Mass of Secondary Charge:

$$m_2 = 1.5 * m_{BP} \qquad [g] \tag{14}$$

Table 18: Final Black Powder Charge Quantities

| **Charge** | **Mass (grams)** |
|---|---|
| Primary Drogue Ejection Charge | 1.8 |
| Redundant Drogue Ejection Charge | 2.2 |
| Primary Main Ejection Charge | 4.1 |
| Redundant Main Ejection Charge | 4.9 |

### 3.3.8 Parachute Sizing

Three major competition constraints were considered in the parachute selection process: the impact kinetic energy of the rocket must be below 75 ft-lbf, the descent time from apogee must be less than 90 seconds, and the rocket must not drift more than 2500 ft from the launchpad. Based on these three requirements, the team derived a process to calculate the optimal parachute size using a series of physics equations.

Table 19 states constant known values as well as final calculated values with their respective equations displayed in Table 20. The maximum allowed kinetic energy given by competition restraints was used to determine maximum terminal velocity. Using the terminal velocity and an estimated drogue parachute area, the minimum area of the main parachute can be calculated. The drogue parachute size is then adjusted to determine a main parachute size that does not exceed drift or kinetic energy requirements.

Table 19: Variables for Parachute Sizing Calculations

| **Symbol** | **Definiton** | **Value** | **Units** |
|---|---|---|---|
| KE | Maximum Kinetic Energy | 75.00 | $ft-lbf$ |
| v | Max Main Terminal Velocity | 16.37 | $ft/s$ |
| m | Mass of Heaviest Section | 0.560 | slugs |
| W | Dry Weight | 38.48 | $lbf$ |
| $\rho$ | Air Density Constant | 2.376e-3 | $slug/ft^3$ |
| $A_{drogue}$ | Area of Drogue Parachute | 1.696 | $ft^2$ |
| $C_{drogue}$ | Drag Coefficient of Drogue Parachute | 1.5 | unitless |
| $D_{drogue}$ | Diameter of Drogue Parachute | 18.00 | $in$ |
| $A_{main}$ | Area of Main Parachute | 75.40 | $ft^2$ |
| $C_{main}$ | Drag Coefficient of Main Parachute | 2.2 | unitless |
| $D_{main}$ | Diameter of Main Parachute | 101.36 | $in$ |
| $KE_{landing}$ | Found kinetic energy at landing | 57.08 | $ft-lbf$ |

The minimum main parachute diameter was calculated to be 105 in. This value was scaled up to the next available size to purchase of 120 in. The resulting kinetic energy of the selected 18 in drogue parachute and the calculated 120 in main parachute was 57.08 ft-lbf. Additionally, the 18 in drogue parachute size aligns with manufacturer recommendation for the 120 in main parachute size.

The following equations were used to calculate the parachute sizing values seen in Table 19.

Max terminal velocity:

$$KE = \frac{1}{2}mV^2 \tag{15}$$

Area of main parachute:

$$V = \sqrt{\frac{2W}{\rho(A_{drogue}C_{drogue} + A_{main}C_{main})}} \tag{16}$$

Minimum diameter of main parachute:

$$A = 4\pi d^2 \tag{17}$$

Table 20: Parachute Sizing Calculations

| Sym | Definition | Method | Value | Units |
|---|---|---|---|---|
| KE | Maximum Kinetic Energy | Equation 12 | 75.00 | $ft-lbf$ |
| v | Max Main Terminal Velocity | Equation 12 | 16.37 | $ft/s$ |
| $A_{main}$ | Area of Main Parachute | Equation 13 | 75.40 | $ft^2$ |
| $D_{main}$ | Diameter of Main Parachute | Equation 14 | 101.36 | $in$ |
| $KE_{landing}$ | Found kinetic energy at landing | Equation 12 | 57.08 | $ft-lbf$ |

### 3.3.9 Descent Time

The WURocketry team aims to achieve a descent time below the competition bonus goal of 80 s. Table 21 states constants as well as final calculated values with their respective equations displayed in Table 22. Drogue and main parachute terminal velocities are calculated using updated area values from Section 3.3.8. Using these velocities, a descent time of 76.88 s is calculated.

Table 21: Variables for Descent Time Calculations

| Symbol | Definition | Value | Units |
|---|---|---|---|
| W | Dry Weight of Rocket | 38.48 | $lb-ft$ |
| $\rho$ | Air Density Constant | 2.376e-3 | $slug/ft^3$ |
| $A_{drogue}$ | Area of Drogue Parachute | 1.696 | $ft^2$ |
| $C_{drogue}$ | Drag Coefficient of Drogue Parachute | 1.5 | unitless |
| $A_{main}$ | Area of Main Parachute | 75.40 | $ft^2$ |
| $C_{main}$ | Drag Coefficient of Main Parachute | 2.2 | unitless |
| $h_{apogee}$ | Target Apogee Altitude | 4650 | $ft$ |
| $h_{main}$ | Main Parachute Deployment Altitude | 600 | $ft$ |
| $v_{t,drogue}$ | Terminal Velocity with Drogue Deployed | 116.2 | $ft/s$ |
| $v_{t,main}$ | Terminal Velocity with Main Deployed | 14.28 | $ft/s$ |
| $t_{descent}$ | Descent Time | 76.88 | $s$ |

The following equations were used to calculate the descent time values seen in Table 22.

Terminal velocity after drogue deployment:

$$v_{t,drogue} = \sqrt{\frac{2W}{C_{drogue}\rho A_{drogue}}} \tag{18}$$

Terminal velocity after main deployment:

$$V_{t,main} = \sqrt{\frac{2W}{\rho(A_{drogue}C_{drogue} + A_{main}C_{main})}} \tag{19}$$

Descent time of the rocket:

$$t_{descent} = \frac{h_{apogee} - h_{main}}{v_{t,drogue}} + \frac{h_{main}}{v_{t,main}} \tag{20}$$

Table 22: Descent Time Calculations

| Symbol | Definition | Method | Value | Units |
|---|---|---|---|---|
| $v_{t,drogue}$ | Terminal Velocity with Drogue Deployed | Equation 15 | 116.2 | $ft/s$ |
| $v_{t,main}$ | Terminal Velocity with Main Deployed | Equation 16 | 14.28 | $ft/s$ |
| $t_{descent}$ | Descent Time | Equation 17 | 76.88 | $s$ |

#### 3.3.10 Recovery System Avionics

Figure 60 displays current design of the avionics bay board on which all electronics will be mounted. A description of those electronics and an explanation of the design is contained in the following sections.

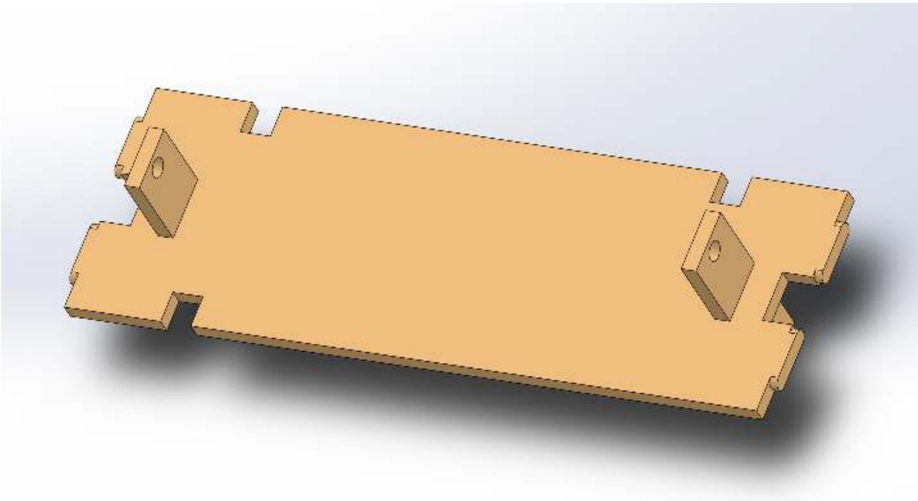

Figure 60: Avionics Bay CAD Model

**Flight Computers** The Altus Metrum EasyMini flight computer (Fig. 61) will be used for both the primary and redundant flight computers in the recovery electronics system. Each flight computer will fire a separate charge within each of the separation chambers with the primary flight computer firing the first charge and the redundant flight computer firing the second charge. Charges will be fired at apogee and apogee plus 1 second for the drogue parachute ejection, and 600 ft and 500 ft for the main parachute ejection.


Figure 61: Altus Metrum EasyMini

**Arming Switches** The EasyMini flight computers will be armed while on the launch pad through the use of self locking rotary switches. These switches will be accessible through cutouts in the airframe and, once switched, will provide power to the flight computers. The status of the flight computers can then be verified by translating the status beeps of each flight computer.

**Ejection Charges** The separation event initiated by the flight computers will be executed through the use of redundant black powder charges in each separation section. These black powder charges will be ignited by e-matches causing an explosion that will pressurize the chamber to the point of separation. As previously stated, each of these charges in each section will be controlled by a single flight computer.

**Recovery Avionics Wiring Diagram** Figure 62 displays the current recovery wiring scheme. This design provides an abundance of redundancy by eliminating any single point of failure. The redundancy of the recovery system is further detailed in Section 3.3.11. Furthermore, the continuity of this circuit is demonstrated in Section 6.1.3.

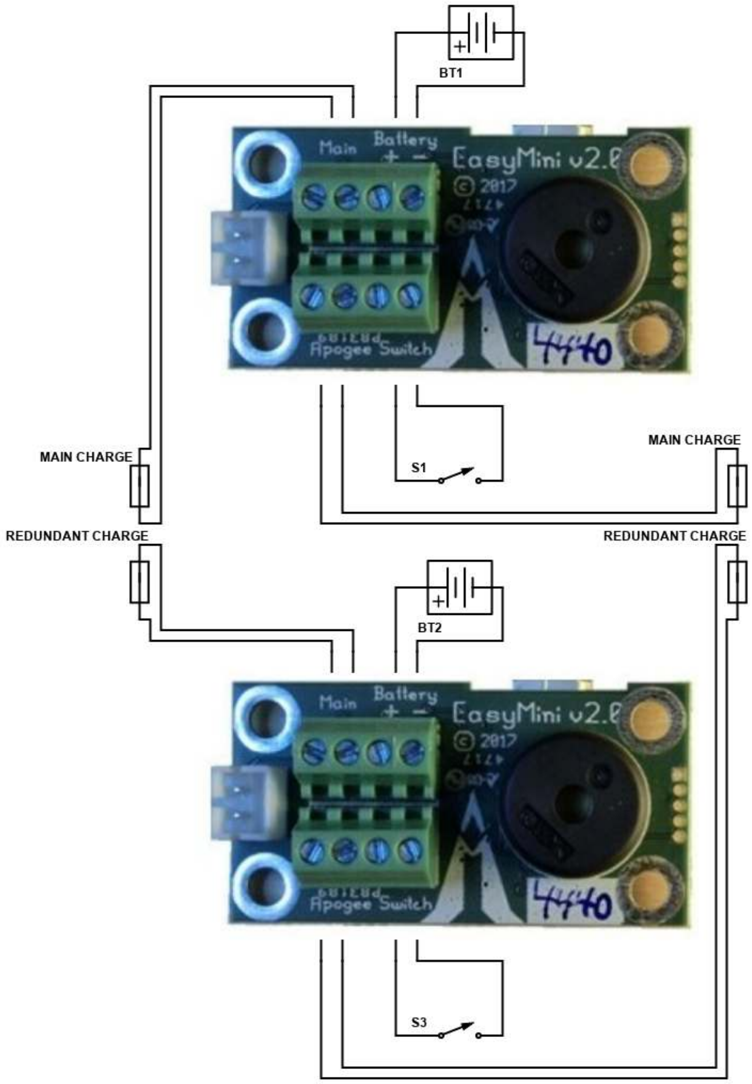


Figure 62: Recovery Avionics Wiring Diagram

**Data Collection/Microprocessor** The Raspberry Pi 4 Model B, pictured in Fig. 63, was decided on as the microprocessor for data collection and collecting GPS data. When compared to the Arduino and the previous generation Raspberry Pi, the Raspberry Pi 4 Model B was weighed as the best option providing both a reliable and powerful microprocessor and a versatile platform. The function of this device is to collect on board data from various sensors to be used in post flight analysis. Specifically, pressure sensors will be utilized to monitor pressure in the separation chambers and an IMU will be used to assess flight kinematics.

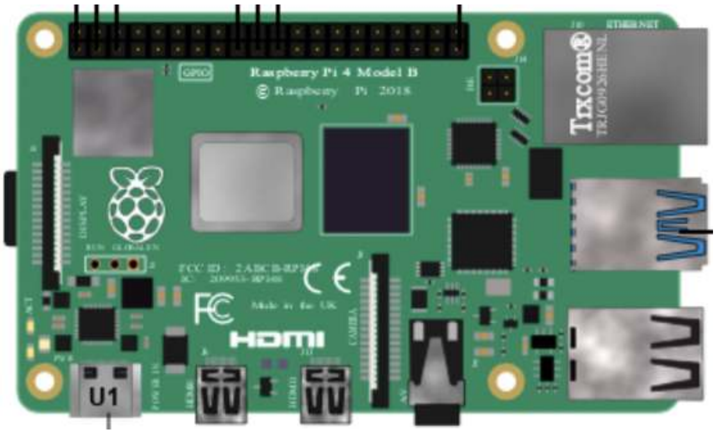


Figure 63: Raspberry Pi Model B (4 GB)

**Vehicle Tracking** The TeleGPS V2 (Fig. 64) will be used as the primary GPS tracking system on the rocket. The TeleGPS will be powered by a 3.7v LiPo battery and will communicate down to a base station system consisting of a 3-element Yagi antenna, base station computer, and TeleBT (Fig. 65). The TeleGPS will communicate with the base station over the 70cm frequency band, specifically 434.55 Hz or channel zero. This system will provide accurate and reliable location data for the rocket enabling easier recovery post launch.


Figure 64: TeleGPS V2

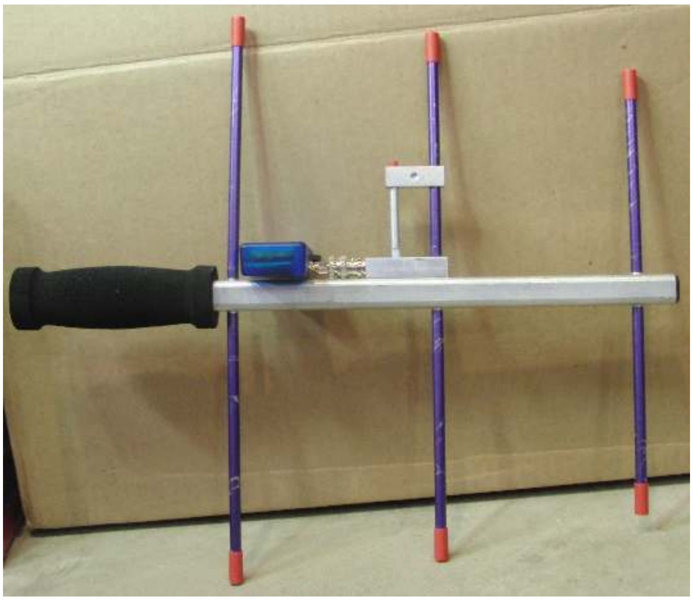

Figure 65: TeleBT Base Station

#### 3.3.11 Redundancy

**Flight Computers** Two separate EasyMini flight computers will be used to monitor the flight status of the rocket and fire the ejection charges for each of the recovery events. These flight computers will be powered and armed using completely independent circuits and will have separate ignition systems for their respective separation charges. This design ensures there is no single point of failure within the flight computer system of the rocket, ensuring a successful execution of all recovery events. This independent wiring is clearly detailed in the wiring diagram above in Fig. 62.

**Ejection Charges** The black powder ejection system, used to power the recovery separation events, will utilize both a primary and redundant charge within each separation chamber. The primary charge in each separation chamber will be fired by the primary EasyMini flight computer using only the circuitry associated with that flight computer. In a similar way, the redundant charges will be fired by the redundant flight computer using only its associated circuitry. Each flight, a new e-match will be wired into the flight computers so as to fit the requirements outlined above. These charges will be fired at apogee and apogee plus 1 second for the drogue parachute separation event and 600 ft and 500 ft for the main parachute separation event. Maintaining two separation charges in each chamber and ensuring proper separation enables a fully redundant ejection system.

## 3.4 Mission Performance Predictions

### 3.4.1 Target Altitude

The official target altitude for WURocketry is 4650 ft. This was determined using OpenRocket software and taking into account the accuracy of the software's apogee prediction. The apogee predicted by OpenRocket is 4712 ft. However, during competition last year, the rocket's actual apogee was approximately 300 feet lower than the prediction. The team believes that this discrepancy may be due to unaccounted mass in the calculation. The predicted apogee is calculated under ideal conditions (0 mph wind and 0° launch angle), which realistically will not happen as wind in Huntsville, AL, historically blows at an average of 12.4 mph in April, and there will be a small launch angle away from the crowd. The team has therefore determined that the 4650 ft apogee is a more accurate estimate, noting to take extra care to accurately account for mass of components. Additionally, the team has accounted for the possibility of increasing the rocket's weight, which could potentially reduce the apogee to 4650 ft. The results of the sub-scale flight also support this prediction, as they suggest that OpenRocket tends to slightly overestimate apogee.

### 3.4.2 Ideal Conditions

Figure 66 displays the flight profile for ideal conditions. Ideal conditions correspond to 0 mph wind, 90 degree wind angle, and a launch angle of 0 degrees. It includes predictions for altitude, velocity, and acceleration.

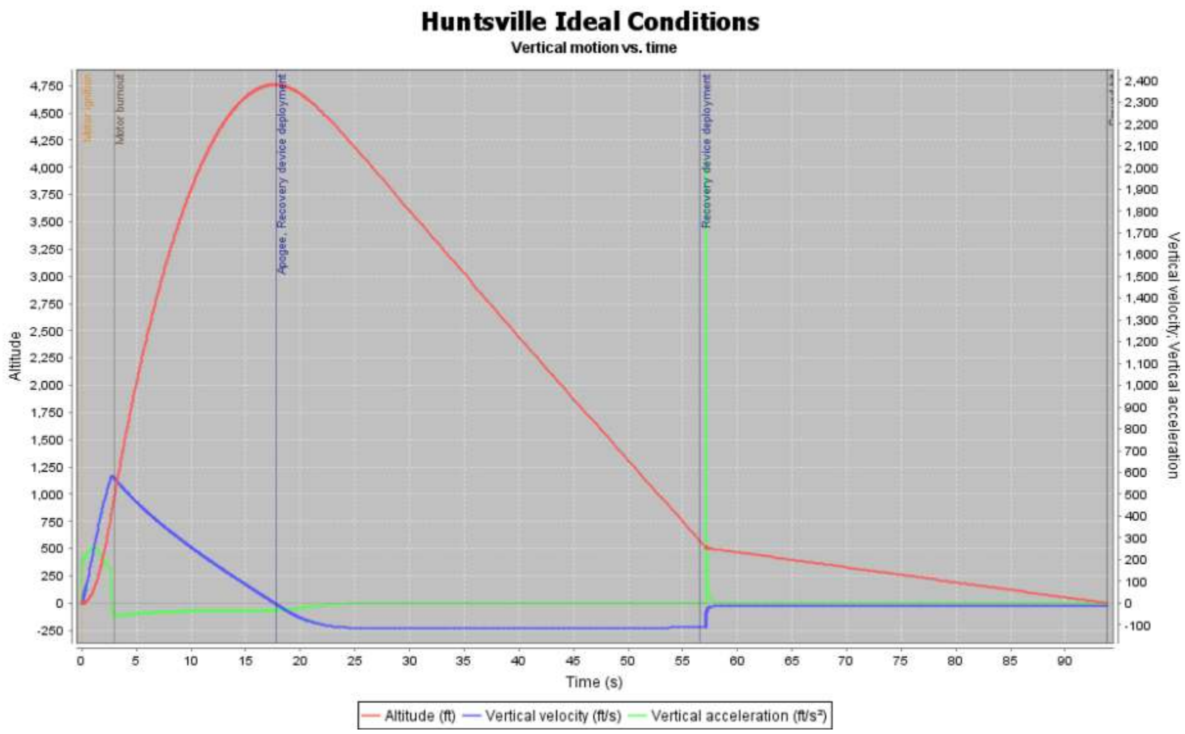


Figure 66: Vertical Motion Open Rocket Flight Profile

### 3.4.3 Flight Predictions and Simulations

The mission performance predictions were compiled using a combination of OpenRocket simulations and hand calculations. Vertical motion, stability, and drag coefficient graphs were used to predict rocket performance. A vertical motion graph displays altitude, velocity, and acceleration of the rocket versus time. A stability graph displays the stability margin calibers, CG location, and CP location versus time. A drag coefficient chart displays the overall, friction, base, and pressure drag coefficients versus time. Table

23 displays the flight predictions for the 2022-2023 design from OpenRocket. Table 24 shows the predicted apogee from OpenRocket at various wind speeds.

Table 23: Mission Performance Predictions Overview

| **Parameter** | **Value** |
|---|---|
| Predicted Apogee | 4759 ft |
| Static Stability Margin | 3.01 cal |
| Drogue Parachute Deployment Altitude | Apogee |
| Main Parachute Deployment Altitude | 600 ft |
| Descent Time | 76.2 sec |
| Velocity Off Rail | 71.8 ft/sec |
| Maximum Velocity | 581 ft/sec |

Table 24: Flight Predictions at Different Wind Speeds

| **Wind Speed** | **Apogee** | **Descent Time** |
|---|---|---|
| 0 mph | 4759 ft | 76.2 sec |
| 5 mph | 4748 ft | 74.9 sec |
| 10 mph | 4722 ft | 77.7 sec |
| 15 mph | 4645 ft | 74.5 sec |
| 20 mph | 4607 ft | 75.1 sec |

The simulated thrust curve is shown in Fig. 67 from OpenRocket. Individual section weights while on the launch pad and at apogee are given in Table 25.

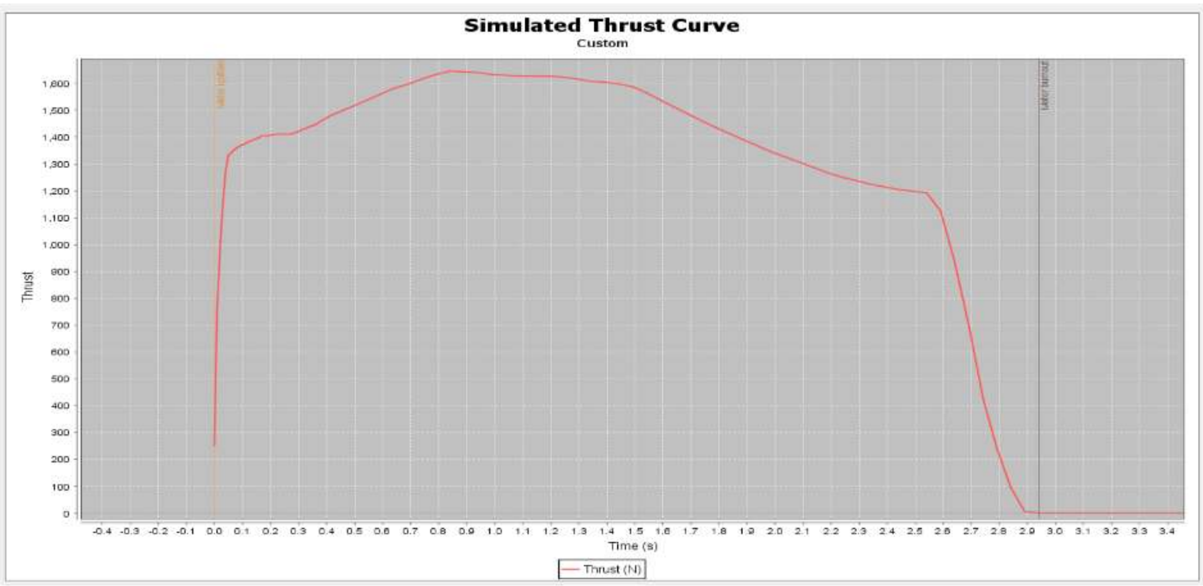


Figure 67: Simulated Motor Thrust Curve

Table 25: Rocket Mass Breakdown

| Mass (lbs) | | |
|---|---|---|
| **Section** | **On Launch Pad** | **Apogee** |
| **Forward** | 18.01 | 18.01 |
| **Middle** | 5.59 | 5.59 |
| **Aft** | 19.24 | 14.88 |
| **Total** | 42.84 | 38.48 |

In order to properly design the rocket and select materials that can withstand the forces generated by the motor, black powder charges, and parachute deployment, it is important to have a thorough understanding of the weight of each section of the rocket. To ensure the integrity and reliability of the rocket, all hardware is designed with a minimum factor of safety of 1.5. This strong and sturdy design minimizes the risk of failure due to hardware issues and can withstand the expected loads during flight.

### 3.4.4 CG and CP

According to the OpenRocket diagram displayed in Fig. 68, the center of pressure (CP) can be found 88.017 inches from the tip of the nosecone, while the center of gravity (CG) is situated 69.464 inches from the same point. The rocket will be stable becasue of the center of gravity being before of center of pressure. With these two values in relationship with the diameter leading to a stability margin of 3.01 cal.

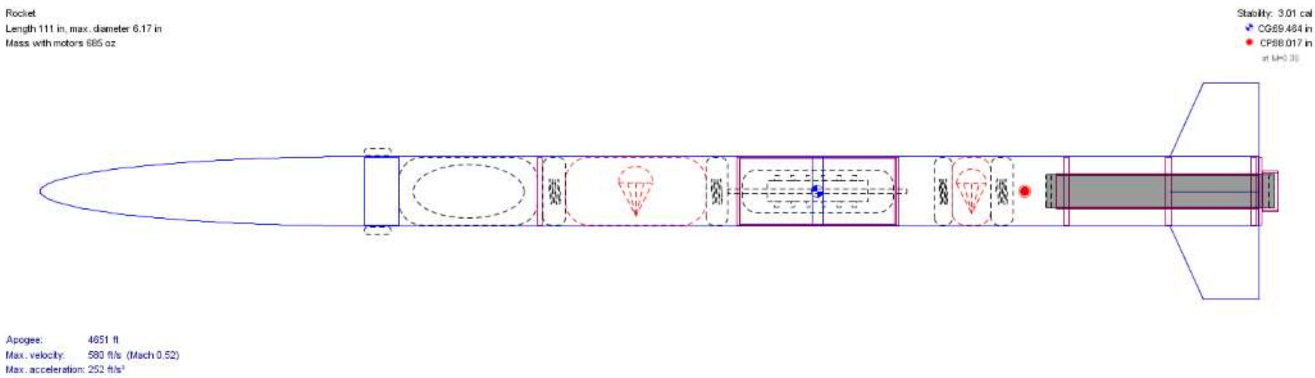


Figure 68: Open Rocket CP and CG Relationship and Locations

### 3.4.5 Kinetic Energy Calculations

Table 26 displays the kinetic energy of each section. These kinetic energies were calculated using the terminal velocity after main deployment, 14.28 ft/s, from Section 3.3.9.

Table 26: Kinetic Energy Values

| Rocket Section | Kinetic Energy At Landing (lbs-ft) |
|---|---|
| Forward Section | 57.08 |
| Mid Section | 17.72 |
| Aft Section | 47.19 |

### 3.4.6 Drift Calculations

Table 27 displays the predicted drifts ranging from 0-20 mph as calculated by-hand and in OpenRocket simulation. By competition requirements, the drift must be less than 2500 ft from launch point. At the maximum launch speeds of 20 mph, the maximum drift experienced is averaged to 2228.9 ft, 271.1 ft below the maximum.

Table 27: Drift Calculation Values

| Wind Speed | Hand Calculation Drift (ft) | Open Rocket Drift (ft) | % Difference |
|---|---|---|---|
| 0 | 0 | 0 | 0 |
| 5 | 563.8 | 549.0 | 2.660 |
| 10 | 1127.5 | 1139.6 | 1.067 |
| 15 | 1691.3 | 1639.0 | 3.141 |
| 20 | 2255.1 | 2202.7 | 2.351 |

Table 27 above displays a small difference in drift values when comparing the hand calculations to the OpenRocket values. The difference in these calculations is due to the non-ideal drift conditions taken into account in the OpenRocket simulation. OpenRocket does not assume the descending vehicle to travel at a constant wind speed.

To verify the precision of the OpenRocket apogees and descent times, and therefore the drift calculations as well, multiple simulations were performed and a standard deviation was calculated from the data. Tables 28 and 29 display three trials for the apogee and descent time at various wind speeds from OpenRocket with an accompanying standard deviation.

Table 28: Simulated Apogee Precision

| Wind Speed | Simulation 1 Apogee (ft) | Simulation 2 Apogee (ft) | Simulation 3 Apogee (ft) | Standard Deviation (ft) |
|---|---|---|---|---|
| 0 | 4759 | 4759 | 4759 | 0 |
| 5 | 4747 | 4748 | 4748 | 0.471 |
| 10 | 4715 | 4718 | 4729 | 6.02 |
| 15 | 4680 | 4671 | 4653 | 11.2 |
| 20 | 4618 | 4629 | 4581 | 15.1 |

Table 29: Simulated Descent Time Precision

| **Wind Speed** | **Simulation 1 Descent Time (s)** | **Simulation 2 Descent Time (s)** | **Simulation 3 Descent Time (s)** | **Standard Deviation (s)** |
|---|---|---|---|---|
| 0 | 76.2 | 76.2 | 76.2 | 0 |
| 5 | 75.5 | 74.9 | 75.8 | 0.374 |
| 10 | 75.8 | 75.4 | 74.7 | 0.455 |
| 15 | 77.7 | 76.3 | 75.9 | 0.771 |
| 20 | 73.5 | 74.2 | 75.5 | 0.829 |

It can be surmised from the data that the OpenRocket simulated apogees and descent times are precise as the standard deviations are small when compared to the apogee (<1%) and descent time (<2%) values. It can be seen that as the wind speed increases, so does the standard deviation. This is due to OpenRocket having a built-in standard deviation of 10% of the wind speed to simulate changes in wind speed and turbulence; the higher the wind speed, the higher the deviation.

# 4 Payload Criteria

The payload experiment must meet several objectives throughout the launch and landing of the vehicle in order to perform the requirements of the payload mission. The general execution procedure of the payload mission is as follows:

1. Payload hardware is loaded into vehicle and software is initialized to await launch.
2. Payload detects launch sequence and awaits landing. Periodically transmits telemetry to base station.
3. Payload detects landing and, if stable, begins separating the nosecone from the body tube.
4. When the vehicle is sufficiently separated, the payload deploys the camera system
5. The payload software enters a RAFCO execution loop that continuously listens and executes RAFCO transmitted over the APRS network

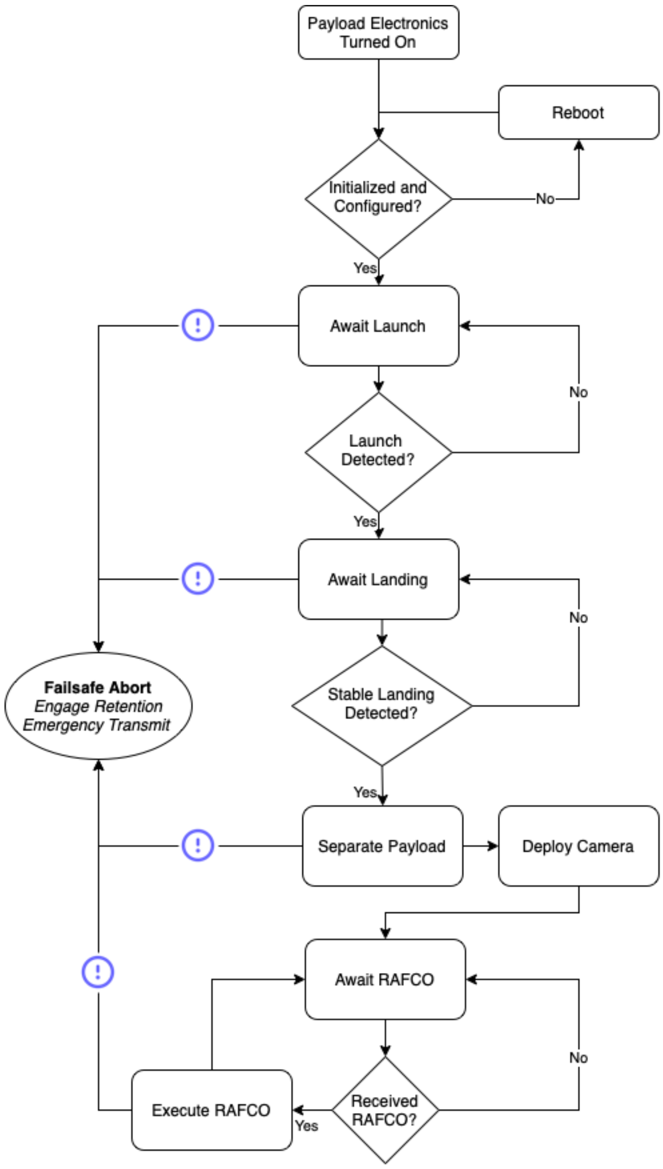


Figure 69: Visual Illustration of Payload Mission Phases

The mechanical and electrical designs of the payload experiment is further discussed in the following sections. As an overview for those two perspectives, the following tables illustrate the mechanical and electrical components that were selected for the final payload design.

| Component | Material | Weight (oz) | Dimensions (in) |
|---|---|---|---|
| 60355K41 Ball Bearing | Steel | 0.35 | 0.375" / 0.125" OD/ID |
| 6832K74 Rack | Steel | 13.23 | 18" x 0.46" x 0.23" LxWxD |
| 7880K18 Pinion Gear | Steel | 0.71 | 0.354" / 0.125" OD/ID |
| Camera & Servo Mount | PETG | 0.34 | 1.97" x 1.18" x 0.59" |
| Centering Rings | PETG | 1.76 | 6" / 3.75" OD/ID |
| Compact Linear Solenoid | Steel | 3.2 | 1.25" OD |
| DC Motor Mount | PETG | 1.6 | 2"/1.22" OD/ID |
| Electronics Board | Plywood | 0.64 | 6"/4.88"/0.25" LxWxH |
| Greartsian 12V DC Motor | Aluminum | 13.11 | 4.54" x 1.58" x 2.6" LxWxD |
| Lazy Susan Turntable | Steel | 7.04 | 3.75" / 2.16" OD/ID |
| Scissor Lift | PETG | 0.64 | 3.75" x 1" LxW, 6" H (ext)/0.65" H (ret) |
| Telescoping Rods | PETG | 0.96 | 11.51" L (ext)/6.9" L (ret), 0.38" OD |

Figure 70: Mechanical Components for Payload Experiment

| Component | Material | Weight (oz) | Dimensions (in) |
|---|---|---|---|
| Adafruit DC Motor Hat | Polycarbonate | 0.8 | 2.6" x 2.2" x 0.5" LxWxD |
| Avionics PCB Shield | Polycarbonate | 1 | 3.8" x 2.5" LxW |
| BMP388 Pressure Sensor | Polycarbonate | 0.11 | 0.8" x 1.1" x 0.2" LxWxD |
| BNO055 Inertial Nav Unit | Polycarbonate | 0.11 | 0.8" x 1.1" x 0.2" LxWxD |
| Dual Band HAM Antenna | Plastic | 1.38 | 4.72 x 6.69 x 0.51 LxWxD |
| ESC Power Distribution Board | Polycarbonate | 0.63 | 4.9" x 4" x 0.2" LxWxD |
| Omnidirectional RFM Antenna | Plastic | 1.06 | 0.25" x 1.73" LxW |
| Parallax 360 Feedback Servo | Steel | 1.62 | 1.6" x 1.5" x 0.8" LxWxD |
| Raspberry Pi 4 | Polycarbonate | 1.62 | 3.5" x 2.3" x 0.76" LxWxD |
| Raspberry Pi Cam Model G | Polycarbonate | 0.39 | 0.98" x 0.94" x 0.5" LxWxD |
| RFM96W LoRa Transceiver | Polycarbonate | 0.25 | 1.14" x 1.0" x 0.2" LxWxD |
| RTL-SDR APRS Adapter | Aluminium | 1.7 | 1" x 4" x 0.5" LxWxD |
| TalentCell DC Battery | Lithium Ion | 13.4 | 1.1" x 3.35" x 5.7" LxWxD |

Figure 71: Electrical Components for Payload Experiment

## 4.1 Payload Mechanical

In the preliminary design, three core aspects of the payload were discussed which involved a self-righting rotating mechanism, retention and deployment systems for imaging, and a dedicated electronics board to house the core logic of the camera system.

Isometric views of the current payload experiment design are shown in Fig. 72 and Fig. 73

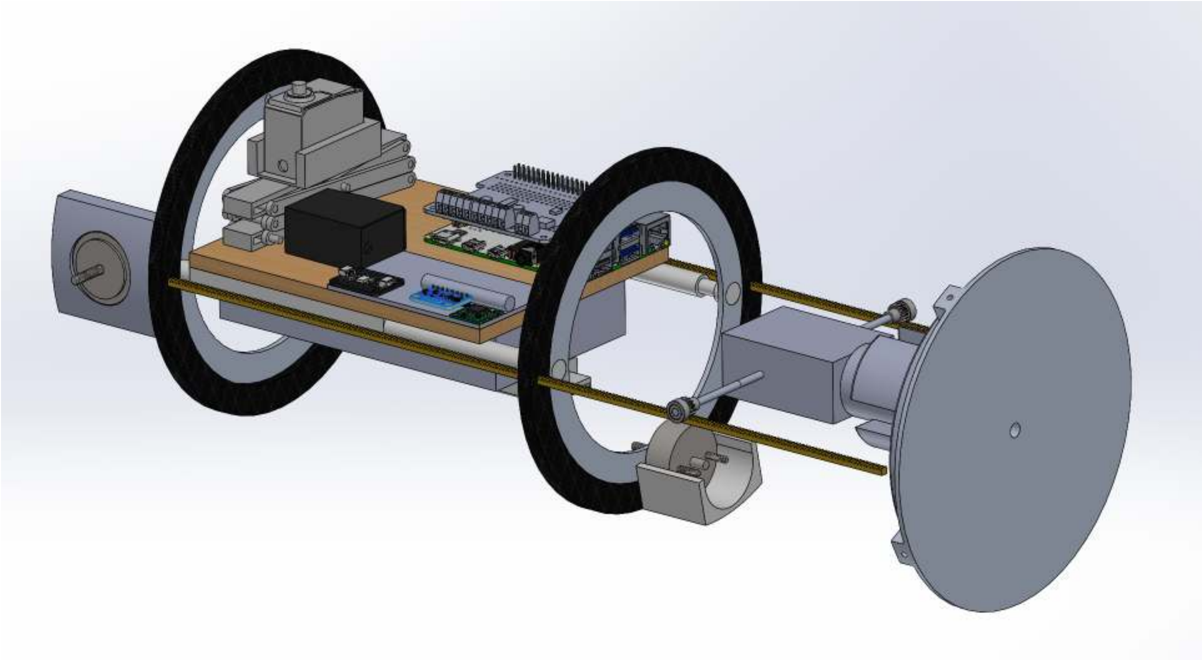

Figure 72: Forward Isometric View of Payload Bay

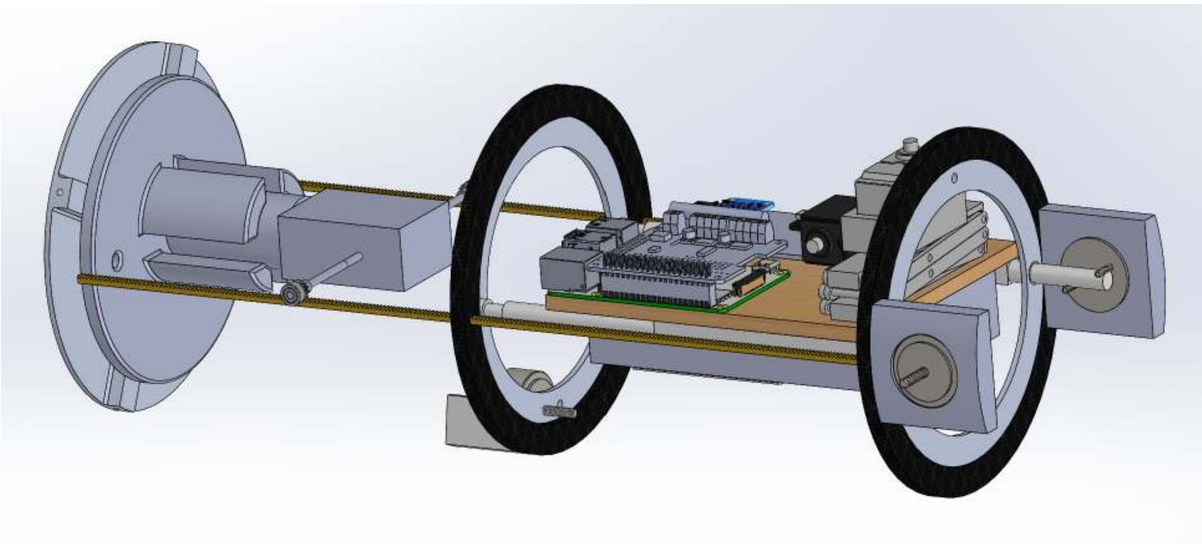

Figure 73: Aft Isometric View of Payload Bay

### 4.1.1 Mechanical System Overview

1. **Self-Righting Design**
   For the self righting design, the team chose to utilize a rotating track design. This allows for the camera board to rotate freely after flight. In order to orient correctly, the camera board is weighted so that the heavier side will always align with the ground. The payload uses solenoids to prevent rotation and therefore damage during flight. The final selected device is the AhCell LS139 steel turntable bearing. This

provides sufficient surface area to mount the camera board rods and enough load support while remaining lightweight at 0.22 lb.

2. **Payload Separation**
For the payload separation, the team chose to utilize a rack and pinion design. The motor will be mounted to the forward bulkhead with a custom designed PETG centering ring piece which is screwed and epoxied. The motor will rotate the pinions, which will then push against the centering rings fixed to the nose cone. This will separate the nose cone and body tube. The pinions are ensured to properly mesh with the rack due to a through-shaft that attaches to the motor and bearings that are mounted to the body tube. This prevents the pinion from lifting from the rack. The overall separation is expected to be roughly 6 in. This allows for the camera to easily deploy. The motor selected to drive the rack and pinion systems is a double shafted DC motor. This allows for enough torque to separate the sections and also eliminates any stress points that would occur due to single-sided separation from a one-shaft motor. The Greartisan 12V 10RPM DC motor was thus selected.

3. **Payload Camera Deployment**
To deploy the camera, the PDR initially selected to use a linear actuator. For this design, the linear actuator would simply lift the camera from the board after flight. After careful analysis and calculation, it was determined that the linear actuator would not fit within the payload size constraints. Therefore, a scissor lift mechanism will now be used instead. The scissor lift mechanism will maintain all 3-D printed parts and will be driven by a servo. The scissor lift will be fixed to the forward side of the camera board.

4. **Retention Mechanisms**
Lastly, the integrity of the entire payload must be taken into consideration in order to ensure successful mission execution. The primary concerns with the current design of the payload are the physically moving components. This includes the self-righting rotating track, as well as the separable nosecone.

### 4.1.2 Self-Righting Design

1. **Self-Righting Rotating Track** The purpose of the self-righting rotating track is to allow the camera board system to achieve the proper orientation (parallel to the ground) after flight. There are two self-righting tracks, one mounted to the nose cone and one mounted to the body tube. Each track is mounted concentrically within a custom machined, PETG centering ring that is fixed via epoxy to the inner diameter of the respective rocket tube portion. PETG was selected for its versatility in being both machinable and relatively sturdy enough to withstand physical stresses during flight. The centering rings account for circumferential changes while also allowing free rotation of the bearings. The camera board is mounted to the self-righting tracks via two telescoping tubes, which passively expand with the payload separation system. There were a number of track component options that were evaluated. Overall, it was decided that the Steel Ball Bearing Rotating Track was the optimal choice. These bearings are extremely lightweight and fit perfectly with our design constraints. Furthermore, they are easily machinable to the desired configuration. The selected bearings also allow the most surface area out of all the

options for fixing the camera board mounts to the rotating bearings. This was a large point of concern, as the camera board mounts will experience heavy torques during in-flight rotation, and therefore require a reliable mount. Finally, the selected bearings are also able to withstand a substantial amount of concentrated force. This is relevant to our separation concept, which will push against the bearings in order to separate the nose cone and body tube after flight. The final drawing design of the self-righting track is illustrated below in Fig 74.

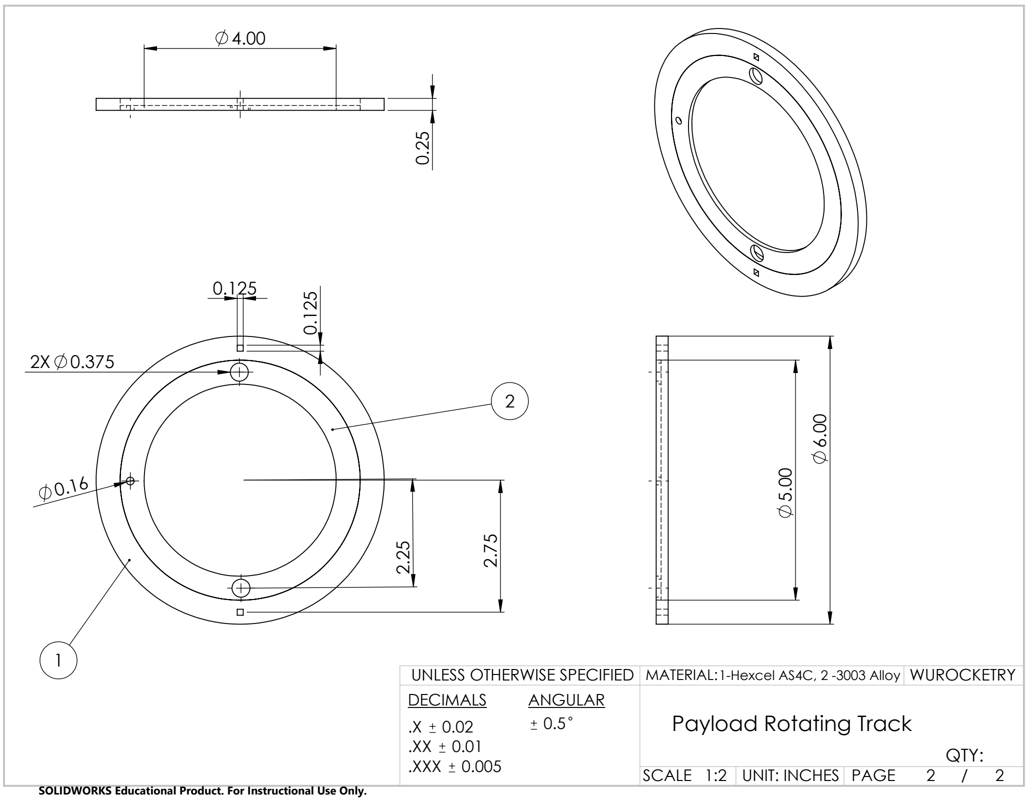


Figure 74: Payload Rotating Track Drawing

### 4.1.3 Payload Separation

1. **Rack and Pinion** The purpose of the rack and pinion is to separate the nose cone from the payload bay and allow for the camera to be deployed. The rack is small yet long enough to push off the nose one and still fit through a hole in the centering rings. The selected material for the rack was steel, which provides the necessary strength to withstand the forces during separation and not suffer damage throughout the flight. There are two of these racks where each is 15 in long. They will work in tandem with the two gears and a motor in order to push off the nose cone. Thereby allowing our camera to deploy and take pictures. The gears in the setup have a pressure angle of 20 degrees with 15 teeth and a 48 gear pitch. These spur gears will be made out of steel as well, also allowing the gears to remain durable and retain its shape when connected with the rack. Their diameter will be 0.354 inches with a thickness of 0.125 inches as shown in Fig. 75. Both of these parts will be placed in the payload section of the rocket. The weight was a main concern along with durability. The rack moves through a hole drilled within the centering rings

of the payload section. The setup is then driven by a motor and pushed forward in order to push off the nose cone thus creating space for the camera to deploy. Risks of utilizing this system include the gear losing contact with the rack meaning the motor could no longer drive the rack. To mitigate this, the motor is locked in place to the rack, unable to move so it cannot separate from the rack. Another possible concern would be the friction of the racks moving through the centering ring holes preventing enough force to push off the nose cone. To prevent this, the rack will be lubricated on the bottom to reduce friction and ensure the rack is effective.

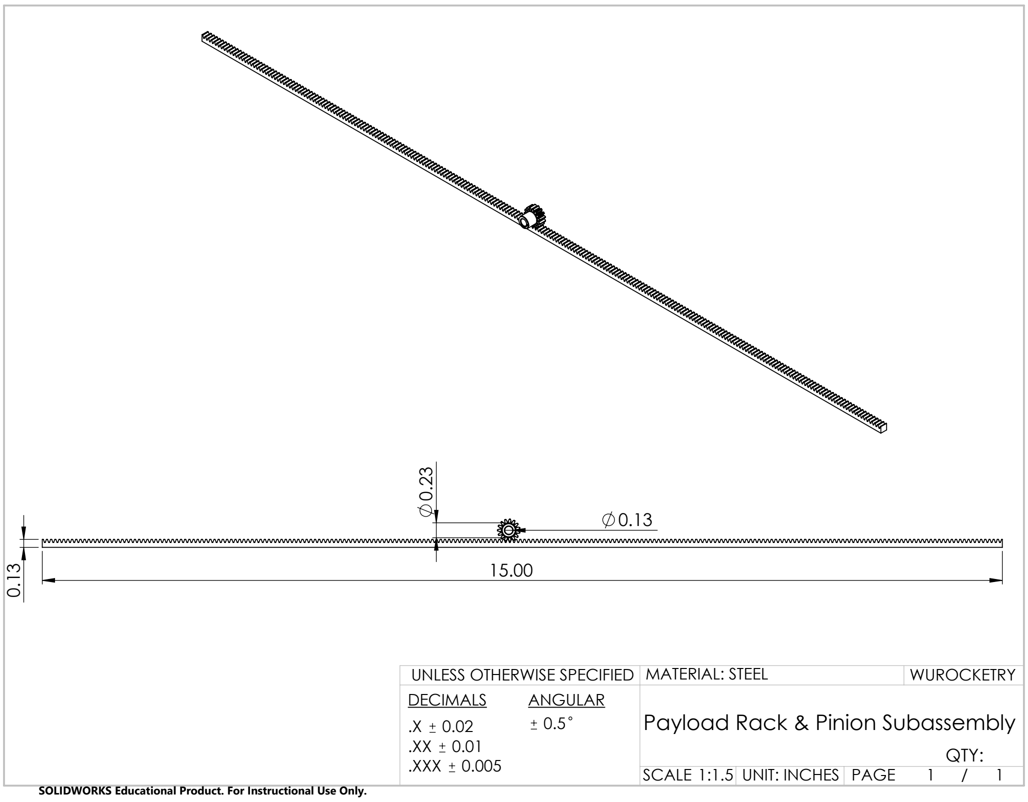


Figure 75: Rack and Pinion Track Drawing

2. **Telescoping Rods** The team will be able to make our own centering rings for payload because the centering rings are simple shapes to machine and will need to have custom dimensions for our design. Using plywood will provide us with the high strength the team needs while also making the machining of the centering rings relatively easy. The team has decided to mount a bearing system and multiple retention systems to the centering rings so using plywood will make our mounts simple and strong. The team manufactures custom telescoping rods using 3D printed parts because PETG provides enough strength to support the weight of our rotation payload subsection. The telescoping rods will be printed with a high 20-30% infill and will have a longitudinal print orientation that gives the rods high shear strength. The complete separation subassembly drawing is illustrated below with the rack and pinion setup implemented with the telescoping rods support.

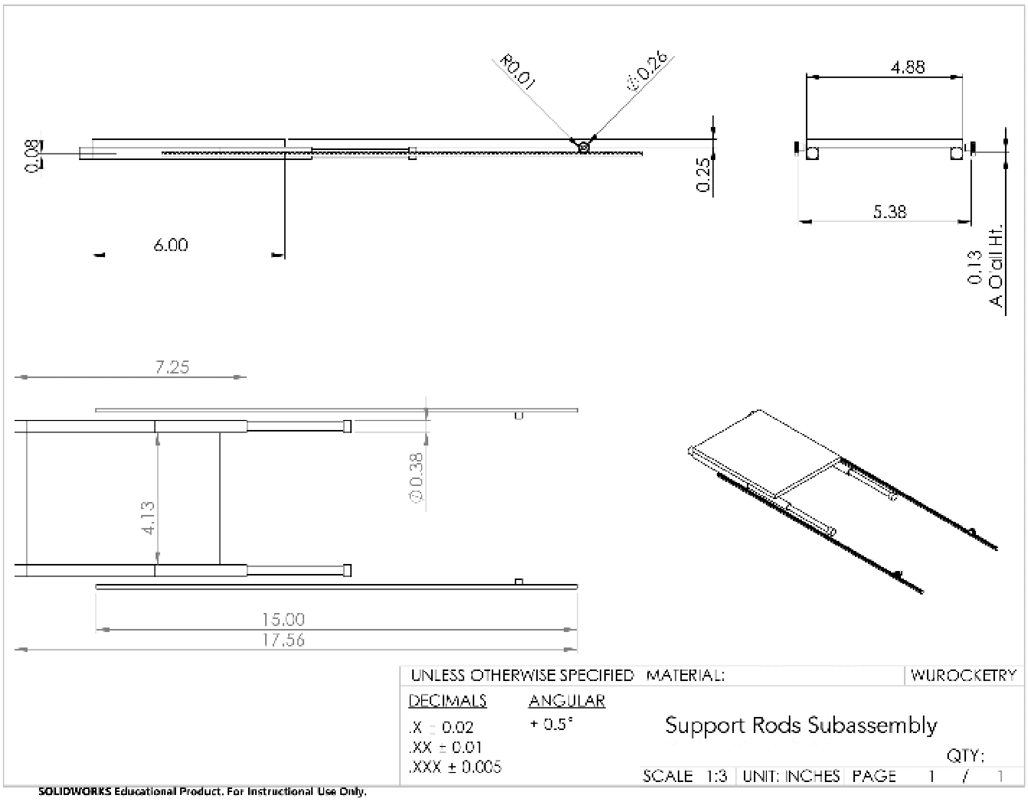


Figure 76: Rack and Pinion with Telescoping Rods Drawing

3. **DC Motor** The rack and pinion separation mechanism will be powered by a 12V double shaft DC motor. This motor is a double shaft because it will turn two gears at the same time to separate the nose cone from the body tube of the rocket. This is more reliable than using two smaller motors and trying to synchronize their movements so that both rack and pinions move at the same time. This motor has a gearbox that revolves at 10 RPM and outputs a rated torque of 2.89 lb/ft, which will ensure the rack and pinion has enough force to separate the nose cone from the body tube, even if the rocket has landed in undesirable terrain. This motor is the heaviest component of this year's payload at 0.82 lb, and this is because the shaft, gearbox, and electric motor are all made of steel. The motor and gearbox together are 11.54 cm in length and 4.01 cm wide. In addition, this is able to operate between 0-70 °C, so it will be able to handle any difficulties during launch. The DC motor is illustrated in Fig. 77.

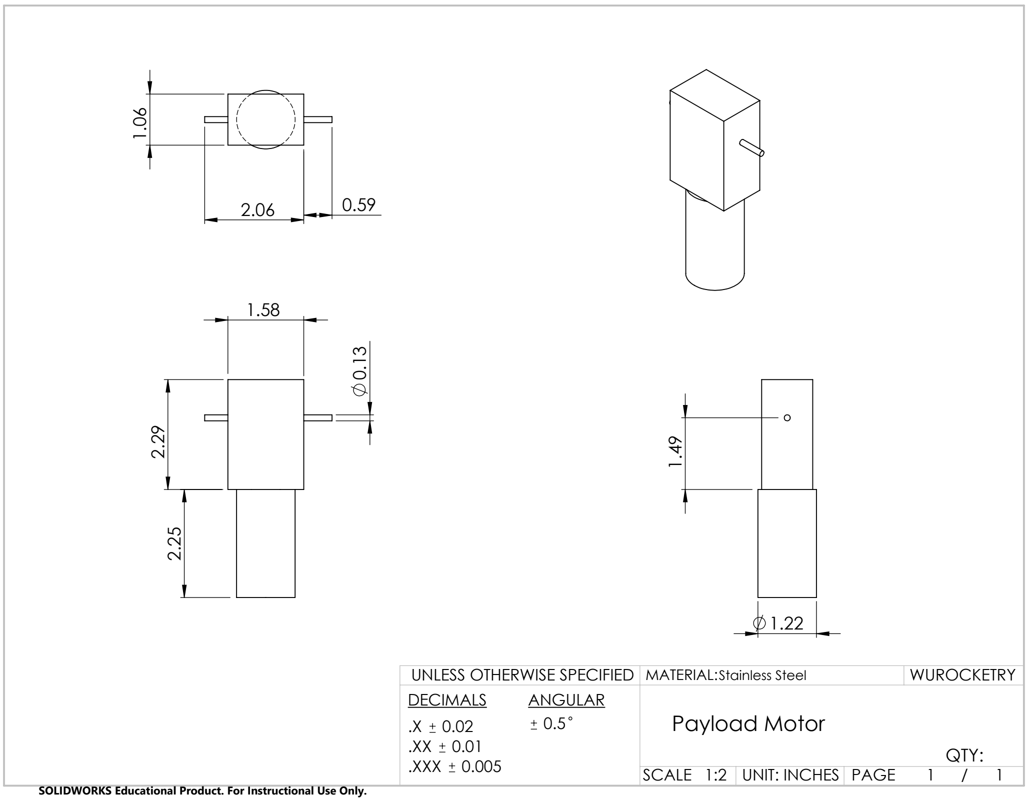


Figure 77: Payload Separation Motor Drawing

4. **Motor Axle Bearings (60355K41)** The purpose of the motor axle bearings is to provide a fixed boundary condition for the pinion shaft. This fixed boundary condition will ensure a proper mesh between the rack and pinion and consequently guarantee that the separation components will function. The two bearings will be mounted directly to the inside of the body tube. The shaft that is connected to the motor will go through the pinion inner diameter and directly fit into the bearings. The selected motor axle bearings that will be included in the final design are the MMC R2-2Z Shielded Bearings with 1/8 in ID (60355K41). These bearings were selected for a number of reasons. First, they are rated to a 50 lb dynamic load, which is within our expected limits for the design. Additionally, the bearings are shielded, which will prevent any debris interference. Third, they utilize a push fit for the shaft mounting, which is much more adaptable to our design. The bearings are pre-lubricated, which limits any error during assembly. Finally, they are lightweight and fit within our geometric design constraints. The OD is 0.375 in and the ID is 0.125 in, and the width is only 0.15625 in. These dimensions are further visualized in Fig. 78.

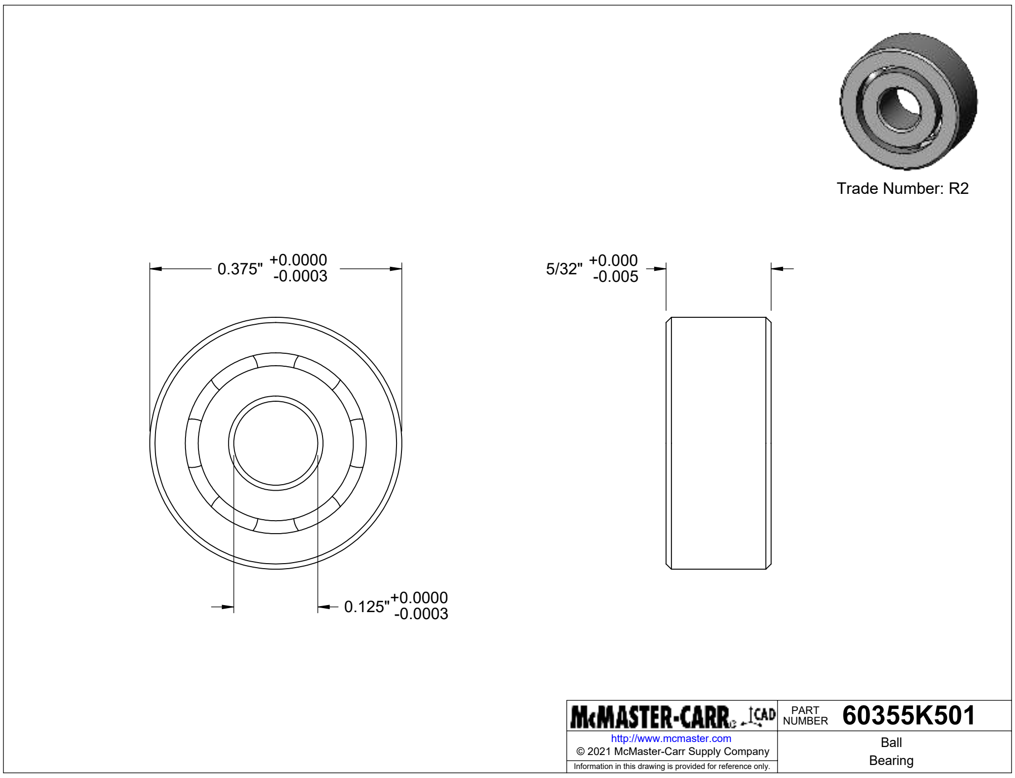


Figure 78: Motor Axle Ball Bearing (Source McMaster [1])

#### 4.1.4 Payload Camera Mechanisms

1. **Pollolu Parallax 360 Servo** In order to rotate the camera various to various positions as required in the payload mission, the Pollolu Parallax 360 Degree servo was selected in the final design for its primary improvements in torque and precision as compared to the previous SG90 servo used in the PDR design. The Parallax is built from a durable plastic housing that contains a steel gears to drive the axle of the servo. The dimension of the servo is around 1.6 × 1.5 × .8 in., which can be seen in Fig. 79. The servo weighs around 1.44 oz, a relatively light component whose increased mass is compensated for its increased stall torque of 35 oz-in when run at 6 volts.

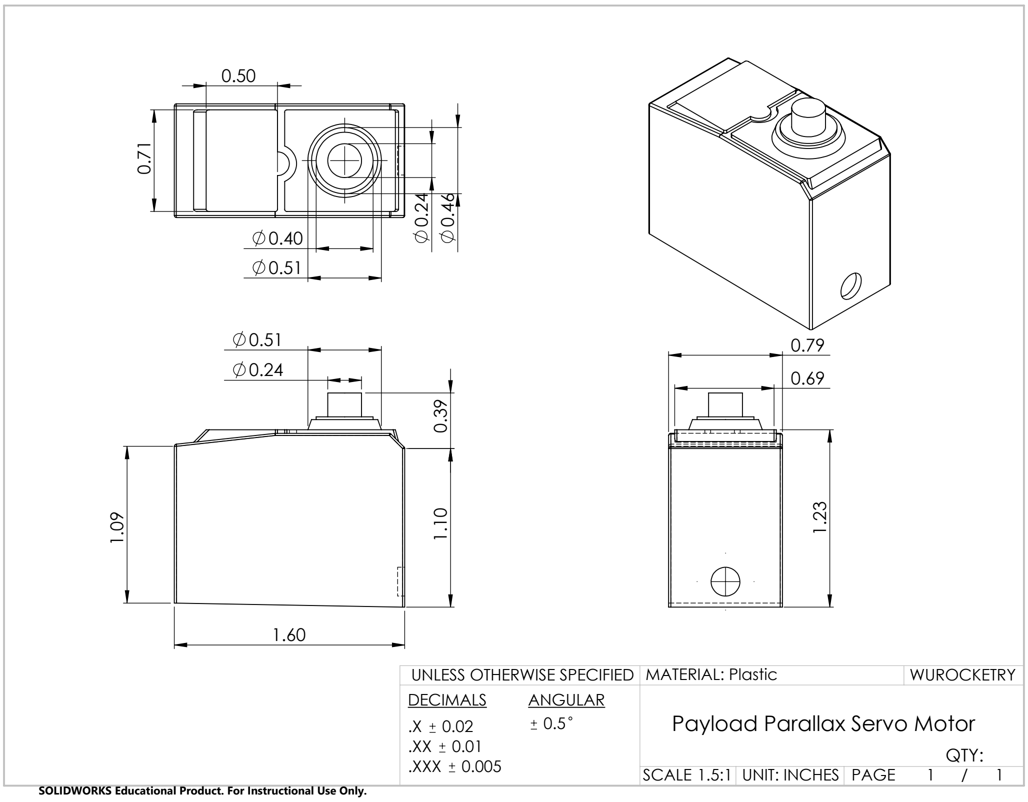


Figure 79: Pollolu Parallax 360 Servo Drawing

2. **Scissor Lift Deployment** To deploy the camera, the PDR design initially selected to use a linear actuator. For this design, the linear actuator would simply lift the camera from the board after flight. After careful analysis and calculation, it was determined that the linear actuator would not fit within the payload size constraints. Therefore, a scissor lift mechanism will now be used instead. The scissor lift mechanism will maintain all 3-D printed parts and will be driven by a SG90 continuous rotation servo that pulls the bottom legs of the lift together. This will cause the lift to extend each layer of rungs upward to ultimately deploy the camera housing above. The scissor lift will be fixed to the forward side of the camera board, nearer to the nosecone during separation. Since the lifting of a scissor lift can introduce changes in the center-of-mass of the payload electronics board, the scissor lift will be oriented in parallel with the axis of the board's rotation to ensure that the COM does not shift to either side of the rotation axis. In addition, the height of the scissor lift is determined by the servo and thus the subteam can determine the optimal height to raise the camera while maintaining stability.

   Both the retracted and extended views of the designed scissor lift can be seen below in Fig 80 and Fig 81.

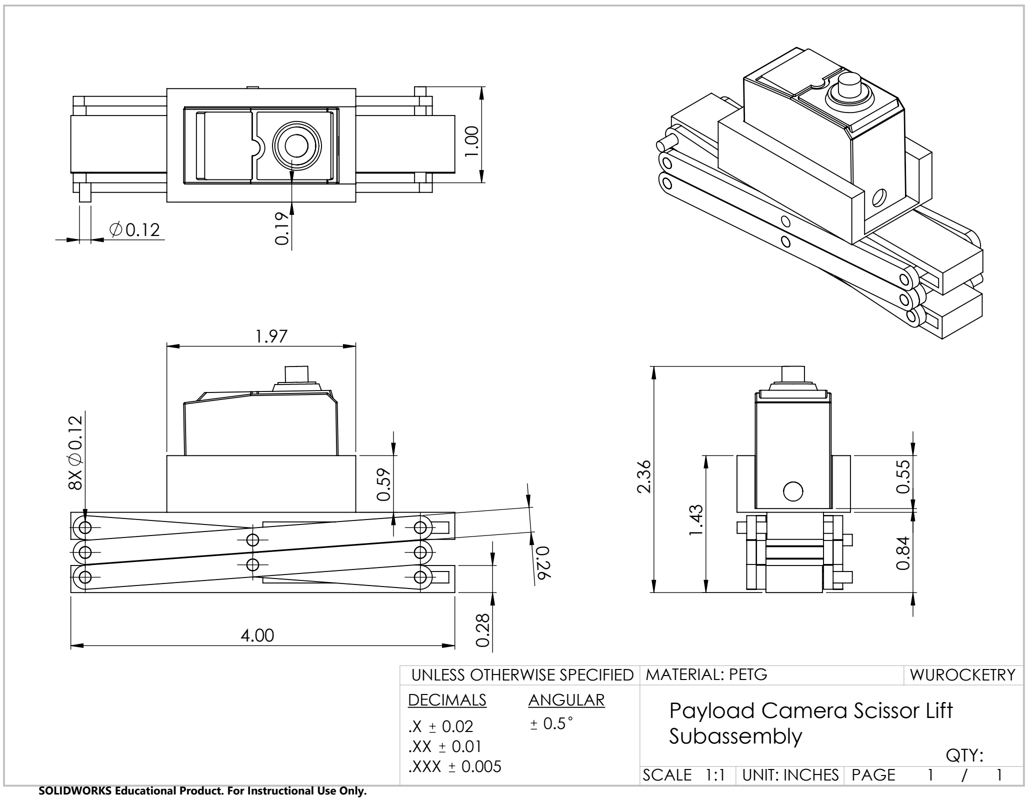


Figure 80: Payload Scissor Lift for Camera Deployment Drawing

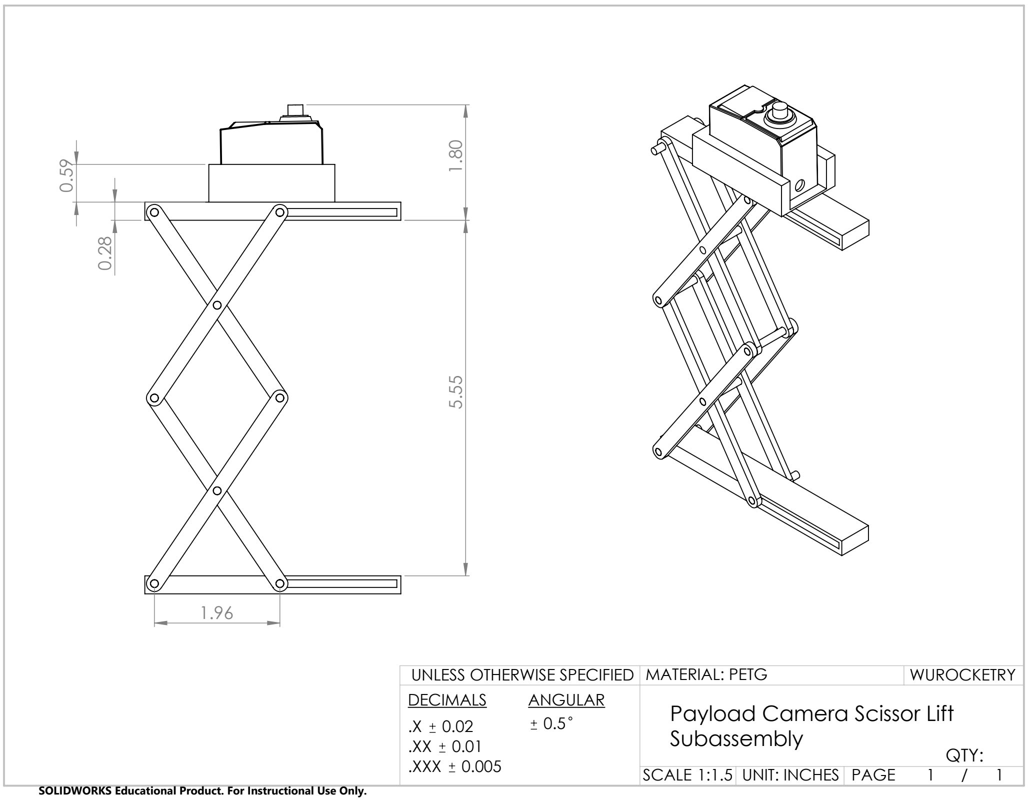


Figure 81: Extended Payload Scissor Lift Drawing

#### 4.1.5 Payload Retention Mechanisms

1. **Linear Solenoid** Since the solenoid will be carrying a large amount of force, the team determined that a steel solenoid with activated retraction would suffice. The solenoid chosen was sturdy yet lightweight, which is important as three of the solenoids will be used for 1. immobilizing self-righting rotation during flight and 2. for nosecone retention. The solenoid is compatible with the battery pack, as it uses 12VDC. The outer diameter is only 1.25 inches and the extended length is 1.5 inches as seen in Fig. 82, which will fit perfectly into position, especially considering that the motor will take up a large amount of room in the back of the payload. The solenoid to stop rotation was added in the empty space below the motor because it could easily fit there. The two solenoids used for nose cone retention are attached to the outer bearing. There will be holes in the body tube where the solenoid can connect. Because of its lightweight nature, having three of them should still allow the team to mount all of the other necessary components without much concern.

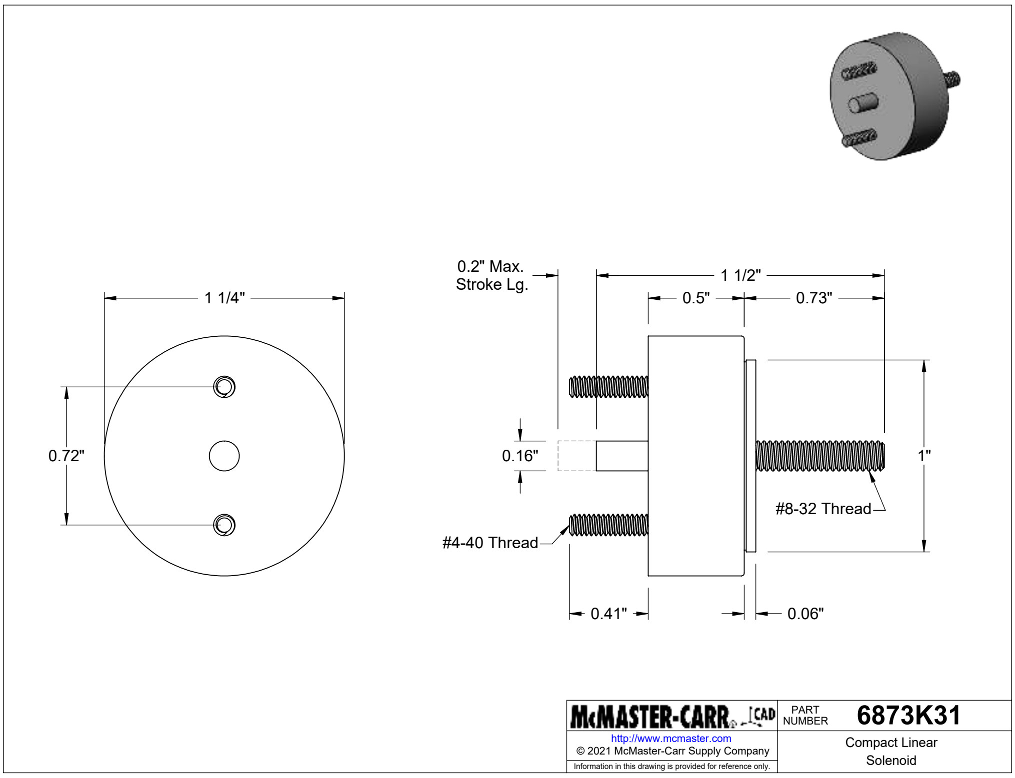


Figure 82: Linear Solenoid for Retention Drawing (Source: McMaster [2])

2. **Nosecone Retention** The nosecone retention mechanism remains as previously designed in the PDR, where a pin-lock mechanism is used by extending pins through the inner lip of the nosecone and body tube at where the two sections connect. The only difference now is that the steel pin will come from the aforementioned linear solenoids. These linear solenoids are composed of a steel housing and are compact enough to be mounted onto the machined, forward section centering ring via screws. The solenoids' implementation into the nosecone retention mechanism is depicted in the below drawing Fig. 83.

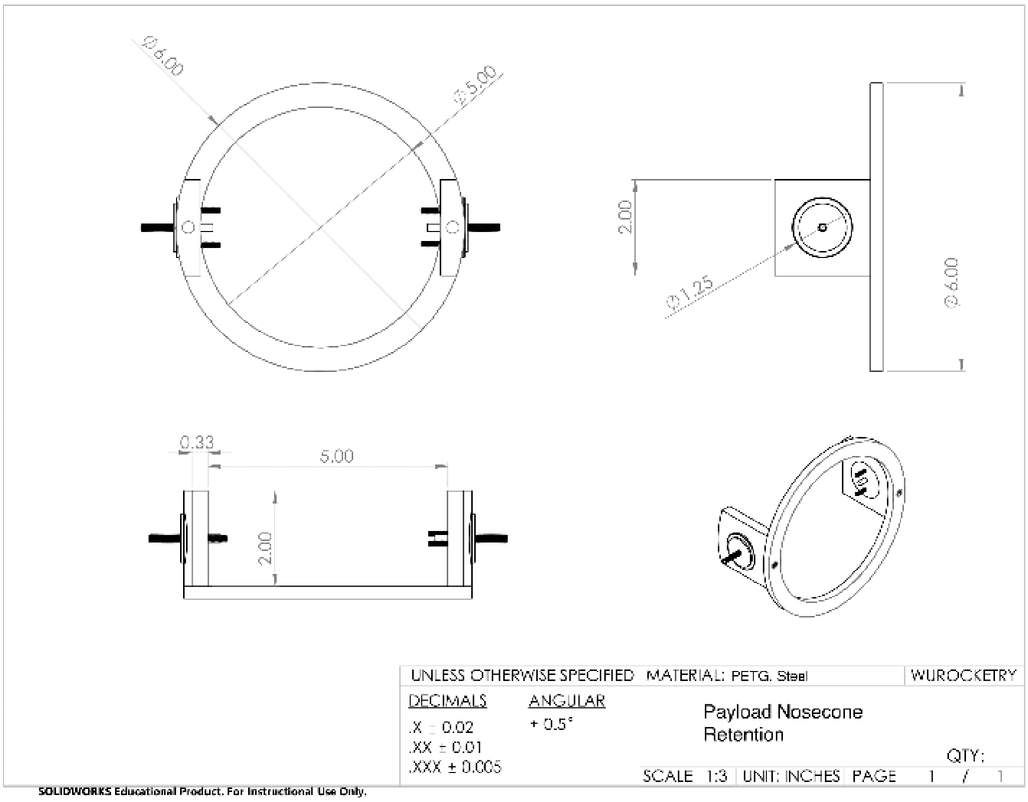


Figure 83: Payload Nosecone Retention Drawing

3. **Rotating Track Retention** In addition to the original nosecone retention, an additional mechanism has been introduced for the self-righting mechanism to ensure that the two rotating tracks do not swivel throughout flight. This was determined as necessary as freely rotating masses will generate variability into the vehicle's center of mass and unwanted torques that may introduce error in flight trajectory. In addition, this helps prevent damage to the internal payload experiment components, particularly the wires that connect static components (such as the separation motor, mounted on the bay aft bulkhead) to components secured on the rotating platform.

   The rotating track retention operates with a similar design as the nosecone retention does. The rotating track itself is a turntable composed of a static center (that is mounted concentrically with the centering ring) which connects to the turntable (that actually rotates and supports the electronics board). Thus, to prevent the turn-table from rotating, a linear solenoid pin will be run through the turn-table's two rotation pieces, locking the two surfaces from rotation. An illustration of this mechanism can be seen in Fig. 84.

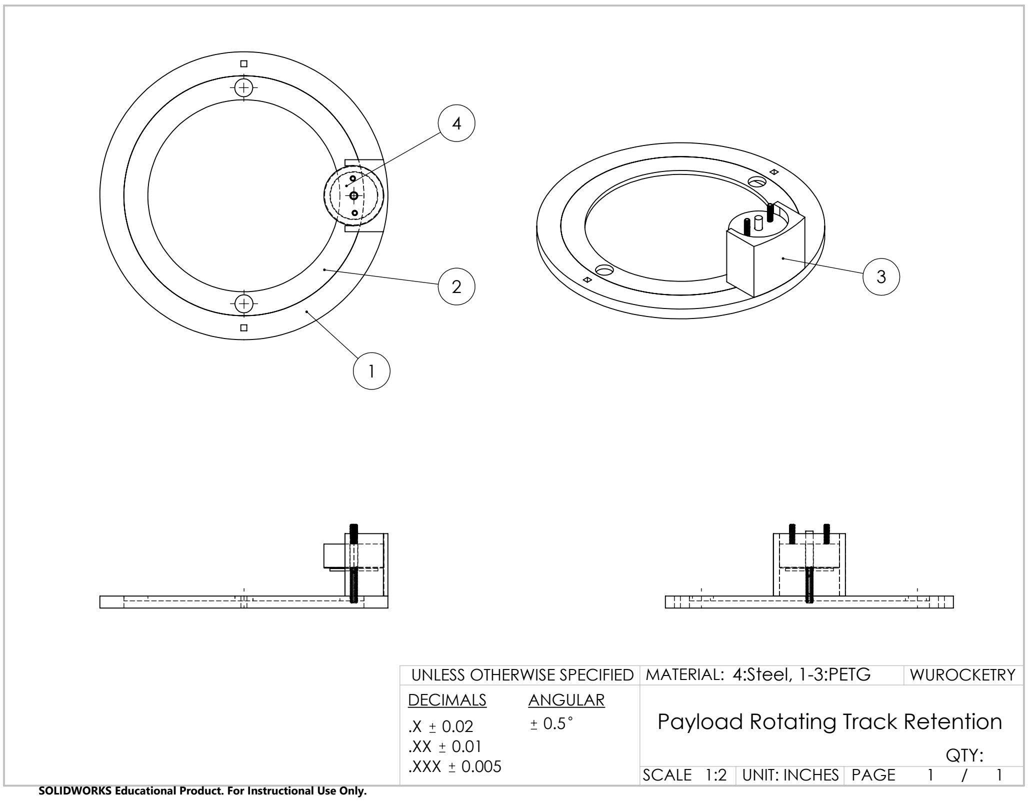


Figure 84: Payload Nosecone Retention Drawing

4. **Separation Motor Retention** In the PDR design, the payload motor was mounted to the inner diameter of the body tube. It is aligned such that the motor is perpendicular to the rocket center axis. It was determined through model dimensions, however, that the motor could not be mounted to the body tube. Thus, it was decided that the motor will instead be mounted to the forward bulkhead. A 3D-printed component will hold the motor in place, and the component will be screwed into the top of the bulkhead. The design can be viewed in Fig. 85 This allows the motor to align perfectly with the rack and pinion design and also allows extra room for additional necessary components. Epoxy will be added to the mount as an added security measure.

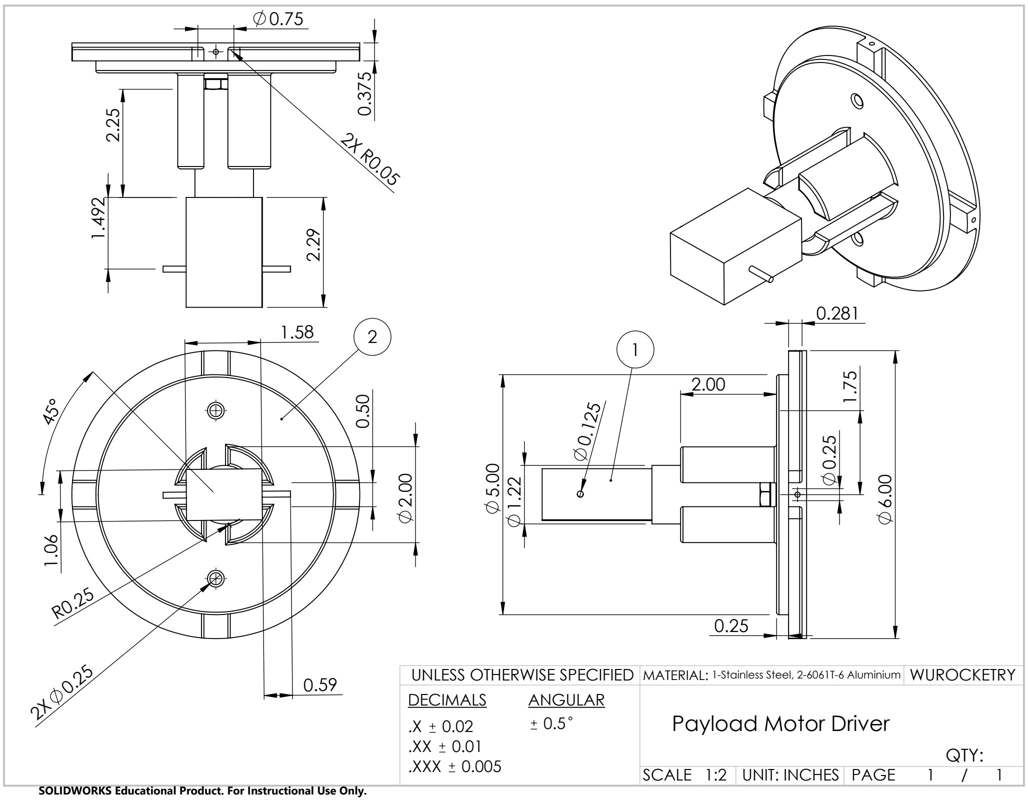


Figure 85: Payload Motor Mount Drawing

5. **Servo and Camera Retention** In order to protect the the servo motor from external forces and to avoid being directly epoxied to any surfaces, a 3D printed PETG housing was designed. It is a minimal housing meant to act as a proxy mount for either being epoxied or drilled into the surfaces it must mount onto. The side walls are also thin as to minimize extra weight being added to the payload.

   Since the camera being used in the payload is a relatively light and fragile component, the same 3D printed housing was also designed to house the camera, its simple design making it universal for housing various light electronics. The mount also features a cutout on the back wall to give room for any wiring such as the camera bus or servo electrical wires. An illustration of the design can be seen in Fig. 86

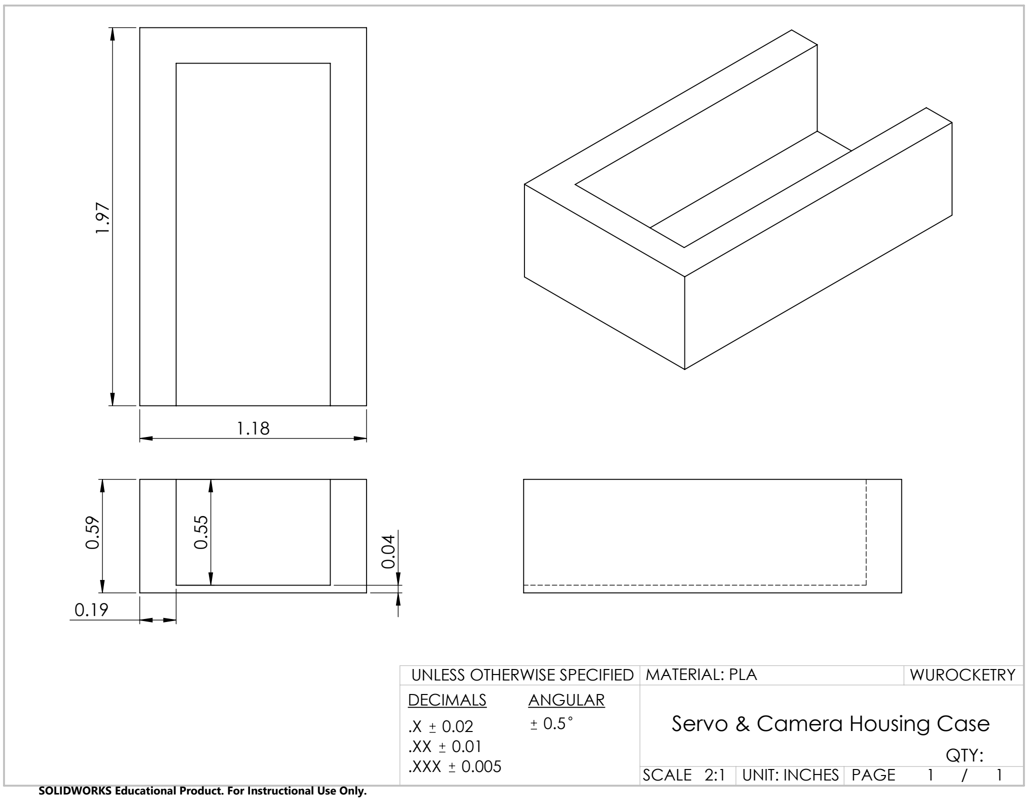


Figure 86: Payload Simple Electronics Mount Drawing

### 4.1.6 Mechanical Component Interaction

Each payload component serves a specific function. During flight, the nosecone retention system is activated, where the solenoids are expanded and prevent the nosecone from separating. Additionally, the anti-rotation solenoids are also expanded to prevent the rotating bearings from turning at all. After flight, all solenoids will contract, allowing the separation to occur and for the rotating bearings to rotate freely. The rotating bearings allow the camera board to orient parallel to the ground after flight. The rack and pinion system will then begin, pushing the nose cone and body tube apart. The racks will move through the body tube centering ring, and push against the nose cone centering ring. This will create a separation distance between the two components of at least 4 in. To deploy the camera, the scissor lift will then raise the imaging system a minimum of 2 in. above the rocket's outer body tube (for a total of at least 5in) to allow for the payload to properly capture images. A top and side view of the payload assembly is shown in Fig. 87 and Fig. 89

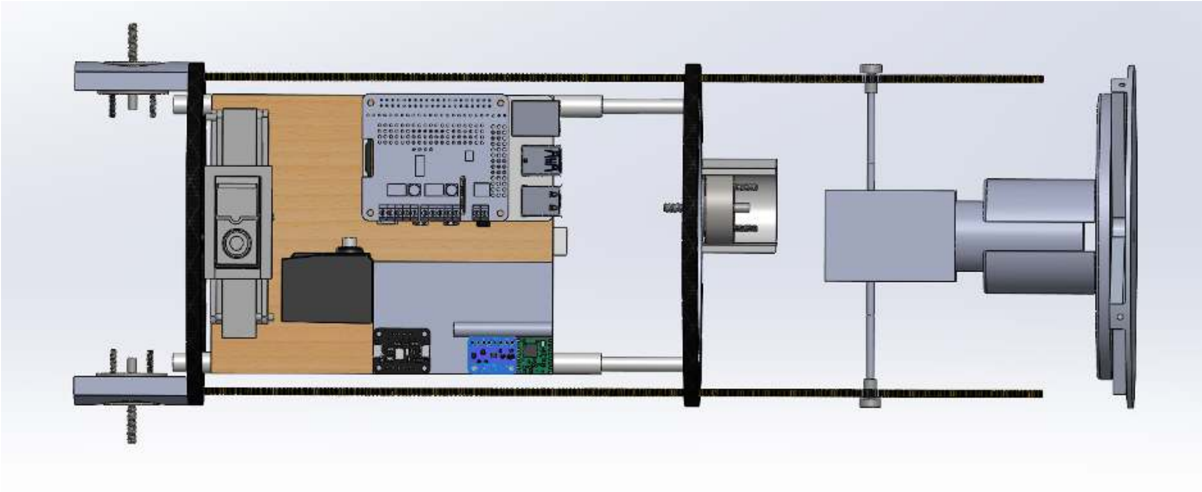

Figure 87: Top View of Payload Component Layout. The nosecone side is on the left and the forward body tube side is on the right.

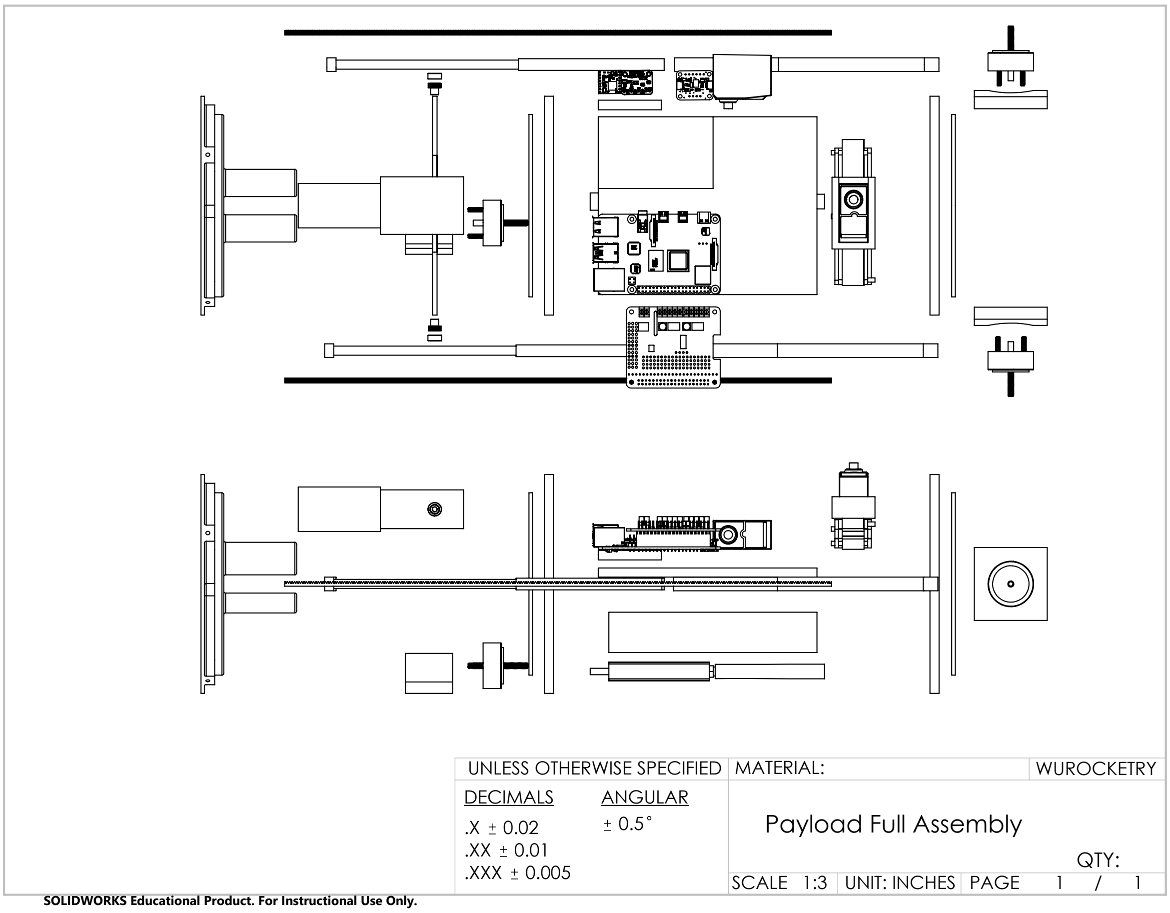


Figure 88: Exploded Top View of Payload Component Layout. The right side inserts into the nosecone and the left side inserts into the forward body tube.

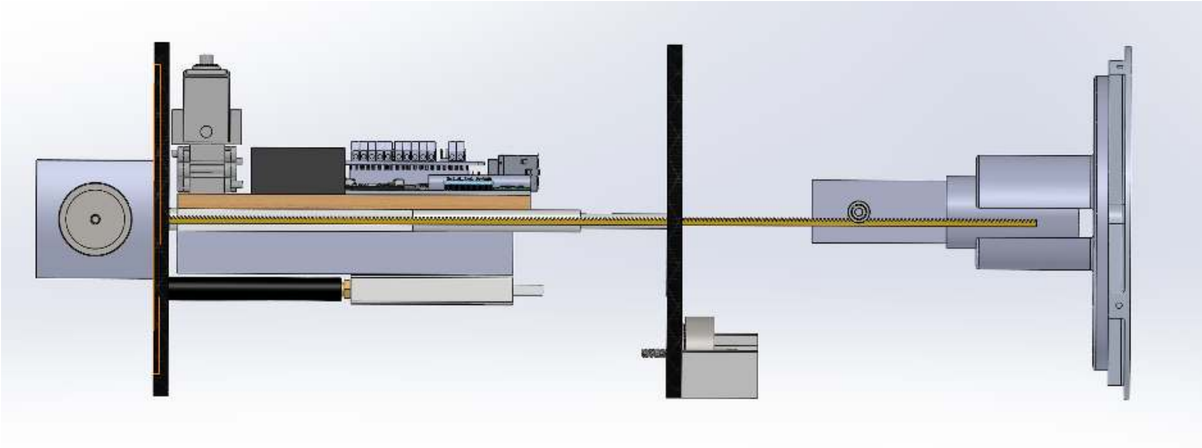

Figure 89: Side View of Payload Component Layout

The specific components of the payload full assembly are shown in the table below, along with an exploded view of the full assembly in Fig. 90

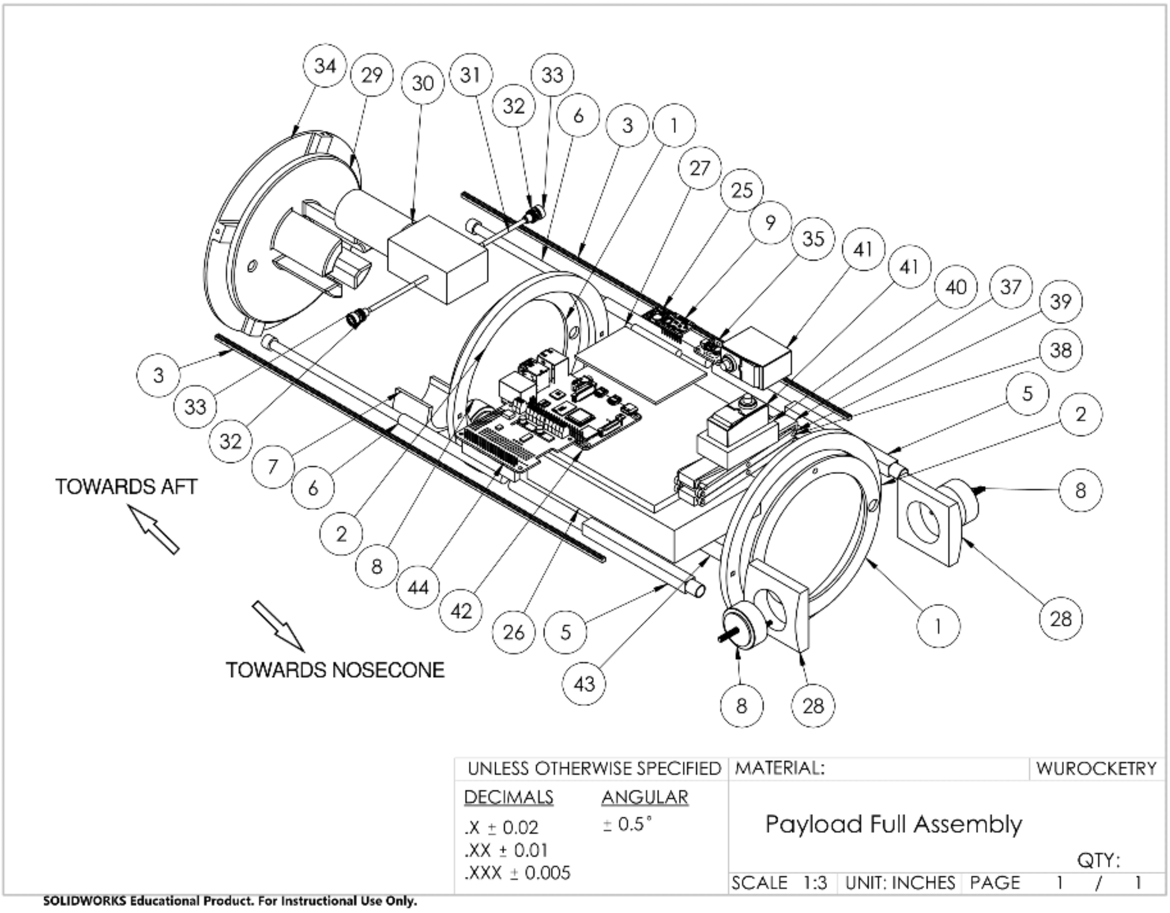


Figure 90: Exploded View of Payload Full Assembly with BoM Callouts (listed in Fig. 91)

| ITEM NO. | PART NUMBER | Material | QTY. |
|---|---|---|---|
| 1 | Inner Rotating Bearing | Steel | 2 |
| 2 | Outer Centering Ring | Fiberglass | 2 |
| 3 | 7854K12 - Metal Gear Rack - 20 Degree Pressure Angle | Steel | 2 |
| 4 | Electronics Board | Plywood | 1 |
| 5 | Telescoping Rod Holder | PETG | 2 |
| 6 | Telescoping Rod | PETG | 2 |
| 7 | Linear Solenoid Mount - Rotation Retention | PETG | 1 |
| 8 | 6873K31 - Compact Linear Solenoid | Steel | 3 |
| 9 | BMP388 | | 1 |
| 10 | RFM96W | | 1 |
| 11 | TelentCell 12V/5V DC Battery | | 1 |
| 12 | Avionics Shield | | 1 |
| 13 | Linear Solenoid Mount - Nosecone Retention | PETG | 2 |
| 14 | DC Motor Mount | PETG | 1 |
| 15 | Geartsian 12V DC Motor | | 1 |
| 16 | Geartsian 12V DC Motor Connecting Rods | | 1 |
| 17 | 7880K18 - Metal Gear - 20 Degree Pressure Angle | Steel | 2 |
| 18 | 60355K501 - Ball Bearing | Steel | |
| 19 | Top Bulkhead | Aluminum | 1 |
| 20 | BNO055 | | 1 |
| 21 | Bingfu Dual Band Antenna | | 1 |
| 22 | Scissor Lift | PETG | 1 |
| 23 | Raspberry Pi 4 Model B | | 1 |
| 24 | RTL SDR Adapter | | 1 |
| 25 | DC Motor Hat | | 1 |
| 26 | Parallax 360 Servo | | 1 |

UNLESS OTHERWISE SPECIFIED

DECIMALS: .X ± 0.02, .XX ± 0.01, .XXX ± 0.005

ANGULAR: ± 0.5°

MATERIAL:

WUROCKETRY

Payload Full Assembly

QTY:

SCALE 1:10 UNIT: INCHES PAGE 1 / 1



Figure 91: BoM of Full Assembly Components

### 4.1.7 Payload Launch Vehicle Integration

The payload sits inside the forward body tube and nosecone. The forward centering ring is a PETG ring which is fixed inside the nosecone via epoxy. The aft centering ring is a PETG ring which is fixed inside the body tube also with epoxy. These centering rings allow the rotating track to maintain proper alignment in the rocket. The centering rings will be fixed to the rocket with epoxy. The nosecone retention solenoids are fixed to the body tube with PETG printed housing and epoxy. The position of the solenoids sit at the section where the nosecone shoulder fits into the body tube so that the pins of the solenoid can extend through both surfaces, locking the nosecone together with the body tube. This can be seen as illustrated in Fig. 92. The rack and pinion motor is fixed to the body tube top bulkhead with a custom printed part, epoxy, and screws. To separate the sections, the rack and pinion system will push against the nose cone centering ring. After separation, the motor will turn the opposite direction to retract the racks and allow the camera to properly deploy.

Illustrations of the payload integration with the vehicle are shown below in Figs. 92 through 95.

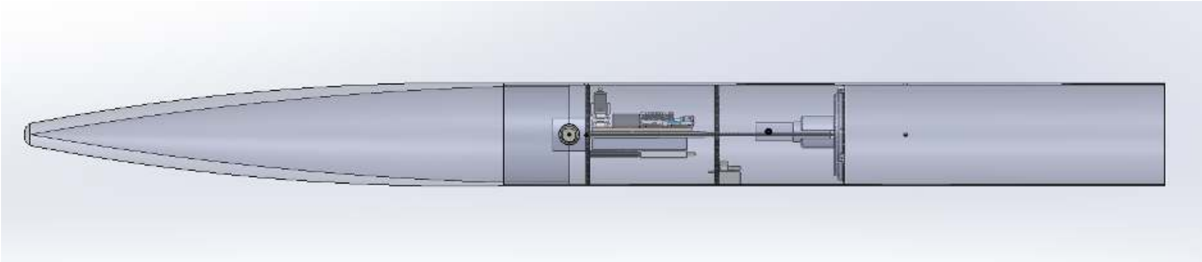

Figure 92: Side view of Payload integration with launch vehicle in a closed state

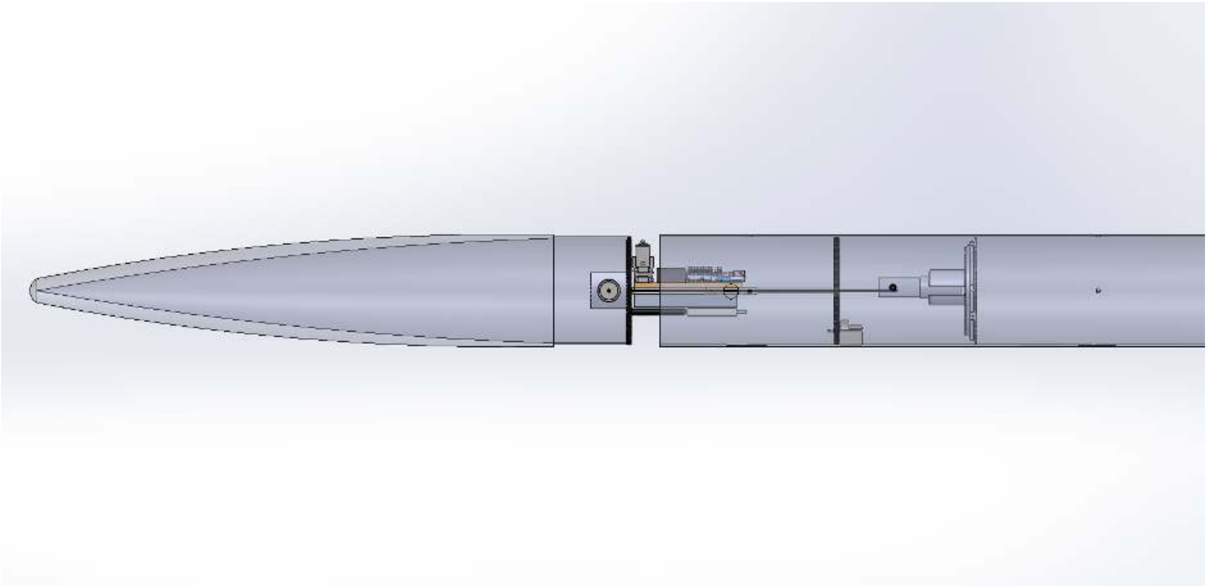

Figure 93: Side view of Payload integration with launch vehicle in a separated state

Figure 94: Isometric view of Payload integration with launch vehicle in a closed state

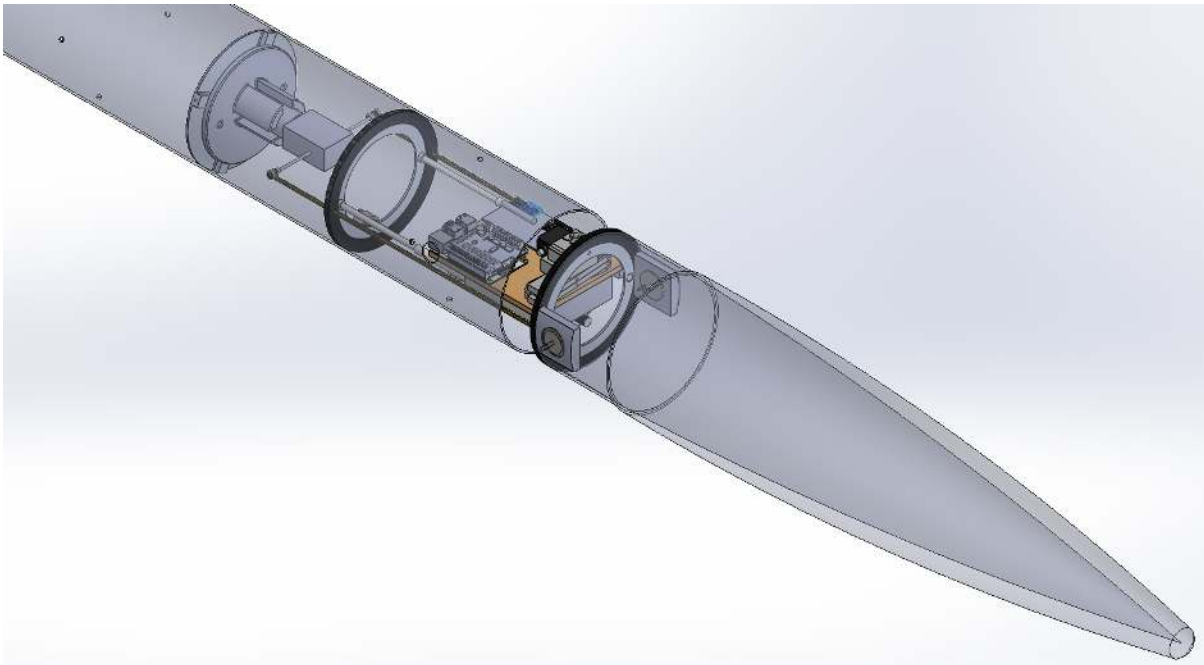

Figure 95: Isometric view of Payload integration with launch vehicle in a separated state

## 4.2 Payload Electrical

### 4.2.1 Electrical System Overview

The electrical system has remained relatively the same as the initial preliminary design. However, the several subsystems that compose the electrical component of VISiON's mission have been further organized into final roles. These subsystems are as listed:

1. **Vision and Image Technology**
   This subsystem is responsible for maintaining the vision capabilities of the payload experiment.

2. **Radio and APRS Communications**
   Maintaining consistent communication with the payload to monitor the progress of the mission is critical for ensuring that VISiON functions as intended, while noticing any potential failures and hazards prior to the event. In addition, the payload mission requires the reception of RAFCO over the APRS network and thus the capture of such packets of data will be facilitated by this subsystem.

3. **Avionic Sensing Capabilities**
   The payload mission requires that the experiment operate and perform certain functions only at specific phases of the flight. Thus, to enable such comprehension of the flight the Avionic Sensing subsystem will perform the necessary data collection through its sensors to achieve this.

4. **Electromotives and Power Distribution**
   Every physical component must be driven by a reliable and adequate power supply, this is especially so for the electromotives that perform controlled mechanical tasks such as retention and separation. This subsystem is responsible for safely powering such components.

5. **Software Control Architecture**
   Lastly, the entirety of the electrical system of the payload experiment must work together cohesively in order to carry out the mission. To achieve this, a main software routine integrates each subsystem under a single, well defined logical path that performs the necessary payload mission phases as well as initiating fail-safe measures at any point of error.

   These electrical subsystems are visualized in an overall payload system as seen in Fig 96.

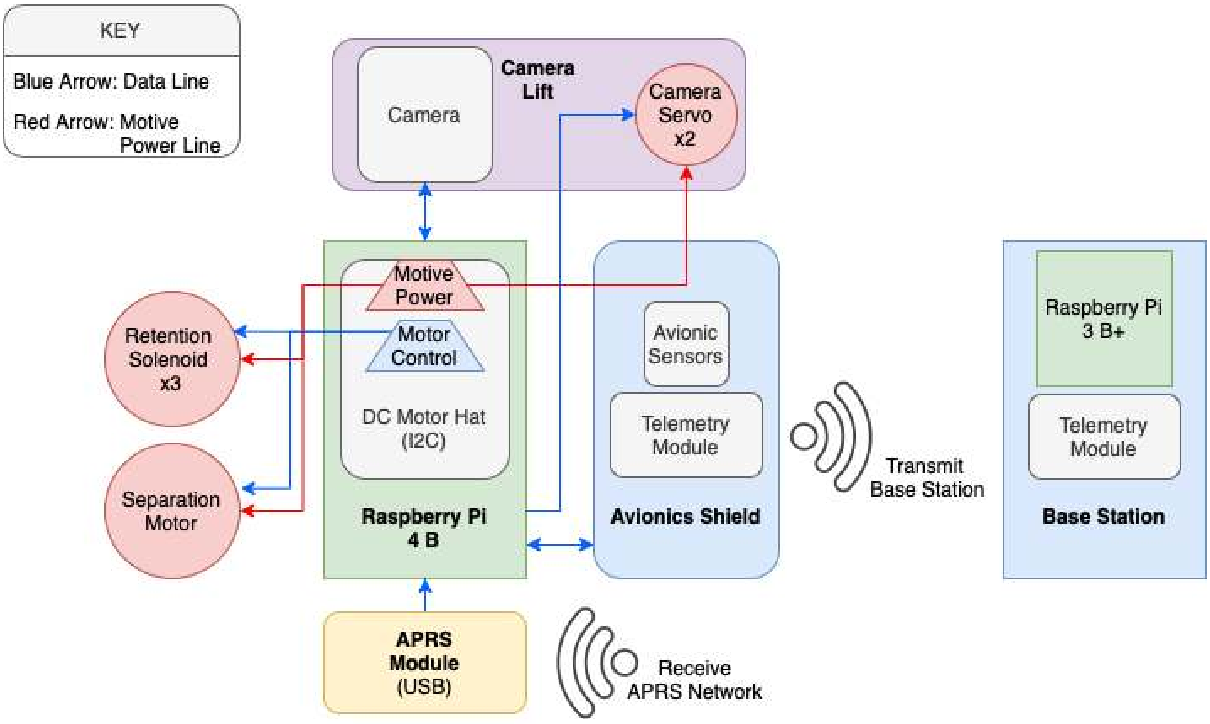


Figure 96: Block Diagram Illustrating Electrical System

The specific electrical components used within this system is also shown in the exploded payload full assembly drawing from Fig. 90

### 4.2.2 Vision and Image Subsystem

1. **Pollolu Parallax 360 Servo** A new servo was selected for the final design for rotating the camera as required per the imaging system. The Pollolu Parallax Feedback servo provides the same functionality as the previous SG90 continuous rotation servo, but includes a signal line from an internal Hall effect sensor providing digital angular position of the servo for use in software. The drawing of the servo is visualized in Fig.79. The servo works well due to its 5V-6V operating voltage, low 15mA idle and 150mA load current draws. The housing of the servo is made of a durable plastic capable of withstanding heat. The servo uses PWM over a singular control pin Only interfaces over the control pin. Unlike other servos, this servo can rotate twice as far (360 degrees v.s 180 degrees) This servo will feedback its angular position allowing for easy calculation of camera direction This servo contains many more features than most servos available on the market and only costing slightly more than the usual continuous servo. Thus the Parallax 360 is used in the final design for its capability handle the rotation of the camera and be controlled using two pins on the Pi 4.

2. **Raspberry Pi Camera Model G** The Raspberry Pi Camera (Model G) fares reasonably well with adjustable focus distance from aperture (F) of 2.35, and focal length of 3.15mm compared to its alternatives. The chosen camera module supports all revisions of the Pi, providing robust driver type supported including libcamera and Raspicam. The design of the camera module can be seen in Fig. 97. The

camera takes commands from the Raspberry Pi to take still pictures and then writes the picture to the Pi's local disk space. For communication protocols, the camera module supports DSI interface (display) and the CSI interface (camera). To support its functionalities, the camera module provides 3.3V power output. With a 160 degree field of angle, the camera module may transfer images up to still resolution of 2592 × 1944 pixels. The camera module also allows for adjustable exposure. Its various functionalities put the altimeter as relatively cost effective (less than 30$ per unit). It weighs around 0.5 pounds, and measures around 25mm x 24mm.

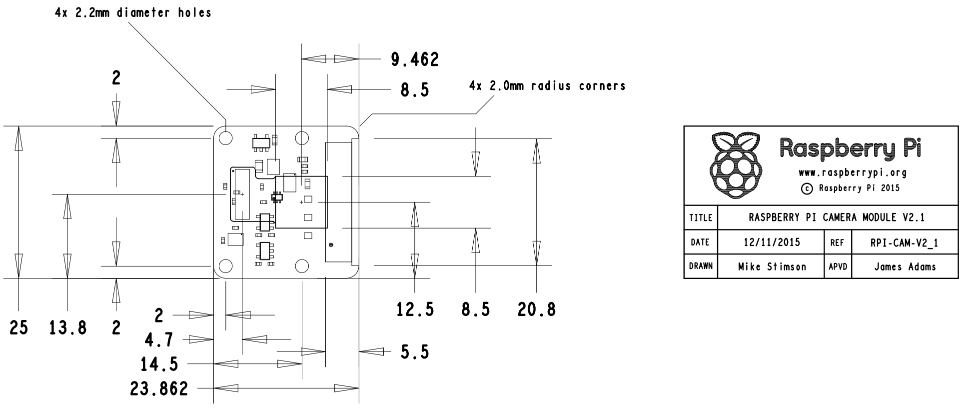


Figure 97: Raspberry Pi Camera Drawing in mm units (Source: RPi Foundation [6])

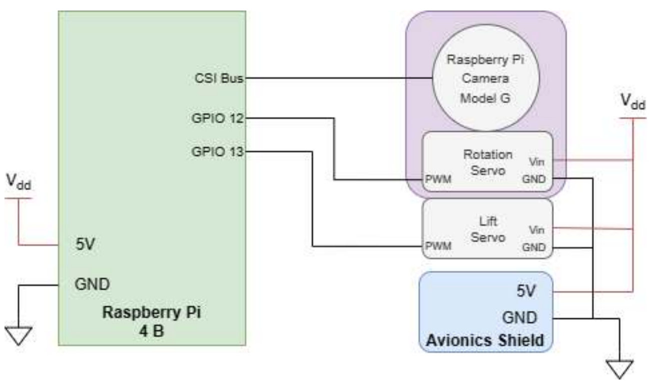


Figure 98: Image and Vision Subsystem Block Diagram

### 4.2.3 Telemetry and Radio Subsystem

This subsystem is composed of two radio setups. One is the team-based telemetry system that enables the transmission of payload mission data from the vehicle to the team's base station. This is accomplished through the use of two UHF transceivers. The second is the USLI-required APRS network receiver for capturing and executing RAFCO sent to VISiON. These two setups are described further below.

1. **VHF/UHF Band Antennas**
   Communication over long distances is difficult, especially when the power output of certain transmitters cannot adequately be picked up by on-board receivers. To resolve this issue, the team decided on the use of two antennas for the two radio communication subsystems.

   The telemetry setup requires the use of a Helical RF Antenna from RF Solutions to provide omnidirectional transmission of telemetry data with 2.5 dBi gain. This allows for the team to maintain communication with the payload over fair distances up to a few kilometers.

   The RTL-SDR receiver is also connected with a UHF/VHF ham band antenna from Bingfu. It is also an omnidirectional antenna to ensure that the payload can reliably capture RAFCO no matter its source transmission location.

2. **RFM96W LoRa Telemetry Receiver**
   Telemetry is maintained through the use of two RFM96W LoRa transceivers that operate around the 433 MHz frequency. One will remain on-board with the payload to transmit data, while the other at the team's base station to receive.

   The RFM96W RF fares reasonably well with three distinct RF power amplifiers, which renders its high sensitivity down to -144 dBm compared to its alternatives. The chosen RF module supports an approximate range of 2Km, depending on obstructions, frequency, antenna and power. The design of the RF module orients itself for communicating with the base station and continuously receiving radio command from NASA. As for communication protocols, the RF module supports SPI. To support its functionalities, the RF module comes a 3.3V voltage regulator and level shifter that can handle 3-5V DC, giving it +5 to +20 dBm up to 100 mW Power Output Capability. The RF module may transfer programmable bit rate up to 300 kbps with a bullet-proof front end with IIP3 of -12.5 dBm. . Its various functionalities put the RF module as relatively cost effective (around $20 per unit). It weighs 0.11 oz, and measures 29mm x 25mm x 4mm / 1.14 in x 1.0 in x 0.2 in. The board dimensions can be further seen in Fig. 99

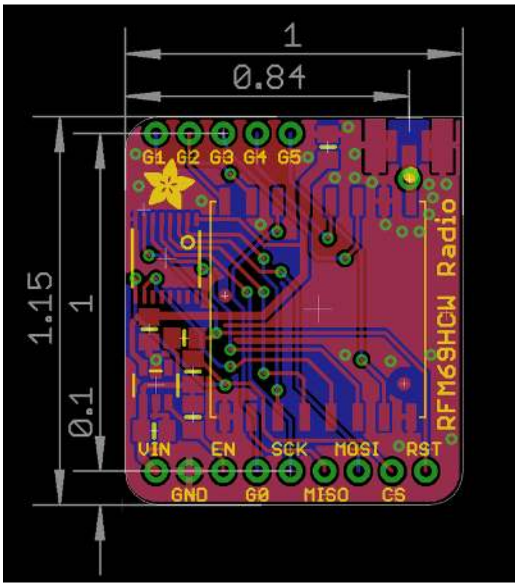


Figure 99: RFM96W Transceiver Layout in inch units (Source: Adafruit Industries [5])

The Adafruit breakout board full wiring schematic is shown below, where the SPI interface pins can be seen interfacing with the RFM96W chip module.

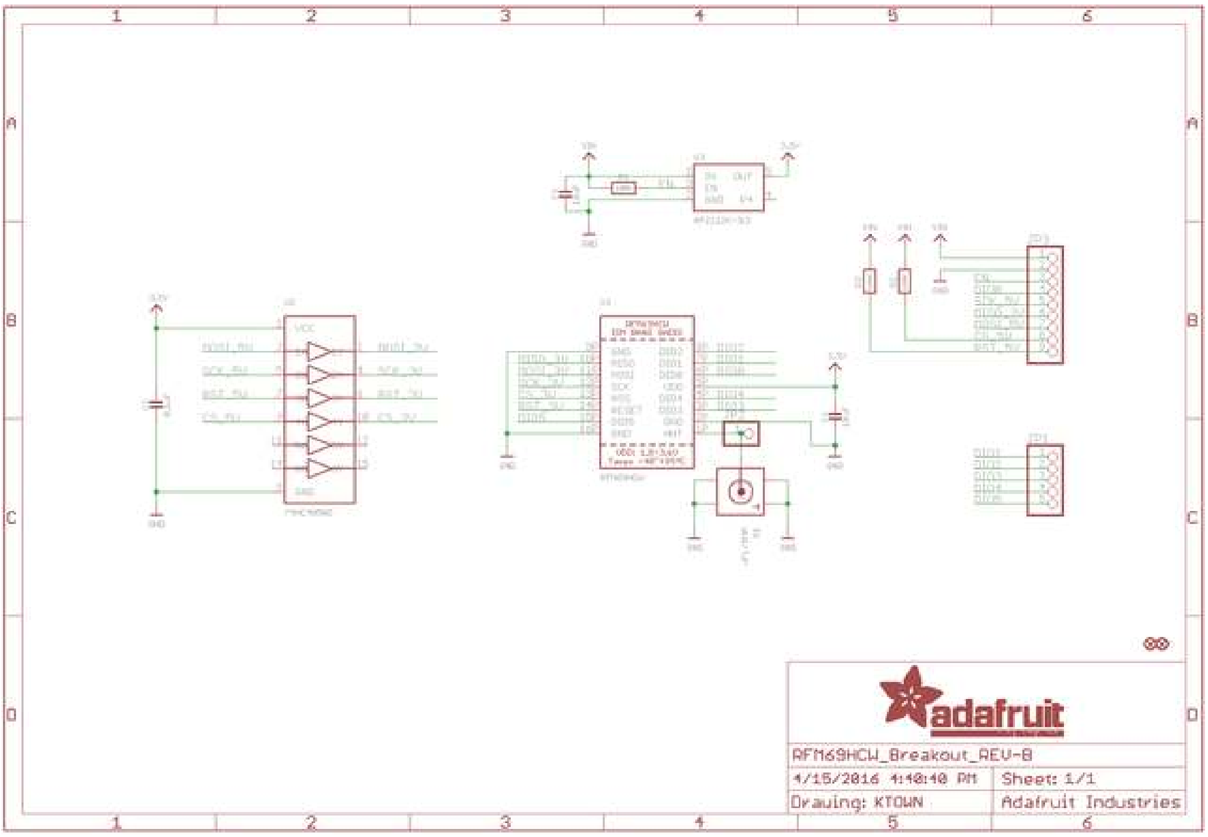


Figure 100: RFM96W Transceiver Wiring Schematic (Source: Adafruit Industries [5])

3. **RTL-SDR APRS Receiver**

In order to receive RAFCO transmissions from the APRS network, the team decided on the use of the RTL-SDR APRS receiver adapter that interfaces with the Raspberry Pi via USB.

The main advantages of the RTL-SDR are its robust capabilities to easily tune to any frequency needed with a simple input. Another important distinction for the RTL-SDR is that it is able to be plugged into one of the Pi 4's USB ports for easy communication access. The RTL SDR also features an aluminium casing pre-installed to protect the components during flight and allow for easier cooling during long receiving times. It uses a simple 5V power over the previous mentioned USB interface and has a slew of python and command line tools for use.

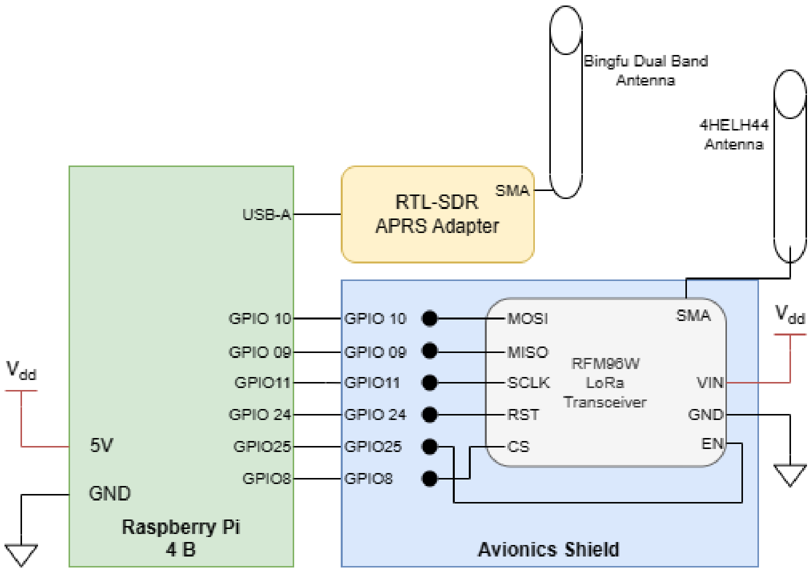


Figure 101: Telemetry and Radio Setup Block Diagram

### 4.2.4 Avionics and Sensing Subsystem

1. **BMP388 Altimeter**
   The Adafruit BMP388 Altimeter fares reasonably well with a relative accuracy of ± 8, Pa and an absolute accuracy of ± 50 Pa. The chosen altimeter supports a variety of digital interfaces, including a variety of read, write functionality, coupled with single byte and multiple byte modality. The digital interface facilitates to track height of the payload, and determine whether the rocket has landed or not as the altimeter feeds its data into python script. As for communication protocols, the altimeter supports $I^2C$ (up to 3.4 MHz) and SPI (3 and 4 wire, up to 10 MHz). To support its functionalities, the altimeter comes with 3.3V regulator and level shifting, interfaceable with a 3V or 5V logic microcontroller. The altimeter's VDD main supply voltage range ranges from 1.65 V to 3.6 V and VDDIO interface voltage range from 1.2 V to 3.6 V. The altimeter operates at rated temperatures ranging from -40 to +85 °C and pressures between 300 and 1250 hPa. Thus the team has determined the component reliable enough to perform optimally in the payload. Its various functionalities put the altimeter as relatively cost effective (around $10 per unit). It weighs around .05 lb and measures 2.0 mm x 2.0 mm x 0.75 mm. The

chassis is primarily composed of a metal lid LGA. The board layout is illustrated in Fig. 102

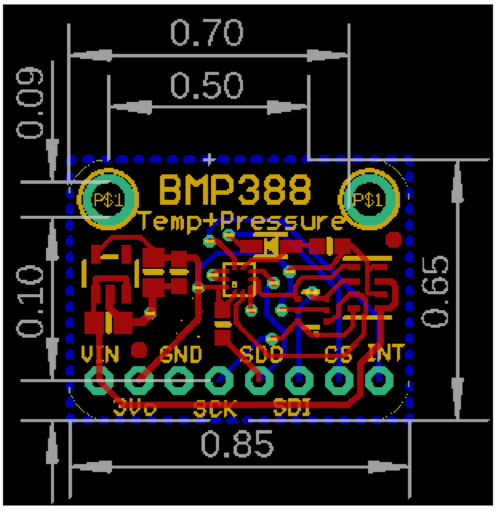


Figure 102: BMP388 Layout in inch units (Source: Adafruit Industries [3])

The wiring schematic for the breakout board is also shown below in Fig. 103

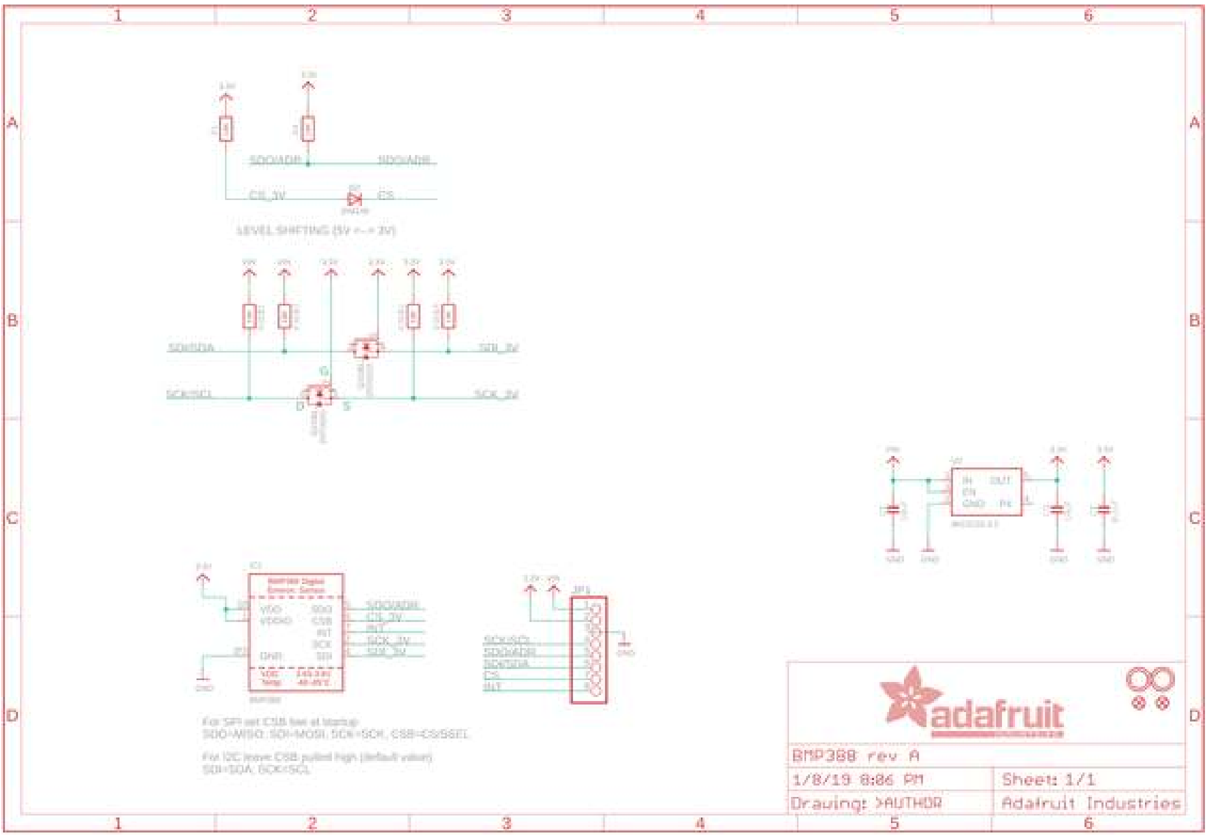


Figure 103: BMP388 Wiring Schematic (Source: Adafruit Industries [3])

2. **BNO055 IMU**
This IMU is a breadboard that uses pins as input to the functionality of the BNO055

IMU. Its dimensions are 20mm x 27mm x 4mm / 0.8 in x 1.1 in x 0.2 in, with its weight at 3 g. Its power requirements support an average of 3 to 5 V.

The BNO055 IMU uses VIN, 3VO, GND (power pins); SCL, SDA (I2C pins); RST, INT, ADR, and PS0/PS1 interface protocols. It can output Absolute Orientation (Euler Vector/Quaternion, 100Hz), Angular Velocity Vector (100Hz), Acceleration Vector (100Hz), Magnetic Field Strength Vector (20Hz), Linear Acceleration Vector (100Hz), Gravity Vector (100Hz), and Temperature (1Hz). This IMU can integrate with the vehicle as it can help move the camera as it is being called on by the FSM control software.

The advantage of this IMU is that it is small, powerful in terms of compatibility, and can output many types of sensor data. There are also many inputs to the breadboard, and it is very resilient and reliable. The board layout is also shown in Fig. 105

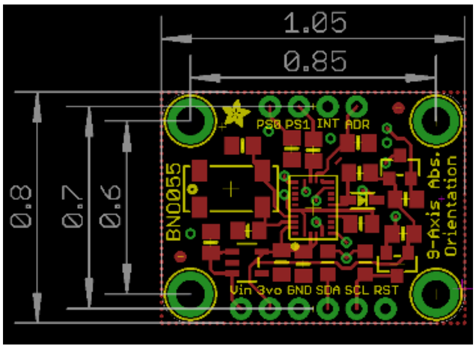


Figure 104: BNO055 Layout in inch units (Source: Adafruit Industries [4])

The wiring schematic for the breakout board is depicted below in Fig. 105

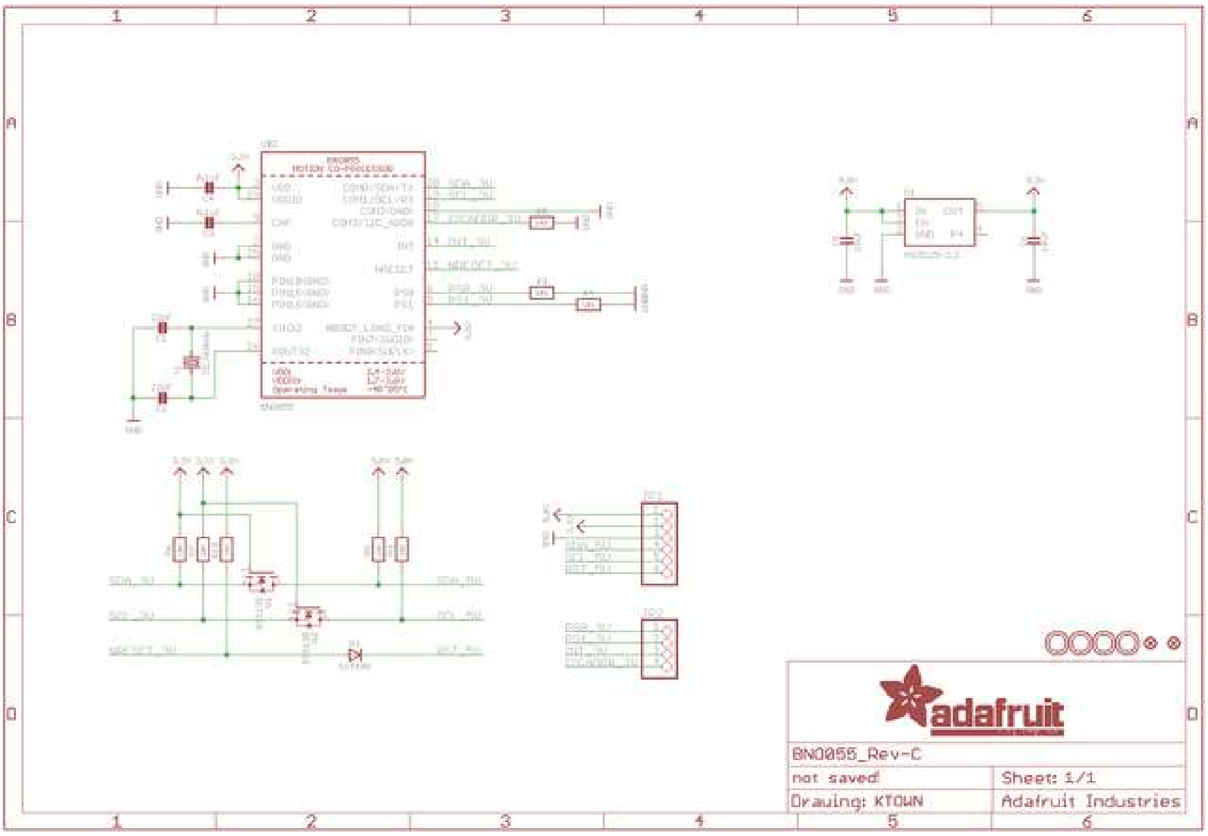


Figure 105: BNO055 Wiring Schematic (Source: Adafruit Industries [4])

The overall avionic sensing subsystem is illustrated in the block diagram of Fig. 106. The I2C protocol is used for both the components to communicate with the Pi. This provides the added benefit of minimal wiring as the two components can share the same bus for synchronization and communication at the cost of greater CPU clock cycles.

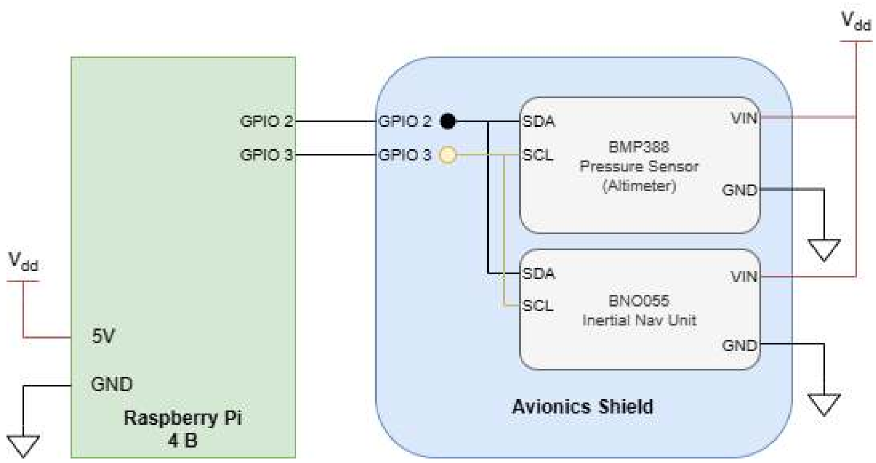


Figure 106: Avionic Sensing Subsystem Block Diagram

### 4.2.5 Electromotive Control and Power Distribution

1. **TalentCell 12v/5v DC Supply**
   The selected power supply is a DC battery pack manufactured by TalentCell. It is a rechargeable lithium ion battery pack capable of outputting both 12V and 5V through two ports, 12V from a coaxial jack and 5V via USB-A. with its dimensions of 1.1 in x 3.35 in x 5.7 in and weighs around 13.4 oz. For 12V, it supports a power requirement of DC5521 12V/3A max. For 5V, it will support 5V USB - 5V/2A max. An image of the battery is shown in Fig. 107.

   
   

   Figure 107: Payload Electronics DC Power Supply

   The primary reason for using the battery in the final design is due to its high capacity-to-weight ratio of almost 900 mAH per oz of its own weight. Moreover, it uses high quality battery cells (18650) and comes with various power supply safety measures, like short-circuit prevention, over-current and over-charging/discharging protection.

2. **Adafruit DC Motor Hat**
   The Adafruit DC motor hat was selected because of its versatility in allowing the team to connect and control up to four 12V devices. The hat can thus support the 12V motor and three linear solenoids for retention.

   This hat was selected as the hat is easily assembled and placed on top of the Raspberry Pi or easily connected via I2C jumper cables if needed. It communicates via the I2C protocol to receive PWM control signals so that it can direct a maximum of 3A at 12V of power from the selected battery. The design also keeps the motor power circuit independent of the power supply for the Pi itself—thus the team avoids the risk of current overdraw damaging the computer during flight. Lastly, there also exists online Python libraries for configuring the hat in software.

   The dimensions of the DC motor hat are similar to the Raspberry Pi, as it was designed to mount on top of the same board dimensions. The specific dimensions are shown in Fig. 108

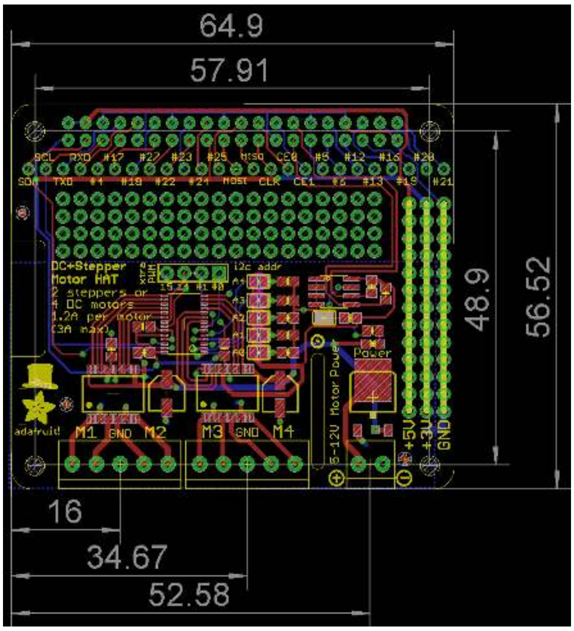


Figure 108: DC Motor Hat Layout (Source: Adafruit Industries [adafruit˙industries:dchat])

The wiring schematic for the DC hat is depicted below in Fig. 109. The I2C protocol that the hat interfaces with is shown on the respective SDA and SCL pins in the diagram.

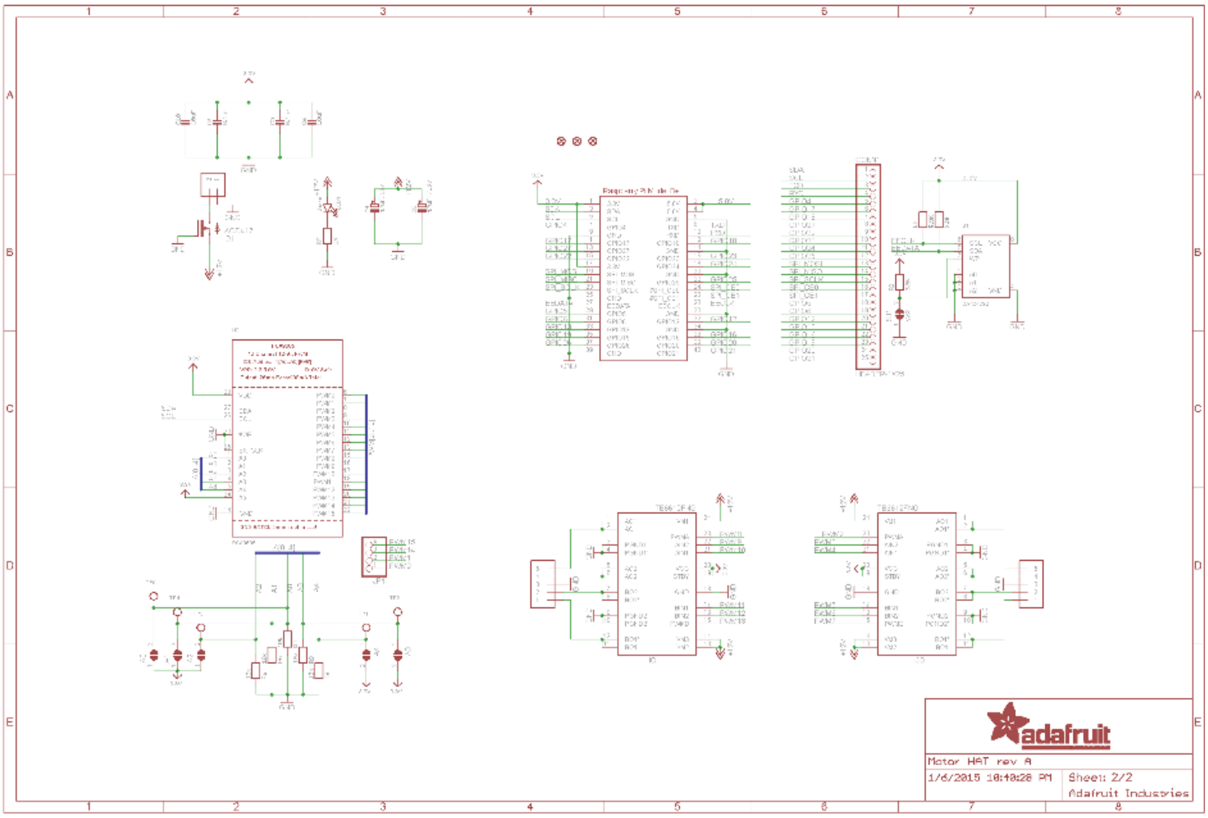


Figure 109: DC Motor Hat Wiring Schematic (Source: Adafruit Industries [**adafruit˙industries:dchat**])

3. **Power Distribution and Motive Subsystem** The overall method of distributing power to the Payload computer and peripheral components are either by cable or PCB connections.

   For powering logic and low-voltage (less than or equal to 5 V) components, the battery first supplies power to the Raspberry Pi via USB. The VIN pin of the Raspberry Pi is also distributed to a custom printed PCB shield that provides power to any 5V components (avionics subsystem, camera, 5V servos, etc.). These connections are made through 22 AWG jumper cables or through the copper traces of the PCB.

   For powering the 12V components, 16 AWG wire cables were selected to support the any current greater than 1000 mA that is necessary to power the solenoids and DC motor. In addition, a simple 8-port power distribution board can be used to separate the 12V power supply into parallel outputs if needed, though the Adafruit motor hat has enough outputs to support the number of solenoids and the DC motor.

### 4.2.6 Payload Software Architecture

The software control of the payload must be both fast and reliable. The primary design concept behind the software is to first perform the necessary setup prior to entering a main execution loop that can perform the necessary tasks of the mission at a high enough frequency such that real-time physical events can be responded to.

The core program will be a single .py file that includes multiple other libraries and Python modules written by the payload team. The components that are contained within this main program are as described below.

1. **Setup and Configuration**
   The first portion of the software is executed as soon as the Raspberry Pi runs the core Python program. This section of code is responsible for initializing all peripheral components communicating with the Raspberry Pi. This includes setting up the communication protocol buses (identifying I2C devices, setting SPI baud rates, etc.), configuring the registers for configuring avionic sensor rates and ranges (IMU sensitivity, altimeter pressure precision, etc.), and establishing RF communication with the base station.

   When all of the setup and checks have been performed, the payload will indicate to the team that setup has been complete, either by outputting to console or sending a RF transmission to the base station. At this point, it will be safe to disconnect the team member from the detached terminal session and to assemble the payload into the rocket.

2. **Delta-Timing Execution Loop**
   The next phase of execution that the program enters after setup is the execution loop. This is a simple infinite loop that is repeated at a fixed frequency, governed by a delta time check. The overall loop will operate at the highest possible frequency, which will also serve as a "base" unit of time that each subroutine executed under this loop can use to count by. This enables the payload to perform various tasks at their appropriate frequencies. For example, avionics sensing will run at the same frequency as the main execution loop to ensure data is read as fast as possible, but basic telemetry monitoring updates can be transmitted to the team only every second.

3. **Avionics Sensing**
   The avionics sensing software is responsible for sampling each avionic component on-board, namely the BNO055 and BMP388, at a fixed interval and preparing the data. Preparation includes filtering noise from read samples and formatting the data into an array of values that can be easily read into other routines.

   In addition, the avionics sensing module will be responsible for setting various global flags that describe the payload's physical activity, such as IS_MOVING and IS_BELOW_50M status bits that can let other routines to test whether the payload has made a stable landing or not.

4. **Imaging**
   Imaging is accomplished through the use of various Python libraries to capture data from the Raspberry Pi camera and then perform the necessary manipulations like timestamping and apply color filters. The libraries in use are PiCamera, numpy, and opencv. The software is capable of executing python commands to take an image from the camera and then saving it to disk where the image can be read into the program as a multidimensional 2d array of pixel data and modified via numpy transformations.

   The subteam chose a custom image filter for the H8 RAFCO execution as a 'rgb2bgr' RGB inversion filter. The filter takes an image coded with RGB values per pixel and reverse the order such that the RGB 8-bit values (0 /-255) for "red" and "blue" are swapped. A snippet of the Python script used for such a filter is shown below in Fig. 110.

```python
'''
input: image
output: image with color space switched from RGB to BGR
'''
def rgb2bgr(img):
    rgb = cv2.cvtColor(img, cv2.COLOR_BGR2RGB)
    return rgb

if __name__ == '__main__':
    # RGB to BGR Image Transformation Demo
    img = cv2.imread("./clear_16_11.jpg")
    path = "./image_results/bgr_transform.jpg"

    img_transformed = rgb2bgr(img)
    cv2.imwrite(path, img_transformed)

    cv2.imshow('RGB2BGR', img_transformed)
    cv2.waitKey(0)
    cv2.destroyAllWindows()
```

Figure 110: Python script snippet of 'rgb2bgr' RGB inversion filter using opencv library

5. **Telemetry and Radio**

Communication with the base station will be maintained through the use of two transceivers, the on-board component being the transmitter and the base station the receiver. The component used is the RFM96W LoRa radio chipset which communicates with data over GFSK modulation at a base frequency of 434.55 MHz on channel 7. Any packets sent will be headed by the team's callsign so that any received data by the base station can validate that the data was from the payload and to minimize interference.

Reception on the APRS network requires the use of a special Raspbian OS that comes prepackaged with APRS packet decoding capabilities. For this, Direwolf was installed with the OS flashed onto the Raspberry Pi. This is a APRS encoding/decoding soundcard implemented in software that enables the Raspberry Pi with several useful commands to interface with the RTL-SDR adapter.

An example of the shell commands used to enable the Raspberry Pi to listen for APRS transmissions on the RTL-SDR adapater is as follows:

```
rtl_fm -f 144.390M -s 22050
| multimon-ng -t raw -a AFSK1200 -f alpha /dev/stdin
> data.txt
```

6. **RAFCO FSM**

A more consolidated version of the originally proposed RAFCO processing FSM has been organized for the final payload software design. This updated FSM operates by transitioning between only three states. The main execution of the FSM is implemented by running the subroutine with an input to its current state and setting the function's return value to the next state. This is then repeatedly done by calling the routine under the main delta timing loop, thus the FSM can be executed at some defined frequency without blocking other routines, as executing certain strings of RAFCO (like taking an image or rotating camera servo) can be time-consuming.

The three states are WAIT, CALL, and EXEC. The FSM follows a Mealy State Machine model, as transitions are based on state and input. There are two inputs to the FSM, a "buffer" input that contains at all times a queue of data from the APRS subsystem that it receives asynchronously with respect to the FSM. The second input is a "RAFCO" string that is used as temporary storage for the FSM execution state.

The generic flow of the FSM is for the state to remain at WAIT when no packets are received and thus only transition to CALL when the buffer has data. The CALL state removes and reads the first packet of the buffer queue received is invalid or not (i.e. the callsign does not match NASA's supplied callsign or the data is corrupted) and returns back to WAIT if so. Else, the packet is valid and the FSM transitions to the EXEC state and returns the current packet into the FSM's temporary RAFCO storage string input. Within the EXEC state, the FSM processes each RAFCO from the temporary string input and runs the corresponding imaging system control sequence (e.g. rotate camera or take image). With each execution in the EXEC state, the temporary string is updated with the remaining RAFCO and remains in the EXEC state until no string remains, at which point it transitions back to WAIT to repeat the process. This is further illustrated by the FSM diagram below.

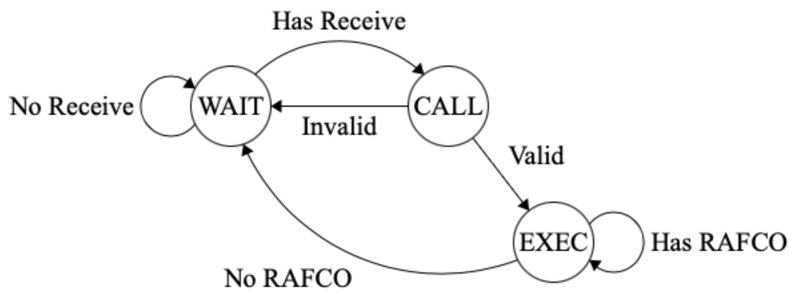


Figure 111: Diagram of the RAFCO FSM with its three states

7. **Failsafe Abort**

Every subroutine that runs underneath the main delta timing execution loop must be programmed to return a special MISSION_ABORT value that can be tested after each execution of the program. These return values will be generated only in the case that the software has detected a severe failure in a critical component or a set of physical flags that should normally not be set. When the abort value is caught, the main execution loop will immediately break and proceed attempting to revert the payload into a failsafe state. This includes re-engaging any retention mechanisms (if they were released), retracting the nosecone separation completely closed, and then locking any electromotives by cutting power.

Only components necessary for transmitting payload information will be kept active, such as the telemetry subsystem, for periodically communicating with the base station while preserving power in the event of an emergency.

# 5 Safety

## 5.1 Safety Officer Responsibilities

The Safety Officer's responsibilities include the following:

1. Oversee the general safety of the team and its members during all aspects of club engagement.

2. Ensure that all broader WURocketry, WashU, and USLI competition safety requirements are being followed throughout the year.

3. Administer safety briefings throughout the school year including pre-testing, pre-machining, and pre-launch safety briefings.

4. Attend all testing, manufacturing, and launch operations to oversee safety guidelines. If the Safety Officer is unable to attend, the team president or chief engineer assumes this responsibility.

5. Monitor the completion of all safety forms that team members are required to sign before machining, testing, and launching.

6. Research any new materials that are used by the team that could be potentially harmful or hazardous in any way.

The procedures for various stages of rocket launch are outlined in the following pages. These procedures are printed and included in the safety binder along with the Material Safety Data Sheet (MSDS) for use on launch day.

# Recovery and Propulsion Procedure

## Supplies

- [ ] Aft body tube
- [ ] Avionics coupler
- [ ] Forward body tube + Nose Cone
- [ ] Toolkit
- [ ] Hardware kit
    - [ ] Shear screws (No. 2 [6] and/or No. 4 [])
    - [ ] Philips head screwdriver
    - [ ] Putty
    - [ ] Superglue
- [ ] Baby powder

## Warnings

⚠**The rocket is live. Do not aim the end of the rocket at any person.**

⚠**Move the rocket slowly and carefully.**

⚠**Be careful with fiberglass edges**

## Procedure

To be completed by R&P Team Lead and Chief Engineer

Component - Drogue Parachute

- [ ] Secure the drogue parachute in the Nomex blanket
- [ ] Attach the 15ft drogue shock cord to the drogue parachute
- [ ] Z-Fold the 15ft drogue shock cord
- [ ] Use painter’s tape to “break band” the 15ft drogue shock cord
- [ ] Attach the other end of the 15ft drogue shock cord to the avionics bottom bulkhead of the avionics coupler
- [ ] Attach the 25ft shock cord to the aft coupler eye bolt
- [ ] Attach the remaining side of the 25ft shock cord to the bottom bulkhead of the avionics coupler
- [ ] Z-Fold the 15ft drogue shock cord
- [ ] Use painter’s tape to “break band” the 25ft drogue shock cord
- [ ] Pack the folded 25ft cord, 15ft cord, and drogue parachute into the aft coupler

Component - Main Parachute

- [ ] Pack the main parachute into the deployment bag
- [ ] Attach the 15ft forward main shock cord to the main parachute
- [ ] Attach the 30ft forward main shock cord to the main parachute

- ☐ Z-fold the 15ft forward main shock cord
- ☐ Use painter's tape to "break band" the 15ft forward main shock cord
- ☐ Z-fold the 30ft aft main shock cord
- ☐ Use painter's tape to "break band" the 30ft aft main shock cord
- ☐ Attach the 15ft forward main shock cord to the nose cone eyebolt
- ☐ Confirm BP charges are correct with team mentor and Chief Engineer

⚠At this point, only the Structure Team Lead, R&P Team Lead, and Chief Engineer should be handling the rocket

- ☐ Attach the 30ft aft main shock cord to the forward bulkhead of the avionics coupler

Team Lead:__________ Safety Officer:__________

# Payload Subsystem Preparation Procedure

## Supplies

- ☐ Philips Head Screwdriver
- ☐ Allen wrench
- ☐ Toolki
- ☐ Payload Bay - board
- ☐ Avionics Electronics (Telemetry)
  - ☐ RPi (1)
  - ☐ Altimeter (1)
  - ☐ IMU (1)
- ☐ Payload Mission Electronics
  - ☐ Micro servos (2)
  - ☐ Micro actuators (2)
  - ☐ RF Transceiver (1)
  - ☐ DC Motor

## Warnings

⚠**The rocket is live. Do not aim the end of the rocket at any person.**

⚠**Move the rocket slowly and carefully.**

⚠**12V Power Supply for the motor - Lithium Ion Battery**

⚠**Wiring - loose wires**

## Procedure

To be completed by Payload Team Lead and Chief Engineer

- ☐ Insert and mount the payload bay

⚠**12V Power Supply for the motor - Lithium Ion Battery**

- ☐ Switch on the electronics (avionics)
  - ☐ Altimeter
  - ☐ IMU
  - ☐ RF Transceiver

⚠**Wiring - loose wires**

- ☐ Check wiring

Team Lead:__________ Safety Officer:__________

# Avionics Procedure

## Supplies

- ☐ Aft body tube
- ☐ Avionics coupler
- ☐ Forward body tube + Nose Cone
- ☐ Toolkit
- ☐ Laptop computer with OpenRocket installed
- ☐ Hardware kit
  - ☐ Shear screws (No. 2 [6] and/or No. 4 [])
  - ☐ Philips head screwdriver
  - ☐ Putty
  - ☐ Superglue
- ☐ Avionics board
- ☐ Avionics hardware (attached to avionics board)

## Warnings

⚠**The rocket is live. Do not aim the end of the rocket at any person.**
⚠**Move the rocket slowly and carefully.**
⚠**Be sure to be able to see the switches in the avionics coupler**
⚠**Be careful with fiberglass edges**

## Procedure

To be completed by Structures Team Lead, R&P Team Lead, and Chief Engineer

- ☐ Setup avionics board
- ☐ Give avionics bay to team mentor to load black powder charges
- ☐ Attach the other end of the 15ft drogue shock cord to the avionics bottom bulkhead of the avionics coupler
- ☐ Attach the remaining side of the 25ft shock cord to the bottom bulkhead of the avionics coupler
- ☐ Insert avionics coupler into the aft tube and ensure holes are lined up
- ☐ Avionics team lead check the holes to ensure power switch is accessible
- ☐ Confirm BP charges are correct with team mentor and Chief Engineer

⚠At this point, only the Structure Team Lead, R&P Team Lead, and Chief Engineer should be handling the rocket

- ☐ Attach the 30ft aft main shock cord to the forward bulkhead of the avionics coupler
- ☐ Pull forward tube over the avionics coupler, ensuring holes are lined up
- ☐ Have avionics team lead check the holes to ensure power switch is accessible
- ☐ Immediately before taking rocket to launch rail, avionics team lead turn on the GPS arming switch and confirm GPS lock and communications with base station

- [ ] When rocket is on launch rail, avionics team lead flip the arming switches for the flight computers and the Raspberry Pi

Team Lead:__________ Safety Officer:__________

# Full Scale Preparation Procedure

## Supplies

- ☐ Aft body tube
- ☐ Avionics coupler
- ☐ Forward body tube + Nose Cone
- ☐ 15 minute epoxy
- ☐ Red Solo Cups
- ☐ Toolkit
- ☐ Scissors
- ☐ 3D printed rocket stands
- ☐ Laptop computer with OpenRocket installed
- ☐ Hardware kit
    - ☐ Shear screws (No. 2 [6] and/or No. 4 [])
    - ☐ Philips head screwdriver
    - ☐ Putty
    - ☐ Superglue
- ☐ Baby powder

## Warnings

⚠**The rocket is live. Do not aim the end of the rocket at any person.**

⚠**Move the rocket slowly and carefully.**

⚠**Line up shear screw holes**

⚠**Be sure to be able to see the switches in the avionics coupler**

⚠**Be careful with fiberglass edges**

## Procedure

To be completed by Structures Team Lead, R&P Team Lead, and Chief Engineer

- ☐ Setup avionics board - see avionics preparation procedure
- ☐ Give avionics bay to team mentor to load black powder charges
- ☐ Secure the drogue parachute in the Nomex blanket
- ☐ Attach the 15ft drogue shock cord to the drogue parachute
- ☐ Z-Fold the 15ft drogue shock cord
- ☐ Use painter's tape to "break band" the 15ft drogue shock cord
- ☐ Attach the other end of the 15ft drogue shock cord to the avionics bottom bulkhead of the avionics coupler
- ☐ Attach the 25ft shock cord to the aft coupler eye bolt
- ☐ Attach the remaining side of the 25ft shock cord to the bottom bulkhead of the avionics coupler
- ☐ Z-Fold the 15ft drogue shock cord
- ☐ Use painter's tape to "break band" the 25ft drogue shock cord

- ☐ Pack the folded 25ft cord, 15ft cord, and drogue parachute into the aft coupler
- ☐ Insert avionics coupler into the aft tube and ensure holes are lined up
- ☐ Have avionics team lead check the holes to ensure power switch is accessible
- ☐ Insert shear screws
    - ☐ 2 No. 2's for subscale - elaborate on exactly how many
- ☐ Pack the main parachute into the deployment bag
- ☐ Attach the 15ft forward main shock cord to the main parachute
- ☐ Attach the 30ft forward main shock cord to the main parachute
- ☐ Z-fold the 15ft forward main shock cord
- ☐ Use painter's tape to "break band" the 15ft forward main shock cord
- ☐ Z-fold the 30ft aft main shock cord
- ☐ Use painter's tape to "break band" the 30ft aft main shock cord
- ☐ Attach the 15ft forward main shock cord to the nose cone eyebolt
- ☐ Confirm BP charges are correct with team mentor and Chief Engineer

⚠At this point, only the Structure Team Lead, R&P Team Lead, and Chief Engineer should be handling the rocket

- ☐ Attach the 30ft aft main shock cord to the forward bulkhead of the avionics coupler
- ☐ Pull forward tube over the avionics coupler, ensuring holes are lined up
- ☐ Have avionics team lead check the holes to ensure power switch is accessible
- ☐ Insert shear screws in forward connection
- ☐ Immediately before taking rocket to launch rail, avionics team lead turn on the GPS arming switch and confirm GPS lock and communications with base station
- ☐ When rocket is on launch rail, avionics team lead flip the arming switches for the flight computers and the Raspberry Pi

Team Lead:__________ Safety Officer:__________

# Motor Procedure

## Supplies

- ☐ Motor
- ☐ Motor Casing

## Procedure

To be completed by team mentor

⚠**The motor is loaded. Do not aim the end of the rocket at any person.**

⚠**Lift the rocket slowly and carefully.**

- ☐ Follow standard High-Power RMS rocket motor preparation procedure below

Team Lead:__________ Safety Officer:__________

## *HIGH-POWER RMS™* Assembly and Operation Instructions

***READ THIS BEFORE YOU BEGIN:***

- Study the illustrations and sequence of assembly. ***THE SEQUENCE OF ASSEMBLY IS EXTREMELY IMPORTANT. READ ALL INSTRUCTIONS BEFORE USE. USE RMS™ MOTORS AND RELOAD KITS ONLY IN ACCORDANCE WITH ALL INSTRUCTIONS.*** Review the parts list and become familiar with all parts before assembly. **IF ANY PARTS ARE MISSING OR DAMAGED, CONTACT RCS AT 1-435-865-7100 or email at warranty@aerotech-rocketry.com.**
- ***DO NOT USE ANY PARTS OF THE RMS™ SYSTEM THAT ARE DAMAGED IN ANY WAY.*** If in doubt, contact RCS at the number above for assistance.
- ***DO NOT MODIFY THE MOTOR IN ANY WAY.*** Modification of the motor or the reload kit parts could result in motor failure, lead to the destruction of both your rocket and motor and may cause personal injury, death and/or property damage. Modification of the motor or reload kit in any way will invalidate your motor warranty.
- ***USE ONLY AEROTECH/RCS RMS™ RELOAD KITS AND MOTOR PARTS TO REFURBISH YOUR RMS™ MOTOR.*** The AeroTech/RCS reload kits have been designed specifically for use in your particular AeroTech/RCS RMS™ motor. Use of imitation components may destroy your motor, rocket and payload and will invalidate your motor warranty. Only use AeroTech/RCS RMS™ reload kits intended for your specific AeroTech/RCS RMS™ motor. ***DO NOT INTERCHANGE PARTS!*** Do not use AeroTech/RCS RMS™ reload kits or motor components for any other purpose than to refurbish an AeroTech/RCS RMS™ motor.
- ***DO NOT REUSE ANY OF THE DISPOSABLE PARTS OF THE RMS™ RELOAD KIT.*** This includes the liner, nozzle and o-rings. These components have been designed for one use only and must be discarded after firing. Reuse can result in motor failure during subsequent operation and will invalidate your motor warranty.
- Motors are hot after firing. Although the RMS™ operates at a lower temperature than most disposable motors, the higher thermal conductivity of the aluminum motor parts may make it seem otherwise. If necessary to handle a motor before it has cooled down, use a rag or similar article.
- Read and follow the safety code of the Tripoli Rocketry Association (TRA) and comply with all federal, state and local laws in all activities involving high power rockets.

***DO NOT OPEN RELOAD KIT UNTIL READY TO USE.***

**PARTS:**

***RMS™-75 HARDWARE***

| | |
|---|---|
| 75mm aft closure | 1 |
| 75/5120 case | 1 |
| 75mm plugged forward closure | 1 |
| 75mm forward seal disk | 1 |

***RELOAD PARTS KIT***

| | |
|---|---|
| Nozzle (large black plastic part) | 1 |
| Liner (2-3/4" O.D. black plastic tube) | 1 |
| Propellant grains (7/8" core) | 4 |
| Fwd & aft o-rings (1/8" thick X 2-3/4" O.D.) | 2 |
| Forward seal disk o-ring (3/32" thick x 2-9/16" O.D.) | 1 |
| Grain spacer o-rings (1/16" thick x 2-1/2" O.D.) | 3 |
| Smoke charge (short solid part) | 1 |
| Smoke charge insulator (1-1/2" O.D. tube) | 1 |
| Nozzle Cap (2-1/4" dia. red cap) | 1 |

***ITEMS NEEDED FOR USE:***

- Synco™ Super Lube™ or other grease
- Hobby knife
- Electric match with thermalite, Firestar™ or other igniter
- Masking tape
- Wet wipes or damp paper towels

**SAVE THE RELOAD KIT PLASTIC BAG FOR THE USED RELOAD PARTS. DISPOSE OF BAG AND PARTS PROPERLY.**

### Chapter 1. Forward Closure Assembly

1-1. Apply a light coat of Synco™ Super Lube™ or other grease to all threads and all o-rings (**except** the grain spacer o-rings). This will facilitate assembly and prevents the threads from seizing.

1-2. **Fig.-1:** Hold the forward (black) closure in a vertical position, smoke charge cavity facing up. Insert the smoke charge insulator into the smoke charge cavity until it is seated against the forward end of the cavity.

1-3. **Fig.-2:** Apply a liberal amount of grease to one end of the smoke charge element. Insert the **greased** end of the smoke charge element into the smoke charge cavity until it is seated against the end of the cavity. Set the completed forward closure assembly aside.

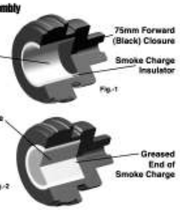


Fig.-1

Fig.-2

### Chapter 2. Case Assembly

2-1. **Fig.-3:** Using a hobby knife or similar tool, carefully deburr (chamfer) both inside edges of the liner tube (2-3/4" O.D. black plastic tube).


Fig.-3

### Chapter 2. Case Assembly (Cont'd)

2-2. **Fig.-4:** Insert the larger diameter portion of the nozzle into one end of the liner, with the nozzle liner flange seated against the liner. **NOTE:** RMS-75/5120 motors use a single large throat nozzle rather than the multiple-throat "Medusa" nozzle shown in the illustrations.

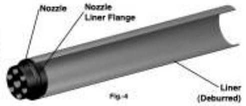


Fig.-4

2-3. **Fig.-5:** Perform the remaining assembly steps with the liner held in a horizontal position. Install the propellant grains into the liner, placing the three (3) grain spacer o-rings (1/16" thick x 2-1/2" O.D.) between each propellant grain. The aft grain should be seated against the nozzle grain flange. **NOTE:** Three propellant grains are shown in all illustrations for simplicity. RMS-75/5120 motors use four (4) grains.

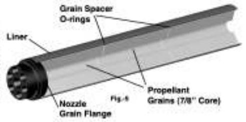


Fig.-5

2-4. **Fig.-6:** Place the greased forward seal disk (3/32" thick X 2-9/16" O.D.) o-ring into the groove in the forward seal disk.

2-5. **Fig.-7:** Insert the smaller (o-ring) end of the seal disk into the open end of the liner tube until the seal disk flange is seated against the end of the liner.


Fig.-6

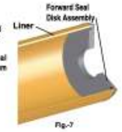


Fig.-7

2-6. **Fig.-8:** Push the liner assembly into the motor case until the nozzle protrudes approximately 1-3/4" from the end of the case. **NOTE:** A coating of grease on the outside surface of the liner will facilitate installation and casing cleanup after motor firing.

2-6. **Fig.-9:** Place the greased forward (1/8" thick X 2-3/4" O.D.) o-ring into the forward (bulkhead) end of the case until it is seated against the forward seal disk.


Fig.-8


Fig.-9

2-7. **Fig.-10:** Thread the previously-completed forward closure assembly into the forward end of the motor case by hand until it is seated against the case. **NOTE:** There will be considerable resistance to threading in the closure during the last 1/8" to 3/16" of travel.


Fig.-10

2-8. **Fig.-11:** Place the greased aft (1/8" thick X 2-3/4" O.D.) o-ring into the groove in the nozzle.

2-9. **Fig.-12:** Thread the aft closure into the aft end of the motor case by hand until it is seated against the case. **NOTE:** There will be considerable resistance to threading in the closure during the last 1/8" to 3/16" of travel. It is normal if a slight (1/32" to 1/16") gap remains between the closure and the case, and the grains rattle slightly in the liner after tightening.


Fig.-11


Fig.-12

# MOTOR PREPARATION PROCEDURE

## Chapter 3. Preparation For Flight


Fig.-13

3-1. **Fig.-13:** Insert the coated end of a Firestar™ or other igniter through the nozzle throat until it stops against the smoke charge element.

3-2. Secure the igniter to the nozzle with a piece of masking tape or the 2-1/4" dia. red nozzle cap supplied with the reload kit. NOTE: Cut a 1/8"-1/4" wide slot in the corner of the cap to allow for igniter venting.

3-3. Install the motor into the rocket's motor mount tube. Ensure that the motor is securely retained in the rocket by using positive mechanical means to prevent it from being ejected during recovery system deployment.

3-4. Prepare the rocket's recovery system and then launch the rocket in accordance with the Tripoli Rocketry Association (TRA) Safety Code and National Fire Protection Association (NFPA) Code 1127.

## Chapter 4. Post-Recovery Cleanup

**NOTE:** Perform motor clean-up as soon as possible after motor firing. Propellant and smoke charge residues become difficult to remove after 24 hours and can lead to corrosion of the metal parts. Place the spent motor components in the reload kit plastic bags and boxes and dispose of properly.

4-1. After the motor has cooled down, unthread and remove the forward and aft closures.

4-2. Remove the smoke charge insulator from the forward closure and discard. Using wet wipes or damp paper towels, remove all smoke charge and propellant residues from the closures.

4-3. Remove and discard the forward and aft o-rings from the motor case. Remove the liner, forward seal disk and nozzle from the casing by pushing on the nozzle end. Remove the forward seal disk from the liner, and remove and discard the forward seal disk o-ring. ***DO NOT DISCARD THE FORWARD SEAL DISK!*** Discard the nozzle and liner. Using wet wipes or damp paper towels, wipe the inside of the casing and the forward seal disk to remove all propellant residue.

4-4. Apply a light coat of grease to all threads and the inside of the motor case. Reassemble metal parts and store motor in a dry place.

## Chapter 5. First Aid

**WARNING:** For a minor burn, apply a burn ointment. For a severe burn, immerse the burned area in ice water at once and see a physician as quickly as possible. In the unlikely event of oral ingestion of the propellant, induce vomiting and see a physician as quickly as possible. The AeroTech/RCS composite propellant consists primarily of Ammonium Perchlorate and a rubber-like plastic elastomer.

## Chapter 6. Disposal

Damaged or defective reload kits should be returned to RCS.

## Chapter 7. Fire Safety

Tests show that the pyrotechnic components of RMS™ reload kits will not explode in fires and normally will not ignite unless subjected to direct flame and then will burn slowly. Use water to fight any fires in which AeroTech/RCS RMS™ reload kit pyrotechnic components may become involved: Direct the water at the AeroTech/RCS RMS™ reload kit pyrotechnic components to keep them below their 550 deg. F autoignition temperature. Foam and carbon dioxide fire extinguishers will NOT extinguish burning propellants of the type used in RMS™ reload kit pyrotechnic components. Keep reload kit pyrotechnic components away from flames, sources of heat and flammable materials.

## Disclaimer and Warranty

**NOTICE:** As we cannot control the storage and use of our products, once sold we cannot assume any responsibility for product storage, transportation or usage. RCS shall not be held responsible for any personal injury or property damage resulting from the handling, storage or use of our product. The buyer assumes all risks and liabilities therefrom and accepts and uses AeroTech/RCS products on these conditions. No warranty either expressed or implied is made regarding AeroTech/RCS products, except for replacement or repair, at RCS's option, of those products which are proven to be defective in manufacture within one year from the date of original purchase. For repair or replacement under this warranty, please contact RCS. Proof of purchase will be required. Note: Your state may provide additional rights not covered by this warranty.

**AeroTech Division**
**RCS Rocket Motor Components, Inc.**
**Cedar City, UT 84720**
**www.aerotech-rocketry.com**

**P/N 20087 Rev. 12/30/09**
**Made in U.S.A.**



AeroTech® Consumer Aerospace — Division of RCS Rocket Motor Components, Inc.

# HIGH-POWER RMS™

## Reloadable Motor System™

## RMS™ 75/5120 BLACK MAX™

### This Package Contains One Reload Kit:

☐ ***L1170FJ-P*** (75/5120)

**NOTE: This reload kit MUST be used with separately packaged L1170FJ propellant grains (P/N 03616-4) and motor liner tube (03035-4). RMS™-75 reload kits do not include an ejection charge. RMS™-75 motors must be used in conjunction with a timer, altimeter or radio-actuated recovery system.**

**NOTE:** This reload kit is *ONLY* for use in AeroTech/RCS, Dr. Rocket™ or Rouse-Tech™ RMS™ 75/5120 high-power motors. Certified by the Tripoli Rocketry Association (TRA).

**DO NOT OPEN RELOAD KIT UNTIL READY TO USE**

### Typical Time-Thrust Curve:

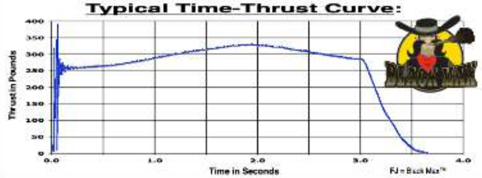


### RMS™ 75MM BLACK MAX RELOAD KIT DATA

| Hardware Designation | Performance Designation | Total Impulse (Typical) | Propellant Weight | Loaded Motor Weight |
|---|---|---|---|---|
| RMS™-75/5120 | *L1170FJ-P* | 4,218 N-sec | 2,800 g (6.17 lb) | 5,021 g (11.06 lb) |

**NOTE:** Total impulse shown is typical.

### RMS™ 75MM HARDWARE DATA

| Hardware Designation | Motor Diameter | Motor Length | Hardware Weight | Reload(s) Used |
|---|---|---|---|---|
| *RMS™-75/5120* | 2.965" (75mm) | 26.20" | 1,408 g (3.10 lb) | L1170FJ-P |

**NOTE:** Motor lengths are measured from end of aft closure to end of forward closure.

**NOTE: SALE TO PERSONS UNDER 18 YEARS OF AGE PROHIBITED BY FEDERAL LAW. WARNING-FLAMMABLE: Read Instructions Before Use. KEEP OUT OF REACH OF CHILDREN. FOR USE ONLY BY CERTIFIED HIGH-POWER USERS 18 YEARS OF AGE OR OLDER. DO NOT SMOKE when loading these motors or use in the vicinity of open flames.**

# Setup on Launch Pad Procedure

## Supplies

- ☐ 1515 Launch Rails
- ☐ Fully Assembled Rocket
- ☐ Flat Head Screwdriver

## Procedure

To be completed by mentor and two L2 certified members

⚠**The rocket is live. Do not aim the end of the rocket at any person.**

⚠**Lift the rocket slowly and carefully.**

- ☐ A minimum of 2 team members, who are High Power Rocket certified, will carry the rocket to the launch rail
- ☐ Inspect the rail to ensure it is in proper condition and ready for launch

⚠**Move the rail slowly to not disturb connections.**

- ☐ With the assistance and oversight of a High Power Rocket certified member or the team mentor, tilt the launch rail to an angle such that the rocket can be easily slid onto the rail, insert the two rail buttons, and return the now connected rail and rocket to the upright position.

⚠**Beware of pinch points when turning on switches.**

- ☐ With a flat head screwdriver, turn the arming switch for one flight computer to the on position and monitor the flash of the LED in conjunction with the audible tone produced by the flight computer to ensure proper startup and power connection to the flight computer. Now, beeping/LED flashes should come 3 beeps at a time, indicating that main and drogue ejection charges have been detected. Repeat these steps with the redundant flight computer.

Team Lead:__________ Safety Officer:__________

# Ignitor Installation Procedure

## Supplies

- ☐ Ignitor
- ☐ Wire Stripper
- ☐ 12VDC Firing Module

## Procedure

To be completed by mentor

⚠**The motor is live. Do not aim the motor at any person.**

⚠**Beware of shock hazards while handling live electronics.**

- ☐ Ensure the 12VDC firing module is turned to off

⚠**Beware of sharp points of lead wires.**

- ☐ Separate the leads on the bottom of the ignitor

⚠**Beware of sharp edges of wire stripper.**

- ☐ Strip each lead to expose approximately 1 inch of wire

⚠**Beware of sharp points of lead wires.**

- ☐ Attach one lead to the positively charged (red wire) alligator clip and wrap the wire around the clip to ensure good connection
- ☐ Attach the other lead to the negatively charged (black wire) alligator clip and wrap the wire around the clip to ensure good connection
- ☐ Bend the ignitor into a Z-shape and place it into the motor opening on the bottom of the aft section of the rocket. The motor should sit as high as possible in this opening.

Team Lead:__________ Safety Officer:__________

# Launch Procedure

## Supplies

- ☐ Ignitor

## Procedure

To be completed by RSO, Mentor, and two L2 Certified Members

⚠**The rocket is live. Do not aim the end of the rocket at any person.**

- ☐ Walk at least 300’ from the rocket and clear a diameter of at least 100’
- ☐ Communicate to the RSO that the rocket is ready to launch

⚠**Ensure all members are quiet and attentive during countdown.**

- ☐ RSO begins countdown from 5 to launch
- ☐ If the rocket does not launch, RSO waits 10 seconds and initiates new countdown
- ☐ If the rocket still does not launch, certified members wait 60 seconds before approaching to inspect the ignitor and attempt to diagnose the issue

Team Lead:__________ Safety Officer:__________

# Troubleshooting Procedure

## Supplies

- ☐ 9V Battery
- ☐ Wire Stripper
- ☐ Soldering Iron
- ☐ WD-40
- ☐ Quick Links
- ☐ Payload Filler Material (paper, cardboard, foil)
- ☐ Scissors
- ☐ Toolkit
- ☐ 15 minute epoxy

## Procedures for Avionics Troubleshooting

<u>Problem to troubleshoot: GPS to Base Station connection failed</u>

Re-check connection upon completion of each step

⚠**Beware of shock hazards from live electronics.**

⚠**Beware of pinch points when connecting wires**

- ☐ Disconnect and reconnect power to the GPS
- ☐ Check all connections to ensure they are secure and not shorted
  - ☐ LiPo to GPS
  - ☐ TeleGPS to Antenna
  - ☐ TeleGPS to Base Station Computer
- ☐ Connect the GPS directly to the Base Station
  - ☐ Open user interface and connect or configure TeleGPS manually
  - ☐ Verify battery charge using Altos to monitor TeleGPS

Team Lead:__________ Safety Officer:__________

<u>Problem to troubleshoot: GPS lock failed</u>

Re-check GPS lock upon completion of each step

⚠**Beware of shock hazards from live electronics.**

⚠**Beware of pinch points when turning on switches.**

- ☐ Verify the charge of the GPS LiPo with user interface
- ☐ Disconnect and reconnect power to the TeleGPS
- ☐ Verify the GPS is out of range of any significant sources of interference (telephones, radios, transmitters, metal barns, etc.)

- ☐ Verify the TeleGPS is not obstructed by any large structures that may inhibit signal transfer (metal barns, etc.)

Team Lead:__________ Safety Officer:__________

Problem to troubleshoot: Wire connections are cut or otherwise disconnected

⚠**Beware of shock hazards from live electronics.**
⚠**Beware of sharp edges of wire stripper.**
- ☐ Strip both sides of disconnected wires. If extra wire length is needed, strip both ends of an additional wire for soldering connection

⚠**Beware of sharp edges on stripped wires.**
- ☐ Twist the wires together where connections are needed to initiate soldering points
- ☐ Obtain damp paper towel that will be used for cleaning the soldering iron

⚠**Beware hot surfaces on solder and soldering iron. Wear eye protection.**
- ☐ After powering on and heating up the solder, use the solder on all solder connections using the damp towel to clean it when necessary
- ☐ Insulate all new solder joints to prevent accidental shorts using electrical tape

Team Lead:__________ Safety Officer:__________



## Procedures for Recovery and Propulsion Troubleshooting

Problem to troubleshoot: Parachutes or shock cords become tangled

⚠**Beware pinch points during detachment**
- ☐ Detach recovery system from the rocket and detangle any knots that developed

⚠**Beware pinch points during attachment**
- ☐ Re-attach recovery system to rocket, refold shock cords, and re-pack parachutes

Team Lead:__________ Safety Officer:__________

Problem to troubleshoot: Threading on recovery connection quick link is damaged

⚠**Beware pinch points when using quick links**
- ☐ Use WD-40 to loosen the opening and closing of the quick link
- ☐ Replace quick link from surplus

Team Lead:__________ Safety Officer:__________

## Procedures for Payload Troubleshooting

Problem to troubleshoot: Body tube diameter interfering with payload install

⚠**Beware of shock hazards from live electronics.**
⚠**Avoids sharp edges of body tube**

- ☐ To fill space that is not reached by the payload bay encasing, use paper or cardboard to fill this space. These materials are chosen because they will not damage electrical components and are not good conductors.
- ☐ To shorten the payload encasing if it is too long, use a mallet to hammer in the payload and ensure holes are lined up

Team Lead:__________ Safety Officer:__________

Problem to troubleshoot: Screws to secure payload fails to tighten

⚠**Beware of shock hazards from live electronics.**
⚠**Avoids sharp edges of body tube**

- ☐ Ensure the payload bay holes are aligned with the proper body tube holes before sliding the payload bay into the body tube.

⚠**Be careful to not over-torque screws and cause damage or injury**

Team Lead:__________ Safety Officer:__________

# Post-flight Inspection Procedure

## Supplies

- ☐ Camera
- ☐ Philips Head Screwdriver
- ☐ Avionics Base Station Computer

## Procedure

To be completed by Structures, Recovery, Avionics, and Payload

⚠**Avoid sharp edges of body tube**

- ☐ Upon approaching the rocket, focus should be on the avionics bay and determining that the black powder charges have all detonated. If Avionics team has any preliminary flight data, they should try to point out drogue detonations
- ☐ Approach rocket cautiously and take photos of landing site
- ☐ Inspect forward, mid, and aft body tubes for any damage
- ☐ Inspect fins and nose cone for damage

⚠**If black powder residue is not present, treat charge cups as live black powder and do not aim at any person**

- ☐ Now, closely inspect black powder charges for proper ignition
    - ☐ If charge has not detonated, ensure there are no loose or frayed wires near the ejections canisters
- ☐ Inspect parachute shock chords for any fraying or singeing
- ☐ Inspect drogue and main parachute for rips, tears, and holes

⚠**Treat aft end of rocket as live and do not aim at any person**

- ☐ Inspect motor tube to ensure proper burn out

⚠**Avoids sharp edges of body tube**

- ☐ After complete outer inspection, remove avionics bay

⚠**Beware of shock hazards from live electronics.**

- ☐ Connect avionics bay to base station computer to obtain flight data
- ☐ Remove payload bay and inspect for proper camera deployment

Team Lead:__________ Safety Officer:__________

Table 30: Risk Assessment Categories

| Category | Represented Percentage Range |
|---|---|
| Rare | 0% - 25% |
| Unlikely | 25% - 50% |
| Possible | 50% - 75% |
| Likely | 75% - 100% |

The primary goal of the likelihood categorization is to quantify the likelihood of some hazard leading to an event that causes harm either to the rocket or to a person. The extent of an injury or rocket damage is independent of these percentages, and high likelihood percentages do not necessarily mean the injury or damage will be extensive and likewise with lower percentages. The primary goal of the severity categorization is to quantify the extent of harm or damage that could occur due to different failures. The safety team analyzed risks for all the materials and facilities that are used during the construction and launch process.

Table 31: Risk Severity Categories

| Category | Severity To Human | Severity To Rocket |
|---|---|---|
| Minor | Injury requiring no treatment. | Superficial damage to rocket requiring no repair. |
| Moderate | Injury requiring some medical care/treatment (bandage, ice, etc.). | Damage to the rocket requiring some repairs (retighten hardware, re-align component, etc.) |
| Major | Injury requiring professional medical care/treatment (sutures, concussion protocol, etc.) | Damage requiring significant repair (Patching parachute, correcting bent components, etc.) |
| Severe | Injury requiring hospitalization or other prolonged treatment | Damage requiring purchase of entirely new component |

Table 32: Personnel Hazard Analysis

| Risk | Likelihood | Cause | Effect | Severity | Mitigation | Verification |
|---|---|---|---|---|---|---|
| Burns to skin from hot tools, machines, or parts | Rare | Incorrect or lacking PPE while performing tasks, insufficient training on machine or tool usage techniques | Damage to skin or body, scarring | Moderate | Members are trained to use each tool and machine properly and wear PPE when necessary | Safety Officer maintains up to date information on trainings and certifications for each team member. Safety Officer or Chief Engineer oversees machining tasks verifying proper PPE and techniques |
| Contact with rotating or fast moving parts in machines | Rare | Incorrect use of machines due to improper training or careless workflow procedures | Bodily injury in the form of lacerations, bruises, burns, or broken bones | Major | All team members complete training and certification for usage of machines in the shop and makerspace, safety briefings conducted before rocket construction begins and immediately after any known breach of safety rules or event in which member is harmed | Safety Officer maintains up to date information on trainings for team members. Safety Officer or Chief Engineer oversees machining tasks verifying correct usage of machines. |

| | | | | | | |
|---|---|---|---|---|---|---|
| Harmful contact with fiberglass parts | Possible | Incorrect or insufficient PPE, careless or rushed movements in machining or transporting fiberglass components | Bodily injury in form of cuts, lacerations, splinters | Minor | Members must wear PPE when working with fiberglass including safety glasses, gloves, long pants, and closed shoes | Safety Officer informs team members of proper PPE required for different tasks, including tasks with fiberglass. Safety Officer or Chief Engineer overses construction activities including working with fiberglass. |
| Inhalation of toxic or inflammatory fumes | Possible | Incorrect or insufficient PPE when working with epoxy and other chemicals | Respiratory harm, difficulty breathing, headaches | Major | Materials Safety Data Sheet is up to date and available to all team members. Safety Officer reviews the location of this file with team members periodically so team always knows where to find it. Members conducting activities with toxic chemicals are briefed by Safety Officer before the activity. | Safety officer keeps up to date list of team members training and certifications, including list with names of members who attended briefings on toxic chemical usage. Safety Officer or Chief Engineer oversee all construction processes including epoxying. |

| | | | | | | |
|---|---|---|---|---|---|---|
| Skin contact with epoxy or other inflammatory materials | Possible | Incorrect or insufficient PPE, careless transport of components or materials | Burns, rashes, inflammation | Minor | Materials Safety Data Sheet is up to date and available to all team members. Safety Officer reviews the location of this file with team members periodically so team always knows where to find it. Members conducting activities with toxic chemicals are briefed by Safety Officer before the activity. | Safety officer keeps up to date list of team members training and certifications, including list with names of members who attended briefings on toxic chemical usage. Safety Officer or Chief Engineer oversee all construction processes. |
| Spread if illness from close contact in meetings | Possible | Viral infections going around, time of year, close contact | Illness | Minor | If illness seems to be spreading at WashU or amongst the team, the Exec team will move meetings to Zoom whenever possible, sick team members will not attend in-person meetings | Safety Officer and President keep track of attendance with reasons why members might miss, allowing for tracking of illness-related absences to monitor health of team |
| Severe illness from weather conditions | Rare | Unprepared members during launches | Heat stroke or frost bite | Major | Safety Officer informs team of the weather conditions prior to launch; Exec team coordinates presence of food and water at launches | Safety Officer confirms launch plan with President and informs team of conditions |

## 5.2 Failure Modes and Effects Analysis (FMEA)

### 5.2.1 Payload FMEA

Table 33: Failure Modes and Effects Analysis

| Failure | Likelihood | Cause | Effect | Severity | Mitigation | Verification |
|---|---|---|---|---|---|---|
| Structural Retention System Failure | Possible | Forces from launch, parachute deployment, and landing exceed load capacity | Components come loose, can not properly execute mission | Severe | Design and select material to withstand launch, deployment, and landing forces | Drop tests and FEA load simulations for retention structures and materials |
| Nosecone Retention Failure | Unlikely | Latching mechanism within the body tube break from shear stress | Fractures the payload camera deployment rails | Severe | Ensure latching mechanism material is durable enough and firmly locked into place prior to flight | Drop tests, and FEA load simulations |
| Battery short | Rare | Poor battery quality; battery overheated | Electronic components die, unable to receive commands, motors unable to drive camera deployment | Severe | Choose battery with reliable and appropriate power output | Payload team leads checks battery requirements and new batteries used for launch |
| Wire detaching | Possible | Battery wiring incorrect | Damage to electronics | Major | Follow proper procedures on battery wiring | Payload team leads review battery wiring |

| | | | | | | |
|---|---|---|---|---|---|---|
| Transmitter interferes with avionics electronics | Possible | Improper frequencies chosen or transmitted due to software mistakes | Loss of connection with avionics electronics including flight computer and loss of ability to initiate timed BP detonations | Severe | Position transmitter as far as possible from avionics bay, use frequency far from avionics frequency range | Test transmitting signals from both avionics and payload prior to launches |
| Camera failure | Unlikely | Lens damage during flight | Unable to provide mission critical imaging upon payload deployment | Major | Camera casing system designed to be durable and withstand launch forces | Drop tests and FEA load simulations |
| Loss of RF Communication | Possible | Vehicle travels out of range, signal interference | Unable to complete mission | Severe | RF module is selected for the simulated vehicle flight range, and electronic components are properly shielded to prevent interference | Payload team inspects the RF component before launch and tests data reception |

### 5.2.2 Avionics FMEA

Table 34: Failure Modes and Effects Analysis

| Failure | Likelihood | Cause | Effect | Severity | Mitigation | Verification |
|---|---|---|---|---|---|---|

| | | | | | | |
|---|---|---|---|---|---|---|
| Battery short | Unlikely | Improper or weak wire connections, possibly caused by movement during setup or flight | Fire that damages electronics and vehicle structures, rendering the vehicle incapable of performing satisfactorily and potentially dangerous to team members | Severe | Use proper soldering techniques and test connections to make sure they are sufficient with multimeter, ensure avionics components are attached securely to the board | Avionics team lead teaches proper soldering techniques, oversees new members demonstrate their soldering abilities before soldering on final components |
| Power loss | Rare | Faulty or disconnected batteries | Disabling of avionics components and other vehicle communication subsystems, resulting in failure to properly initiate altitude-triggered events like separation and parachute deployment | Major | Maintain and follow a procedure for charging each type of battery and test each battery before rocket assembly, ensure stable connections when batteries are placed into rocket by testing power before and after insertion | Practice battery assembly for rocket prior to launch daya, Safety Officer reviews charging procedures for each type of battery, Chief Engineer oversees battery insertion and placement into subsystems |

| | | | | | | |
|---|---|---|---|---|---|---|
| Loss of communication signal | Unlikely | Poor positioning of directional antenna at base station | Interruption of real-time flight data transmission making recovery difficult without GPS data on landing location, poor quality and continuity of test launch data for test launch review | Minor | Use procedure for proper antenna setup and positioning, with pre-launch checks to confirm that the handshake between rocket and base station is complete and signal is received | Avionics lead tests the signal after assembly, Chief Engineer certifies connection and results before launch |
| Improper GPS calibration | Rare | Failure to establish or loss of satellite connection due to interference | Poor quality GPS data for test launch analysis and difficulty locating the rocket via GPS data | Moderate | Test connectivity with GPS satellites prior to launch | Avionics lead ensures that reliable GPS connection is established before launch, Chief Engineer approves final connection before rocket is assembled with avionics bay inside |
| Raspberry Pi Bug | Rare | Software issues not discovered prior to launch | Reliable data not retrieved from computer, issues with GPS data and locating rocket | Moderate | Test all code before launch | Avionics team conducts peer review of code included in all avionics subsystem components, peer-review process overseen by Chief Engineer and other skilled coders on the team |

| | | | | | | |
|---|---|---|---|---|---|---|
| Ejection Timing Failure | Unlikely | Improper pressure reading due to blocked pressure port on flight computer | Failure to initiate ejection events at correct times or altitudes, parachute failures and damage to rocket | Severe | Design avionics bay with extra room for flight computer to ensure unblocked pressure ports | Test flight computer pressure readings before launch |
| Lipo Fire | Rare | Improper lipo battery connection, or overcharged battery | Fire and damage to components on avionics board and other rocket subsystems | Severe | Design lipo battery casing to withstand launch forces to prevent battery disconnection, obtain documentation on proper lipo charging times and capacity | Test lipo connection prior to launch, charge lipos ahead of launch only to proper charge capacity, Safety Officer obtains and maintains proper battery charging procedures |



### 5.2.3 Recovery and Propulsion FMEA

Table 35: Failure Modes and Effects Analysis

| Failure | Likelihood | Cause | Effect | Severity | Mitigation | Verification |
|---|---|---|---|---|---|---|

| | | | | | | |
|---|---|---|---|---|---|---|
| Shear pins not sheared | Unlikely | Incorrect (low) black powder charges, charges fail to detonate | Parachute does not eject, catastrophic damage to the rocket due to free fall, danger to humans in landing area | Major | Use more black powder than calculated based on Factor of Safety, Include redundant black powder charge which is 1.25x the amount of the preliminary charge | Test the black powder charge with mentor present, Present results to be confirmed by Chief Engineer |
| Fire damage to parachutes | Possible | Insufficient protection from flames from black powder detonation, parachute material becomes exposed during flight | Parachute fails to deploy, catastrophic rocket damage from free-fall, Endangerment of humans in landing area with decreased reaction time | Severe | Utilized a deployment bag for main parachute, protective nomex blanket for drogue parachute, include parachutes using final folding and assembly during black powder testing and look for any singes parachute material during these tests, Add dog barf when necessary | Recovery and Propulsion team lead packs parachutes using careful documentation written in conjunction with Safety Officer, Confirm test results with Chief Engineer, Confirm final installation with Chief Engineer |
| Tangled shroud lines | Likely | Improper parachute packing, movement during flight | Incomplete parachute opening, Catastrophic rocket damage from free-fall or partial free-fall, Unpredictable drift | Moderate | Research and document appropriate packing methods in parachute packing procedures, Test packing methods with drop tests when possible | Demonstrate packing Chief Engineer, Practice parachute packing prior to any launches, Confirm final installation with Chief Engineer |

| | | | | | | |
|---|---|---|---|---|---|---|
| Eye bolt failure | Rare | Underestimated snatch forces, Insufficient bolt strength, Eye bolt not screwed in fully | Catastrophic rocket damage from free-fall | Severe | Research proper calculation methods for snatch forces, Calculate worst cases snatch force for eye bolt connection design | Confirm calculations with CAD models when possible, Confirm values with Chief Engineer during design reviews, Confirm that eye bolts are properly secured and tightened in final assembly with Chief Engineer |

### 5.2.4 Structures FMEA

Table 36: Failure Modes and Effects Analysis

| Failure | Likelihood | Cause | Effect | Severity | Mitigation | Verification |
|---|---|---|---|---|---|---|
| Plywood board fracture | Possible | Snatch force from parachute deployment | Structural fracture/failure and damage to rocket, New weaknesses in airframe due to structural damage | Major | Research plywood force ratings and calculated allowable forces with factor of safety, design with worst case flight forces considered | Use CAD models to simulate forces and ensure plywood can withstand these forces |

| | | | | | | |
|---|---|---|---|---|---|---|
| Fin fracture | Unlikely | Flutter in fins from high flight turbulence, or impact damage, increased drag on fins due to failure of new fin covers | Fin damage leading to unstable flight path, critical damage to rocket | Severe | Research flutter calculations and consult Chief Engineer to choose best calculation method, multiple structures members calculate these flutter values to cross-check and verify results | Use CAD models when possible to check the allowable forces, Chief Engineer confirms calculated vibrations are allowable given fin design |
| Bulkhead fracture | Rare | Large shear force at connection points | Catastrophic damage to rocket due to free-fall, danger to humans in landing area | Severe | Research calculation methods for shear of bulkheads and verify these methods with Chief Engineer, test bulkhead shear strength in school labs when available | Use CAD models to check the allowable forces, Chief Engineer confirms the forces calculated are below requirements with factor of safety considerations, Require larger safety factor to reduce likelihood of failure |
| Airframe buckling | Rare | Compression force from rocket during launch or upon landing impact | Catastrophic damage to rocket due to free-fall, Danger to human in landing area, Unstable flight conditions and unstable flight path | Severe | Test airframe material in school labs when possible, calculate compressive forces from both maximum motor forces and maximum ground impact forces | Use CAD models when possible to check the allowable forces with large safety factor, Chief Engineer confirms that the forces involved are below requirements |

## 5.3 Environmental Concerns for Launch Site

Table 37: Environmental Concerns for Launch Site

| Failure | Likelihood | Cause | Effect | Severity | Mitigation | Verification |
|---|---|---|---|---|---|---|
| Fire hazard | Unlikely | Crashed rocket, motor ignition failure, improper connection of ignitors, battery failure/short | Damage to environment at launch site, risk of injury to team members, harm to wildlife if fire spreads | Severe | Verify black powder connections and e-match connections with team mentor, purchase motor from reputable dealer, use safe storage techniques for batteries | Confirm final installations of ignitors with Chief Engineer and Safety Officer, follow prescribed launch preparations procedures and operations |
| Debris and material pollution to surrounding area | Unlikely | Crashed rocket, Loose hardware, careless rocket preparation and cleanup procedures | Pollution of launch site habitat, harm to local wildlife | Moderate | Test components connections, test hardware for sufficient fastening; follow construction procedure without rushing, clean up after launch | Chief engineer confirms finals attachments and fastenings, exec team supervises cleanup procedure after launch |
| Chemical pollution | Rare | Crashed rocket, improper application of epoxy, unfavorable weather conditions for paint | Pollution of launch site habitat from motor exhaust, battery leaks, chipped paint, epoxy fragments, epoxy fumes | Major | Practice safe battery storage and usage, purchase motors from reputable dealers to ensure acceptable emissions, minimize last minute epoxy or painting activities on the launch field | Chief engineer and structures team lead inspect paint and epoxy for chips or deterioration, clean up as much as possible if paint chips or epoxy fragments are released onto ground |
| Noise pollution | Likely | Motor ignition; black powder ignition | Potential damage to nearby structures and harm to local wildlife | Minor | Follow NAR regulations which require launch to occur a safe distance from buildings and roads, check with RSO for noise issues with wildlife at launch site | Safety Officer confirms launch site is in compliance with NAR codes, Safety Officer confirms with RSO that noise will not have impact on wildlife |

# 6 Project Plan

## 6.1 Testing and Demonstrations

### 6.1.1 Vehicle Component Testing

1. **Snatch Force Testing**
   **Introduction**

The possibility of the snatch force from the parachute deployment deforming the rocket bulkhead necessitates this test. Whether or not the Delrin plate yields at the calculated forces below will determine the viability of using the lower-weight Delrin material on a full-scale rocket and verifies the use of a stronger material like 6061-T6 Aluminum.

| Objective | Criteria for Success | Test Variables |
|---|---|---|
| Determine whether Delrin bulkhead can withstand the calculated snatch force without visual deformation. | Bulkhead is placed into a tensile tester. Delrin structural limits must meet or exceed calculated force with no visible yielding after load is removed, assuming a safety factor of 1.5. | Delrin bulkheads are tested. |

Delrin bulkheads were tested to determine whether the structural limits of Delrin would withstand the calculated and experimental snatch force data. The bulkheads must have a yield strength that meet or exceed the snatch force from parachute deployment. The three methods used to calculate snatch forces are displayed in Table 38.

Using the OSCALC snatch force calculator, a maximum force of 4,096.215 N was obtained. Calculating the max drag force on the parachute using its drag coefficient, and substituting the values in for air density, the velocity at the moment before the parachute opens, and the area of the main parachute into the equation provided by NASA results in a predicted force of 11,488 N. In addition, the team utilized a set of coupled differential equations to estimate the peak tension force in the shock cord, taking into account the spring coefficient of the shock cord. The differential equations approximate the rocket system on descent as the main parachute and a high mass object, with a tension force applied between them. The appropriate drag and mass terms are applied to both object considered.

$$M_p\ddot{y}_p = \frac{1}{2}C_p\rho A_p\dot{y}_p^2 - M_pg - Tension(y_p, y_r) \tag{21}$$

$$M_r\ddot{y}_r = \frac{1}{2}C_r\rho A_r\dot{y}_r^2 - M_rg + Tension(y_p, y_r) \tag{22}$$

$$Tension(y_p, y_r) = \begin{cases} (y_p - y_r - L) * k & \text{if } y_p - L > y_r \\ 0 & \text{if } y_p - L <= y_r \end{cases} \tag{23}$$

In equations 21 to 23, all terms with a subscript of p and refer to the quantities associated with the parachute and rocket respectively. The quantities that are considered are the positions of the two objects, y [m], the mass of the objects, M [kg], the drag coefficient C, the characteristic area, A [m$^2$], the density of air, $\rho$ [$\frac{kg}{m^3}$], the spring coefficient, k $[\frac{kg}{m}]$ and the length of the shock cord, L [m]. The spring coefficient was determined by multiplying the elastic modulus of nylon by the cross-sectional area of the shock cord and dividing by the length. This system of coupled differential equations was solved with Wolfram Mathematica, yielding a predicted max tension force of 5750 N.

Below are the calculated force values derived from each method.

Table 38: Snatch Force Success Criteria

| **Method** | **Equation** | **Force (N)** | **Safety Factor** | **Calculated Force with Safety Factor (N)** |
|---|---|---|---|---|
| NASA | $\frac{1}{2}C_p\rho A_p V_{open}^2$ | 11,488 | 1.5 | 17,232 |
| OSCALC | N/A | 4,096.22 | 1.5 | 6,144.32 |
| Diff. Eq. | N/A | 5750 | 1.5 | 8625 |

**Testing Procedure**

1. Attach both bulkheads with 3/8-16 lead screws and 1/4-28 flange nuts.
2. Mount eye-bolts to bulkheads with flange nuts.
3. Secure eye-bolts to Instron Load Frame with wedge action tensile grips.
4. Calibrate load frame until there there is no tension applied to the testing sample.
5. Perform tensile test using 68TM-30 Load Frame, increasing force applied by 2.5kN increments to observe any deformations.
6. Compare yielding results to calculated snatch force data to determine whether Delrin bulkhead reaches required yield strength.

Table 39 contains the results for this test.

Table 39: Delrin Bulkhead Yielding Results

| **Force Applied (N)** | **Maximum Displacement (mm)** | **Visible Yielding After Load Removed** |
|---|---|---|
| 2500 | 1.79 | No |
| 5000 | 3.71 | No |
| 7500 | 5.61 | No |
| 10000 | 9.29 | No |
| 12000 | 13.07 | No |
| 15000 | 26.06 | Yes |

Below are images of the bulkhead while a load was applied and an image of the bulkhead's deformation after being removed from the testing apparatus.

Figure 112: Visible Bending Of Bulkhead Testing Sample With 15 kN Applied

Figure 113: Permanent Deformation of Delrin Bulkheads After Released from 15 kN Test

For the tensile test, an Instron 68TM-30 Load Frame stretched the bulkheads apart with a tensile force, as seen in Figure 112. The tensile force within the test simulated the snatch force of the parachute. The tensile force was increased by approximately 2.5kN in each trial until the bulkheads yielded at 15kN. Figure 113 shows the Delrin bulkheads after 15kN of force were applied, and visible, permanent deformation can be seen after release from the load frame. The test results in Table 39 demonstrate that the Delrin bulkheads could withstand up to 15kN before yielding. Testing results exceeded expectations from FEA simulations. Based on the data gained, Delrin seems to be an appropriate choice for a sub scale application as it was able to withstand more force than what was calculated for expected maximum snatch force based off the OSCALC and Diff. Eq methods.

### 2. Fin Shell Material Testing

#### Introduction

The team performed two tests in order to drive the design for the 3D-printed fin shells: a subjective smoothness test and an empirical compression test. The following table contains the objectives, success criteria, and variables for these tests.

| Test | Objective | Criteria for Success | Test Variables |
|---|---|---|---|
| Smoothness | Determine which print material will have the most aerodynamic finish in order to aid in reaching the expected apogee. | Print material is ranked based on the roughness of the surface. Ideal smoothness has little to no ridges and should feel completely even to the touch. | PLA and PETG prints are tested both as printed and after sanding. Resin is tested as printed and Polysmooth is tested after smoothing using alcohol according to the manufacturer's instructions. |
| Compression | Determine which print material can withstand the most force in order to ensure that surface finish is not traded for structural stability. | Small samples of each print material are placed into a compression machine. The print material with the highest yielding force is determined to be the strongest. | PLA, PETG, Resin, and Polysmooth are tested. |

PLA, PETG, and resin print materials were tested for smoothness and compressive strength. WURocketry intended to test an additional polysmooth filament, but a shipping delay necessitated that the polysmooth material results be omitted from the initial test. The team plans to perform these tests in January of 2023.

The purpose of the subjective smoothness test was to determine which of the tested materials will produce the least aerodynamic drag. During the October 29th, 2022, subscale launch, the vehicle undershot its calculated apogee. The team theorized that the ridges (caused by the manufacturing method of extrusion printing) in the sub-scale's PLA fin shells increased drag. The subjective smoothness test provided the team with a uniform subject to compare each material's relative smoothness.

**Testing Procedure**

1. Print PLA, PETG, Resin, and Polysmooth testing cylinders.
2. Smooth each material (see below for techniques for each material).
3. Perform subjective smoothness test.
4. Perform compression test using 68TM-30 Load Frame to the point of material failure.
5. Analyze the maximum force each print can sustain to determine which material can sustain the highest force.

The PLA and PETG were sanded until smooth to touch to reduce ridges along the outside of the print caused by extrusion printing. Polysmooth is a specific type of extrusion print material that smooths when in contact with Isopropyl Alcohol. Two methods for distributing the alcohol across the part will be tested; spraying and dipping. The Resin print was not smoothed because resin prints are comparably smooth by nature.

After smoothing, resin was the smoothest, followed by sanded PLA, sanded PETG, un-sanded PLA, and un-sanded PETG.

For the compression test, an Instron 68TM-30 Load Frame applied a force via compression plates, as seen in Figure 114. The PLA and PETG samples were compressed to the point of clear plastic deformation, but the resin sample reached the maximum load of the testing apparatus before yielding. As such, the compression test for the resin sample was deemed inconclusive.

Table 40 contains the results for this test along with each sample's weight and manufacturing cost.

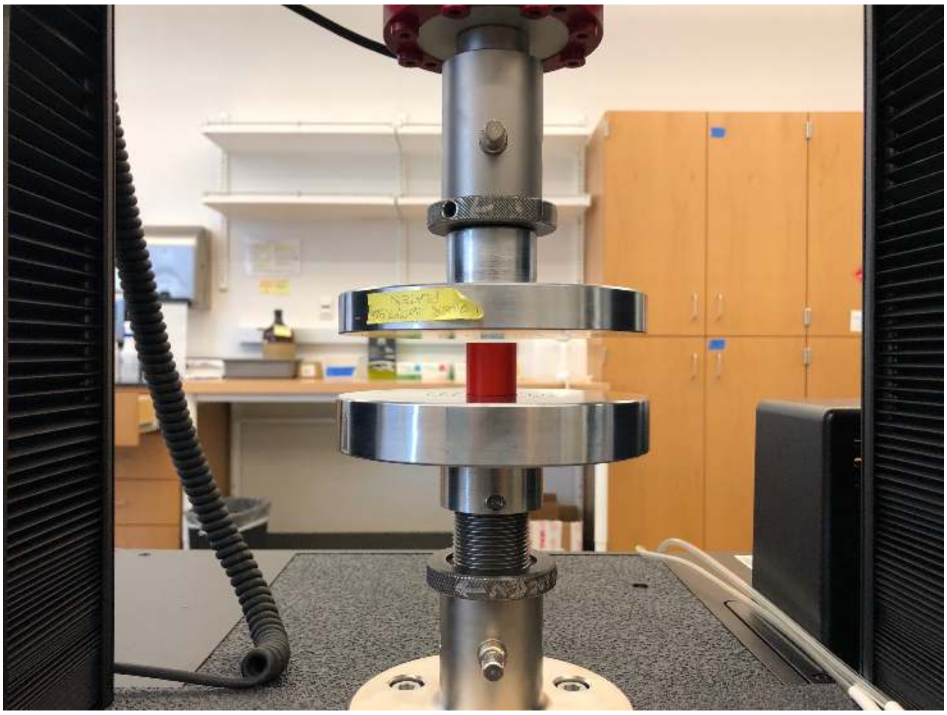

Figure 114: Compression Test Setup

Table 40: Fin Shell Test Results

| | PLA | PETG | Resin | Polysmooth |
|---|---|---|---|---|
| Weight (g) | 5 | 5 | 15 | N/A |
| Yielding Force (kN) | 4.92 | 3.75 | Inconclusive | N/A |
| Ultimate Force (kN) | 4.92 | 3.75 | Inconclusive | N/A |
| Cost (USD) | 0.255 | 0.265 | 3.2125 | N/A |

As shown in Table 40, the PLA experienced a yielding and ultimate force of 4.92kN which was the highest compared to the other materials tested. While the Resin exceeded the force range of the Load Frame, the material is far more expensive and heavy so Structures has elected to not use this material. Thus no further testing will occur for the resin, despite inconclusive results. Additionally, sanded PLA was smoother compared to PETG which is why, based on the data collected, Structures will use sanded PLA for the full-scale rocket's fin shells for its strength-weight ratio. However, the team has plans to test the Polysmooth filament in January, 2023 before finalizing the material selection. If the Polysmooth filament is of strength to the PLA and is significantly smoother, as WURocketry predicates, then the team will use Ploysmooth for the full-scale rocket's fin shells.

**3. Body Tube Compression Testing**

The objective of this test is to understand how the body tube deforms in compression to simulate launch forces from the motor. The thrust forces from the motor are transferred to the thrust plate, which transfers the forces to the body tubes. The test will be successful if the body tube survives the max thrust force times the factor of safety without damage. This test will demonstrate the reusability of the body tubes between launches. If the test fails, an alternate body tube material will need to be chosen because the motor cannot be changed. The team will use an Instron Compression Testing in the Shared Instrument Lab at Washington University to apply compressive force to a sample of the body tube in January of 2023.

**Testing Procedure**

1. Acquire a sample of a G12 Fiberglass body tube from scrap.
2. Ensure that both sides of the body tube are level and flat.
3. Place the sample in the center of the 68TM-30 Instron Load Frame.
4. Perform compression test using the load frame. Compress the sample until the maximum force value is 1.5 (safety factor) times the thrust force from the motor.
5. Inspect the sample when it is removed from the load frame to ensure that there are no cracks.

### 6.1.2 Recovery and Propulsion Testing and Demonstrations

#### 1. Deployment Bag Demonstration

**Introduction** The Deployment Bag Demonstration ensures that the main parachute is not packed too tight in its associated deployment bag. A successful demonstration is when the parachute can be pulled out of the bag with little applied force. If the test fails, the folding procedure or method will be reconsidered and re-tested.

| Objective | Criteria for Success | Test Variables |
|---|---|---|
| Demonstrate successful deployment of the parachutes | Parachutes deploy with minimal applied force | Applied Force |

**Testing Procedure**

1. Fully assemble the rocket to reflect launch readiness; neglecting shear screws
2. Pull the Aft and Forward sections apart in parallel opposite directions while supporting the avionics bay.

**Results**
The Sub-scale and Full-scale Deployment Bag Demonstrations have both been completed successfully. No changes have been made as a result of their performance

#### 2. Black Powder Separation Test

**Introduction** The objective of this test is to ensure the forward and aft chamber pressurization from black powder ignition is neither too low nor too high, as the first would prevent the parachute from deploying and the latter could cause damage to the components of the rocket. If testing fails, increasing or decreasing the mass of black powder by 25%-35% may be an effective solution. The percentage of increase or decrease will be chosen with the advice of the team mentor, Mike Walsh.

| Objective | Criteria for Success | Test Variables |
|---|---|---|
| Demonstrate the resulting separation of the rocket due to calculated black powder quantities | Full rocket separation with no resulting damage to the rocket | The mass of black powder for primary drogue and main section charges |

**Procedure**

1. The Safety Officer, Drew DeRupertis, and the Recovery Propulsion Team will travel to Team Mentor Mike Walsh's house for the separation test.
2. Mike Walsh, Drew DeRupertis, and the Recovery and Propulsion team will put on appropriate protective equipment, including safety glasses and gloves. The rocket will be assembled following launch procedures.
3. Mike Walsh will place the following quantity of black powder into the primary charge ejection canister to test the first section separation for the drogue parachute deployment.

Full-Scale Charge: 1.8 g

Sub-Scale Charge: 0.9 g

4. Mike Walsh will insert an e-match into the main ejection canister.

5. The recovery and propulsion team lead, Mikayla Jenkins, will close the rocket with two 4 shear pins.

6. Team members will distance themselves at least fifteen feet from the side of the rocket. Caution is taken not to stand in line with either ends of the rocket.

7. Mike Walsh will wire the e-match to a nine volt (9V) battery. The team will observe the separation of the rocket sections.

8. If the rocket does not separate successfully, the mass of black powder will be increased by 25-35 percent of the previous test value.

9. Steps 3-8 will be repeated with new black powder quantity until successful separation occurs.

10. The same steps will also be repeated with the following quantity of black powder, and four 4 shear pins, for the second section separation for the deployment of the main parachute.

    Full-Scale Charge: 4.1 g

    Sub-Scale Charge: 1.8 g

11. Once both sections' separation tests are successful, black powder masses will be recorded and the tests will be complete.

    Note: The redundant charge is not tested in any separation test.

**Results**
Table 41 contains the calculated black powder quantities for the sub-scale rocket.

Table 41: Initial Sub-scale Black Powder Charge Quantities

| **Charge** | **Mass (grams)** |
|---|---|
| Primary Drogue Ejection Charge | 0.9 |
| Redundant Drogue Ejection Charge | 1.1 |
| Primary Main Ejection Charge | 1.8 |
| Redundant Main Ejection Charge | 2.2 |

Table 42 contains the results for this test. The main and drogue parachute deployments were both successful, however the drogue deployment black powder quantities was increased by approximately 35% for improved performance.

Table 42: Final Sub-scale Black Powder Charge Quantities

| **Charge** | **Mass (grams)** |
|---|---|
| Primary Drogue Ejection Charge | 1.3 |
| Redundant Drogue Ejection Charge | 1.6 |
| Primary Main Ejection Charge | 1.8 |
| Redundant Main Ejection Charge | 2.2 |

The Sub-scale Black Power Separation Test has been completed successfully with an approximate 35% increase in drogue deployment charge quantity for ideal performance. The Full-scale Black Power Separation Test has not been completed.

### 3. Parachute Durability Test

**Introduction** The objective of the parachute durability test is to determine various parachute models' ability to withstand harsh environmental conditions or obstacles, such as corn stalks upon landing. This is to be done by plotting the resulting stress-strain curves of the parachutes from their output yield strength values. The following procedure is conducted with an ADMET eXpert puncture testing machine.

| Objective | Criteria for Success | Test Variables |
|---|---|---|
| Determine the durability of various parachute models | Minor to no visible tearing of the material during testing | Material Yield Strength |

**Testing Procedure**

1. Lay the parachute flat on the base of the machine and pull on all sides to make sure there are no wrinkles in the parachute
2. Secure the parachute down to the base of the machine using the circular mount and the clamps
3. Attach a probe with a diameter of 30 mm to the head of the machine (to mimic conditions the parachute may experience)
4. Set the machine to slowly lower the probe down towards the parachute
5. Once the probe breaks through the parachute, the max values of force and energy applied will be shown on the digital readout
6. Raise the probe back to its starting position and release the clamps holding down the parachute
7. Remove the parachute from the machine
8. Repeat steps for two trials per parachute model

**Results**
The Parachute Durability Test has not been completed.

### 4. Hardware Tensile Test

**Introduction** The hardware tensile test sets out to prove that the hardware apparatus connecting the shock cords to the body of the rocket can withstand a minimum load of 550 Ibf, which was smallest quoted force for a component of the apparatus. The test will run with constant increasing load until maximum yield strength is determined. The Recovery and Propulsion (R&P) Subteam will perform this test through the use of a Universal Testing Machine. This test will determine if the components of the hardware apparatus reflect the expected tensile strengths quoted by their manufacturers, and therefore can withstand the separation force of the rocket. If the test fails, new hardware will be purchased with greater maximum strength.

| Objective | Criteria for Success | Test Variables |
|---|---|---|
| Validate the maximum instantaneous load of our hardware | No visible deformation or breakage after 550 lbf is applied | Maximum strength of hardware apparatus |

**Testing Procedure**

1. Assemble the hardware in the following order: eyebolt, quicklink, swivel joint, quicklink, eyebolt.
2. Screw the eyebolts into steel blocks to be held by the tensile tester clamps.
3. Adjust the lower and upper clamps to fit the length of the hardware and blocks.
4. Clamp the steel blocks, ensuring that the hardware is vertically aligned between the tensile clamps.
5. The machine will separate the tensile clamps with a constantly increasing force until deformation is detected.
6. Once deformation occurs, the maximum yield strength will be recorded from the digital readout

**Results**
The Hardware Tensile Test has not been completed.

### 5. Masking Tape Strength Test

**Introduction** The objective of the masking tape strength test is to determine the amount of force needed to break the loops of masking tape wrapped around the shock cords. This force will indicate if break banding is a useful practice in reducing snatch force experienced on the rocket. If the test is successful, break banding will be used on the drogue shock cords to further prevent premature separation of the main parachute at deployment. If the test is unsuccessful, break banding will no longer be utilized in launch procedures. The following procedure is conducted with a Universal Tensile Testing Machine.

| Objective | Criteria for Success | Test Variables |
|---|---|---|
| Determine the maximum strength of various masking tape thicknesses | The amount of force required to break the masking tape is greater than 25% of the snatch force experienced by the drogue parachute | Masking tape loop thickness and maximum strength |

The decent velocity after drogue deployment is 116.2ft/s, with a coefficient of drag of 1.5 and drogue parachute area of 1.696 $ft^2$. Using NASA's method in Section 6.1.1

Snatch Force Testing, a snatch force of 180.7 N (40.6 lbf) was calculated. If a masking tape band can withstand up to 10.15 lbf, this quantity would be considered substancial enough to utilize in launch configurations.

**Testing Procedure**

1. Prepare 4 loops of masking tape; varying from one layer of tape to 4 layers of masking tape
2. Align the loop of tape vertically and insert into the machine
3. Adjust the clamps such the masking tape is held securely on both ends
4. Align and attach the extensometer to the masking tape (if using non-contact extensometer, ensure it is aligned with the center of the loop of tape)
5. Ensure all clamps are attached to the tape
6. Use the software in the machine to set the machine to slowly separate the crosshead and stretch the tape
7. Once the loop of tape breaks, the max force will be recorded and graphs of the data will be shown
8. Remove the extensometer from the tape and remove the tape from the clamps
9. Repeat steps 2-8 until two trials for each loop thickness is completed. The average of the two trials will be taken.

**Results**
The Masking Tape Strength Test has not been completed.

### 6. Snatch Force Testing

**Introduction** The objective of the Snatch Force test is to determine the force experienced on the rocket from main and drogue parachute deployments. The Recovery and Propulsion (R&P) Subteam will perform this test with the use of a load cell during test launches. If the testing fails, causes of failure will be considered and improved before re-testing at a following launch. The snatch force values read will be compared to calculations found in Section 6.1.1 Snatch Force Testing.

| Objective | Criteria for Success | Test Variables |
|---|---|---|
| Determine the snatch force experienced after main and drogue parachute deployments | Parachute fully inflates and a value for snatch force is read | Main and Drogue parachute snatch force values |

**Testing Procedure**

This procedure is designed to determine the snatch force experienced by the rocket. This aids in the understanding of the minimum strength required for the hardware chosen based on the sizes, descent speeds, and drag coefficients of the parachutes. Two load cells will be used and attached to the shock cords associated with the heaviest sections after drogue and main parachute deployment stages.

1. Follow the Parachute Folding Procedure.

   Main Parachute: *Main Parachute Folding Procedure*

   Drogue Parachute: *Drogue Parachute Folding Procedure*

2. Attach a load cell to the parachute

3. Attach the shock cord to the load cell

   Main Parachute: 15ft Forward Main shock cord

   Drogue Parachute: 15ft Drogue shock cord

4. Follow launch day procedures

5. Launch rocket and record snatch forces experienced

**Results**
The Snatch Force Test has not been completed.

**7. Shock Cord Tensile Test**

**Introduction** The shock cord tensile test sets out to compare the percent difference in the elasticity of nylon shock cords and its alternative, kevlar shock cords, when under a force of 2100 Ibf. The Recovery and Propulsion (R&P) Subteam will perform this test through the use of a Universal Testing Machine. This test will provide more accurate elasticities of the two shock cord materials for calculations due to their variation in braid and thicknesses.

| **Objective** | **Criteria for Success** | **Test Variables** |
|---|---|---|
| Compare nylon's elasticity to kevlar's under the stress of 2100 Ibf | Recorded values of elasticity | The extension of the shock cords measured by the extensometer |

**Testing Procedure**

1. Cut the nylon shock cord into 3 separate 5 in. strips.

2. Adjust the lower and upper clamps to fit the length of the shock cord.

3. Place the shock cord between the tensile clamps, gripping at least $\frac{3}{4}$ of the material's surface area into the vise.

4. Ensure that the material is vertically aligned between the clamps.

5. Attach the extensometer at both ends of the exposed shock cord.

6. The machine will separate the tensile clamps with a force of 2100 Ibf.

7. Remove the deformed shock cord from the clamps.

8. Record the extensions given by the extensometer.

9. Repeat this process for a total of three trials and take the average extension value.

10. Repeat steps 1-9 for the kevlar shock cord.

11. Calculate and compare the percent differences in extension of the two materials.

**Results**
The Shock Cords Tensile Test has not been completed.

### 6.1.3 Avionics Testing and Demonstrations

#### GPS Demonstration

**Introduction** The purpose of this demonstration is to verify that the TeleGPS V2 and base station computer/device are properly communicating with each other via the TeleBT and a bluetooth connection. This is done by checking the "age" datapoint on the base station software and confirming that the GPS coordinates from the software are accurate.

| Objective | Criteria for Success | Demonstration Variables |
|---|---|---|
| Prove the proper function of the GPS Vehicle Tracking system | Verify proper GPS start up, communication, and data transmission | Transmitted GPS coordinates and signal age |

#### Materials

- TeleGPS V2
- TeleBT
- Bluetooth Capable Base Station Computer/Device and Receiver
- 3-Element Yagi Antenna
- Cellular Device

#### Procedure

1. Assemble 3-element yagi antenna and connect antenna to TeleBT via SMA connection.
2. Connect TeleBT to the base station computer/device via a bluetooth connection.
3. Verify that the "age" datapoint on the base station software is 0 or 1 that indicates that data is being received from the TeleGPS V2.
4. Verify that the GPS coordinates are accurate by checking GPS coordinates online with a cellular device.

**Conclusion** The TeleGPS V2 successfully turned on, and the data stream of GPS coordinates was validated and compared using Google Maps and Google Earth. Furthermore, the TeleGPS V2 efficiently connected to more than ten satellites offering a stable and precise connection.

**GPS Accuracy Test**

**Introduction** The purpose of this test is to measure the accuracy of the TeleGPS V2's distance tracking. This is conducted by moving the TeleGPS V2 by a set of predetermined distances and comparing and contrasting the predetermined distances with the distances given by the base station software.

| Objective | Criteria for Success | Test Variables |
|---|---|---|
| Determine the accuracy of the reported GPS coordinates provided by the TeleGPS | Reported GPS coordinate's standard deviation is minimal | Distance from base station |

**Materials**

- TeleGPS V2
- TeleBT
- Bluetooth Capable Base Station Computer/Device and Receiver
- 3-Element Yagi Antenna
- 2 Individuals to Perform the Test
- Measuring Tape

**Procedure**

1. Assemble 3-element yagi antenna and connect antenna to TeleBT via SMA connection.
2. Connect TeleBT to the base station computer/device via a bluetooth connection.
3. Person 1 holds the TelegGPS V2 and walks away from the base station, while person 2 monitors the data appearing at the base station.
4. The place where person 1 stopped is marked using a piece of tape, and the distance between the piece of tape and the base station measured using a measuring tape. All measurements and GPS recordings are recorded.
5. Steps 1 and 2 are repeated for 5 trials. In each trial a different distance is covered by person 1: 5 m, 10 m, 15 m, 20 m, and 25 m.
6. The data from the base station is compared with the data physically measured with the measuring tape, and several key statistics such as percent error and standard deviation are calculated.

Table 43: GPS Testing Data

| Distances (m) | Trial 1 (m) | Trial 2 (m) | Trial 3 (m) | Trial 4 (m) | Average (m) | Standard Deviation (m) |
|---|---|---|---|---|---|---|
| **20** | 30 | 18 | 22 | 25 | 23 | 4.69 |
| **50** | 52 | 48 | 49 | 50 | 49.8 | 1.48 |
| **100** | 97 | 96 | 102 | 99 | 98.8 | 2.39 |

**Conclusion** The TeleGPS V2 successfully sent its location to the TeleBT with good accuracy. The average of all the trials were within five meters of the desired distance, and on average, the distance was off by less than three meters, approximately 2.85 meters, based on the standard deviation of the trials. It is important to also note that the TeleGPS V2 was more accurate as the distance increased and less accurate at very close distances from the base station. This can be seen by the standard deviation for a distance of twenty meters is much higher than that of the fifty meter distance and one hundred meter distance. Overall, the TeleGPS V2 and the TeleBT can be successfully used to pinpoint the location of the rocket with less than 1% error across an average of all the differences. This accuracy will give us accurate measurement for the rocket's location at all times, increasing efficiency of recovery, safety, and a redundant measurement for the apogee.

**Recovery Circuit Continuity Demonstration**

**Introduction** This demonstration sets out to prove the complete continuity of the flight computer circuit by using a multimeter to authenticate that each section of the circuit is flowing as expected. The tested variable is whether or not a connection has continuity. If continuity is true for all connections, then the criteria for success is reached. The continuity of this circuit is vital to ensuring that no components are set off prematurely or act in an unpredictable manner.

| Objective | Criteria for Success | Demonstration Variables |
|---|---|---|
| Prove the continuity of the recovery avionics circuit | The multi meter shows continuity across each solder joint and temporary connection in the circuit | Electrical continuity |

**Materials**

1. Multimeter
2. Circuit
   (a) Two EasyMini v2.0 flight computers
   (b) Two Lithium Polymer 3.7V 900mA batteries

(c) 2 Rotary Switches

(d) Terminal Blocks

(e) Wires

**Procedure**

1. Test for continuity at the appropriate locations. Turn on multimeter, turn dial to continuity setting.
2. Touch the test leads to each point indicated on the figure below. Each pair of triangles of the same color indicate a pair where continuity should be tested (i.e. one test lead should be at one location indicated by a triangle in figure —, the other should be at the other location with the triangle of the same color).
3. If the multimeter beeps, continuity is true.

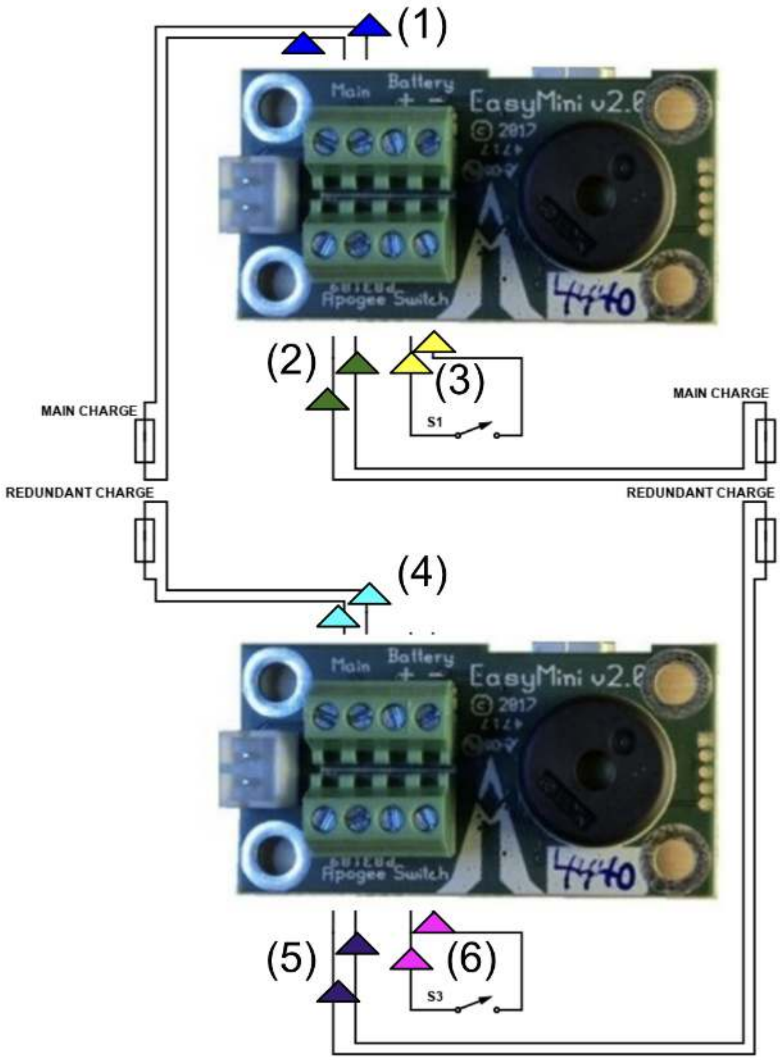


Figure 115: Places to test for continuity. Each set of colored triangles represents the location of the multimeter prongs for each individual test. (Note: locations 1,2,4, and 5 are being tested at the respective terminal blocks for those charges)

Table 30. Continuity of each connection in circuit

| Connection Number | Continuous |
|---|---|
| 1 | True |
| 2 | True |
| 3 | True |
| 4 | True |
| 5 | True |
| 6 | True |

After testing the continuity of all connections, all were found to be true. Assuming each individual component is continuous (a reasonable assumption, as the components were bought and presumed to be quality-tested), this confirms the continuity of the entire circuit.

### Flight Computer Deviation Test

**Introduction** This test aims to determine the average differences in data between the main and redundant flight computer using flight information from a previous sub-scale launch. The flight computers should experience the same data as input and should therefore have no significant difference in data. Thus, if the redundant data is within one standard deviation of the main, then the criteria for success is reached. This information can then be utilized to distinguish outliers in recorded flight data as well as provide an understanding of the range of error of the data.

| Objective | Criteria for Success | Test Variables |
|---|---|---|
| Determine the average difference between data read by the two on board flight computers | The data between the two flight computers is precise with a low standard deviation | Acceleration, height, and speed |

#### Materials

1. AltosUI
2. Flight Data
3. Flight computers
4. Micro USB Cable

#### Procedure

1. Pull flight data from each flight computer.
2. Open AltosUI on computer, connect USB cable to computer and flight computer of interest(main or redundant).
3. Download data in spreadsheet form.
4. Transfer data into spreadsheet(Google sheets and excel work well)

5. Convert data points into imperial.
6. Calculate difference between the redundant and main data points for each tick.
7. Find the average difference and standard deviation for each data column(acceleration, height, speed, etc.).

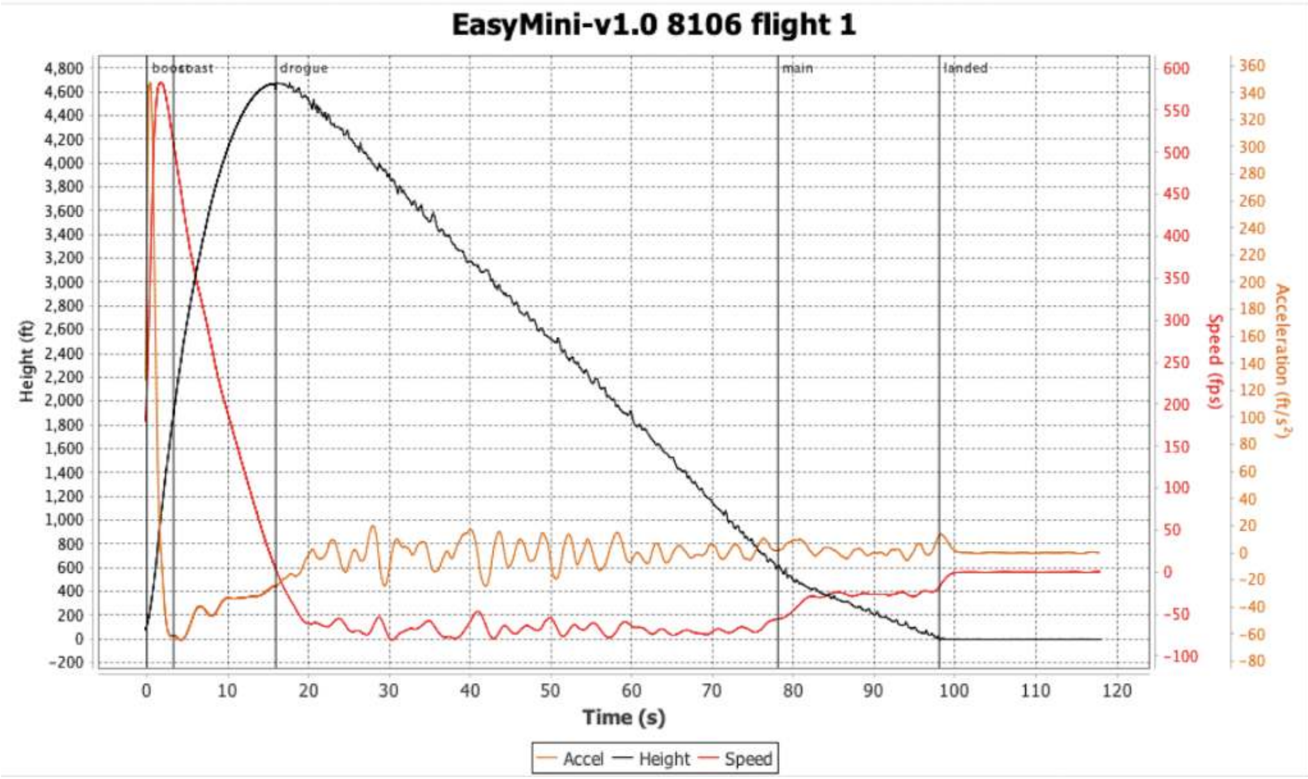


Figure 116: Primary flight computer acceleration, height, speed plotted

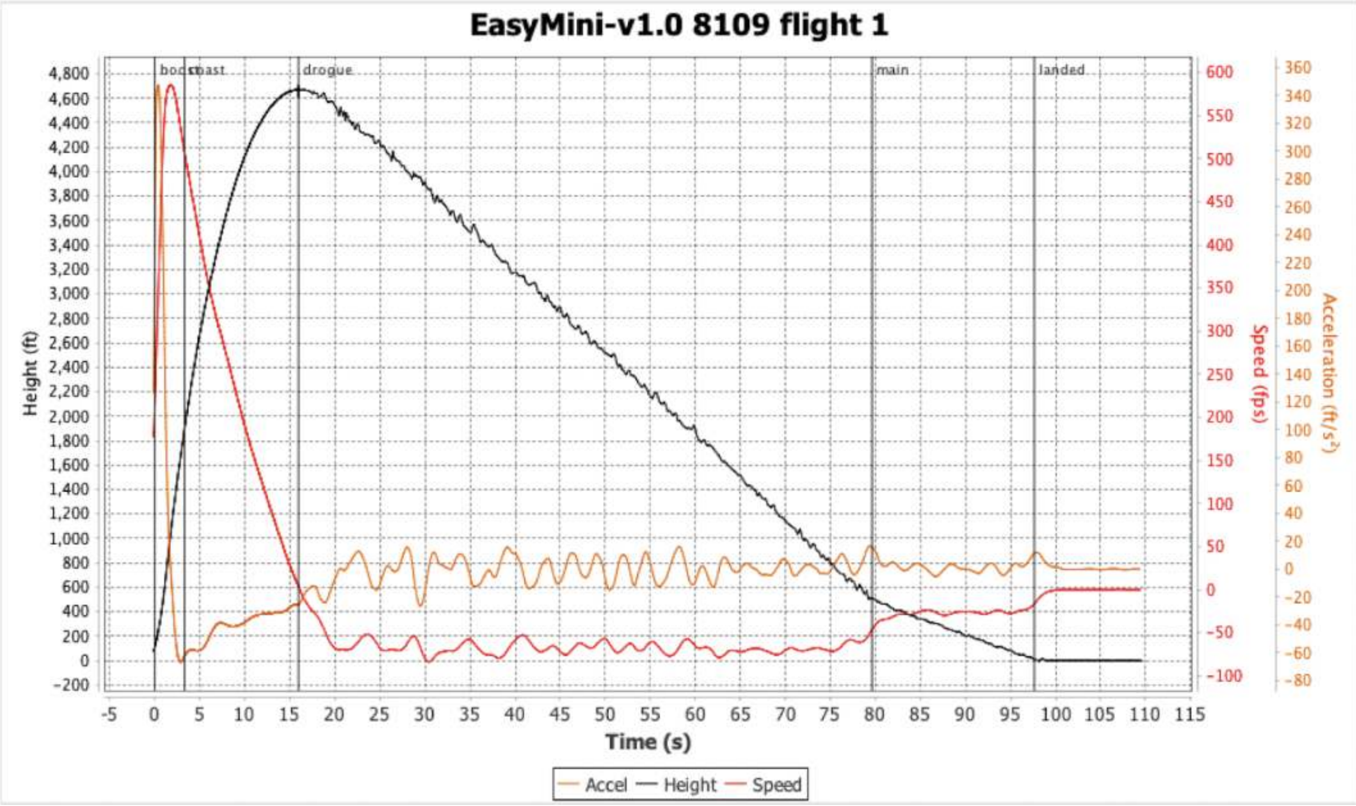


Figure 117: Redundant flight computer acceleration, height, speed plotted

Table 31. Acceleration, Height, and Speed Differences for Subscale Flight

| | Acceleration Difference (ft) | Height Difference (ft) | Speed Difference (ft) |
|---|---|---|---|
| Average | 0.0946 | 0.5333 | 0.0661 |
| St. Dev | 3.3849 | 5.8856 | 2.3627 |

**Conclusion** Observing this data, we concluded that the main and redundant altimeters should have an average difference of .0946 ft in their acceleration, an average difference of 0.5333 ft in recorded height, and an average difference of 0.0661 ft in recorded speed. These values can be used, along with the calculated standard deviation, to determine whether or not data from a given flight is anomalous in some way. Seeing as the average differences for all variables are within one standard deviation of zero, as seen in Table 31, our test's success criterion was reached.

### Pressure Sensor Demonstration

**Introduction** The purpose of this demonstration is to verify that the Sparkfun Qwiic MicroPressure Sensors are accurately reading the atmospheric pressure, writing to the data to a file, and correctly interfacing with the Raspberry Pi 4B+. To do this, both pressure sensors read data at 20 Hz for a duration of 10 seconds. This was then compared to the actual pressure obtained from the weather app in inHg.

| Objective | Criteria for Success | Demonstration Variables |
|---|---|---|
| Verify proper function of the Raspberry Pi 4B+ and the pressure sensors | Verify that proper pressure data is read from the pressure sensors by the Raspberry Pi | Pressure data |

**Materials**

- 2x Sparkfun Qwiic MicroPressure Sensors
- RaspberryPi 4B+ 4GB Model
- Jumper Cables
- LED light
- Base Station Computer
- USB-C Cable
- Weather App to Read Actual Pressure

**Procedure**

1. The Pi was connected to via an ssh connection with an Ethernet cable to the base station computer.
2. A Python script using the adafruit mprls library was written locally on the RaspberryPi in order to read the data from each of the sensors configured on I2C Bus 3 and I2C Bus 4 at a frequency of 5 Hz that would run on boot.
3. An LED was added to the RaspberryPi and output high each time the read function returned a value that was not type None to ensure the function was actually returning a value.
4. The script was ran outside and the data.txt file was produced with the measurements from each pressure sensor and the time the value was returned from the read function.
5. The values were plotted as a function of time for the ten seconds the script was running to compare the values to each other and to the actual atmospheric pressure (14.87 psi).

**Collected Data** The actual atmospheric pressure was measured at 14.87 psi.

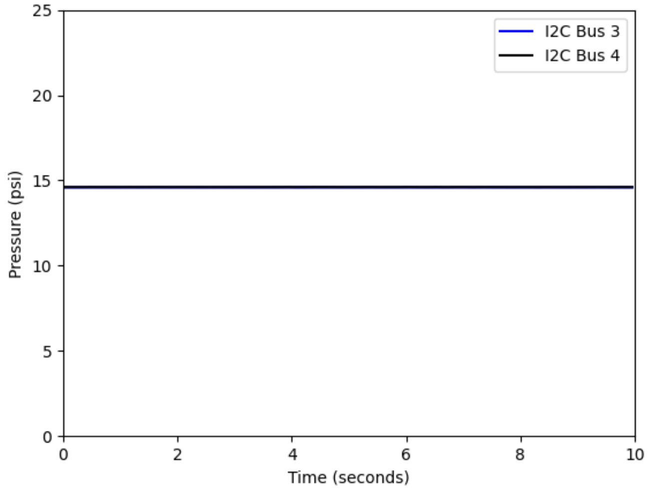


Figure 118: Both Sparkfun Pressure Sensors Plotted over 10 second duration while outside

**Conclusion** The values from both pressure sensors overlap just below where the actual atmospheric pressure would be. These pressure sensors are intended to troubleshoot possible separation failures by tracking the change in both the forward and aft chambers at a frequency of 20 Hz. Based on the accuracy for both pressure sensors, seeing that the values were writing to a text file, and the LED continuously blinking, the pressure sensors will be able to troubleshoot these issues post-flight.

**Pressure Sensor Accuracy Test**

**Introduction** Attached to our Raspberry Pi 4B, there are two identical pressure sensors that will be used to collect pressure data throughout our rocket's flight to troubleshoot possible separation failures. In order to determine the accuracy of our pressure sensor, a test must be conducted to find the uncertainty range that its outputted data lies within. This will be achieved by running pressure tests and finding the uncertainty of one of our sensors.

| **Objective** | **Criteria for Success** | **Test Variables** |
|---|---|---|
| Determine the accuracy of the pressure data read by the Raspberry Pi 4B+ from the pressure sensors | Pressure data is accurate to actual environmental readings | Pressure data |

**Materials**

- 2x Sparkfun Qwiic MicroPressure Sensors
- RaspberryPi 4B+ 4GB Model
- Jumper Cables
- LED light

- Base Station Computer
- USB-C Cable

**Procedure**

1. The Pi was connected to via an ssh connection with an Ethernet cable to the base station computer.
2. The data collected from the first and second pressure sensor respectively.
3. Ten short trial periods with 6 pieces of pressure data each were collected for each pressure sensor using a Pyhton script and the Raspberry Pi.
4. The average for each trial period was taken by adding the 6 values together and dividing them by 6.
5. The standard deviation was also taken so that both values could be compared to measure the accuracy and similarities of the values being read from each of the sensors.

**Collected Data** The following tables below show the collected data for both pressure sensors:

Table 44: Data for Pressure Sensor Test 1

| **Trial Number** | **Value 1** | **Value 2** | **Value 3** | **Value 4** | **Value 5** | **Value 6** | **Average (psi)** |
|---|---|---|---|---|---|---|---|
| **Trial 1** | 14.2967 | 14.2983 | 14.2972 | 14.2961 | 14.2959 | 14.2985 | 14.2971 |
| **Trial 2** | 14.2849 | 14.2816 | 14.2854 | 14.2827 | 14.2839 | 14.2840 | 14.2837 |
| **Trial 3** | 14.2868 | 14.2856 | 14.2850 | 14.2819 | 14.2833 | 14.2853 | 14.2847 |
| **Trial 4** | 14.2816 | 14.2813 | 14.2838 | 14.2842 | 14.2819 | 14.2843 | 14.2829 |
| **Trial 5** | 14.2859 | 14.2842 | 14.2828 | 14.2833 | 14.2828 | 14.2834 | 14.2838 |
| **Trial 6** | 14.2823 | 14.2832 | 14.2825 | 14.2859 | 14.2831 | 14.2841 | 14.2835 |
| **Trial 7** | 14.2833 | 14.2832 | 14.2830 | 14.2838 | 14.2830 | 14.2834 | 14.2833 |
| **Trial 8** | 14.2854 | 14.2798 | 14.2838 | 14.2849 | 14.2843 | 14.2840 | 14.2837 |
| **Trial 9** | 14.2827 | 14.2837 | 14.2841 | 14.2822 | 14.2816 | 14.2825 | 14.2828 |
| **Trial 10** | 14.2837 | 14.2859 | 14.2826 | 14.2856 | 14.2825 | 14.2849 | 14.2842 |

Table 45: Data for Pressure Sensor Test 2

| **Trial Number** | **Value 1** | **Value 2** | **Value 3** | **Value 4** | **Value 5** | **Value 6** | **Average (psi)** |
|---|---|---|---|---|---|---|---|
| **Trial 1** | 14.2967 | 14.2983 | 14.2972 | 14.2961 | 14.2959 | 14.2985 | 14.2971 |
| **Trial 2** | 14.2969 | 14.2956 | 14.2965 | 14.2979 | 14.2949 | 14.2965 | 14.2964 |
| **Trial 3** | 14.2997 | 14.2956 | 14.2955 | 14.2965 | 14.2952 | 14.2947 | 14.2962 |
| **Trial 4** | 14.2960 | 14.2958 | 14.2982 | 14.2957 | 14.2959 | 14.2980 | 14.2966 |
| **Trial 5** | 14.2920 | 14.2949 | 14.2977 | 14.2962 | 14.2966 | 14.2964 | 14.2956 |
| **Trial 6** | 14.2979 | 14.2949 | 14.2962 | 14.2963 | 14.2969 | 14.2955 | 14.2963 |
| **Trial 7** | 14.2969 | 14.2966 | 14.2990 | 14.2970 | 14.2971 | 14.2948 | 14.2969 |
| **Trial 8** | 14.2975 | 14.2965 | 14.2979 | 14.2937 | 14.2940 | 14.2966 | 14.2960 |
| **Trial 9** | 14.2977 | 14.2966 | 14.2958 | 14.2950 | 14.2965 | 14.2972 | 14.2964 |
| **Trial 10** | 14.2978 | 14.2952 | 14.2977 | 14.2963 | 14.2966 | 14.2946 | 14.2964 |

**Conclusion** The individual uncertainties of each pressure sensor is mostly negligible, as their measurements are very consistent under equivalent conditions. However, there seems to be a small discrepancy between the two sensors themselves of about 0.013 psi.

#### 6.1.4 Payload Testing and Demonstrations

**Payload Mechanical Tests and Demos**

1. **Rotating Track Efficacy Test**
   **Introduction**
   The objective of this test is to confirm the viability of the rotating track design. The rotating track is the component of payload which allows the camera board and electronics to properly orient in a position that is parallel to the ground after flight. The prototype used for testing mimics the final construction of the rotating track. Results indicate a successful design concept.

| Objective | Criteria for Success | Test Variables |
|---|---|---|
| Observe self-righting efficacy of rotating track concept under various weight distributions. | Rotating track consistently uprights its orientation | Orientation angle of rotating track (degrees) and weight of ballast (grams) |

   **Materials**

   - 2x Prototype Rotating Track Mounts
   - Prototype Rotating Track and Support Board
   - Mock weights (items of various mass)
   - Duct Tape
   - 2x Vice Clamps
   - Protractor

   **Procedure**

   (a) Sand the axles of the Rotating Track and Support Board prototype component to minimize friction between the Track Mounts
   (b) Assemble the 3D printed Rotating Track prototype
   (c) Fix the Rotating Track mounts to a surface via vice clamps
   (d) Align protractor to base of a mount to measure orientation of Support Board
   (e) Attach desired ballast weight to bottom of support board
   (f) Attach desired load weight to top of support board
   (g) Orient support board to a desired initial angle
   (h) Release board
   (i) Record final orientation of support board
   (j) Repeat step D until all trials have been completed

   **Results**
   A visual representation of the setup is shown below in Fig. 119

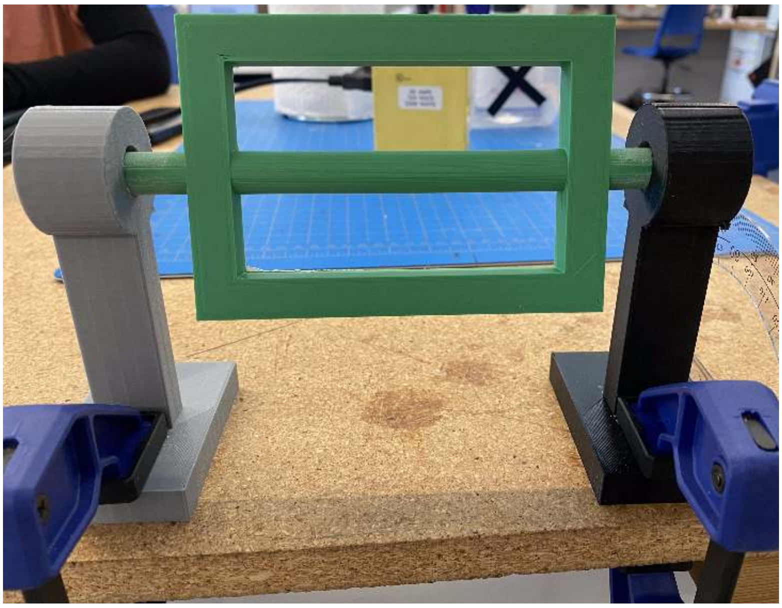

Figure 119: Setup of Rotating Track Mechanical Test

In this setup, the green support board maintains two degrees of freedom, and is able to rotate freely around the central axis between the two supports. Each support is mounted to the table via clamps, and are completely static. The protractor was used to measure the starting orientation.

The mock weights used and their weight distributions are as follows:

- Gray PLA disk (top) / Black PLA disk (bottom)
- Gray PLA disk and black PLA disk (top) / Battery (bottom)
- Mobile Phone (top) / Battery (bottom)
- Gray PLA disk, Black PLA disk, tape rolls (top) / Battery (bottom)

The initial orientations that were tested are as follows. *Note that a 0 degree orientation is specified as the camera board oriented parallel to the ground, with the bottom of the board closer to the ground and the top of the board farther from the ground.*

- 90 degrees (vertical)
- 45 degrees (slant)
- 180 degrees (horizontal, heavy weight on top)

The resulting outcomes of each various weight distribution between the self-righting track's initial and final orientation are shown in the table below.

| Test Number | Initial Position (deg) | Final Position (deg) |
|---|---|---|
| Test 1 (27 g top, 26 g bottom) | 90 | 90 |
| | 45 | 70 |
| | 180 | 180 |
| | Spin | 80 |
| | Spin | 80 |
| Test 2 (53 g top, 376 g bottom) | 90 | 0 |
| | 45 | 0 |
| | 180 | 0 |
| | Spin | 0 |
| | Spin | 0 |
| Test 3 (242 g top, 376 g bottom) | 90 | 0 |
| | 45 | 0 |
| | 180 | 180 |
| | Spin | 0 |
| | Spin | 0 |
| Test 4 (182 g, 376 g bottom) | 90 | - 70 |
| | 45 | - 70 |
| | 180 | - 70 |
| | Spin | - 70 |
| | Spin | - 70 |

Figure 120: Outcomes of rotating track orientations given various weight distributions (grams versus degrees)

The results of the testing provided verification of the rotating track design. For each test, the desired final orientation was 0 degrees. Test 1 utilized an even weight distribution on the top and bottom of the camera board, and obtained a final orientation that was not the desired 0 degrees. This proves that with an even weight distribution, the camera board will not achieve the final orientation parallel to the ground. Test 2 utilized an uneven weight distribution with low weight on top of the camera board and obtained all successful tests. Test 3 utilized an uneven weight distribution with high weight on top of the camera board and obtained almost all successful tests. The only test which failed was the 180 degree starting orientation test, which had a final orientation of 180 degrees. This is likely due to the heavy weight of the phone as well as the rough edges of the PLA printed components. It is not a concerning result, as it is extremely unlikely that the camera board will ever be at a completely static position at the end of flight. Test 4 utilized an uneven weight distribution with a high weight on top, and furthermore maintained an uneven center of mass for the added weight. The final orientation for each test was 70 degrees. While this is not the intended 0 degree final orientation, it is expected and a successful test. This is because the initial, base orientation for the Test 4 configuration is 70 degrees off-center due to the uneven center of mass for the added weight.

**Conclusion**
The results of the verification testing are positive. Through a series of tests, it was confirmed that the rotating track will function properly. It is important that the initial, base orientation of the camera board is perfectly level with the ground. This ensures that the camera board will achieve the desired final orientation after any disturbance.

2. **Proposed Scissor Lift Load Test**
**Introduction**
The objective of this test is to ensure that the scissor lift will be able to raise the camera and rotating camera components into the air so unobstructed pictures can be taken. The scissor lift will need to be powered by an electric motor, and must be able to extend the camera components.

The scissor lift will be composed of two mounting boards, 12 arms, and 8 middle pins.

| **Objective** | **Criteria for Success** | **Test Variables** |
|---|---|---|
| Determine whether the scissor lift can deploy the camera system | The camera must be raised a minimum of 2" above the body tube | Height of extended scissor lift and final camera lens height (inches) |

**Materials**

- Prototype Scissor Lift
- Pulley Tension String
- Parallax Servo
- Power Supply
- Mock Weights (items of various mass)

**Procedure**

(a) Assemble the 3D Printed Scissor Lift prototype
(b) Fix the bottom mounting board to a surface with the scissor lift collapsed on top
(c) Mount a servo with its axle parallel to the scissor lift's bottom rung
(d) Attach a spool of tension wire to the servo axle and connect wire to bottom rung of scissor lift
(e) Add a desired weight to the platform of the collapsed scissor lift
(f) Drive the servo at PWM values of increasing intervals of power (25%, 50%, 75%, 100%)
(g) Record the height of the scissor lift

(h) Repeat step E until all trials have been completed

**Results**
No data has yet been collected as the test must still be prototyped. The proposed date for completing this test will be mid-January when the is able to meet again.

**Conclusion**
The test will be considered successful if the scissor lift is capable of extending a supported weight of around 2 oz at least 5 in. and holding the position. This height was determined by the necessity to extend the camera at least 2 inches above the body tube, with an added 3 inches from the radius of the body tube.

3. **Proposed Telescoping Rods Stress Test**
**Introduction**
The objective of this test is to ensure the 3D printed telescoping rods can hold the weight of the payload, and that they can extend up to 7 in. and retract even when weight is added. The separation rods are the components that passively expand when the nose cone is pushed forward to release the camera. The subteam plans to 3D print the rods in the final payload, so this test will prove whether or not a stronger material is required.

Note that the collapsed (retracted) rod position will not be evaluated in this test. This is due to the fact that the collapsed rod position has a significantly higher strength due to stacked rods. Thus, testing the collapsed position would be redundant and unnecessary.

| **Objective** | **Criteria for Success** | **Test Variables** |
|---|---|---|
| Gauge the amount of stress the telescoping rods can withstand when supporting weight | Telescoping rods do not deform and are capable of supporting payload board | Mass of weight (grams) and curve deformation of rods when extended (degrees) |

**Materials**

- 2x Centering Rings
- 2x Outer Telescoping Rods
- 2x Inner Telescoping Rods
- Plywood Support Board
- Mock Weights (items of various mass)

**Procedure**

(a) Assemble the 3D printed Telescoping Rod prototype

(b) Run the two rods through the two centering rings following the rotating track design

(c) Mount the plywood support board to the outer telescoping rod

(d) Place desired weight on support board

(e) Apply a constant force to pull apart the inner telescoping rod from the outer rod to bring the telescoping rods into a extended position

(f) Record curve deformation of telescoping rods across its length in degrees

(g) Repeat step D until all trials have been completed

**Results**
No data has yet been collected as the test must still be prototyped. The proposed date for completing this test will be mid-January when the is able to meet again.

**Conclusion**
A successful test would require minimal deformation of the physical rod structures when under at least 2.5 lbs of weight, as this is the estimated mass of the electronics with a +20% margin. The telescoping rods must also be capable of being extended even when under this stress at a maximum of 1.45 lb/ft of torque, which is a margin half of the expected rated torque of the DC separation motor.

### Payload Electrical Tests and Demos

1. **RTL-SDR Adapter Demonstration**
**Introduction**
The purpose of this demonstration was to verify that the RTL-SDR receiver could power on and receive APRS transmissions from local sources. This is done by having the RTL-SDR set to receive APRS transmissions on the North American standard frequency of 144.39Mhz and print any received transmission strings onto the console.

| Objective | Criteria for Success | Test Variables |
|---|---|---|
| Demonstrate RTL-SDR adapter is capable of receiving from a local APRS network | Receiving messages from RTL-SDR in the form of a string output to console | Transmitted data |

**Materials**

- 1x RTL-SDR Adapter
- 1x Raspberry Pi 4 B
- 1x Bingfu Dual Band Antenna
- 1x Power Supply

**Procedure**

(a) Screw on the dual band antenna to the RTL-SDR adapter's coaxial SMA connector

(b) Plug the RTL-SDR adapter into the Raspberry Pi's USB-A port

(c) Power the Raspberry Pi via the 5V supply through the USB-C port

(d) SSH into the Pi

(e) Execute the following command to activate the RTL-SDR to listen for packets on the local APRS network

```
rtl-fm -f 144.390M -s 22050
| multimon-ng -t raw -a AFSK1200 -f alpha /dev/stdin
```

(f) Await received packet strings that are printed to console

**Results**
The RTL-SDR successfully printed out a transmission from a local radio station stating: "Listening on the St. Louis Metro DMR Talk Group. Email is (user's email)"

**Conclusion**
The RTL-SDR successfully received a localized transmission, proving that it would be able to receive the RAFCO as sent by NASA during RAFCO.

2. **Avionic Sensors Demonstration**
**Introduction**
The purpose of this system demonstration is to show that the avionic sensors onboard of the payload mission are properly working and capable of reading accurate data from the surrounding physical environment. Reliable and accurate data is key for the payload to run autonomously, and this demonstration will evaluate the quality of the sensor data received.

| Objective | Criteria for Success | Test Variables |
|---|---|---|
| Demonstrate avionic sensors are properly reading physical world data | Receiving data for each respective component and viewing data | Transmitted data |

**Materials**

- Raspberry Pi 4 B
- BMP388 Pressure Sensor
- BNO055 Inertial Measurement Unit
- Jumper Cables
- Breadboard
- 5V Power Supply

**Procedure**

(a) Wire BMP388 and BNO055 to Raspberry Pi's SDA and SCL pins
(b) Connect 5V and GND to the two component's power pins
(c) Power the Raspberry Pi via the 5V supply through the USB-C port
(d) SSH into the Pi
(e) Run the BMP388 and BNO055 test scripts
(f) Record readings output to console

**Results**

Two Python scripts were written to test the sensors, the first script initialized the I2C bus for the BMP388. When communication with the component was successful, the script then began to read temperature, pressure, and altitude from the sensor. The altitude is dependent on a base pressure of the region in order to determine height above sea level. At the zip code of 63132, the air pressure was around 1016 mb and was configured as such. It should be noted that during launch day the base air pressure will be set to an averaged reading of the sensor to use the launch pad as the base altitude.

The second script was written for the BNO055, where the script first initializes the sensor in a 9 degrees-of-freedom operation mode and then awaits calibration of the IMU. Calibration of the IMU is achieved by orienting the IMU in various angles along each of the three physical absolute axes and then holding the position for three seconds. When the IMU was calibrated, the program begins sampling the IMU at 50 Hz. The data recorded included gyroscope, magnetometer, and accelerometer data for each reading that was written to the console.

The following values were collected data from the BMP388 component.

| Reading | Pressure (hPa) | Altitude (m) |
|---|---|---|
| 1 | 994.7871332 | 0.2418098999 |
| 2 | 994.8176663 | -0.01696334459 |
| 3 | 994.7983058 | -0.1116557856 |
| 4 | 994.8186604 | 0.9843963832 |
| 5 | 994.8186604 | 0.2249340123 |
| 6 | 994.7697566 | 0.9843963832 |
| 7 | 994.7697566 | -0.1116557856 |
| 8 | 994.8186604 | 0.2249340123 |
| 9 | 994.858377 | 0.05243301114 |
| 10 | 994.8980937 | 0.8981454315 |
| 11 | 994.8186604 | 0.2249340123 |
| 12 | 994.8390148 | -0.03381620638 |
| 13 | 994.8186604 | -0.5344867371 |
| 14 | 994.7992974 | 0.05243301114 |
| 15 | 994.8186604 | -0.1116557856 |
| 16 | 994.8390148 | 0.2249340123 |
| 17 | 994.8288376 | 0.2249340123 |
| 18 | 994.858377 | 0.138683084 |
| 19 | 994.8980937 | 0.2249340123 |
| 20 | 994.8186604 | -0.7848035622 |
| 21 | 994.849192 | -0.1116557856 |
| 22 | 994.7290506 | -0.1116557856 |
| 23 | 994.9082717 | -0.1116557856 |
| 24 | 994.9184497 | -0.1116557856 |
| 25 | 994.8787322 | 0.2249340123 |

The following two figures are the BMP388 pressure and altitude values plotted, shown respectively in figures Fig. 121 and Fig. 122

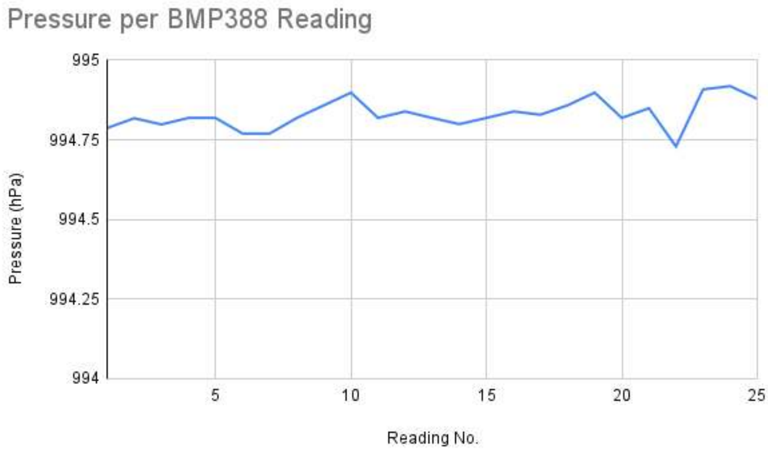


Figure 121: Pressure Readings in hectoPascals from BMP388


Figure 122: Altitude Readings in meters from BMP388

The following values are the sensor readings from the BNO055 component in the form of a 3-dimensional tuple, each dimension representing the (x,y,z) axes respectively, relative to the component's orientation.

| Reading | Angular Velocity (rad/s) | Acceleration (m/s^2) | Magnetic Strength (uT) |
|---|---|---|---|
| 1 | (-0.001090830782496456, -0.007635815477475192, 0.001090830782496456) | (-0.43, 0.03, 9.78) | (5.375, 21.875, -35.6875) |
| 2 | (-0.001090830782496456, -0.008726646259971648, 0.001090830782496456) | (-0.46, 0.04, 8.52) | (5.0, 21.875, -36.875) |
| 3 | (0.001090830782496456, -0.013089969389957472, 0.0) | (-0.44, 0.0, 9.78) | (4.25, 22.25, -36.5) |
| 4 | (-0.001090830782496456, -0.015271630954950384, -0.009817477042468103) | (-0.44, 0.06, 9.76) | (5.75, 21.875, -36.5) |
| 5 | (-0.00545415391248228, -0.04908738521234052, -0.002181661564992912) | (-0.41000000000000003, 0.06, 9.81) | (4.25, 22.5625, -35.6875) |
| 6 | (-0.00545415391248228, -0.03381575425739013, -0.001090830782496456) | (-0.4, 0.06, 9.78) | (4.25, 22.25, -35.6875) |
| 7 | (0.001090830782496456, -0.03381575425739013, -0.1407171709420428) | (-0.48, 0.15, 9.8) | (4.25, 22.25, -35.6875) |
| 8 | (0.003272492347489368, 0.03381575425739013, -0.007635815477475192) | (-0.44, 0.06, 9.76) | (4.5625, 22.5625, -36.0625) |
| 9 | (0.002181661564992912, 0.007635815477475192, -0.002181661564992912) | (-0.44, 0.1, 9.78) | (4.25, 21.5, -36.0625) |
| 10 | (-0.002181661564992912, -0.019634954084936207, 0.0) | (-0.41000000000000003, 0.06, 9.78) | (4.5625, 21.875, -36.875) |
| 11 | (0.002181661564992912, -0.006544984694978736, 0.001090830782496456) | (-0.42, 0.07, 9.81) | (4.5625, 21.1875, -36.875) |
| 12 | (0.00545415391248228, 0.03490658503988659, -0.002181661564992912) | (-0.45, 0.04, 9.81) | (4.0, 21.1875, -36.0625) |
| 13 | (0.001090830782496456, 0.004363323129985824, 0.0) | (-0.4, -0.23, 9.78) | (5.375, 21.5, -35.6875) |
| 14 | (-0.007635815477475192, -0.039269908169872414, -0.007635815477475192) | (-0.44, 0.06, 9.77) | (3.5625, 21.5, -35.6875) |
| 15 | (0.003272492347489368, 0.001090830782496456, 0.001090830782496456) | (-0.43, 0.03, 9.75) | (4.25, 21.875, -34.875) |
| 16 | (0.001090830782496456, 0.02181661564992912, 0.00545415391248228) | (-0.43, 0.03, 9.790000000000001) | (4.25, 21.875, -35.6875) |
| 17 | (-0.007635815477475192, -0.04581489286485115, 0.0) | (-0.4, 0.02, 9.81) | (4.25, 21.0625, -35.25) |
| 18 | (-0.003272492347489368, -0.02399827721492203, 0.0) | (-0.41000000000000003, -0.02, 9.8) | (4.0, 21.5, -35.25) |
| 19 | (-0.001090830782496456, 0.016362461737446838, -0.001090830782496456) | (-0.41000000000000003, 0.02, 9.78) | (4.0, 20.75, -36.5) |
| 20 | (0.002181661564992912, 0.007635815477475192, 0.0) | (-0.4, 0.02, 9.77) | (4.0, 20.75, -36.5) |
| 21 | (0.00545415391248228, 0.02399827721492203, 0.001090830782496456) | (-0.43, 0.04, 9.76) | (5.0, 21.875, -36.0625) |
| 22 | (-0.007635815477475192, -0.038179077387375956, -0.002181661564992912) | (-0.41000000000000003, 0.02, 9.78) | (5.375, 21.875, -36.875) |
| 23 | (-0.003272492347489368, -0.011999138607461015, -0.001090830782496456) | (-0.4, 0.01, 9.78) | (5.0, 21.875, -36.5) |
| 24 | (0.002181661564992912, -0.001090830782496456, 0.001090830782496456) | (-0.39, 0.0, 9.790000000000001) | (5.0, 21.875, -35.25) |
| 25 | (0.002181661564992912, -0.00545415391248228, 0.002181661564992912) | (-0.41000000000000003, 0.02, 9.77) | (4.5625, 22.25, -35.6875) |

Figure 123: BNO055 9-DOF Sensor Readings

**Conclusion**
The demonstration has shown that the avionic sensing components, both the BMP388 and BNO055 are in working order and capable of reading physical world data for the payload mission to use. It should be noted, however, that the sensor readings have a fair amount of noise (fluctuations from zero, small inconsistencies, etc.) that have been addressed through the use of rolling mean filters. Should more advanced noise suppression techniques be required, the subteam will implement algorithms like the Kalman filter.

3. **Camera PoV Test**
   **Introduction**
   The aim of this test was to calculate the angle of view of the Payload Raspberry Pi camera to ensure that the resulting field of view image is within 100 to 180 degrees. This test was conducted by taking images with the camera set at some specified distance to determine the angle of view.

| Objective | Criteria for Success | Test Variables |
|---|---|---|
| Determine the imaging system's physical field of view to ensure competition requirements are met | The calculated physical field of view to be within 100 and 180 degrees | The calculated field of view (degrees) |

**Materials**

- Raspberry Pi Camera Model G

- Raspberry Pi 4 B
- 5V DC Power Supply
- Marker
- Yardstick
- Vice Grip

**Procedure**

(a) Connect Raspberry Pi camera to Raspberry Pi 4 B via CSI bus interface

(b) Mark a target wall's surface with inch-wide ticks that span its width

(c) Position camera such that its lenses height is level with the tick-marks and the lenses angle of depression is perpendicular with respect to the ground.

(d) Power Raspberry Pi via 5V DC power supply through its USB-C port

(e) SSH into Raspberry Pi

(f) Position camera to desired subject distance

(g) Execute the following command to capture a picture named "image.png" to current directory

```
raspistill -o ./image.png
```

(h) Record width of image as counted by the inch tick-marks in "image.png" to the corresponding subject distance

(i) Repeat step (F) for desired number of trials

**Results**

The above procedure was run for three trials, as camera hardware does not fluctuate much only a few number of trials would be needed to verify whether the camera's field of view were well within the range.

The field of view was roughly calculated as the physical angle of the resulting image's width as seen in the real world. This indicates that the width of the marked wall would be the hypotenuse and the distance to the wall the height of the triangle. From this, the following equation shown in Fig. 124 was used to calculate the defined field of view with image width denoted as l and subject distance d.

$$FoV = 2 * arctan(\frac{l}{2d})$$

Figure 124: Physical PoV of Camera Image Equation

The following results of the three trials are recorded below.

| Subject Dist (in) | Measured Width (in) | Physical FoV (deg) |
|---|---|---|
| 10 | 32.25 | 116.3893422 |
| 15 | 55.5 | 123.2139612 |
| 16 | 60.5 | 124.2489792 |

**Conclusion**

The resulting data indicates that the physical field of view is at least above 100 degrees and below 180 degrees for all three trials. The calculated FoVs have a standard deviation of around 4.27 which is likely to error introduced by how the instruments were positioned and the resolution of the marked wall. Regardless, the test is successful in providing a reasonable average margin of around 22 degrees above the minimum FoV and well below the 180 maximum, thus the selected camera will perform as required during the payload mission.

4. **Proposed DC Motor Hat Test**
**Introduction**
The purpose of this test is to show that the DC Motor Hat component received will be in working condition and capable of driving the selected electromotives for the payload mission within reasonable power consumption. This requires using the Raspberry Pi to interface with the hat via an I2C protocol to send motor power that drives the separation motor, three linear solenoids, and two servos. The selected DC battery supply will be used and current draw measured to ensure that it remains below the motor hat's rated current of 3A.

| **Objective** | **Criteria for Success** | **Test Variables** |
|---|---|---|
| Demonstrate that the DC Motor Hat is capable of driving electromotives without exceeding maximum current draw of 3A | Driving both the DC separation motor and payload servos via Raspberry Pi control | Current draw of DC Motor Hat (Amperes) |

**Materials**

- Adafruit DC Motor Hat
- Raspberry Pi 4 B
- 12V DC Separation Motor
- 3x McMaster Linear Solenoid
- 2x Pollolu Parallax 360 Servo
- TalentCell 12V/5V Battery
- 14 AWG 12V Cable
- Ammeter

**Procedure**

(a) Assemble the DC Motor Hat on top of the Raspberry Pi
(b) Connect DC motor to hat's motor block terminal
(c) Connect three linear solenoids to remaining hat's motor block terminals
(d) Connect two servos to the 5V and GND outputs of the hat
(e) Connect the two servos' PWM signals to the PWM pins routed from the Pi to the hat
(f) Connect battery 12V to motor hat's power terminal block with ammeter in series to the circuit

(g) Connect battery 5V to Raspberry Pi's power through USB-C port

(h) Switch battery on

(i) Record current draw

(j) SSH into Raspberry Pi

(k) Run Python script to drive each individual component set of components (1. DC Motor, 2. Solenoids, 3. Servos)

(l) Record current draw from each trial, stopping if current draw begins to exceed 2.75 A

**Results**

No data has yet been collected as the test must still be prototyped. The proposed date for completing this test will be mid-January when the is able to meet again.

**Conclusion**

A successful test would drive each set of electromotives pulling current under the 3A maximum. If these requirements are not met, the team must determine ways to minimizing power consumption by either driving motors and servos at lower speeds.

5. **Proposed RTL-SDR Temperature Test**

**Introduction**

The goal of this test is to determine whether the RTL-SDR adapter can operate under long durations of active listening without overheating. The major chip component of the RTL-SDR must remain under 257 degrees Fahrenheit and the RTL-SDR must be able to receive packets for at least 3 hours.

| **Objective** | **Criteria for Success** | **Test Variables** |
|---|---|---|
| Measure operating temperature of RTL-SDR adapter under various durations of active listening to ensure component does not overheat during mission execution | RTL-SDR remains below its rated temperature of 257 degrees Fahrenheit for at least 3 hours | Temperature of RTL-SDR casing (Fahrenheit) and time of measurement (minutes) |

**Materials**

- RTL-SDR Adapter
- Bingfu Dual Band Antenna
- Raspberry Pi 4 B
- IR Wireless Thermometer Gun
- 5V Power Supply
- Electrical Tape

**Procedure**

(a) Wrap electrical tape around aluminium casing of RTL-SDR to provide a surface for IR temperature monitoring

(b) Connect Bingfu dual band antenna to RTL-SDR coaxial SMA connector

(c) Connect RTL-SDR to Raspberry Pi through the USB-A port

(d) Connect 5V power supply to Raspberry Pi through the USB-C port

(e) SSH into the Pi

(f) Execute the following command on the terminal to bring the RTL-SDR into active listening

```
rtl-fm -f 144.390M -s 22050
| multimon-ng -t raw -a AFSK1200 -f alpha /dev/stdin
```

(g) Monitor RTL-SDR temperature every 30 minutes by using the IR thermometer gun over the duration of 3 hours

**Results**

No data has yet been collected as the test must still be prototyped. The proposed date for completing this test will be mid-January when the is able to meet again.

**Conclusion**

A successful test would indicate no reading ever exceeding 257 degrees Fahrenheit over the duration of the experiment. Additionally, the rate of change in temperature should approach zero as the experiment continues.

6. **Proposed RAFCO FSM Timing Test**

**Introduction**

The aim of this test is to determine whether or not the automated imaging system software is capable of executing RAFCO within the imposed 30 second time constraint allowed for each command run. This test will indicate to the subteam whether optimizations must be made to either the hardware or software of the overall system to improve runtime.

| **Objective** | **Criteria for Success** | **Test Variables** |
|---|---|---|
| Determine the runtime of the payload imaging system execution when receiving RAFCO | Each RAFCO is executed within 30 seconds | Runtime of execution (seconds) |

**Materials**

- Raspberry Pi 4 B
- Raspberry Pi Camera
- DC Motor Hat
- Parallax Servo
- 2x Camera/Servo Mount
- 2x 5V Power Supply

**Procedure**

(a) Connect the Raspberry Pi Camera to the Raspberry Pi via the CSI bus interface

(b) Assemble the DC Motor Hat ontop of the Raspberry Pi via the four screws

(c) Power the Raspberry Pi via the 5V supply and the DC motor hat by another supply

(d) Wire the Parallax servo to the Motor Hat +5V and GND for power and any PWM signal routed from the Raspberry Pi

(e) Mount the servo and camera in their respective housings, with the camera mounted on top of the servo axle

(f) SSH into the Raspberry Pi

(g) Run the FSM RAFCO timing program that will run each RAFCO and record the runtime in software

(h) Record the runtimes

**Results**
No data has yet been collected as the test must still be prototyped. The proposed date for completing this test will be mid-January when the is able to meet again.

**Conclusion**
A successful test would result in all RAFCO execution subroutines in properly running with an average runtime of less than 30 seconds and not a single execution taking longer than 30 seconds. If these requirements are not met, the team will analyze certain points of the software that take longest and attempt to optimize its performance, although certain factors like servo rotation speed is a hardware limitation that will be addressed from a mechanical perspective.

## 6.2 Requirements Compliance

### 6.2.1 Statement of Work Requirements

Table 46: General Requirements

| Item | Requirement | Verification Method | Verification Plan | Verification Status | Reference |
|---|---|---|---|---|---|
| SOW1.1 | Students on the team will do 100% of the project, including design, written reports and presentations. Teams will submit new work. Excessive use of past work will merit penalties | Inspection | The leadership structure of the team is implemented in a way that ensures the full completion of work by team members on all project milestones, construction, and design. The executive board of the team oversees the design, construction, and documentation process to ensure that the work is done fully by team members. The Program Manager schedules and outlines the details regarding the work that needs to be done, and communicates this information to the team. Documentation will undergo a careful review from the executive board as well as a plagiarism checker program to ensure that team members have not copied documentation from past work. | In progress, subteam leaders and the executive board have ensured that no one outside of the team has contributed to any aspect of the overall project. Plagiarizing of documentation has been periodically assessed throughout the writing process. The Safety Officer has indicated that handling of dangerous material has been left to only the people with proper certification. | N/A |

*Continued on next page*

Table 46 – *Continued from previous page*

| Item | Requirement | Verification Method | Verification Plan | Verification Status | Reference |
|---|---|---|---|---|---|
| SOW1.2 | The team will provide and maintain a project plan to include, but not limited to the following items: project milestones, budget and community support, checklists, personnel assignments, STEM engagement events, and risks and mitigations. | Inspection | The President and the Program Manager have created a project plan outline that details a schedule of deadlines to be completed for each of the project milestones for each of the subteams. Each subteam lead will then delegate these tasks to team members to ensure that they are completed properly. The project plan includes details related to budgeting, community support, checklists, personnel assignments, STEM Engagement events, and risks and mitigation. The risks and mitigation section of the project plan will be assisted by the Safety Officer to ensure accuracy and attention to detail in the process. | In progress, the aforementioned project plan is checked daily by the executive team to ensure deadlines are being met. The plan is updated as changes are made, with the Safety Officer signing off to ensure changes are safe. | Section 6 |

*Continued on next page*

Table 46 – *Continued from previous page*

| **Item** | **Requirement** | **Verification Method** | **Verification Plan** | **Verification Status** | **Reference** |
|---|---|---|---|---|---|
| SOW1.3 | The team shall identify all team members who plan to attend Launch Week activities by the Critical Design Review (CDR). Team members will include: 1.4.1. Students actively engaged in the project throughout the entire year. 1.4.2. No more than two adult educators. | Inspection | The President has collected contact information of team members attending Launch Week using a Google Form. The compiled results will be submitted as part of the WURocketry CDR package. | Complete, emailed to Allison Chouinard in Excel Format. | N/A |
| SOW1.4 | Teams shall engage a minimum of 250 participants in Educational Direct Engagement STEM activities in order to be eligible for STEM Engagement scoring and awards. These activities can be conducted inperson or virtually. To satisfy this requirement, all events shall occur between project acceptance and the FRR due date. A template of the STEM Engagement Activity Report can be found on pages 77-80. | Inspection | These events will be documented by the STEM Engagement Chair in the STEM Engagement Activity Report that has been provided by the USLI team, and will be submitted completely at the FRR deadline. The STEM Engagement Chair and President are currently planning events to engage over 250 kids. It is required that all team members attend two STEM engagement events to ensure participation and success for the kids at these events | In progress, WURocketry has already completed two large STEM engagement events, with several more already planned throughout the months of January and February. The completed events have been documented and are ready to submit once all STEM engagements have been completed. | N/A |

*Continued on next page*

Table 46 – *Continued from previous page*

| Item | Requirement | Verification Method | Verification Plan | Verification Status | Reference |
|---|---|---|---|---|---|
| SOW1.5 | The team will establish and maintain a social media presence to inform the public about team activities. | Inspection | The social media accounts on Instagram, LinkedIn, Facebook, Twitter, and TikTok are consistently used to document construction and design processes for all of the followers. The social media pages the team uses have dramatically increased visibility for the team as well as NASA and provides insights into the team that strum up interest from students not currently involved. All team events are posted on social media so that the public can keep up with team progress. | In progress. The Social Media chair ensures that posts go up on a regular basis and are documenting all important events in which the team might participate. The Social Media Chair is kept accountable by the executive board. | N/A |

*Continued on next page*

Table 46 – *Continued from previous page*

| Item | Requirement | Verification Method | Verification Plan | Verification Status | Reference |
|---|---|---|---|---|---|
| SOW1.6 | Teams will email all deliverables to the NASA project management team by the deadline specified in the handbook for each milestone. In the event that a deliverable is too large to attach to an email, inclusion of a link to download the file will be sufficient. Late submissions of PDR, CDR, FRR milestone documents shall be accepted up to 72 hours after the submission deadline. Late submissions shall incur an overall penalty. No PDR, CDR, FRR milestone documents shall be accepted beyond the 72-hour window. Teams that fail to submit the PDR, CDR, FRR milestone documents shall be eliminated from the project. | Inspection | Milestone documentation is checked on a periodic basis in the two weeks leading up to the submission deadline. The executive board independently reviews the necessary materials for submission and creates each milestone package together to ensure nothing is missing and all information is complete. | In progress. The executive board continuously reviews the deadlines and requirements to ensure that submissions happen properly | N/A |

*Continued on next page*

Table 46 – *Continued from previous page*

| Item | Requirement | Verification Method | Verification Plan | Verification Status | Reference |
|---|---|---|---|---|---|
| SOW1.7 | Teams who do not satisfactorily complete each milestone review (PDR, CDR, FRR) shall be provided action items needed to be completed following their review and shall be required to address action items in a delta review session. After the delta session the NASA management panel shall meet to determine the teams' status in the program and the team shall be notified shortly thereafter. | Inspection | The executive board will work as quickly and accurately to assess the necessary changes that need to be made following the possibility of an unsatisfactory submission. The delta review session will be scheduled efficiently through effective communication between the team and the USLI board. | In Progress. The team has so far not had to deal with this issue, but should it arise, the executive team will call a meeting to sort out the issues so that whatever documentation needs to be altered can be done as efficiently as possible. | N/A |
| SOW1.8 | All deliverables shall be in PDF format. | Inspection | The executive board is responsible for ensuring all documentation is in PDF format | In Progress. All milestones have been submitted in PDF format. All upcoming milestones will be submitted in this format as well. | N/A |

*Continued on next page*

Table 46 – *Continued from previous page*

| Item | Requirement | Verification Method | Verification Plan | Verification Status | Reference |
|---|---|---|---|---|---|
| SOW1.9 | In every report, teams will provide a table of contents including major sections and their respective sub-sections. | Inspection | The executive board will ensure upon review of documentation that all sections and sub-sections are accounted for in the table of contents | In Progress. Milestone reports so far submitted have all included a table of contents that has been checked for accuracy. This will be the standard moving forward with future milestone documents. | N/A |
| SOW1.10 | In every report, the team will include the page number at the bottom of the page. | Inspection | The executive board will ensure that page numbers are included at the bottom of each page of the deliverable reports | In Progress. All submitted reports have thus far included page numbers. Future reports will include page numbers at the bottom of the page. | N/A |
| SOW1.11 | The team will provide any computer equipment necessary to perform a video teleconference with the review panel. This includes, but is not limited to, a computer system, video camera, speaker telephone, and a sufficient Internet connection. Cellular phones should be used for speakerphone capability only as a last resort. | Demonstration | WURocketry has meetings scheduled in Washington University conference rooms with reliable network connection and video/audio capabilities for teleconferences with the USLI board. These systems are checked to ensure reliability by the Washington University IT staff prior to the conferences | In progress. A reliable conference room has been reserved with the audio and video capabilities necessary for a successful conference | N/A |

*Continued on next page*

Table 46 – *Continued from previous page*

| Item | Requirement | Verification Method | Verification Plan | Verification Status | Reference |
|---|---|---|---|---|---|
| SOW1.12 | Teams will track and report the number of hours spent working on each milestone. | Inspection | Each subteam leader is required to ensure that subteam members record all time worked on each milestone to provide an accurate value for the hours worked on each report. | In Progress. For each of the previously submitted milestones, data regarding time spent on each report has been submitted to the executive team. | Section 1 |

Table 47: Vehicle Requirements

| **Item** | **Requirement** | **Verification Method** | **Verification Plan** | **Verification Status** | **Reference** |
|---|---|---|---|---|---|
| SOW2.1 | The vehicle will deliver the payload to an apogee altitude between 4,000 and 6,000 feet above ground level (AGL). | Analysis | OpenRocket will be utilized to design a rocket that can deliver a payload to an apogee between 4,000 and 6,000 feet AGL. | Complete. The OpenRocket simulation of the full-scale vehicle showed that expected apogee altitude is 4,712 ft. | Section 3.4 |
| SOW2.2 | Teams shall declare their target altitude goal at the PDR milestone. | Analysis | The team will declare the target altitude based on OpenRocket simulations and cumulative experience from previous flights. | Complete. A target altitude of 4,650 feet AGL was declared in the PDR. | Section 3.4 |
| SOW2.3 | The launch vehicle will be designed to be recoverable and reusable. Reusable is defined as being able to launch again on the same day without repairs or modifications. | Inspection | The rocket will be designed to be robust and sturdy enough to be recoverable and reusable on the same day. Motors will be chosen that can be replaced on the same day. | Complete. The rocket was constructed using sturdy, high strength materials and designed to be recoverable and reusable on the same day. An Aerotech L1390G motor was chosen for its reloading capabilities. | Section 3 |

*Continued on next page*

Table 47 – *Continued from previous page*

| Item | Requirement | Verification Method | Verification Plan | Verification Status | Reference |
|---|---|---|---|---|---|
| SOW2.4 | The launch vehicle will have a maximum of four (4) independent sections. An independent section is defined as a section that is either tethered to the main vehicle or is recovered separately from the main vehicle using its own parachute. | Inspection | The team will design a launch vehicle to ensure that there are a maximum of four independent sections which are tethered to each other. The launch vehicle will not jettison a section. | Complete. The vehicle is designed to have three separation points. The payload pushes the nose cone off of the forward body tube on the ground. The forward body tube separates from the mid body tube and coupler for the main parachute deployment. The aft body tube separates from the mid body tube and coupler for the drogue parachute deployment. | Section 3.1 |
| SOW2.4.1 | Coupler/airframe shoulders which are located at in-flight separation points will be at least 2 airframe diameters in length. (One body diameter of surface contact with each airframe section) | Inspection | The team will inspect each part of the launch vehicle to ensure that the coupler will have one body diameter of surface contact with the airframe. | Complete. The launch vehicle will have three independent sections. All coupler shoulders are double the length of the body diameter of the launch vehicle, which is 6.17 in. The avionics coupler is 14 in. | Section 3.1.3 |

*Continued on next page*

Table 47 – *Continued from previous page*

| **Item** | **Requirement** | **Verification Method** | **Verification Plan** | **Verification Status** | **Reference** |
|---|---|---|---|---|---|
| SOW2.4.2 | Nosecone shoulders which are located at in-flight separation points will be at least $\frac{1}{2}$ body diameter in length. | Inspection | The team will inspect each part of the launch vehicle to ensure that the nose cone shoulder will have one half of a body diameter of surface contact with the airframe. | Complete. The Structures subteam designed the nose cone shoulder to be 3.1 in long, which is over half the diameter of 6.17 in. | Section 3.1.8 |
| SOW2.5 | The launch vehicle will be capable of being prepared for flight at the launch site within 2 hours of the time the Federal Aviation Administration flight waiver opens | Test | Calculations will be run to determine the minimum total battery power necessary for each component to properly function for at least 2 hours in the launch-ready configuration. The power supplies for each component well be selected accordingly. | Complete. The on-board batteries have been selected such that they will satisfy operational capacity for a comfortable margin beyond 2 hours. | Flysheet |

*Continued on next page*

Table 47 – *Continued from previous page*

| Item | Requirement | Verification Method | Verification Plan | Verification Status | Reference |
|---|---|---|---|---|---|
| SOW2.6 | The launch vehicle and payload will be capable of remaining in launch-ready configuration on the pad for a minimum of 2 hours without losing the functionality of any critical on-board components, although the capability to withstand longer delays is highly encouraged. | Test | Power consumption of each electrical component at their rated voltage and current draw will be calculated to determine if the selected battery provides enough capacity to remain launch-ready for at least 2 hours. | Complete. The on-board batteries have been selected such that they will satisfy operational capacity for a comfortable margin beyond 2 hours. | Section 5.2 |
| SOW2.7 | The launch vehicle will be capable of being launched by a standard 12-volt direct current firing system. The firing system will be provided by the NASA-designated launch services provider. | Inspection | Motors will be chosen such that they can be fired by a standard 12-volt direct current firing system. | Complete. The Aerotech L1390G motor is capable of being launched by a standard 12-volt direct current firing system. | Section 3.1.16 |

*Continued on next page*

Table 47 – *Continued from previous page*

| Item | Requirement | Verification Method | Verification Plan | Verification Status | Reference |
|---|---|---|---|---|---|
| SOW2.8 | The launch vehicle will require no external circuitry or special ground support equipment to initiate launch (other than what is provided by the launch services provider). | Inspection | The design of the vehicle will include the incorporation of all electrical components within its structure. It will be designed to launch without the need for external circuitry or special equipment on the ground. | Complete. The vehicle design incorporates all electrical components within its structure. It can launch without the need for external circuitry or special equipment on the ground. | Section 3.1.3 |
| SOW2.9 | Each team shall use commercially available ematches or igniters. Hand-dipped igniters shall not be permitted. | Inspection | The igniters used for the ignition of the black powder charges will not be made by the students nor the mentor nor purchase from anywhere other than a commercial vendor. | Complete. | N/A |

*Continued on next page*

Table 47 – *Continued from previous page*

| **Item** | **Requirement** | **Verification Method** | **Verification Plan** | **Verification Status** | **Reference** |
|---|---|---|---|---|---|
| SOW2.10 | The launch vehicle will use a commercially available solid motor propulsion system using ammonium perchlorate composite propellant (APCP) which is approved and certified by the National Association of Rocketry (NAR), Tripoli Rocketry Association (TRA), and/or the Canadian Association of Rocketry (CAR). | Inspection | NAR S&T's Combined Motor List will be used to verify the certification of the chosen motor | Complete. The L1390G-PS is certified by TRA | Section 3.1.16 |
| SOW2.10.1 | Final motor choices will be declared by the Critical Design Review (CDR) milestone. | Inspection | The final motor selection will be presented in the CDR | Complete. The final motor selection has been declared in the CDR. | 3.1.16 |

*Continued on next page*

Table 47 – *Continued from previous page*

| Item | Requirement | Verification Method | Verification Plan | Verification Status | Reference |
|---|---|---|---|---|---|
| SOW2.10.2 | Any motor change after CDR shall be approved by the NASA Range Safety Officer (RSO). Changes for the sole purpose of altitude adjustment will not be approved. A penalty against the team's overall score will be incurred when a motor change is made after the CDR milestone, regardless of the reason. | Analysis | Any motor change due to motor restrictions or other non-altitude related reasons will be checked and approved with the NASA Range Safety Officer. | Complete. The team is using a TRA approved Aerotech L1390G motor which will not be changed for altitude or non-altitude reasons. | Section 3.1.16 |
| SOW2.11 | The launch vehicle will be limited to a single motor propulsion system. | Inspection | The team will ensure that any motor system on the launch vehicle adheres to the requirements. | Complete. The current proposed launch vehicle is limited to a single motor system. | Section 3.1.16 |
| SOW2.12 | The total impulse provided by a College or University launch vehicle will not exceed 5,120 Newton-seconds (L-class). | Inspection | The team will ensure that any motor system on the launch vehicle does not exceed L-class. | Complete. The Aerotech L1390G-P has a total impulse of 3949 N-s. | Section 3.1.16 |

*Continued on next page*

Table 47 – *Continued from previous page*

| Item | Requirement | Verification Method | Verification Plan | Verification Status | Reference |
|---|---|---|---|---|---|
| SOW2.13 | 2.13. Pressure vessels on the vehicle will be approved by the RSO and will meet the following criteria: 2.13.1. The minimum factor of safety (Burst or Ultimate pressure versus Max Expected Operating Pressure) will be 4:1 with supporting design documentation included in all milestone reviews. 2.13.2. Each pressure vessel will include a pressure relief valve that sees the full pressure of the tank and is capable of withstanding the maximum pressure and flow rate of the tank. 2.13.3. The full pedigree of the tank will be described, including the application for which the tank was designed and the history of the tank. This will include the number of pressure cycles put on the tank, the dates of pressurization/depressurization, and the name of the person or entity administering each pressure event. | Inspection | The team will ensure that any pressure vessels on the launch vehicle adhere to the requirements. | Complete. The current proposed launch vehicle does not have any pressure vessels. | Section 3.1.3 |

*Continued on next page*

Table 47 – *Continued from previous page*

| **Item** | **Requirement** | **Verification Method** | **Verification Plan** | **Verification Status** | **Reference** |
|---|---|---|---|---|---|
| SOW2.14 | The launch vehicle will have a minimum static stability margin of 2.0 at the point of rail exit. Rail exit is defined at the point where the forward rail button loses contact with the rail. | Analysis | The team will use OpenRocket to verify that the launch vehicle design meets the static stability requirement at rail exit. | Complete. Using the proposed vehicle design, OpenRocket has confirmed that the static stability margin at rail exit is 3.0 cal. | Section 3.1.10 |
| SOW2.15 | The launch vehicle will have a minimum thrust to weight ratio of 5.0 : 1.0. | Analysis | Thrust to weight ratio will be verified by dividing the maximum acceleration predicted for the launch vehicle from OpenRocket by Earth's gravitational constant. | Complete. The thrust to weight ratio of the rocket is significantly above this 5:1 ratio. The full-scale maximum acceleration was determined to be 252 $\frac{ft}{s^2}$ using OpenRocket. Dividing this acceleration by 32.2 $\frac{ft}{s^2}$ yields a thrust to weight ratio of 7.86:1. | Section 3.1 |

*Continued on next page*

Table 47 – *Continued from previous page*

| Item | Requirement | Verification Method | Verification Plan | Verification Status | Reference |
|---|---|---|---|---|---|
| SOW2.16 | Any structural protuberance on the rocket will be located aft of the burnout center of gravity. Camera housings will be exempted, provided the team can show that the housing(s) causes minimal aerodynamic effect on the rocket's stability. | Inspection | The rail buttons and fins on the rocket will be located below the burnout CG. The camera housings will be placed forward of the burnout CG. | Complete. The fins and rail buttons on the rocket will be placed aft of the burnout center of gravity. The cameras are located forward of the burnout center of gravity but weigh a total of 1 oz, which will not significantly affect the center of gravity location, according to OpenRocket. Additionally, fluid dynamics simulations have shown that the cameras do not significantly affect the aerodynamics of the rocket. | Section 3.4.4 |
| SOW2.17 | The launch vehicle will accelerate to a minimum velocity of 52 fps at rail exit. | Analysis | The team will use OpenRocket to verify that the launch vehicle will accelerate to a minimum velocity of 52 fps at rail exit. | Complete. Using the proposed vehicle design, OpenRocket has confirmed that the rail exit velocity is 71.8 fps. | Section 3.4.3 |

*Continued on next page*

Table 47 – *Continued from previous page*

| Item | Requirement | Verification Method | Verification Plan | Verification Status | Reference |
|---|---|---|---|---|---|
| SOW2.18 | All Lithium Polymer batteries will be sufficiently protected from impact with the ground and will be brightly colored, clearly marked as a fire hazard, and easily distinguishable from other payload hardware | Inspection | Lithium Polymer Batteries will be securely attached to the avionics board and marked as a fire hazard. This will prevent any danger of damage upon landing. | Complete. The Lithium Polymer batteries in the avionics bay of the rocket are securely attached to the board via Velcro and zip ties. | N/A |
| SOW2.19.1 | The launch vehicle will not utilize forward firing motors. | Inspection | The team will ensure that launch vehicle will not utilize forward firing motors | Complete. The current proposed launch vehicle does not include forward firing motors. | Section 3.1.16 |
| SOW2.19.2 | The launch vehicle will not utilize motors that expel titanium sponges (Sparky, Skidmark, MetalStorm, etc.) | Inspection | The team will ensure that the launch vehicle will not utilize motors that expel titanium sponges | Complete. The current declared motor does not expel titanium sponges. | Section 3.1.16 |
| SOW2.19.3 | The launch vehicle will not utilize hybrid motors. | Inspection | The team will ensure that the launch vehicle will not utilize hybrid motors. | Complete. The current proposed launch vehicle does not include a hybrid motor. | Section 3.1.16 |
| SOW2.19.4 | The launch vehicle will not utilize a cluster of motors. | Inspection | The team will ensure that the launch vehicle will not utilize a cluster of motors. | Complete. The current proposed launch vehicle does not include a cluster of motors. | Section 3.1.16 |

*Continued on next page*

Table 47 – *Continued from previous page*

| Item | Requirement | Verification Method | Verification Plan | Verification Status | Reference |
|---|---|---|---|---|---|
| SOW2.19.5 | The launch vehicle will not utilize friction fitting for motors. | Inspection | The team will not use friction fitting to secure the motor to the launch vehicle. | Complete. Retainers are used to secure the motor to the launch vehicle. | Section 3.1.17 |
| SOW2.19.6 | The launch vehicle will not exceed Mach 1 at any point during flight. | Analysis | The team will use OpenRocket simulations to verify that the launch vehicle design does not exceed Mach 1. | Complete. Using the proposed vehicle design, OpenRocket has confirmed that the maximum velocity is at Mach 0.52. | Section 3.4.2 |
| SOW2.19.7 | Vehicle ballast will not exceed 10% of the total unballasted weight of the rocket as it would sit on the pad (i.e., a rocket with an unballasted weight of 40 lbs. on the pad may contain a maximum of 4 lbs. of ballast). | Inspection | The team will ensure that any ballast designed for the rocket meets the requirements. | Complete. The vehicle design does not have a ballast. | Section 3.1.3 |
| SOW2.19.8 | Transmissions from onboard transmitters, which are active at any point prior to landing, will not exceed 250 mW of power (per transmitter). | Inspection | All transmitters will be selected and programmed to successfully communicate without exceeding the maximum power of 250mW. | Complete. All selected transmitters are capable of functioning for the team's purposes without exceeding the power cap. | Flysheet |

*Continued on next page*

Table 47 – *Continued from previous page*

| Item | Requirement | Verification Method | Verification Plan | Verification Status | Reference |
|---|---|---|---|---|---|
| SOW2.19.9 | Transmitters will not create excessive interference. Teams will utilize unique frequencies, handshake/passcode systems, or other means to mitigate interference caused to or received from other teams. | Inspection | All transmitter systems will not utilize excessive means to communicate or mitigate interference that may cause greater interference for other teams. | Complete. The selected transmitters make use of handshake systems to mitigate interference | N/A |
| SOW2.19.10 | Excessive and/or dense metal will not be utilized in the construction of the vehicle. Use of lightweight metal will be permitted but limited to the amount necessary to ensure structural integrity of the airframe under the expected operating stresses | Inspection | All vehicle prohibitions of excessive or dense metal will be adhered to throughout the conception, design, manufacturing, and testing process. | Complete. The vehicle has been designed with the only metal being 6061 aluminum for the bulkheads as it is a material deemed necessary to maintain structural integrity of the body tubes. | Section 3.1.4 |

Table 48: Recovery System Requirements

| Item | Requirement | Verification Method | Verification Plan | Verification Status | Reference |
|---|---|---|---|---|---|

*Continued on next page*

Table 48 – *Continued from previous page*

| Item | Requirement | Verification Method | Verification Plan | Verification Status | Reference |
|---|---|---|---|---|---|
| SOW3.1 | The full scale launch vehicle will stage the deployment of its recovery devices, where a drogue parachute is deployed at apogee, and a main parachute is deployed at a lower altitude. Tumble or streamer recovery from apogee to main parachute deployment is also permissible, provided that kinetic energy during drogue stage descent is reasonable, as deemed by the RSO. | Inspection | Flight computers will use altitude and velocity data to detonate black powder charges inside the recovery sections of the rocket, pressurizing the vessel and severing the shear pins for the separation events. When flight velocity reaches zero, the flight computers will ignite the primary drogue separation charge, releasing the drogue parachute at apogee. A larger, redundant black powder charge will ignite one second following the primary charge to ensure the deployment of the drogue parachute within 2 seconds of reaching apogee. The main parachute will be deployed in a similar process when the rocket has reached 600 ft above ground level, and redundant charges will ignite at 500 ft. | Complete. | Section 3.3.2 |

*Continued on next page*

Table 48 – *Continued from previous page*

| Item | Requirement | Verification Method | Verification Plan | Verification Status | Reference |
|---|---|---|---|---|---|
| SOW3.1.1 | The main parachute shall be deployed no lower than 500 feet. | Inspection | The EasyMini flight computers will be set to main parachute ejection altitudes of 600ft and 500ft respectively, ensuring the separation and safe ejection of the main parachute before 500ft | Complete. | Section 3.3.10 |
| SOW3.1.2 | The apogee event may contain a delay of no more than 2 seconds. | Inspection | The apogee separation, releasing the drogue parachute, will be set to occur at apogee for the primary flight computer and 1 second after apogee for the redundant, ensuring proper drogue separation before 2 seconds after apogee. | Complete. | Section 3.3.10 |
| SOW3.1.3 | Motor ejection is not a permissible form of primary or secondary deployment. | Inspection | The team will not use motor ejection as a form of primary or secondary deployment. | Complete. | Section 3.3.2 |

*Continued on next page*

Table 48 – *Continued from previous page*

| Item | Requirement | Verification Method | Verification Plan | Verification Status | Reference |
|---|---|---|---|---|---|
| SOW3.2 | Each team will perform a successful ground ejection test for all electronically initiated recovery events prior to the initial flights of the subscale and full scale vehicles. | Test | A ground ejection test will be conducted for the primary black powder charges of both the drogue and main parachute separation events. Testing will be completed at any change of black powder quantity and two weeks prior to each launch of subscale and full scale rockets. | Incomplete. | Section 3.3.7 |
| SOW3.3 | Each independent section of the launch vehicle will have a maximum kinetic energy of 75 ft-lbf at landing. | Analysis | OpenRocket simulations will be conducted to verify an impact kinetic energy below competition requirements | Complete. The forward, mid, and aft sections have kinetic energy values of 57.08, 17.72, and 47.19 ft-lbf, respectfully. | Section 3.4.5 |
| SOW3.4 | The recovery system will contain redundant, commercially available barometric altimeters that are specifically designed for initiation of rocketry recovery events. The term "altimeters" includes both simple altimeters and more sophisticated flight computers. | Inspection | The recovery electronics will consist of two Altus Metrum EasyMini flight computers. | Complete. | Section 3.3.10 |

*Continued on next page*

Table 48 – *Continued from previous page*

| Item | Requirement | Verification Method | Verification Plan | Verification Status | Reference |
|---|---|---|---|---|---|
| SOW3.5 | Each altimeter will have a dedicated power supply, and all recovery electronics will be powered by commercially available batteries. | Inspection | Both EasyMini flight computers will have their own 3.7v Lithium Polymer battery. | Complete. | Section 3.3.10 |
| SOW3.6 | Each altimeter will be armed by a dedicated mechanical arming switch that is accessible from the exterior of the rocket airframe when the rocket is in the launch configuration on the launch pad. | Inspection | Each flight computer will be armed by a separate rotary arming switch that will be accessible via a cutout in the airframe at all stages of assembly. | Complete. | Section 3.3.10 |
| SOW3.7 | Each arming switch will be capable of being locked in the ON position for launch (i.e. cannot be disarmed due to flight forces). | Inspection | The rotary switches used for arming the flight computers lock upon changing state and are designed such that flight forces cannot disarm the flight computers. | Complete. | Section 3.3.10 |

*Continued on next page*

Table 48 – *Continued from previous page*

| Item | Requirement | Verification Method | Verification Plan | Verification Status | Reference |
|---|---|---|---|---|---|
| SOW3.8 | The recovery system, GPS and altimeters, electrical circuits will be completely independent of any payload electrical circuits. | Inspection | The recovery system electronics, although positioned within the avionics bay with the rest of the avionics system, will be entirely independent of the rest of the avionics system or payload system for power, function, and arming. | Complete. | Fig. 62 |
| SOW3.9 | Removable shear pins will be used for both the main parachute compartment and the drogue parachute compartment. | Inspection | The Structures team will hand drill shear screw holes onto the airframe and coupler connections to be fitted for the necessary shear pins. | Complete. | Section 3.1.14 |
| SOW3.10 | The recovery area will be limited to a 2500 ft. radius from the launch pads. | Analysis | The rocket's drift was calculated to be 2255 ft at maximum windspeeds of 20 mph, 245 ft below the maximum | Complete | Section 3.4.6 |
| SOW3.11 | Descent time of the launch vehicle will be limited to 90 seconds (apogee to touch down). | Analysis | The rocket's descent time was calculated to be 76.88 seconds, 13.12 s below the maximum and 3.12 seconds below the bonus goal | Complete | Section 3.3.9 |

*Continued on next page*

Table 48 – *Continued from previous page*

| **Item** | **Requirement** | **Verification Method** | **Verification Plan** | **Verification Status** | **Reference** |
|---|---|---|---|---|---|
| SOW3.12 | An electronic GPS tracking device will be installed in the launch vehicle and will transmit the position of the tethered vehicle or any independent section to a ground receiver. | Inspection | The Altus Metrum TeleGPS will be fitted to the avionics bay and will track the rocket (consisting of only one independent section) transmitting down to the TeleBT ground receiver. | Complete. | Section 3.3.10 |
| SOW3.12.1 | Any rocket section or payload component, which lands untethered to the launch vehicle, will contain an active electronic GPS tracking device. | Analysis | Any section that fits the requirements previously stated will be fitted with its own GPS tracking device. Presently, there is no such section aside from the main rocket section. | Complete | N/A |
| SOW3.13 | The recovery system electronics will not be adversely affected by any other on-board electronic devices during flight (from launch until landing). | Inspection | The EasyMini flight computers will be shielded from any RF interference by use of an aluminum Faraday cage. All continuities will be verified preflight and no bare wires will be present within the avionics bay. | Complete. | N/A |

*Continued on next page*

Table 48 – *Continued from previous page*

| Item | Requirement | Verification Method | Verification Plan | Verification Status | Reference |
|---|---|---|---|---|---|
| SOW3.13.1 | The recovery system altimeters will be physically located in a separate compartment within the vehicle from any other radio frequency transmitting device and/or magnetic wave producing device. | Inspection | The EasyMini flight computers will be located in the avionics bay and separated from the TeleGPS system by the avionics bay board by as much distance as possible | Complete. | N/A |
| SOW3.13.2 | The recovery system electronics will be shielded from all onboard transmitting devices to avoid inadvertent excitation of the recovery system electronics. | Inspection | The EasyMini flight computers will be shielded from any RF interference by use of an aluminum Faraday cage. All continuities will be verified preflight and no bare wires will be present within the avionics bay. | Complete. | N/A |
| SOW3.13.3 | The recovery system electronics will be shielded from all onboard devices which may generate magnetic waves (such as generators, solenoid valves, and Tesla coils) to avoid inadvertent excitation of the recovery system. | Inspection | The EasyMini flight computers will be shielded from any RF interference by use of an aluminum Faraday cage. All continuities will be verified preflight and no bare wires will be present within the avionics bay. | Complete. | N/A |

*Continued on next page*

Table 48 – *Continued from previous page*

| Item | Requirement | Verification Method | Verification Plan | Verification Status | Reference |
|---|---|---|---|---|---|
| SOW3.13.4 | The recovery system electronics will be shielded from any other onboard devices which may adversely affect the proper operation of the recovery system electronics. | Inspection | The EasyMini flight computers will be shielded from any RF interference by use of an aluminum Faraday cage. All continuities will be verified preflight and no bare wires will be present within the avionics bay. | Complete. | N/A |

Table 49: Payload Requirements

| Item | Requirement | Verification Method | Verification Plan | Verification Status | Reference |
|---|---|---|---|---|---|
| SOW4.2.1 | Launch Vehicle shall contain an automated camera system capable of swiveling 360º to take images of the entire surrounding area of the launch vehicle. | Demonstration | The team will transmit RAFCO commands for the camera to take images at various positions. These positions can include clockwise and counterclockwise rotations that sum to 360 degrees of rotation. The team can visually verify that the camera system is capable of swiveling 360 degrees. | In Progress. Final designs have been prototyped and software has been outlined. Further work will be done to consolidate all the components together into a cohesive automated system. | Section 4.5 |

*Continued on next page*

Table 49 – *Continued from previous page*

| Item | Requirement | Verification Method | Verification Plan | Verification Status | Reference |
|---|---|---|---|---|---|
| SOW4.2.1.1 | The camera shall have the capability of rotating about the z axis. The z axis is perpendicular to the ground plane with the sky oriented up and the planetary surface oriented down. | Demonstration | This will be confirmed by performing multiple tests of the rotating track (on both the prototype and final design) with mock weights to simulate pulling the camera upright about the z-axis. Demonstrations will also be made to prove that a selected servo can rotate the Raspberry Pi camera. | In Progress. The Payload subteam has made and tested a proof of concept design of the rotating track demonstrating its ability to remain upright, as well as software for rotating a servo with the camera mounted on top to capture different image angles. | Section 4.5. Future work involves transitioning the prototype to the final parts. |
| SOW4.2.1.2 | The camera shall have a FOV of at least $100^{\circ}$ and a maximum FOV of $180^{\circ}$ | Test | Will take various images of a flat plane with a viewing angle perpendicular to the plane. The plane will be marked with measured lengths so that calculations can be performed to ensure that the selected camera produced images of FoV between $100^{\circ}$ and $180^{\circ}$. | Complete. The camera test resulted in a calculated PoV of around $160^{\circ}$. | Section 6.1.2 |

*Continued on next page*

Table 49 – *Continued from previous page*

| Item | Requirement | Verification Method | Verification Plan | Verification Status | Reference |
|---|---|---|---|---|---|
| SOW4.2.1,3 | The camera shall time stamp each photo taken. The time stamp shall be visible on all photos submitted to NASA in the PLAR. | Inspection | After the imaging program modifies the image file captured by the camera, the team will visually inspect the file on a computer display for the timestamp. | Complete. The team has successfully take images and added a timestamp to the resulting image. | Section 4.6 |
| SOW4.2.1.4 | The camera system shall execute the string of transmitted commands quickly, with a maximum of 30 seconds between photos taken. | Demonstration | The routine used to execute the camera system functions will have code to time the runtime of each RAFCO execution. | In Progress. Once the entire automated camera system is working, the team will rerun the timing code to demonstrate that each RAFCO executes under 30 seconds. | Section 4.8 |

*Continued on next page*

Table 49 – *Continued from previous page*

| Item | Requirement | Verification Method | Verification Plan | Verification Status | Reference |
|---|---|---|---|---|---|
| SOW4.2.2 | NASA Student Launch Management Team shall transmit a RF sequence that shall contain a radio call sign followed by a sequence of tasks to be completed. The list of potential commands to be given on launch day along with their radio transcriptions which shall be sent in a RF message using APRS transmission in no particular order are: A1—Turn camera 60º to the right. B2—Turn camera 60º to the left. C3—Take picture. D4—Change camera mode from color to grayscale. E5—Change camera mode back from grayscale to color. F6—Rotate image 180º (upside down). G7—Special effects filter (Apply any filter or image distortion you want and state what filter or distortion was used). H8—Remove all filters. | Inspection and Demonstration | Black powder or energetics will not be utilized to fulfill the goals of the payload mission. Code will be written in Python and demonstrated through multiple field tests. | In Progress. The Payload subteam has not interacted with any energetics on the payload. Future work involves assembling payload and using field tests to demonstrate filtering capabilities. | Section 4.5. |

*Continued on next page*

Table 49 – *Continued from previous page*

| **Item** | **Requirement** | **Verification Method** | **Verification Plan** | **Verification Status** | **Reference** |
|---|---|---|---|---|---|
| SOW4.2.3 | The NASA Student Launch Management Panel shall transmit the RAFCO using APRS. | Demonstration | The payload mission will not include drones or any jettisoned objects, this ensure the rocket abides by FAA and NAR rules and regulations. | Complete | Section 4.5 |
| SOW4.2.3.1 | NASA will use dedicated frequencies to transmit the message. NASA will operate on the 2-Meter amateur radio band between the frequencies of 144.90 MHz and 145.10 MHz. No team shall be permitted to transmit on any frequency in this range. The specific frequency used will be shared with teams during Launch Week. NASA reserves the right to modify the transmission frequency as deemed necessary. | Inspection | No payload element will be jettisoned from the rocket | Complete | Section 4.5 |

*Continued on next page*

Table 49 – *Continued from previous page*

| Item | Requirement | Verification Method | Verification Plan | Verification Status | Reference |
|---|---|---|---|---|---|
| SOW4.3.1 | The NASA Management Team shall transmit the RAFCO every 2 minutes. | Demonstration | The Payload subteam will simulate transmission of a RAFCO sequence every 2 minutes to verify that the RAFCO is received as expected. | In Progress. The Payload team has successfully received APRS transmissions from the on-board SDL adapter. However, the team has yet to perform personal APRS transmissions. | Section 4 |
| SOW4.2.3.3 | The payload system shall not initiate and begin accepting RAFCO until AFTER the launch vehicle has landed on the planetary surface. | Demonstration | The Payload software that controls initialization of RAFCO execution will only begin once the on-board avionics subsystem has detected a stable landing. | Complete. The Payload team has been able to sample the on-board IMU and altimeter for data and process it to determine whether the payload is moving or not below a certain altitude. | Section 4 |
| SOW4.2.4 | The payload shall not be jettisoned. | Demonstration | The Payload subteam will not eject any portion of the payload from the vehicle. | Complete | Section 4 |
| SOW4.2.5 | The sequence of time-stamped photos taken need not be transmitted back to ground station and shall be presented in the correct order in your PLAR. | Demonstration | The Payload subteam will not tranmist any images to the ground station, but will save the images on-disk in order that they were taken so that the PLAR can be easily organized. | Complete. The subteam has been able to save the images captured with the filename incorporating a timestamp such that they are sorted on the filesystem. | Section 4 |

*Continued on next page*

Table 49 – *Continued from previous page*

| Item | Requirement | Verification Method | Verification Plan | Verification Status | Reference |
|---|---|---|---|---|---|
| SOW4.3.1 | Black Powder and/or similar energetics are only permitted for deployment of in-flight recovery systems. Energetics shall not be permitted for any surface operations. | Demonstration | The Payload subteam will not interact with any energetic for the payload. | Complete | Section 4 |
| SOW4.3.2 | Teams shall abide by all FAA and NAR rules and regulations. | Demonstration | WURocketry will thoroughly read and review the rules with members prior to launch to ensure no regulations are violated. | Complete | Section 4 |
| SOW4.3.3 | Any secondary payload experiment element that is jettisoned during the recovery phase will receive real-time RSO permission prior to initiating the jettison event, unless exempted from the requirement the CDR milestone by NASA. | Demonstration | WURocketry will not fly a secondary payload experiment. | Complete | Section 4 |

*Continued on next page*

Table 49 – *Continued from previous page*

| Item | Requirement | Verification Method | Verification Plan | Verification Status | Reference |
|---|---|---|---|---|---|
| SOW4.3.4 | Unmanned aircraft system (UAS) payloads, if designed to be deployed during descent, will be tethered to the vehicle with a remotely controlled release mechanism until the RSO has given permission to release the UAS. | Demonstration | WURocketry will not fly a UAS as part of the payload mission. | Complete | Section 4 |
| SOW4.3.5 | Teams flying UASs will abide by all applicable FAA regulations, including the FAA's Special Rule for Model Aircraft (Public Law 112-95 Section 336; see https://www.faa.gov/uas/faqs). | Demonstration | WURocketry will not fly a UAS as part of the payload mission. | Complete | Section 4 |
| SOW4.3.6 | Any UAS weighing more than .55 lbs. shall be registered with the FAA and the registration number marked on the vehicle. | Demonstration | WURocketry will not fly a UAS as part of the payload mission. | Complete | Section 4 |

Table 50: Safety Requirements

| Item | Requirement | Verification Method | Verification Plan | Verification Status | Reference |
|---|---|---|---|---|---|
| SOW5.1 | Each team will use a launch and safety checklist. The final safety checklists will be included in the FRR report and used during the Launch Readiness Review and any Launch Day Operations. | Inspection | Safety checklists will be written by the Safety Officer using the launch regulations and the safety plans in Section 5 of this document. | Complete. Checklists and procedures with safety warning are written | Section 5.1 |
| SOW5.2 | Each team shall identify a student safety officer who will be responsible for all items in section 5.3. | Inspection | WURocketry Safety Officer is Andrew DeRubertis and he is responsible for the items in section 5.3. | Complete. Andrew DeRubertis is aware of his responsibility for all items in section 5.3 of this document. | N/A |

*Continued on next page*

Table 50 – *Continued from previous page*

| **Item** | **Requirement** | **Verification Method** | **Verification Plan** | **Verification Status** | **Reference** |
|---|---|---|---|---|---|
| SOW5.3.1 | Monitor team activities with an emphasis on safety during: 5.3.1.1. Design of vehicle and payload. 5.3.1.2. Construction of vehicle and payload components. 5.3.1.3. Assembly of vehicle and payload. 5.3.1.4. Ground testing of vehicle and payload. 5.3.1.5. Subscale launch test(s). 5.3.1.6. Full-scale launch test(s). 5.3.1.7. Competition launch. 5.3.1.8. Recovery activities. 5.3.1.9. STEM Engagement Activities. | Inspection | The Safety Officer is responsible for reading and understanding all safety requirements and regulations regarding the USLI competition and WashU club affairs. The Safety Officer will use this knowledge to monitor all WURocketry activities. | In Progress. Andrew DeRubertis has read and understands all safety requirements and regulations from the NASA Student Launch Handbook and from WashU. | N/A |
| SOW5.3.2 | Implement procedures developed by the team for construction, assembly, launch, and recovery activities. | Inspection | The Safety Officer will review all construction and assembly procedures for subteams, as well as enforcing school required training for specific machine use. | In Progress. The Safety Officer will review construction, assembly, launch and recovery plans with the team and brief them any time a change or addition is made to these procedures. | N/A |

*Continued on next page*

Table 50 – *Continued from previous page*

| **Item** | **Requirement** | **Verification Method** | **Verification Plan** | **Verification Status** | **Reference** |
|---|---|---|---|---|---|
| SOW5.3.3 | Manage and maintain current revisions of the team's hazard analyses, failure modes analyses, procedures, and MSDS/chemical inventory data. | Inspection | The Safety Officer is responsible for updating all safety documents including but not limited to the documents mentioned here. | In Progress. The Safety Officer attends all WURocketry activities to ensure that all safety documentation is up to date and encompasses all related procedures and team activity. | N/A |
| SOW5.3.4 | Assist in the writing and development of the team's hazard analyses, failure modes analyses, and procedures. | Inspection | The Safety Officer is responsible for writing team safety documents. | Complete. The Safety Officer and auxiliary safety officer(s) write all safety documents | N/A |

*Continued on next page*

Table 50 – *Continued from previous page*

| Item | Requirement | Verification Method | Verification Plan | Verification Status | Reference |
|---|---|---|---|---|---|
| SOW5.4 | During test flights, teams will abide by the rules and guidance of the local rocketry club's RSO. The allowance of certain vehicle configurations and/or payloads at the NASA Student Launch does not give explicit or implicit authority for teams to fly those vehicle configurations and/or payloads at other club launches. Teams should communicate their intentions to the local club's President or Prefect and RSO before attending any NAR or TRA launch. | Inspection | The Safety Officer is responsible for contacting the RSO and the team-mentor prior to test flights to go over the local rocketry associations rules and launch location rules. The Safety Officer is responsible for explaining the payload mission and confirming with the RSO and local regulations that the payload is permissible for test flight at the local launch. | In Progress. The Safety Officer and any members conducting the launch discuss the payload and any pertinent rules or regulations with the RSO and team mentor prior to a test launch with the payload. | N/A |
| SOW5.5 | Teams will abide by all rules set forth by the FAA. | Inspection | In pre-flight safety briefings, the Safety Officer will discuss the rules of the local rocketry association, the configuration of the launch vehicle, and the recommendations of the RSO. | In Progress. The Safety Officer and any members conducting the launch discuss rules and regulations with the RSO and team mentor prior to launch. | N/A |

### 6.2.2 Team-Derived Vehicle Requirements

Table 51: Team-Derived Vehicle Requirements

| Item | Requirement | Justification | Verification Method | Verification Plan |
|---|---|---|---|---|
| TDVR 1 | The Status LED for the Raspberry Pi 4B needs to be visible from the outside of the rocket | Since no audible status notification is provided by the Raspberry Pi 4B it is neccessary to include a status LED indicating proper function of the microcontroller. | Demonstration and Inspection | A status LED will be attached to the Raspberry Pi 4B and programmed to provide a useful indication of the pi's status. A hole will be cut into the airframe to allow visual access to the status LED. |
| TDVR 2 | The launch vehicle must be able to fit in the back of a car trunk. | The budget limits the team transportation options to students' cars, so the launch vehicle must fit within the back of a car to be easily transported. | Inspection | The team will determine if the launch vehicle fits in the back of a car by placing each section and its components in the back of a team member's car. |
| TDVR 3 | Zippered body tubes and couplers must be avoided. | The team observed a zippered coupler in a previous launch due to the placement of the shock cords and couplers within the body tubes. | Inspection | All couplers must have an anti-zipper design. The attachment points of the shock cords are placed at the end of the couplers in the design using eye bolts. |

*Continued on next page*

Table 51 – *Continued from previous page*

| Item | Requirement | Justification | Verification Method | Verification Plan |
|---|---|---|---|---|
| TDVR 4 | There must be a fully self-contained telemetry down-link. | In order to provide a simplified method for tracking the rocket that does not risk communication errors brought on by running GPS data through a separate micro controller before transmission to the base station, a fully self contained telemetry down link is necessary. | Demonstration | The Altus Metrum TeleGPS will be used to transmit telemetry data to the base station. This design has been demonstrated in Section 6.1.3. |
| TDVR 5 | The e-matches should be able to connect to the avionics bay after it has been fully constructed. | The ability to fully construct the avionics bay prior to launch day will dramatically reduce the time necessary to assemble the rocket. In order to fully enable prior assembly of the avionics bay, it is necessary to attach terminal blocks to the bulk heads of the avionics bay that will be used to attach E-matches to the flight computers on launch day. | Inspection | Two sets of terminal blocks will be attached to the bulkheads for each separation chamber enabling the attachment of E-matches for both the primary and redundant charges contained within each separation section. |

*Continued on next page*

Table 51 – *Continued from previous page*

| **Item** | **Requirement** | **Justification** | **Verification Method** | **Verification Plan** |
|---|---|---|---|---|
| TDVR 6 | The fins do not break during launch. | The team wants to ensure that the rocket is stable throughout its entire flight from rail exit to landing. If the rocket lands in free fall, the fins must be designed to withstand the force of hitting the ground at a high velocity. | Inspection | Many different materials were studied for the fin design. WURocketry chose to create four G10 fiberglass non-removable fin cores. Additionally, the team will 3D print PETG fin protective shells with an airfoil as a removable option to decrease the likelihood of fin fracture during launch (the vehicle hits the ground in free fall). |
| TDVR 7 | The bulkheads do not degrade below required strength. | The bulkheads will be reused multiple times for each launch and the bulkheads must remain capable of supporting the applied loads repeatedly. | Demonstration | As part of the testing campaign the strength of the sample bulkheads over cycles will be examined and recorded. The second-to-last cycle before the cycle at which the loads can no longer maintain structural integrity will be used as the cycle limit of the bulkhead part. |

*Continued on next page*

Table 51 – *Continued from previous page*

| Item | Requirement | Justification | Verification Method | Verification Plan |
|---|---|---|---|---|
| TDVR 9 | The fastener holes on both the airframe and coupler do not degrade and widen after multiple assemblies and dis-assemblies | If holes wear out, they will need to be drilled in new locations. It is difficult to move hole locations once holes are drilled in the airframe because the avionics bay must sit in a particular orientation and cannot be rotated with new holes. | Inspection | At each hole in the airframe and couplers where the fasteners sit, a small amount of super glue on the outside edge of the hole will be applied after one or two uses of the rocket. |
| TDVR 10 | The bulkheads should be as light as possible. | Bulkheads should help allow for other design freedom for the rocket by being as light as possible while still being able to support the required load. | Demonstration and Inspection | Finite element analysis will be used on the bulkhead designs in SolidWorks to apply a constant load resembling that of the snatch force of the parachutes on the bulkheads. The bulkheads will be designed by mass so that they do not have displacement of more than 0.01 in under the snatch force load but are still as light as possible. |
| TDVR 11 | Components manufactured must be sanded or filed to prevent injuries to team members during assembly and testing. | WURocketry prioritizes the safety of all team members. | Demonstration | The team will acquire sandpaper and a file from the Student Machine Shop to borrow after each part is delivered, machined, or constructed. |

*Continued on next page*

Table 51 – *Continued from previous page*

| Item | Requirement | Justification | Verification Method | Verification Plan |
|---|---|---|---|---|
| TDVR 12 | The bulkheads and ballast must be manufacturable by WURocketry members in the Washington University Student Machine Shop. | The team minimizes extraneous manufacturing expenses and gains valuable hands-on experience by turning design drawings into parts. | Demonstration | The team members will consult the Machine Shop Manager for guidance to construct the bulkheads. All members of the Structures subteam are strongly encouraged to obtain machine shop training and to attend machining hours for the bulkheads. |
| TDVR 13 | All permanent screws are 6-32 Phillips head screws on the launch vehicle. | Standardizing fasteners reduces the required equipment on site and makes transportation, assembly, and repairs simpler. | Inspection | The team members will design and purchase 6-32 size Phillips head screws for the bulkheads for the 2022-2023 season. |

### 6.2.3 Team-Derived Recovery Requirements

Table 52: Team-Derived Recovery Requirements

| Item | Requirement | Justification | Verification Method | Verification Plan |
|---|---|---|---|---|

*Continued on next page*

Table 52 – *Continued from previous page*

| Item | Requirement | Justification | Verification Method | Verification Plan |
|---|---|---|---|---|
| TDRR 1 | Drogue and Main parachutes must be protected during black powder charge ignition. | Black powder detonations can damage the parachute, potentially threatening a safe recovery. Parachute protection methods can be taken to prevent this. | Inspection | The drogue and main parachute deployment systems will be designed to ensure a deployment bag or blanket can be used alongside the parachute. The packing of the parachute will be checked by the R&P Team Lead to ensure the parachutes are properly covered before placed into the rocket. |
| TDRR 2 | Black powder quantity must be less than 5 g. | Too much black powder risks damage to the launch vessel and components within. | Testing and Inspection | In testing and launch preparation, the R&P team lead and WURocketry mentor will ensure that no more than 5g of black powder will be used. |
| TDRR 3 | Black powder charges must properly remove shear pins and separate sections of the rocket. | If black powder charges fail to remove shear pins and separate sections of the rocket, parachute deployment will fail, leading to a high impact velocity, major damage to the rocket, and a potential hazard to observers. | Testing and Inspection | Ground ejection tests will be performed two weeks prior to each launch to ensure the amounts of black powder chosen will successfully remove shear pins and seperate the rocket's sections. The R&P Team Lead and WURocketry Mentor will both conduct, monitor, and verify the testing and results. |

*Continued on next page*

Table 52 – *Continued from previous page*

| Item | Requirement | Justification | Verification Method | Verification Plan |
|---|---|---|---|---|
| TDRR 4 | Shock cords used must be three to five times the length of the rocket section attached in the use of nylon shock cords. | Nylon shock cords dampen the snatch force on the rocket due to a greater elastic strength. This elasticity is most effective in greater lengths to disperse energy without causeing the rocket section to bounce back and collide. | Inspection, Testing | The R&P Team lead will verify the length of each shock cord. The R&P Team lead will also inspect the camera footage recorded during launches to determine if bounce or collision occurred. |
| TDRR 5 | Shock cord colors must correlate to their size group. | Color coding aids in the visual analysis of shock cord behavior in the camera footage taken during launch. Additionally, color coding reduces likeliness of incorrect shock cord attachments on launch day. | Inspection | Different colored shock cords will be selected for the main and drogue parachute systems, and will be chosen based on specific size. The shock cords will be visually examined by the R&P Team Lead before launch to ensure the colored shock cords are connected to their respective sections. |
| TDRR 6 | Pressure sensors will be used to verify the ignition of the separation charges within in both separation chambers. | A secondary method of separation verification is necessary to provide crucial information in the event of a recovery failure. | Demonstration | The ported pressure sensors will be mounted such that they are able to read the pressure in the separation chambers. Activation of the Raspberry Pi will provide verification of pressure readouts. |

### 6.2.4 Team-Derived Payload Requirements

Table 53: Team-Derived Payload Requirements

| Item | Requirement | Justification | Verification Method | Verification Plan |
|---|---|---|---|---|
| TDPR 1 | The payload must not exceed 16" in length. | The team has designed the payload bay to be at most 15.5" in length this year. | Design and Analysis | CAD software has been used to model the machined structures and overall assembly of the payload experiment to ensure it does not exceed the length. Post-build measurements will also be taken to verify the physical build does not exceed 16". |
| TDPR 2 | The payload must not exceed 6" in diameter. | The team has designed the launch vehicle with an inner diameter of 6" this year. | Design and Analysis | CAD software has been used to model the machined structures and overall assembly of the payload experiment to ensure it does not exceed the diameter. Post-build measurements will also be taken to verify the physical build does not exceed 6". |
| TDPR 3 | The payload should weigh 5 pounds. | The team has determined launch vehicle stability and conducted Open Rocket simulations with a calculated weight of 5 pounds. | Design and Analysis | CAD software has provided an estimate mass for each model that composes the payload, in addition to component commercial weight specifications. |

*Continued on next page*

Table 53 – *Continued from previous page*

| Item | Requirement | Justification | Verification Method | Verification Plan |
|---|---|---|---|---|
| TDPR 4 | The payload imaging camera must be able to rotate | In order to properly take images of the surrounding environment, a servo will be used to rotate the camera left and right at 60 degree intervals. | Test | Test the Full Stop, and Full Speed duty cycle values. From there reduce the Servo speed by changing the duty cycle values and use a spreadsheet and timer to calculate rotation. |
| TDPR 5 | The payload will automatically upright itself physically, normal to the ground plane and aligned to the z-axis | In order to properly take images of the surrounding environment, the camera must be deployed upright | Test | The subteam has performed multiple tests on the efficacy of the rotating track design by placing various weights at different CGs on a rotating board to test the orientation of the track. The tests have shown that a ballast weight is capable of self-righting the payload track. |
| TDPR 6 | The payload must be securely retained within the vehicle throughout flight | During flight, the nosecone must not separate and rotating tracks must remain stable, and will only deploy when the vehicle has made a stable landing. | Test and Analysis | On SolidWorks, the team will use a simulation with an added force added in the normal direction to the end of the linear solenoid to ensure there is minimal deflection and that the stress value is not too high. |

*Continued on next page*

Table 53 – *Continued from previous page*

| **Item** | **Requirement** | **Justification** | **Verification Method** | **Verification Plan** |
|---|---|---|---|---|
| TDPR 7 | The payload deployment must separate the nosecone and extend the imaging camera with enough clearance to provide good imaging of surrounding environment. | The payload deployment will involve separation of the nosecone from the payload bay of at least 4" and extending the camera above the body tube by at least 2" to provide good imaging clearance. | Test | Test how much force the rack and pinion can generate. The team will have the rack and pinion plus motor run at various speeds to push into a force sensor. Force will be recorded in newtons and analyses to ensure the nose cone can be separated. In addition we can demonstrate it by pushing a mock or real nose cone. |
| TDPR 8 | The payload camera, radio communication, and deployment mechanisms will be run autonomously by a Raspberry Pi. | It is more efficient to have a system capable of running independently and not relying on external influences. | Test and analyze. | Each phase of the payload mission execution (stand-by, launch, landing, self-righting, separation, deployment, and RAFCO execution) will be all run together to ensure the overall components can run under the single main program without team input. |

*Continued on next page*

Table 53 – *Continued from previous page*

| Item | Requirement | Justification | Verification Method | Verification Plan |
|---|---|---|---|---|
| TDPR 9 | The payload software will utilize VHF transceiver hardware to listen for RAFCO on the 2-meter radio frequency band to process and execute camera control and transformation operations. | The USLI launch competition will use a NASA hosted APRS network to communicate RAFCO to the payload experiment. | Inspection and Demonstration | The selected hardware for receiving RAFCO signals has been chosen to listen on the 2-meter band and has been demonstrated to receive APRS transmissions from the local area. |
| TDPR 10 | The team will be capable of maintaining reliable communication with the payload during standby, launch, and operation of the system throughout the flight. | This allows the team more insight into the payload mission as it is being executed in real-time. | Demonstration | The RFM96W transceivers have been demonstrated to communicate over 700ft in direct line of sight of each other. The data sent can be of packets of varying sizes, and specifically ASCII data can be transmitted to send informative strings of the payload operation to the base station |

## 6.3 Budgeting and Timeline

### 6.3.1 Line Item Budgets

Tables 54 to 63 show the budgets for the different subteams as well as budgets for travel and manufacturing. Recovery and Propulsion was broken out and divided into sub-scale and full-scale budgets for clarity. Table 64 shows the total budget of the team.

Table 54: Structures Budget

| **Item** | **Vendor / Manufacturer** | **QTY** | **Unit Price** | **Total Price** |
|---|---|---|---|---|
| 6" Diameter, 10' Length G12 Fiberglass Airframe | Madcow Rocketry | 1 | $366.00 | $366.00 |
| 4" Diameter, 8' Length G12 Fiberglass Airframe | Madcow Rocketry | 1 | $211.20 | $211.20 |
| 6" Diameter, 14" Length G12 Fiberglass Coupler | Madcow Rocketry | 1 | $93.22 | $93.22 |
| 4" Diameter, 12" Length G12 Fiberglass Coupler | Madcow Rocketry | 1 | $41.20 | $41.20 |
| 6" inch Nosecone Fiberglass 5:1 with rounded aluminum tip | Madcow Rocketry | 1 | $149.99 | $149.99 |
| 4" inch Nosecone Ogive 5:1 Goblin & Redmax with rounded composite tip | Madcow Rocketry | 1 | $90.94 | $90.94 |
| Universal AstroCam HD Rocket Camera and Holder | Belleville Hobby | 2 | $29.49 | $58.98 |
| 6061 T6 Aluminum 6" x 6" x 3/8" | McMaster-Carr | 10 | $18.07 | $180.70 |
| 6-32 Metal Screws 100 count | McMaster-Carr | 1 | $6.46 | $6.46 |
| 2-56 Shear Screws 3/16" 100 Pack | McMaster-Carr | 1 | $8.69 | $8.69 |
| 2-56 Shear Screws 1/4" 100 Pack | McMaster-Carr | 1 | $8.74 | $8.74 |
| 316 Stainless Steel Flange Nuts 3/8"-16 Thread Size 25 Pack | McMaster-Carr | 1 | $12.65 | $12.65 |
| Eyebolt - For Lifting 1/4"-28 | McMaster-Carr | 8 | $6.28 | $50.24 |
| Rail Buttons for 1.5" rail | Apogee Components | 2 | $5.70 | $11.40 |
| 3/8" lead Screw | Ace Hardware | 2 | $7.30 | $14.60 |
| G10 Fiberglass Sheet 24" x 24" x 1/8" | McMaster-Carr | 1 | $76.71 | $76.71 |
| **Total** | | | | **$1381.72** |

Table 55: Avionics Budget

| Item | Vendor / Manufacturer | QTY | Unit Price | Total Price |
|---|---|---|---|---|
| SparkFun GPS Breakout - NEO-M9N, SMA (Qwiic) | Sparkfun | 1 | $74.95 | $74.95 |
| RockBLOCK External Patch Antenna | RockBLOCK | 1 | $69.95 | $69.95 |
| Easy Mini | AltusMetrum | 2 | $80.00 | $160.00 |
| Micro USB Cord | Apogee Components | 2 | $6.99 | $13.98 |
| 3.7V LiPo Battery, 900 mAh | AltusMetrum | 2 | $12.12 | $24.24 |
| Raspberry Pi 4 Model B 2019 | Raspberry Pi | 1 | $135.00 | $135.00 |
| Adafruit MCP3008 8-Channel 10-Bit ADC | Adafruit | 1 | $9.00 | $9.00 |
| Adafruit MPRLS Ported Pressure Sensor Breakout - 0 to 25 PSI | Adafruit | 2 | $14.95 | $29.90 |
| USB-C to USB-A Cable (0.5ft) | Cable Creations | 2 | $7.79 | $15.58 |
| USB Battery Pack for Raspberry Pi - 10000mAh - 2 x 5V outputs | Adafruit | 1 | $39.95 | $39.95 |
| Perf Bread Boards | Generic | 2 | $10.05 | $20.10 |
| Base Transceiver (EVK-M91-00) | Mouser Electronics | 1 | $175.00 | $175.00 |
| Quad-band Cellular Duck Antenna SMA | Sparkfun | 2 | $8.95 | $17.90 |
| Rotary Switches | Apogee Components | 3 | $20.15 | $60.45 |
| Zip Ties, 6” Long, Pack of 200 | Amazon | 1 | $8.99 | $8.99 |
| Velcro, Pack of 6 | Amazon | 1 | $9.99 | $9.99 |
| LiPo Guard Bag | Amazon | 2 | $7.90 | $15.80 |
| **Total** | | | | **$880.78** |

Table 56: Fullscale Recovery Budget

| **Item** | **Vendor / Manufacturer** | **QTY** | **Unit Price** | **Total Price** |
|---|---|---|---|---|
| Iris Ultra 120" Standard Parachute | Fruity Chutes | 1 | $475.71 | $475.71 |
| 18" Elliptical Parachute | Fruity Chutes | 1 | $62.89 | $62.89 |
| 15 ft 5/8" 3,200lb Tubular Nylon Shock Cords | Rocketman | 2 | $30.00 | $60.00 |
| 25 ft 5/8" 3,200lb Tubular Nylon Shock Cords | Rocketman | 1 | $45.00 | $45.00 |
| 30 ft 5/8" 3,200lb Tubular Nylon Shock Cords | Rocketman | 1 | $53.00 | $53.00 |
| Nomex Cord Protector | Sirius Rocketry | 3 | $18.95 | $56.85 |
| Main Deployment Bag | Fruity Chutes | 1 | $56.76 | $56.76 |
| Drogue Nomex Blanket | Fruity Chutes | 1 | $17.60 | $17.60 |
| "Dog Barf" Recovery Wadding | Rocketry Works | 1 | $1.99 | $1.99 |
| Ejection Canister | McMaster-Carr | 4 | $1.24 | $4.96 |
| 9V Batteries, 2 pack | Energizer | 1 | $7.19 | $7.19 |
| FFFFg Black Powder | Goex | 1 | $21.50 | $21.50 |
| Gloves for Packing Black Powder and Motor | Amazon | 1 | $9.99 | $9.99 |
| Baby Wipes for Assembling the Motor | Amazon | 1 | $9.97 | $9.97 |
| Baby Powder for Packing Recovery System | Amazon | 1 | $6.19 | $6.19 |
| **Total** | | | | **$889.60** |

Table 57: Subscale Recovery Budget

| Item | Vendor / Manufacturer | QTY | Unit Price | Total Price |
|---|---|---|---|---|
| Iris Ultra 84” Standard Parachute | Fruity Chutes | 1 | $326.66 | $326.66 |
| 12”Compact Elliptical Parachute | Fruity Chutes | 1 | $67.41 | $67.41 |
| 10 ft 5/8” 3,200lb Tubular Nylon Shock Cords | Rocketman | 1 | $25.00 | $50.00 |
| 15 ft 5/8” 3,200lb Tubular Nylon Shock Cords | Rocketman | 1 | $30.00 | $30.00 |
| 25 ft 5/8” 3,200lb Tubular Nylon Shock Cords | Rocketman | 1 | $45.00 | $45.00 |
| 13” Nomex Blanket Cord Protector | Sirius Rocketry | 1 | $17.60 | $17.60 |
| 4” Deployment Bag | Fruity Chutes | 1 | $50.60 | $50.60 |
| ”Dog Barf” Recovery Wadding | Rocketry Works | 1 | $1.99 | $1.99 |
| Ejection Canister | McMaster-Carr | 4 | $1.24 | $4.96 |
| 9V Batteries, 2 pack | Energizer | 1 | $7.19 | $7.19 |
| FFFFg Black Powder | Goex | 1 | $21.50 | $21.50 |
| **Total** | | | | **$622.91** |

Table 58: Fullscale Propulsion Budget

| Item | Vendor / Manufacturer | QTY | Unit Price | Total Price |
|---|---|---|---|---|
| L1390G Motor | Aerotech | 4 | $223.54 | $894.16 |
| Aerotech 75/3840 Complete Motor Hardware | Aerotech | 1 | $503.99 | $503.99 |
| 6” - 75mm Thrust Plate | SC Precision | 1 | $68.30 | $68.30 |
| Aeropack 75mm Retaining Ring | AeroPack | 1 | $75.83 | $75.83 |
| Motor Shipping and Handling | | | | $50.00 |
| **Total** | | | | **$1592.28** |

Table 59: Subscale Propulsion Budget

| **Item** | **Vendor / Manufacturer** | **QTY** | **Unit Price** | **Total Price** |
|---|---|---|---|---|
| K805G-P Motor | Aerotech | 1 | $151.99 | $151.99 |
| 54mm 1706 motor kit (Casing, Forward closure, Aft Closure, Forward Seal disk) | Wildman Rocketry | 1 | $187.99 | $187.99 |
| 4" - 54mm Thrust Plate | SC Precision | 1 | $44.87 | $44.87 |
| Aeropack 54mm Retaining Ring | AeroPack | 1 | $46.66 | $46.66 |
| Motor Shipping and Handling | | | | $50.00 |
| **Total** | | | | **$481.51** |

Table 60: Payload Budget

| Item | Vendor / Manufacturer | QTY | Unit Price | Total Price |
|---|---|---|---|---|
| Raspberry Pi 4B 4GB RAM | RPI Foundation | 1 | $152.98 | $152.98 |
| SanDisk SD 32GB Pack of 2 | SanDisk | 2 | $13.49 | $26.98 |
| TalentCell Rechargeable 12V/5V Pack | TalentCell | 1 | $39.99 | $39.99 |
| DC 5521 Cable Pack of 2 | DTV | 1 | $9.99 | $9.99 |
| Drone Power Distribution Board | KK MWC | 1 | $8.79 | $8.79 |
| Adafruit BMP388 Precision Altimeter | Adafruit | 1 | $9.95 | $9.95 |
| Adafruit RFM96W RF | Adafruit | 1 | $19.95 | $19.95 |
| SMA ANT 6.1mm | Adafruit | 1 | $2.50 | $2.50 |
| Smraza 160 Wide-Angle | Smraza | 1 | $16.99 | $16.99 |
| USB RTL-SDR Dongle | RTL-SDR | 1 | $29.95 | $29.95 |
| SG90 360 Degree Servo Pack of 2 | Jianniu | 1 | $8.99 | $8.99 |
| Adafruit DC Motor Driver Hat | Adafruit | 1 | $22.50 | $22.50 |
| 360* Servo with Angle Feedback | Pollolu | 1 | $27.99 | $27.99 |
| 2.54mm Breakaway PCB Board 40Pin Male and Female Header Connector | Orcity | 1 | $8.99 | $8.99 |
| Dual Band VHF UHF Male SMA Antenna | Bingfu | 1 | $9.99 | $9.99 |
| USB Extension Cord | Amazon | 1 | $2.95 | $2.95 |
| Raspberry Pi Camera (Model G) | RPI Foundation | 1 | $24.99 | $24.99 |
| Infrared Thermometer Temp Gun | Etekcity | 1 | 18.99 | 18.99 |
| Handheld Ham Radio UV-S9 | BaoFeng | 1 | 27.99 | 27.99 |
| BTECH APRS-K1 Cable | BaoFeng | 1 | 22.49 | 22.49 |
| Lazy Susan Turntable 3.75" | DMSTECH | 2 | $5.99 | $11.98 |
| 12V DC Double Shafted Motor | Greartsian | 1 | $29.99 | $29.99 |
| Compact Linear Solenoid | McMaster | 2 | $82.06 | $164.12 |
| 6832K74 Steel Rack | McMaster | 2 | $180.50 | $361.00 |
| 7880K18 Steel Pinion Gear | McMaster | 2 | $17.96 | $35.92 |
| 60355K41 Ball Bearing | McMaster | 2 | $7.09 | $14.18 |
| Shipping and Handling | | | | $40.00 |
| **Total** | | | | **$1111.13** |

Table 61: Manufacturing Budget

| **Item** | **Total Price** |
|---|---|
| Additive Manufacturing | $200.00 |
| Machine Tools | $100.00 |
| **Total Cost** | **$300.00** |

Table 62: STEM Engagement Budget

| **Item** | **Total Price** |
|---|---|
| Printer Paper | $20.00 |
| Gallon Bags | $20.00 |
| Rubber Bands | $5.00 |
| Paperclips | $5.00 |
| Markers | $20.00 |
| Miscellaneous Other Supplies | $20.00 |
| Hand Sanitizer | $10.00 |
| **Total Cost** | **$100.00** |

Table 63: Travel Budget

| **Item** | **Total Price** |
|---|---|
| Hotel | $2500.00 |
| Transportation | $2500.00 |
| **Total Cost** | **$5000.00** |

Table 64: Total Budget

| **System** | **Total Cost** |
|---|---|
| Structures | $1381.72 |
| Avionics | $880.78 |
| Fullscale Recovery | $889.60 |
| Subscale Recovery | $622.91 |
| Fullscale Propulsion | $1592.28 |
| Subscale Propulsion | $481.51 |
| Payload | $1111.13 |
| Manufacturing | $300.00 |
| STEM Engagement | $100.00 |
| Travel Budget | $5000.00 |
| **Total Cost** | **$12359.93** |

### 6.3.2 Funding Plan

The budget in Section 6.3.1 is paid for through several avenues in which WURocketry has been seeking to raise money. The major sources of funding are four different Washington University in St. Louis student group grants, which WURocketry has had to write up proposals and give presentations for in order to win prize money. Two of the grants, the

Engineering Project Review Board Grant (EPRB) and the McKelvey Grant are awarded on a semester basis, requiring the team to put together two proposals and presentations for each presentation each school year. The EPRB grant is required to be used on a specific set of materials that are indicateed during the grant presentations. This year, EPRB money has and will be used for the development of the payload as well as many structural components like the air frame and nose cone. The McKelvey grant provides more flexibility in spending, and was therefore used for materials not budgeted for in the EPRB and some transportation costs. In the fall semester, the team received $1775 and $2000 from the EPRB and McKelvey grant, respectively. The team has recently been awarded $1500 and $1850 for the EPRB and the McKelvey grant, respectively, for the spring semester. In addition to the aforementioned engineering school grants, the team was awarded $2375 from the Washington University in St. Louis Student Union. This money may be spent over the course of the school year and is required to be spent on a line-item budget that is proposed the previous year, thereby allowing very little flexibility in how it can be spent. The items that this grant covers include remaining structural components for both the sub-scale and full-scale rocket that were not purchased using the EPRB grant money, all avionics components for the sub-scale rocket and the full-scale rocket, and recovery & propulsion materials including parachutes, hardware, deployment bags, and shock cords. On top of these grants, WURocketry has been awarded a $1400 transportation grant through Washington University in St. Louis that is meant to cover a portion of the costs associated with traveling to Huntsville for the competition in April. The team has developed a sponsorship brochure that has recently been approved by the school that will serve to market WURocketry to businesses in the St. Louis region and beyond in order to develop relationships that might turn into sponsorships down the road. The goal is to eventually phase out the need for school-related grants so that the team can operate completely on outside investment money. The school has indicated that there are leads with Milwaukee Tools and Relativity Space that could prove to help the sponsorship efforts.

All materials that have been purchased or will be purchased have been ordered online and delivered to the engineering office at Washington University in St. Louis. These materials typically come within a week, and the vendors that are being used (see Section 6.3.1) have been reliable in their shipments and deliveries. For materials like motors and black powder, the team mentor, Mike Walsh, who has the proper certification for purchase, will complete the orders and store the materials until they are needed to be used during a launch. Using these processes, the team has found it comfortable to acquire everything that is needed for successful construction of the subscale rocket.

## 6.4 Timeline

WURocketry's timeline for the 2022-2023 competition year is split up into five milestones/phases: the proposal phase, preliminary design review phase, critical design review phase, flight readiness review phase, and competition phase. In each of these phases, all necessary tasks were compiled and assigned to a subteam. The leaders of each subteam then assigned individual tasks to subteam members. The tasks and Gantt charts for each milestone were made in Microsoft Project and are shown in Figs. 125, 126, 127, 128. and 129.

The focus for the proposal phase was to absorb the information presented in the USLI Competition Handbook, devise a plan for the rocket and team, and begin research for design considerations. Another large focus in this phase was social media presence and recruitment, as shown in the tasks and Gantt chart for the first month of the competition year.

| Task Mode | Task Name | Duration | Start | Finish |
|---|---|---|---|---|
| | **Proposal Phase** | **24 days** | **Wed 8/17/22** | **Mon 9/19/22** |
| | Request for Proposal (RFP) Released | 1 day | Wed 8/17/22 | Wed 8/17/22 |
| | Team Kickoff Meeting | 1 day | Sun 9/11/22 | Sun 9/11/22 |
| | Recovery & Propulsion, Structures, and Avionics Research and Preliminary Design Development | 14 days | Sun 9/11/22 | Wed 9/28/22 |
| | Payload: Research and Design Development | 14 days | Wed 8/24/22 | Mon 9/12/22 |
| | Safety: Develop Safety Section of Proposal | 17 days | Sun 8/21/22 | Mon 9/12/22 |
| | STEM Engagement: Develop New Activities for Students | 21 days | Sun 9/4/22 | Fri 9/30/22 |
| | Social Media: Recruitment-Focused Social Media Posts | 30 days | Sun 8/21/22 | Thu 9/29/22 |
| | STEM Engagement: Contact Local Schools | 35 days | Sun 9/18/22 | Thu 11/3/22 |
| | Business/Funding: Request for Funds/Sponsorships | 47 days | Sun 8/21/22 | Mon 10/24/22 |
| | Recruitment: Engineering Student Group Activities Fair | 0.2 days | Mon 8/29/22 | Mon 8/29/22 |
| | Recovery & Propulsion, Structures, and Avionics Detailed Design Development | 7 days | Sun 9/11/22 | Sun 9/18/22 |
| | Develop CAD Model of Subscale and Full-Scale Rockets | 7 days | Sun 9/11/22 | Sun 9/18/22 |
| | Recruitment: Student Union Student Group In-Person Activities Fair | 1 day | Fri 9/2/22 | Fri 9/2/22 |
| | Recovery & Propulsion, Structures, and Avionics Develop Technical Design Portion of Proposal | 5 days | Sun 9/11/22 | Thu 9/15/22 |
| | Payload: Choose Design and Complete Design Validation with Chief Engineer | 1 day | Sun 9/4/22 | Sun 9/4/22 |
| | Payload: Develop Payload Technical Design Portion of Proposal | 5 days | Sun 9/4/22 | Thu 9/8/22 |
| | Recovery & Propulsion, Structures, and Avionics Bill of Materials Due | 1 day | Sun 9/11/22 | Sun 9/11/22 |
| | Proposal Rough Draft Due | 1 day | Mon 9/12/22 | Mon 9/12/22 |
| | Edit, Compile, and Proofread Proposal | 7 days | Sun 9/11/22 | Sun 9/18/22 |
| | Build Sub-Scale Rocket | 14 days | Sun 10/2/22 | Wed 10/19/22 |
| | Payload: Create Detailed Design | 22 days | Sun 9/18/22 | Mon 10/17/22 |
| | Submit Proposal | 0.2 days | Fri 9/16/22 | Fri 9/16/22 |
| | Recovery & Propulsion, Structures, and Avionics Design Refinement | 7 days | Mon 9/19/22 | Tue 9/27/22 |
| | Proposal Due at 8am CDT | 1 day | Tue 9/20/22 | Tue 9/20/22 |
| | Recovery & Propulsion, Structures, and Avionics Updated Bill of Materials Due | 1 day | Tue 9/27/22 | Tue 9/27/22 |

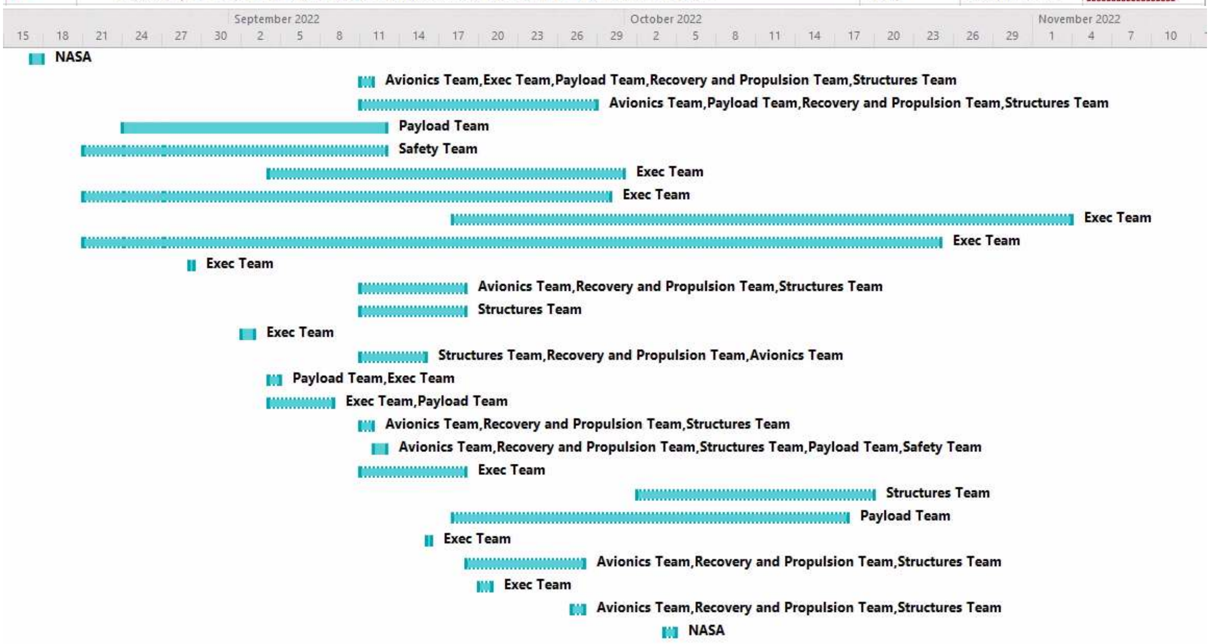


Figure 125: WURocketry Proposal Timeline for the 2022-2023 Competition Year

The focus for the preliminary design review phase was to develop the design considerations and continue to do research into the best alternatives. Sub-teams made their first prototypes and started refining the ideas and designs based on preliminary results. The main focus of the structures sub-team was building the sub-scale rocket, paying special attention to detail to ensure a successful launch.

| Task Mode | Task Name | Duration | Start | Finish |
|---|---|---|---|---|
| | PDR Phase | 34 days | Wed 10/5/22 | Mon 11/21/22 |
| | Social Media: Update Social Media Weekly | 172 days | Wed 10/5/22 | Thu 6/1/23 |
| | Social Media: Update Website as Needed for Documentation | 172 days | Wed 10/5/22 | Thu 6/1/23 |
| | Recovery & Propulsion, Structures, and Avionics Testing | 4 days | Wed 10/5/22 | Sun 10/9/22 |
| | Payload: Complete CAD and Bill of Materials | 11 days | Wed 10/5/22 | Wed 10/19/22 |
| | Recovery & Propulsion, Structures, and Avionics PDR Vehicle Section | 17 days | Wed 10/5/22 | Thu 10/27/22 |
| | PDR Q&A | 1 day | Thu 10/6/22 | Thu 10/6/22 |
| | Build Full-Scale Rocket | 7 days | Sat 10/8/22 | Sat 10/15/22 |
| | Payload: Complete Payload Section of PDR | 14 days | Sat 10/8/22 | Wed 10/26/22 |
| | STEM Engagement: Francis Howell North Engineering Students | 1 day | Sat 10/15/22 | Sat 10/15/22 |
| | Payload: Manufacture Prototype | 7 days | Sat 10/15/22 | Sat 10/22/22 |
| | Social Media Handle List sent to project office by 8am CDT | 1 day | Fri 10/21/22 | Fri 10/21/22 |
| | PDR Rough Draft Due | 1 day | Sat 10/22/22 | Sat 10/22/22 |
| | Payload: Test Prototype | 14 days | Sat 10/22/22 | Wed 11/9/22 |
| | Payload: Refine Design Based on Protoype Test Results | 17 days | Tue 10/25/22 | Wed 11/16/22 |
| | PDR Report, Presentation Slides, and Flysheet Due by 8am CDT | 1 day | Wed 10/26/22 | Wed 10/26/22 |
| | PDR Teleconferences | 20 days | Tue 11/1/22 | Mon 11/28/22 |
| | STEM Engagement: North Kirkwood Middle School Engineering Students | 1 day | Sat 11/5/22 | Sat 11/5/22 |
| | Payload: Build Refined Payload | 5 days | Tue 11/8/22 | Sun 11/13/22 |
| | Fly Sub-Scale Rocket | 1 day | Sun 11/13/22 | Sun 11/13/22 |
| | Payload: Validate Refined Payload | 5 days | Sun 11/13/22 | Thu 11/17/22 |
| | STEM Engagement: Brittany Woods Middle School | 0.5 days | Tue 11/15/22 | Tue 11/15/22 |
| | Payload Demonstration Flight: Fly Full-Scale Rocket with Payload | 1 day | Sun 11/20/22 | Sun 11/20/22 |

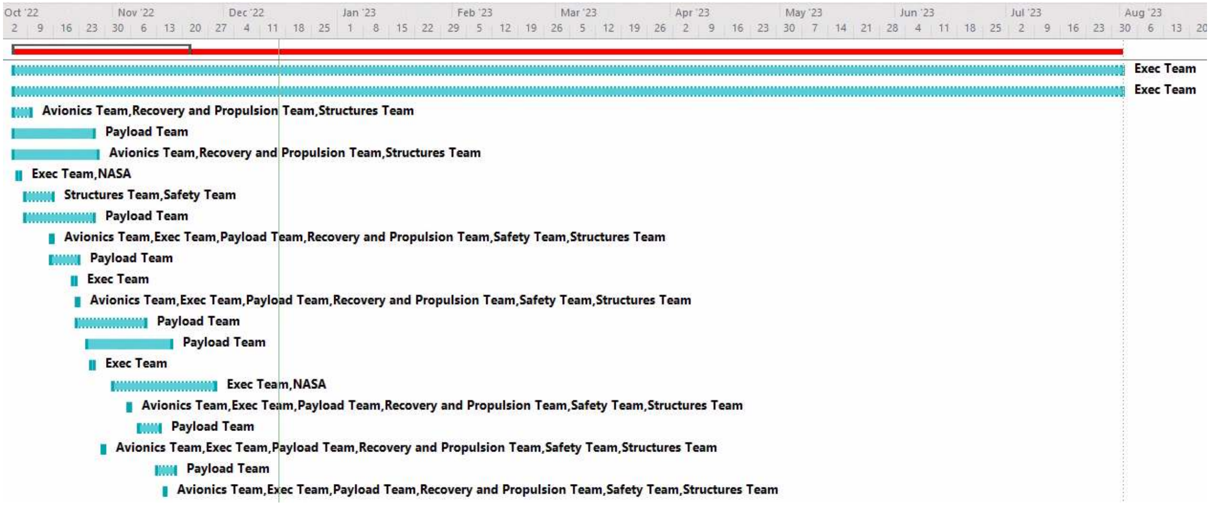


Figure 126: WURocketry Preliminary Design Review Timeline for the 2022-2023 Competition Year

The focus for the critical design review phase was to continue to refine the design of the rocket and payload. In this phase, the sub-scale rocket had already successfully launched, so the focus shifted to building the full-scale rocket and learning from the experiences and shortcomings of the sub-scale launch. For all sub-teams, there was also a shift to testing the final design choices. All tests were compiled and prepared for physical testing. If the tests could be completed in this phase utilizing 3D printing, those tests were performed, analyzed, and a report was written detailing the results and lessons learned.

| Task Mode | Task Name | Duration | Start | Finish |
|---|---|---|---|---|
| | **CDR Phase** | **58 days** | **Wed 11/30/22** | **Fri 2/17/23** |
| | CDR Q&A | 0.5 days | Thu 12/1/22 | Thu 12/1/22 |
| | Recovery & Propulsion, Structures, and Avionics Write Vehicle and Recovery Design Portions of CDR and CDR Presentation Slides | 14 days | Wed 11/30/22 | Mon 12/19/22 |
| | Payload: Write Payload Design Portion of CDR and CDR Presentation Slides | 14 days | Wed 11/30/22 | Mon 12/19/22 |
| | CDR Rough Draft Due | 1 day | Mon 12/12/22 | Mon 12/12/22 |
| | Fly Full-Scale Rocket | 1 day | Sun 11/13/22 | Sun 11/13/22 |
| | Subscale Flight Deadline | 1 day | Mon 1/9/23 | Mon 1/9/23 |
| | CDR Report, Presentation Slides, and Flysheet due by 8am CST | 0.5 days | Mon 1/9/23 | Mon 1/9/23 |
| | CDR Teleconferences | 18 days | Fri 1/13/23 | Tue 2/7/23 |

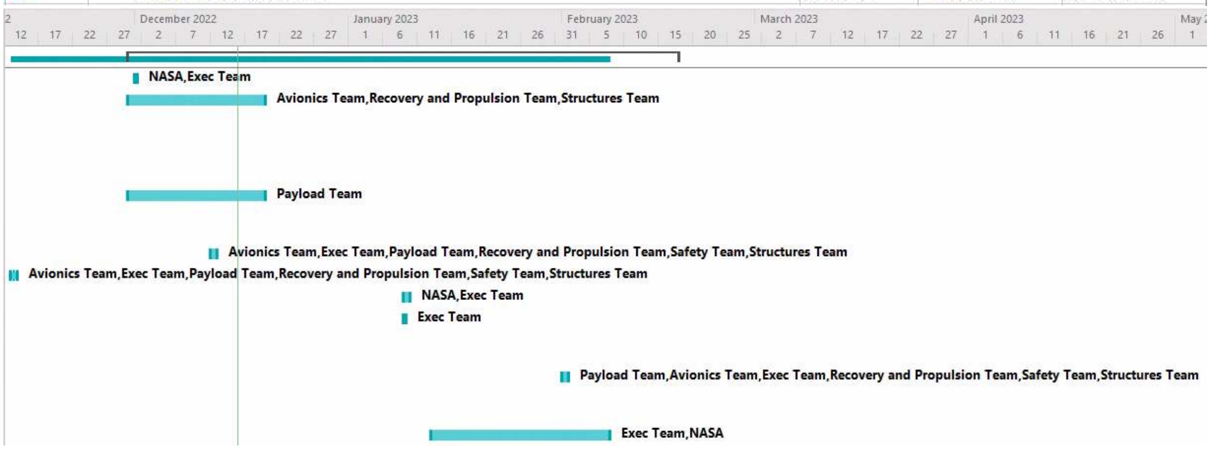


Figure 127: WURocketry Critical Design Review Timeline for the 2022-2023 Competition Year

In the flight readiness review phase, the focus will again be mostly on testing and demonstrations. The full-scale rocket will be flown both with a simulated payload and the actual payload to prepare for the competition phase. In addition, the payload team will begin construction of the payload using the final design choices made in the CDR phase. Once the payload has been constructed, more tests and demonstrations will be performed to ensure viability of the design and concepts before the payload is launched with the rocket.

| Task Mode | Task Name | Duration | Start | Finish |
|---|---|---|---|---|
| | **FRR Phase** | **46 days** | **Fri 1/27/23** | **Fri 3/31/23** |
| | FRR Q&A | 0.5 days | Thu 2/9/23 | Thu 2/9/23 |
| | Recovery & Propulsion, Structures, and Avionics Write Vehicle and Recovery Design Portions of FRR and FRR Presentation Slides | 18 days | Fri 1/27/23 | Tue 2/21/23 |
| | Payload: Write Payload Design Portion of FRR and FRR Presentation Slides | 18 days | Fri 1/27/23 | Tue 2/21/23 |
| | STEM Engagement: Girl Scouts of Eastern Missouri Rocket Team | 0.5 days | Sat 2/4/23 | Sat 2/4/23 |
| | FRR Rough Draft Due | 1 day | Tue 2/14/23 | Tue 2/14/23 |
| | Fly Full-Scale Rocket (Vehicle Demonstraton Try #2) | 1 day | Sun 2/26/23 | Sun 2/26/23 |
| | STEM Engagement: UCity Kindergarteners: Jackson Park Elementary | 1 day | Sat 3/4/23 | Sat 3/4/23 |
| | STEM Engagement: UCity Kindergarteners: Flynn Park Elementary | 1 day | Sat 3/4/23 | Sat 3/4/23 |
| | STEM Engagement: Girl Scouts of Eastern Missouri Rocket Team | 1 day | Mon 3/6/23 | Mon 3/6/23 |
| | Vehicle Demonstration Flight Deadline | 0.5 days | Mon 3/6/23 | Mon 3/6/23 |
| | FRR Report, Presentation Slides, and Flysheet due by 8am CST | 0.5 days | Mon 3/6/23 | Mon 3/6/23 |
| | FRR Teleconferences | 18 days | Mon 3/13/23 | Wed 4/5/23 |
| | Payload Demonstration Flight and Vehicle Re-flight (Back-up Date: March 26, 2022) | 1 day | Sun 3/19/23 | Sun 3/19/23 |
| | Payload Demonstration Flight and Vehicle Re-flight deadline | 0.5 days | Mon 4/3/23 | Mon 4/3/23 |
| | FRR Addendum due by 8am CST | 0.5 days | Mon 4/3/23 | Mon 4/3/23 |

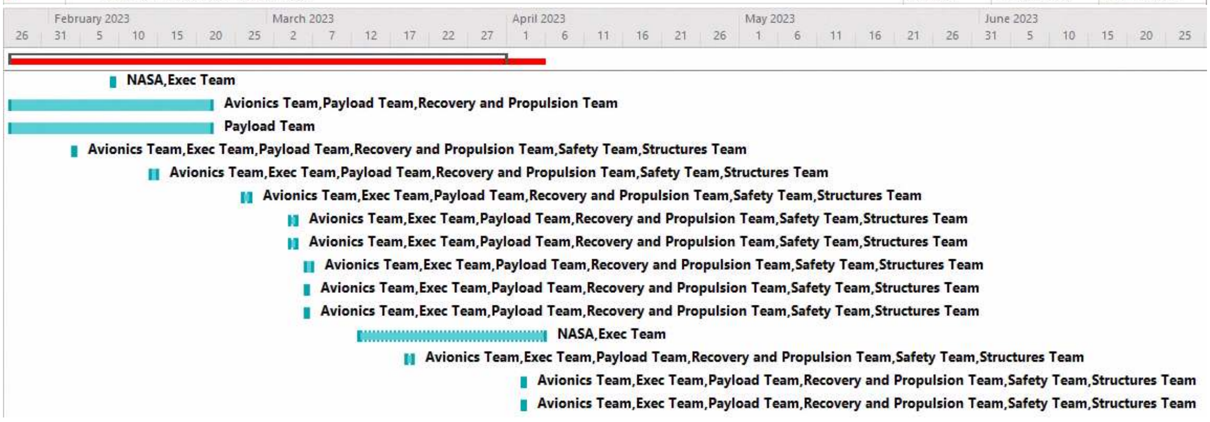


Figure 128: WURocketry Flight Readiness Review Timeline for the 2022-2023 Competition Year

The competition phase will mostly focus on traveling to Huntsville to launch with the other USLI Competition teams. This consists of final hardware checks, code pushes, and the final competition launch. This phase also entails the Post Launch Assessment Report, in which teams will analyze how the rocket and payload performed on launch day.

| Task Mode | Task Name | Duration | Start | Finish |
|---|---|---|---|---|
| | **Competition Phase** | **22 days** | **Sat 4/1/23** | **Mon 5/1/23** |
| | Launch Week Q&A | 0.6 days | Thu 4/6/23 | Thu 4/6/23 |
| | Teams travel to Huntsville, AL | 1 day | Wed 4/12/23 | Wed 4/12/23 |
| | Hardware Checks in Huntsville, AL | 1 day | Thu 4/13/23 | Thu 4/13/23 |
| | Launch Day and Awards Ceremony | 0.75 days | Sat 4/15/23 | Sat 4/15/23 |
| | Backup launch day | 0.75 days | Sun 4/16/23 | Sun 4/16/23 |
| | Post-Launch Assessment Review (PLAR) submitted to NASA project management team by 8:00 a.m. CDT. | 1 day | Mon 5/1/23 | Mon 5/1/23 |

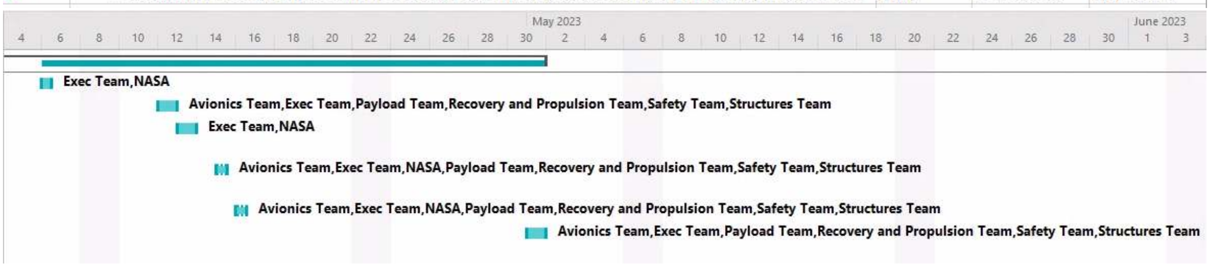


Figure 129: WURocketry Competition Timeline for the 2022-2023 Competition Year

The status of WURocketry's progress throughout the year is being tracked by pivot charts to ensure the project is staying on time and progressing as expected. The overall status of the project is shown in Fig. 130.

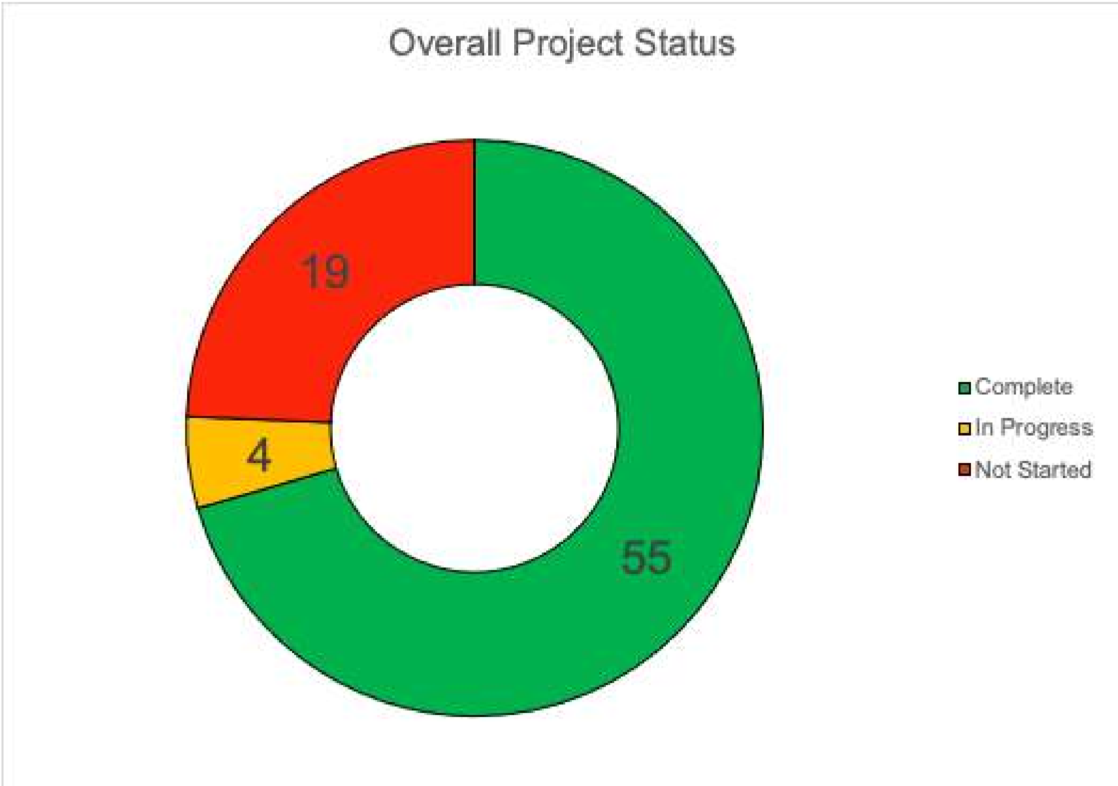


Figure 130: High-Level Status of WURocketry's 2022-2023 Competition Year Tasks.

This status can also be broken down by phase to determine where most of the work still lies. This is shown in Fig. 131.

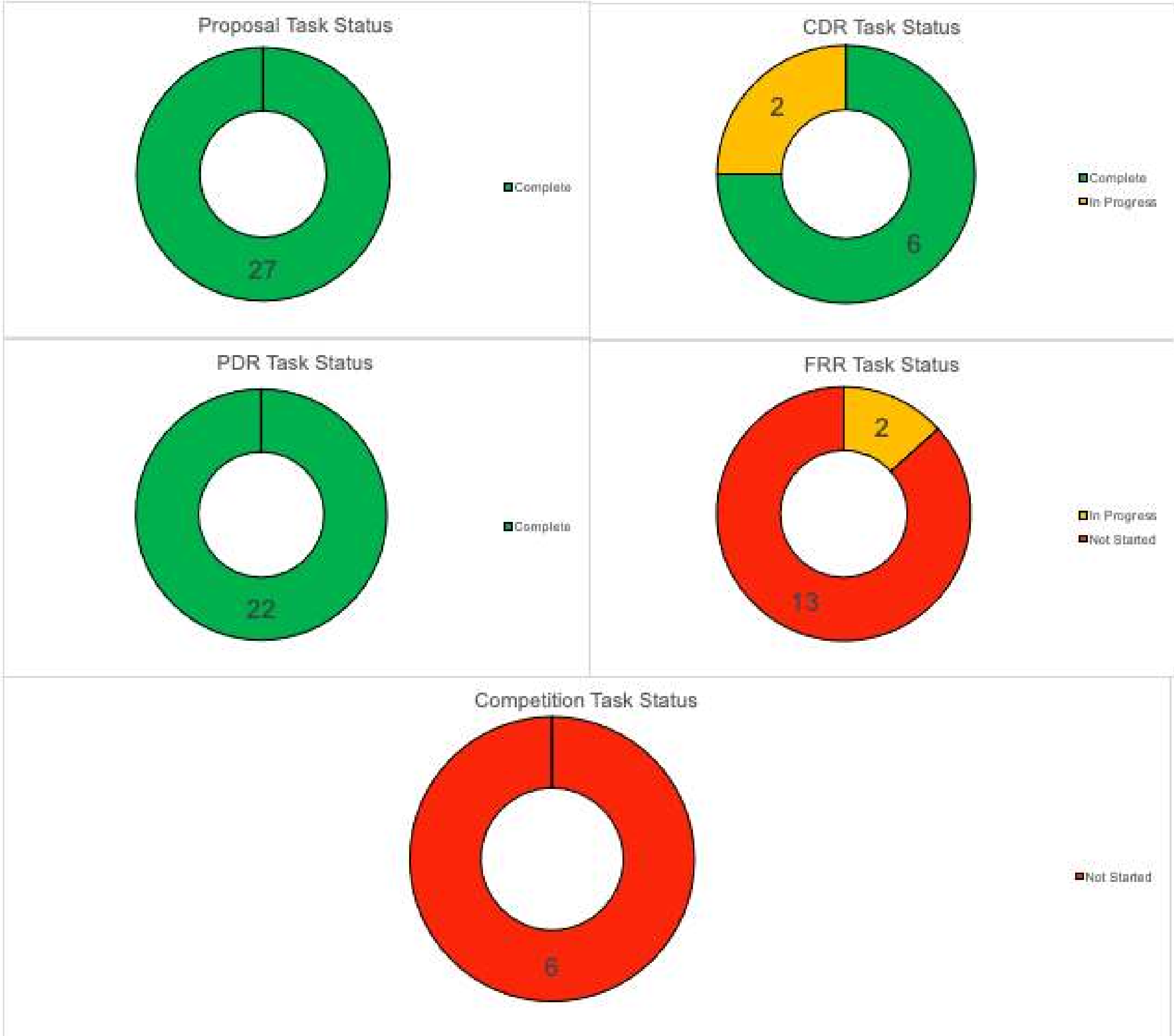


Figure 131: Status of each phase in WURocketry's 2022-2023 competition year.

It can be noted that there are still two items in the CDR Task Status chart that are "In Progress." These include the submission of the final CDR package and the CDR presentation. Both of these items are still expected to be completed on time.

Figure 130 shows that WURocketry is about halfway through the tasks associated with this competition year and Fig. 131 shows that most of these tasks are associated with future phases of the project. This leads the team to believe that the project is on schedule, will progress as expected, and will be ready to present at the final competition.

# 7 Appendix

## 7.1 Subscale Flight Raw Data

| #version | serial | flight | time | state | state_name | acceleration | pressure | altitude | height | speed | temperature | drogue_volta | main_voltage | battery_voltage |
|---|---|---|---|---|---|---|---|---|---|---|---|---|---|---|
| 6 | 8106 | 1 | -0.14 | 3 | boost | 38.95 | 99945 | 115.51 | 23.12 | 54.69 | 29.3 | 4.21 | 4.17 | 4.17 |
| 6 | 8106 | 1 | -0.13 | 3 | boost | 40.98 | 99938 | 116.1 | 23.71 | 55.48 | 29.3 | 4.21 | 4.17 | 4.17 |
| 6 | 8106 | 1 | -0.12 | 3 | boost | 43.08 | 99928 | 116.94 | 24.55 | 56.28 | 29.3 | 4.21 | 4.17 | 4.17 |
| 6 | 8106 | 1 | -0.11 | 3 | boost | 45.24 | 99919 | 117.7 | 25.31 | 57.08 | 29.3 | 4.21 | 4.17 | 4.17 |
| 6 | 8106 | 1 | -0.1 | 3 | boost | 47.47 | 99918 | 117.79 | 25.39 | 57.9 | 29.3 | 4.21 | 4.17 | 4.18 |
| 6 | 8106 | 1 | -0.09 | 3 | boost | 49.77 | 99898 | 119.47 | 27.08 | 58.72 | 29.3 | 4.21 | 4.17 | 4.18 |
| 6 | 8106 | 1 | -0.08 | 3 | boost | 52.12 | 99891 | 120.06 | 27.67 | 59.55 | 29.3 | 4.21 | 4.17 | 4.17 |
| 6 | 8106 | 1 | -0.07 | 3 | boost | 54.52 | 99873 | 121.58 | 29.18 | 60.4 | 29.3 | 4.21 | 4.18 | 4.18 |
| 6 | 8106 | 1 | -0.06 | 3 | boost | 56.96 | 99865 | 122.25 | 29.86 | 61.24 | 29.3 | 4.2 | 4.2 | 4.18 |
| 6 | 8106 | 1 | -0.05 | 3 | boost | 59.45 | 99869 | 121.91 | 29.52 | 62.1 | 29.3 | 4.21 | 4.17 | 4.18 |
| 6 | 8106 | 1 | -0.04 | 3 | boost | 61.95 | 99839 | 124.44 | 32.05 | 62.97 | 29.3 | 4.21 | 4.17 | 4.2 |
| 6 | 8106 | 1 | -0.03 | 3 | boost | 64.48 | 99832 | 125.03 | 32.64 | 63.84 | 29.3 | 4.18 | 4.18 | 4.17 |
| 6 | 8106 | 1 | -0.02 | 3 | boost | 67.02 | 99830 | 125.2 | 32.81 | 64.72 | 29.3 | 4.21 | 4.17 | 4.18 |
| 6 | 8106 | 1 | -0.01 | 3 | boost | 69.55 | 99817 | 126.29 | 33.9 | 65.61 | 29.3 | 4.21 | 4.17 | 4.18 |
| 6 | 8106 | 1 | 0 | 3 | boost | 72.06 | 99800 | 127.72 | 35.33 | 66.51 | 29.3 | 4.21 | 4.17 | 4.18 |
| 6 | 8106 | 1 | 0 | 3 | boost | 72.06 | 99800 | 127.72 | 35.33 | 66.51 | 29.3 | 4.21 | 4.17 | 4.18 |
| 6 | 8106 | 1 | 0 | 3 | boost | 72.06 | 99800 | 127.72 | 35.33 | 66.51 | 29.3 | 4.21 | 4.17 | 4.18 |
| 6 | 8106 | 1 | 0 | 3 | boost | 72.06 | 99800 | 127.72 | 35.33 | 66.51 | 29.3 | 4.21 | 4.17 | 4.18 |
| 6 | 8106 | 1 | 0 | 3 | boost | 72.06 | 99800 | 127.72 | 35.33 | 66.51 | 29.3 | 4.21 | 4.17 | 4.18 |
| 6 | 8106 | 1 | 0 | 3 | boost | 72.06 | 99800 | 127.72 | 35.33 | 66.51 | 29.3 | 4.21 | 4.17 | 4.18 |
| 6 | 8106 | 1 | 0 | 3 | boost | 72.06 | 99800 | 127.72 | 35.33 | 66.51 | 29.3 | 4.21 | 4.17 | 4.18 |
| 6 | 8106 | 1 | 0 | 3 | boost | 72.06 | 99800 | 127.72 | 35.33 | 66.51 | 29.3 | 4.21 | 4.17 | 4.18 |
| 6 | 8106 | 1 | 0 | 3 | boost | 72.06 | 99800 | 127.72 | 35.33 | 66.51 | 29.3 | 4.21 | 4.17 | 4.18 |
| 6 | 8106 | 1 | 0 | 3 | boost | 72.06 | 99800 | 127.72 | 35.33 | 66.51 | 29.3 | 4.21 | 4.17 | 4.18 |
| 6 | 8106 | 1 | 0 | 3 | boost | 72.06 | 99800 | 127.72 | 35.33 | 66.51 | 29.3 | 4.21 | 4.17 | 4.18 |
| 6 | 8106 | 1 | 0 | 3 | boost | 72.06 | 99800 | 127.72 | 35.33 | 66.51 | 29.3 | 4.21 | 4.17 | 4.18 |
| 6 | 8106 | 1 | 0 | 3 | boost | 72.06 | 99800 | 127.72 | 35.33 | 66.51 | 29.3 | 4.21 | 4.17 | 4.18 |
| 6 | 8106 | 1 | 0 | 3 | boost | 72.06 | 99800 | 127.72 | 35.33 | 66.51 | 29.3 | 4.21 | 4.17 | 4.18 |
| 6 | 8106 | 1 | 0 | 3 | boost | 72.06 | 99800 | 127.72 | 35.33 | 66.51 | 29.3 | 4.21 | 4.17 | 4.18 |

Figure 132: Primary EasyMini Flight Data

Figure 132 above is a 30 line preview of the full primary flight data file that can be accessed at the following link: Primary Flight Data

| #version | serial | flight | time | state | state_name | acceleration | pressure | altitude | height | speed | temperature | drogue_volta | main_voltage | battery_voltage |
|---|---|---|---|---|---|---|---|---|---|---|---|---|---|---|
| 6 | 8109 | 1 | -0.14 | 3 | boost | 38.69 | 99849 | 123.6 | 23.22 | 54 | 29.2 | 4.12 | 4.12 | 4.12 |
| 6 | 8109 | 1 | -0.13 | 3 | boost | 40.71 | 99845 | 123.93 | 23.56 | 54.78 | 29.2 | 4.12 | 4.11 | 4.12 |
| 6 | 8109 | 1 | -0.12 | 3 | boost | 42.79 | 99827 | 125.45 | 25.08 | 55.57 | 29.2 | 4.12 | 4.11 | 4.12 |
| 6 | 8109 | 1 | -0.11 | 3 | boost | 44.95 | 99817 | 126.29 | 25.92 | 56.37 | 29.2 | 4.12 | 4.12 | 4.12 |
| 6 | 8109 | 1 | -0.1 | 3 | boost | 47.17 | 99820 | 126.04 | 25.67 | 57.18 | 29.2 | 4.12 | 4.12 | 4.12 |
| 6 | 8109 | 1 | -0.09 | 3 | boost | 49.45 | 99813 | 126.63 | 26.26 | 57.99 | 29.2 | 4.12 | 4.11 | 4.12 |
| 6 | 8109 | 1 | -0.08 | 3 | boost | 51.79 | 99799 | 127.81 | 27.44 | 58.82 | 29.2 | 4.12 | 4.11 | 4.12 |
| 6 | 8109 | 1 | -0.07 | 3 | boost | 54.18 | 99789 | 128.65 | 28.28 | 59.65 | 29.2 | 4.12 | 4.11 | 4.12 |
| 6 | 8109 | 1 | -0.06 | 3 | boost | 56.61 | 99774 | 129.92 | 29.54 | 60.5 | 29.2 | 4.12 | 4.11 | 4.12 |
| 6 | 8109 | 1 | -0.05 | 3 | boost | 59.08 | 99763 | 130.84 | 30.47 | 61.35 | 29.2 | 4.12 | 4.11 | 4.12 |
| 6 | 8109 | 1 | -0.04 | 3 | boost | 61.58 | 99761 | 131.01 | 30.64 | 62.2 | 29.2 | 4.11 | 4.15 | 4.12 |
| 6 | 8109 | 1 | -0.03 | 3 | boost | 64.1 | 99750 | 131.94 | 31.57 | 63.07 | 29.2 | 4.12 | 4.12 | 4.12 |
| 6 | 8109 | 1 | -0.02 | 3 | boost | 66.62 | 99734 | 133.29 | 32.92 | 63.95 | 29.2 | 4.12 | 4.11 | 4.12 |
| 6 | 8109 | 1 | -0.01 | 3 | boost | 69.15 | 99725 | 134.05 | 33.67 | 64.83 | 29.2 | 4.12 | 4.12 | 4.12 |
| 6 | 8109 | 1 | 0 | 3 | boost | 71.65 | 99712 | 135.14 | 34.77 | 65.72 | 29.2 | 4.12 | 4.11 | 4.12 |
| 6 | 8109 | 1 | 0 | 3 | boost | 71.65 | 99712 | 135.14 | 34.77 | 65.72 | 29.2 | 4.12 | 4.11 | 4.12 |
| 6 | 8109 | 1 | 0 | 3 | boost | 71.65 | 99712 | 135.14 | 34.77 | 65.72 | 29.2 | 4.12 | 4.11 | 4.12 |
| 6 | 8109 | 1 | 0 | 3 | boost | 71.65 | 99712 | 135.14 | 34.77 | 65.72 | 29.2 | 4.12 | 4.11 | 4.12 |
| 6 | 8109 | 1 | 0 | 3 | boost | 71.65 | 99712 | 135.14 | 34.77 | 65.72 | 29.2 | 4.12 | 4.11 | 4.12 |
| 6 | 8109 | 1 | 0 | 3 | boost | 71.65 | 99712 | 135.14 | 34.77 | 65.72 | 29.2 | 4.12 | 4.11 | 4.12 |
| 6 | 8109 | 1 | 0 | 3 | boost | 71.65 | 99712 | 135.14 | 34.77 | 65.72 | 29.2 | 4.12 | 4.11 | 4.12 |
| 6 | 8109 | 1 | 0 | 3 | boost | 71.65 | 99712 | 135.14 | 34.77 | 65.72 | 29.2 | 4.12 | 4.11 | 4.12 |
| 6 | 8109 | 1 | 0 | 3 | boost | 71.65 | 99712 | 135.14 | 34.77 | 65.72 | 29.2 | 4.12 | 4.11 | 4.12 |
| 6 | 8109 | 1 | 0 | 3 | boost | 71.65 | 99712 | 135.14 | 34.77 | 65.72 | 29.2 | 4.12 | 4.11 | 4.12 |
| 6 | 8109 | 1 | 0 | 3 | boost | 71.65 | 99712 | 135.14 | 34.77 | 65.72 | 29.2 | 4.12 | 4.11 | 4.12 |
| 6 | 8109 | 1 | 0 | 3 | boost | 71.65 | 99712 | 135.14 | 34.77 | 65.72 | 29.2 | 4.12 | 4.11 | 4.12 |
| 6 | 8109 | 1 | 0 | 3 | boost | 71.65 | 99712 | 135.14 | 34.77 | 65.72 | 29.2 | 4.12 | 4.11 | 4.12 |
| 6 | 8109 | 1 | 0 | 3 | boost | 71.65 | 99712 | 135.14 | 34.77 | 65.72 | 29.2 | 4.12 | 4.11 | 4.12 |
| 6 | 8109 | 1 | 0 | 3 | boost | 71.65 | 99712 | 135.14 | 34.77 | 65.72 | 29.2 | 4.12 | 4.11 | 4.12 |

Figure 133: Redundant EasyMini Flight Data

Figure 133 above is a 30 line preview of the full redundant flight data file accessible at the following link: Redundant Flight Data

## 7.2 Structures Testing Raw Data

### 7.2.1 Snatch Force Test

The figures below are the raw data from the Instron tensile testing machine.

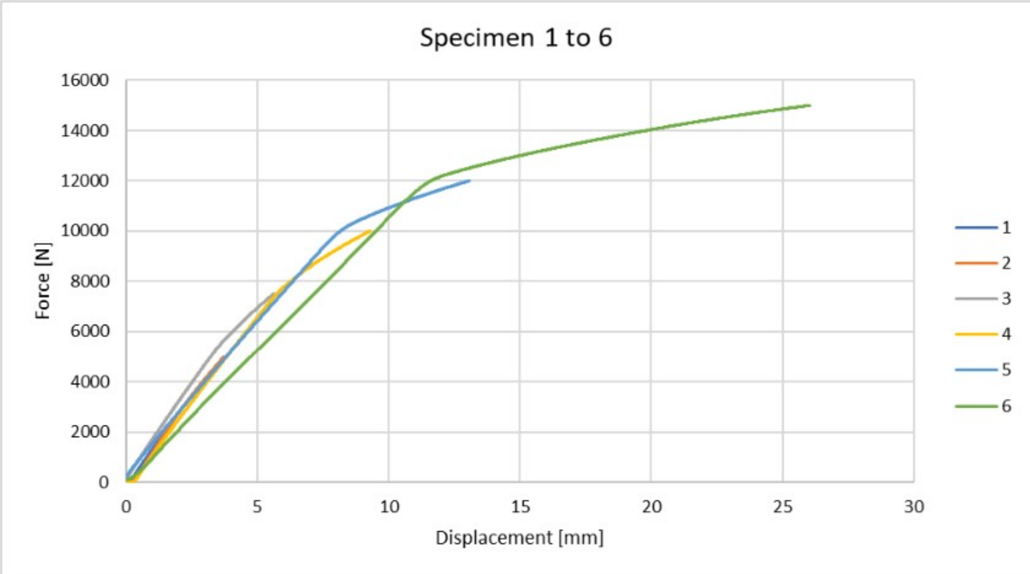


| | Specimen Name | Rate [mm/min] |
|---|---|---|
| 1 | Delrin 2.5kN | 2.00 |
| 2 | Delrin 5.0kN | 2.00 |
| 3 | Delrin 7.5kN | 2.00 |
| 4 | Delrin 10kN | 2.00 |
| 5 | Delrin 12.5kN | 2.00 |
| 6 | Delrin 15kN | 2.00 |

| | Maximum Load [N] | Extension at Maximum Load [mm] | Modulus (Modulus of Elasticity) [mPa] |
|---|---|---|---|
| 1 | 2500.02 | 1.79 | 603.15 |
| 2 | 5000.02 | 3.71 | 643.25 |
| 3 | 7500.02 | 5.61 | 630.97 |
| 4 | 10000.00 | 9.29 | 585.70 |
| 5 | 12001.73 | 13.07 | 503.88 |
| 6 | 15000.01 | 26.06 | 438.22 |

Figure 134: Snatch Force Tensile Test Raw Data

### 7.2.2 Fin Material Test

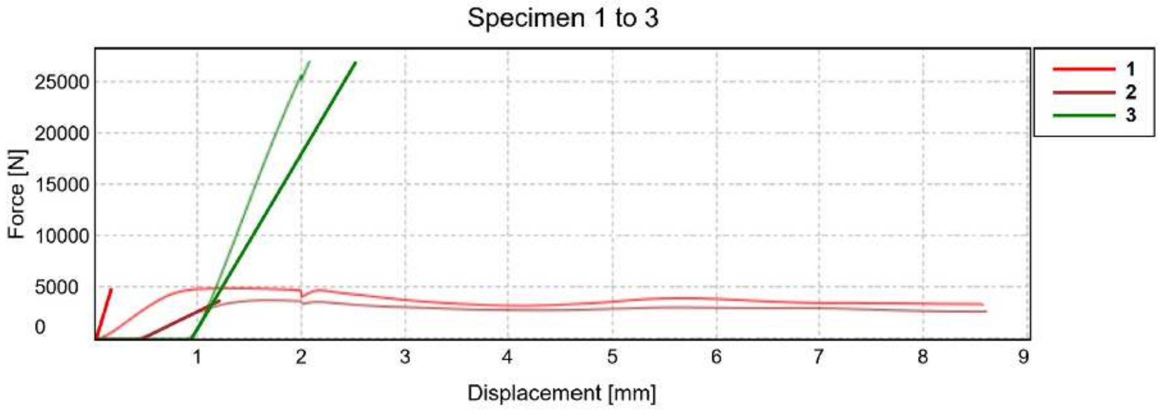


| | Specimen number (included) | Specimen label | Rate 1 [mm/min] |
|---|---|---|---|
| 1 | 1 | PLA | 1.00 |
| 2 | 2 | PETG | 1.00 |
| 3 | 3 | Resin | 1.00 |

| | Diameter [mm] | Height [mm] | Maximum Force [kN] |
|---|---|---|---|
| 1 | 25.24 | 25.60 | 4.92 |
| 2 | 25.24 | 25.60 | 3.75 |
| 3 | 25.23 | 25.11 | 27.00 |

| | Force at Yield (Zero slope) [kN] | Modulus (Young's Compressive stress 0.8 mm - 1 mm) [MPa] |
|---|---|---|
| 1 | 4.92 | 381.40 |
| 2 | 3.75 | 253.81 |
| 3 | ----- | 853.32 |

Figure 135: Fin Material Test Raw Data

The following are data collected from the Payload rotating track test.

| Test Number | Initial Position (deg) | Final Position (deg) |
|---|---|---|
| Test 1 (27 g top, 26 g bottom) | 90 | 90 |
| | 45 | 70 |
| | 180 | 180 |
| | Spin | 80 |
| | Spin | 80 |
| Test 2 (53 g top, 376 g bottom) | 90 | 0 |
| | 45 | 0 |
| | 180 | 0 |
| | Spin | 0 |
| | Spin | 0 |
| Test 3 (242 g top, 376 g bottom) | 90 | 0 |
| | 45 | 0 |
| | 180 | 180 |
| | Spin | 0 |
| | Spin | 0 |
| Test 4 (182 g, 376 g bottom) | 90 | - 70 |
| | 45 | - 70 |
| | 180 | - 70 |
| | Spin | - 70 |
| | Spin | - 70 |

Figure 136: Raw rotating track observation data of orientations given various weight distributions (grams versus degrees)

The following are data collected from the Payload avionic sensor demonstrations.

| Reading | Pressure (hPa) | Altitude (m) |
|---|---|---|
| 1 | 994.7871332 | 0.2418098999 |
| 2 | 994.8176663 | -0.01696334459 |
| 3 | 994.7983058 | -0.1116557856 |
| 4 | 994.8186604 | 0.9843963832 |
| 5 | 994.8186604 | 0.2249340123 |
| 6 | 994.7697566 | 0.9843963832 |
| 7 | 994.7697566 | -0.1116557856 |
| 8 | 994.8186604 | 0.2249340123 |
| 9 | 994.858377 | 0.05243301114 |
| 10 | 994.8980937 | 0.8981454315 |
| 11 | 994.8186604 | 0.2249340123 |
| 12 | 994.8390148 | -0.03381620638 |
| 13 | 994.8186604 | -0.5344867371 |
| 14 | 994.7992974 | 0.05243301114 |
| 15 | 994.8186604 | -0.1116557856 |
| 16 | 994.8390148 | 0.2249340123 |
| 17 | 994.8288376 | 0.2249340123 |
| 18 | 994.858377 | 0.138683084 |
| 19 | 994.8980937 | 0.2249340123 |
| 20 | 994.8186604 | -0.7848035622 |
| 21 | 994.849192 | -0.1116557856 |
| 22 | 994.7290506 | -0.1116557856 |
| 23 | 994.9082717 | -0.1116557856 |
| 24 | 994.9184497 | -0.1116557856 |
| 25 | 994.8787322 | 0.2249340123 |

Figure 137: Raw BMP388 Sensor Reading Data

| Reading | Angular Velocity (rad/s) | Acceleration (m/s^2) | Magnetic Strength (uT) |
|---|---|---|---|
| 1 | (-0.001090830782496456, -0.007635815477475192, 0.001090830782496456) | (-0.43, 0.03, 9.78) | (5.375, 21.875, -35.6875) |
| 2 | (-0.001090830782496456, -0.008726646259971648, 0.001090830782496456) | (-0.46, 0.04, 8.52) | (5.0, 21.875, -36.875) |
| 3 | (0.001090830782496456, -0.013089969389957472, 0.0) | (-0.44, 0.0, 9.78) | (4.25, 22.25, -36.5) |
| 4 | (-0.001090830782496456, -0.015271630954950384, -0.009817477042468103) | (-0.44, 0.06, 9.76) | (5.75, 21.875, -36.5) |
| 5 | (-0.00545415391248228, -0.04908738521234052, -0.002181661564992912) | (-0.41000000000000003, 0.06, 9.81) | (4.25, 22.5625, -35.6875) |
| 6 | (-0.00545415391248228, -0.03381575425739013, -0.001090830782496456) | (-0.4, 0.06, 9.78) | (4.25, 22.25, -35.6875) |
| 7 | (0.001090830782496456, -0.03381575425739013, -0.1407171709420428) | (-0.48, 0.15, 9.8) | (4.25, 22.25, -35.6875) |
| 8 | (0.003272492347489368, 0.03381575425739013, -0.007635815477475192) | (-0.44, 0.06, 9.76) | (4.5625, 22.5625, -36.0625) |
| 9 | (0.002181661564992912, 0.007635815477475192, -0.002181661564992912) | (-0.44, 0.1, 9.78) | (4.25, 21.5, -36.0625) |
| 10 | (-0.002181661564992912, -0.019634954084936207, 0.0) | (-0.41000000000000003, 0.06, 9.78) | (4.5625, 21.875, -36.875) |
| 11 | (0.002181661564992912, -0.006544984694978736, 0.001090830782496456) | (-0.42, 0.07, 9.81) | (4.5625, 21.1875, -36.875) |
| 12 | (0.00545415391248228, 0.03490658503988659, -0.002181661564992912) | (-0.45, 0.04, 9.81) | (4.0, 21.1875, -36.0625) |
| 13 | (0.001090830782496456, 0.004363323129985824, 0.0) | (-0.4, -0.23, 9.78) | (5.375, 21.5, -35.6875) |
| 14 | (-0.007635815477475192, -0.039269908169872414, -0.007635815477475192) | (-0.44, 0.06, 9.77) | (3.5625, 21.5, -35.6875) |
| 15 | (0.003272492347489368, 0.001090830782496456, 0.001090830782496456) | (-0.43, 0.03, 9.75) | (4.25, 21.875, -34.875) |
| 16 | (0.001090830782496456, 0.02181661564992912, 0.00545415391248228) | (-0.43, 0.03, 9.790000000000001) | (4.25, 21.875, -35.6875) |
| 17 | (-0.007635815477475192, -0.04581489286485115, 0.0) | (-0.4, 0.02, 9.81) | (4.25, 21.0625, -35.25) |
| 18 | (-0.003272492347489368, -0.02399827721492203, 0.0) | (-0.41000000000000003, -0.02, 9.8) | (4.0, 21.5, -35.25) |
| 19 | (-0.001090830782496456, 0.016362461737446838, -0.001090830782496456) | (-0.41000000000000003, 0.02, 9.78) | (4.0, 20.75, -36.5) |
| 20 | (0.002181661564992912, 0.007635815477475192, 0.0) | (-0.4, 0.02, 9.77) | (4.0, 20.75, -36.5) |
| 21 | (0.00545415391248228, 0.02399827721492203, 0.001090830782496456) | (-0.43, 0.04, 9.76) | (5.0, 21.875, -36.0625) |
| 22 | (-0.007635815477475192, -0.038179077387375956, -0.002181661564992912) | (-0.41000000000000003, 0.02, 9.78) | (5.375, 21.875, -36.875) |
| 23 | (-0.003272492347489368, -0.011999138607461015, -0.001090830782496456) | (-0.4, 0.01, 9.78) | (5.0, 21.875, -36.5) |
| 24 | (0.002181661564992912, -0.001090830782496456, 0.001090830782496456) | (-0.39, 0.0, 9.790000000000001) | (5.0, 21.875, -35.25) |
| 25 | (0.002181661564992912, -0.00545415391248228, 0.002181661564992912) | (-0.41000000000000003, 0.02, 9.77) | (4.5625, 22.25, -35.6875) |

Figure 138: Raw BNO055 Sensor Reading Data

The following are image data collected from the Payload camera FoV test.

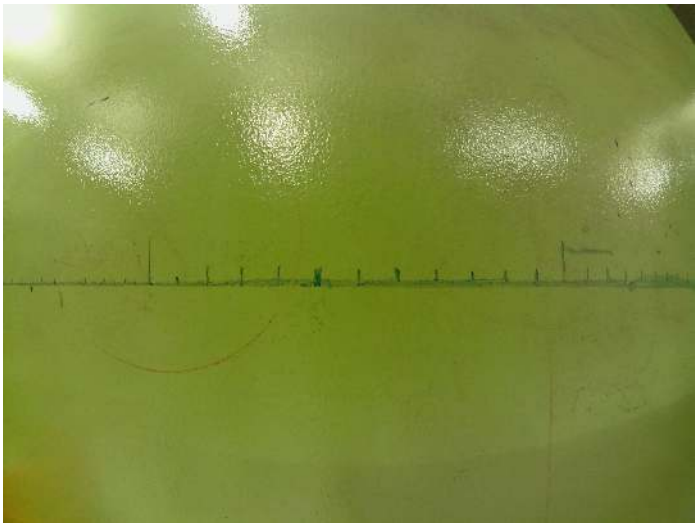

Figure 139: Raw Camera Image Data at 10" Subject Distance

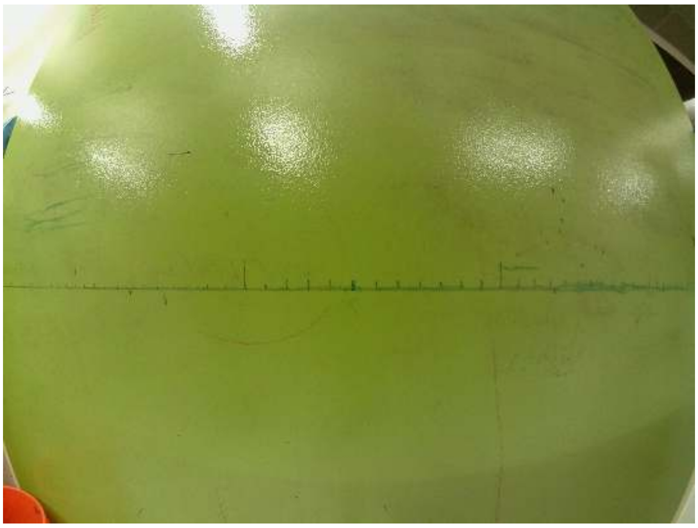

Figure 140: Raw Camera Image Data at 12" Subject Distance

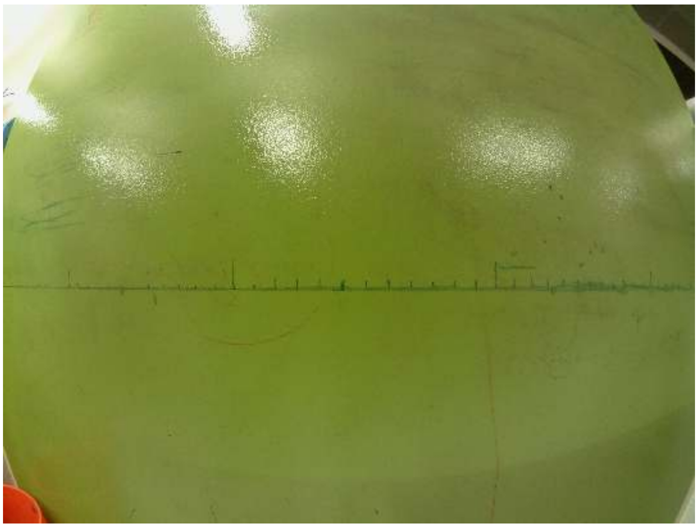

Figure 141: Raw Camera Image Data at 15” Subject Distance

Figure 142: Raw Camera Image Data at 16” Subject Distance